Issue: 11 | September 2023
www.fortishealthcare.com

Fortis

Clinical Connect

Fostering a culture of innovation and excellence

Diagnostic Special

Detect, Diagnose, Deliver!

IN THIS ISSUE

CONTENTS

Inspirational Messages

Mr Anand K
Managing Director and CEO,
Agilus Diagnostics Ltd.

Diagnosis is not the end, but the beginning of practice

……Martin H. Fischer

The perception of the diagnostics has been forever altered due to the pandemic. The significance of the lab cannot be overstated enough; suffice to say that laboratory data forms 70% of the structured clinical data.

Over a span of 4,000 years, concepts about medicine and illness have evolved, as a result of remarkable contributions from scientists and more recently, a result of the continuous advancement of technology. The four humours and other theories enthralled physicians for almost 2000 years, yielding to the idea of organ-based disease only in the last few hundred years. The concept of disease slowly changed from organ to tissue to a cellular level that led to the evolution of histopathology that has held sway in pathology for a century and half. As the second millennium drew to a close, powerful new technologies began to force yet another revision of our ideas, from cell-based disease, to gene-based disease, to individual molecules and their interplay.

The Human Genome Project is a watershed moment not just for human science but also for pathology and laboratory. In March 2022, the first truly complete human genome sequence was produced. Highly accurate and long-read sequencing has finally removed technology limitations, enabling comprehensive studies of genomic variations across the entire human genome, which we expect to drive future discovery in human genomic health and disease. Today, we not just have multiple methods to sequence DNA, but we can also do so quickly and affordably. Genomics is transforming the way we diagnose and study cancer and is enabling hereditary cancer screening. In addition, pharmacogenomics is empowering clinicians to find the right medication for the right patient and at the right dose. Genomics is also revolutionising rare disease diagnosis and prenatal testing.

Omics based diagnostics and computational biology has taken precedence in the current times and holds great potential for laboratory medicine in the near future. As the pace of technological advancement accelerates, it behoves us to harness the potential of emerging informatics, genomics, and proteomics applications.

In India, the diagnostic industry has undergone a significant shift in the last five decades. Today, patients have the option to undergo the most advanced tests at one of the lowest costs across the globe and from the convenience of their homes. The industry today is able to offer affordability, access, quick turnaround time, high quality reports of global standards and a seamless customer experience. Agilus Diagnostics in many ways has led the change in the industry through its rich legacy of diagnostic excellence.

Agilus Diagnostics is India's first NABL Accredited Laboratory as well as the first PAN India Lab to be accredited by College of American Pathologists. We are the largest chain in India in terms of number of laboratories besides also having the largest network or NABL accredited laboratories. Our team of 400+ highly qualified and experienced panel of pathologists work with clinicians to arrive at the right diagnoses for patients. We have three Centres of Excellence focused on Histopathology, HLA & Transplant Immunology and Molecular Pathology. These three units led by expert pathologists work on some of the most complex diagnostic cases each day that raise the bar of diagnostic excellence. Our robust DSIR approved R&D team undertakes clinical research studies, co–marketing projects, contract validations, and collaborations. Our work in digital pathology and advanced genomics is at par with global standards. This year in addition to launching whole genome sequencing for tuberculosis, we also launched several new genomic solutions in the area of reproductive genetics, oncology, and hereditary and rare disorders. Several state-of-the-art technologies were implemented, notably the Golden Helix software for exome and NGS panel reporting. We also installed S5 NGS PLUS and Sanger Sequencing 24 capillary with a better turnaround time.

We have also partnered with Path Presenter's clinical consultation platform to empower specialist pathologists at our reference laboratories to quickly and easily sign out pathology cases uploaded from remote locations in Agilus' laboratory network. Through this partnership, we are proud and excited to pioneer this on a large scale in India and raise the bar of diagnostic excellence. In addition to enabling multi-site collaborations, the Path Presenter platform will also aid in disease research involving pathology informatics that requires the archival, retrieval, organization, and seamless sharing and analysing of data sets created by anatomic pathologists.

Needless to say that Agilus will always remain guided by the latest in laboratory medicine and endeavour to deliver the best in diagnostic care.

I am pleased to be a part of this wonderful 'Clinical Connect' issue that has been dedicated to diagnostics and laboratory medicine. I also take this opportunity to congratulate the team at Fortis for this unique initiative that bolsters our position of 'Care for Good'.

Happy reading!

Dr Rakesh K Gupta
Chair - Radiology Specialty Council,
Principal Director and Head - Radiology,
Fortis Memorial Research Institute, Gurugram

Radiology has become an integral part of hospital services and is being used for evaluation of clinical situations in different systems and subsystems of the body. It is imperative for us to use innovation in the applications and implementation of techniques especially in CT and MRI. Recent advances in CT like the use of photon CT and spectral CT have been able to reduce the radiation dose with improved resolution and faster image acquisition. Similarly, in MRI, newer techniques like AI based compressed sensing acquisition that improves the resolution with reduced imaging time that is likely to help in better patient through put and will help in developing innovative techniques and clinical application in future. Use of Radiomics based approach in future is likely to improve our understanding in better tissue characterization of the disease process in future. Recently an entity has been recognized in brain referred to as GLYMPHATIC SYSTEM which helps to clear the toxic brain products along the perivascular space besides CSF and has been implicated in a number of neurological disorders like dementia, atherosclerosis which can be quantified using different MRI techniques. I feel that use of advanced imaging techniques with the help of artificial intelligence, will improve biological understanding of the disease process and will help in improved patient care.

Dr Mona Bhatia
Director and Head - Radiology,
Fortis Escorts Heart Institute, Okhla

Radiology, has revolutionized healthcare, and plays an indispensable role in modern medicine, with its diagnostic and interventional capabilities shaping the landscape of patient care. In this dynamic and ever-evolving field, the exchange of knowledge and ideas among radiologists, clinicians, and researchers becomes paramount.

My heartiest congratulations to the editorial team of Fortis Clinical Connect and the vision of Fortis as an organization, for providing this platform designed to facilitate seamless communication, knowledge sharing, research and mutual learning. The Clinical Connect indeed connects clinicians, radiologists, stakeholders, and even patients, fostering a dynamic ecosystem of knowledge exchange, academic pursuits that drive innovation and elevate patient care.

Radiology has expanded beyond traditional imaging techniques, encompassing cutting-edge technologies, artificial intelligence, and advanced interventional procedures. As we navigate these advancements, it is imperative that we nurture a robus academic foundation.

We firmly believe that collaboration is the cornerstone of progress and interdisciplinary collaborations offer exciting potentials. Whether you're a radiologist with insights into the latest imaging technologies, a clinician with a unique perspective on patient care, or a researcher exploring the boundaries of medical science, your contribution is invaluable. By pooling our talents, we can develop ground breaking solutions that address the most pressing challenges in healthcare.

Learning from one another's experiences and perspectives enriches our collective knowledge and empowers us to better serve our patients. Together, we can leverage our strengths and pool our resources to tackle even the most complex medical challenges.

Artificial intelligence has become an indispensable partner, enhancing our ability to interpret images, streamline workflows, and uncover insights that were once unimaginable. This convergence of human expertise and AI capabilities forms the foundation of our progressive approach to patient care.

The heart of our mission lies in the well-being of our patients. We are all essential pieces of a greater puzzle, each contributing unique strengths to the intricate tapestry of healthcare. By harnessing our collective potential, we can drive forward innovations that reshape the future of medicine.

As we stand at the precipice of innovation, united by a common passion for healthcare, let us embark on this journey with renewed enthusiasm. Together, we will continue to redefine the boundaries of medicine, armed with knowledge, collaboration, and an unwavering commitment to our patients.

We envision a future where radiology and clinical practice are seamlessly integrated, driving transformative outcomes for patients worldwide. We look forward to embarking on this journey of collaboration and discovery with each and every one of you.

Dr Ishita Sen
Senior Director - Nuclear Medicine,
Fortis Memorial Research Institute, Gurugram

"In the long history of humankind those who learned to collaborate and improvise most effectively, have prevailed."

……Charles Darwin

In this ever changing and fiercely competitive healthcare landscape, to provide an effective platform for the exchange of ideas between its doctors and healthcare professionals is possibly one of the greatest mantras of success for any healthcare organisation. The clinical connect team has effectively promoted and cross promoted achievements, ideas and technological advances across various hospitals in the Fortis Hospitals

network over the last many months. We acknowledge and appreciate the professionals of the clinical connect team who have worked tirelessly to create a platform for all the professionals across the Fortis Hospitals network to come together, showcase their clinical work and learn from each other.

Nuclear medicine is undergoing a kind of renaissance, with a steady introduction and approval of new radiopharmaceuticals, theranostics, and instrumentation. The Fortis Hospitals management has been there every step of the way to support the field of nuclear medicine, promoting quality of practice, research, outreach, and advocacy. The new state of the art digital PET CT with its ability to perform advanced AI based parametric imaging and the new SPECT CT installations at the Fortis Memorial Research Institute, is just one more evidence of the same. Today at FMRI we can boast of having one of the finest nuclear medicine programs, at par with the many of the finest institutions of the world.

With more than nine, state of the art nuclear medicine facilities across various hospitals in the Fortis healthcare group, together we are probably the largest combined nuclear medicine group in the country. This large footprint opens up a huge opportunity for us to standardize the practice protocols, share best practices and perform multicentric collaborative research. We hope we can increase our collaborative efforts in the months and years to come, establishing Nuclear Medicine at the Fortis group as a formidable force in driving excellence in patient care and research, both in the country and beyond.

Once again, I congratulate the team at clinical connect and salute their efforts to bring us all together. I wish them all the best and look forward to lot of academic and research initiatives from the team in future.

Dr Pradeep Srinivasan
Director- Radiology and Fetal Medicine,
Fortis Hospitals, Bangalore

Dear Fortisians,

At the outset I take immense pleasure and pride to call myself a happy Fortisian. After graduating in Radiology, I wanted an apt Organisation to pursue my skills and serve the sick community. This required state of the art X ray, fluoroscopy, CT, MRI, Sonography, mammography, PET etc all of which I could find at Fortis. In my 21 years at Fortis, we as a team have built a strong Radiologist and Technologist and para medic manpower base and run a robust DNA programme for students which fulfils all the needs of a practising doctor. Radiology and fetal medicine are the most opted fields for fresh MBBS graduates since 2 decades and will continued to be so.

Interventional Neuroradiology and body Radiology have branched out smartly and offer Radiologists scope to fulfil their surgical desires and act like clinicians. PET CT and PET MR are indispensable in oncology treatment. Robotic surgeries cannot function without the navigation provided by Advanced CT and MRI images. Artificial intelligence has its best bet in Radiological image interpretations and are threatening to reduce the requirements of large number of radiologists per hospital.

PACS and networking and cloud storage are making Teleradiology so robust that mass migration of multimodality studies from one continent to other in a second is a reality. This threatens the very basic requirements of onsite radiologist concept at hospitals.

Fetal medicine and fetal interventions are of such advanced stage that many Gynecologists are crossing borders and taking fetal medicine as their future speciality of practise.

Thus, Radiologist continues to be *A CONSULTANT TO THE CONSILTANTS.*

I thank all my colleagues, specialists, administrators, technicians, paramedics, nurses, and of course patients for all the good things over the last 2 decades of my practise at Fortis.

Thanking you !

Dr Narayan Pendse
Vice President - Medical Strategy and Operations,
Fortis Corporate

Dear Colleagues

Diagnostics including Radiology, Nuclear Medicine, Lab Medicine, contribute significantly in reducing the burden of disease, frequency and duration of hospitalizations and its associated financial strain, and lead to better clinical outcomes. The rapid and ever-evolving landscape of modern medicine has brought us to the confluence of ground-breaking advancements in diagnostics and therapeutics in the pursuit of precision healthcare. Precise clinical care requires timely, reliable and accurate diagnostics followed by evidence based clinical case management delivered through cutting edge technology by skilled clinicians.

The future of medicine lies in early diagnosis and targeted treatments. Diagnostic specialties have revolutionized healthcare and are witnessing unprecedented advancements and are venturing into the realm of Molecular Imaging, Theranostics and Genomics - combining medical imaging with lab medicine to predict the probability of various diseases and foretell effectiveness of various treatment options to deliver customized care through predictive medicine. A holistic therapeutic approach now focuses on collaboration among radiologists, nuclear medicine specialists, clinicians, and other stakeholders to bring positive outcomes with effective use of forums like Tumor Boards, Multi Disciplinary Team Consults etc. In today's digital age, the field is set to grow exponentially thanks to technological advances like digitization and rapid image acquisition – we are now at the cusp of a new era heralded by application of Artificial Intelligence and Machine Learning to Diagnostics.

Diagnostics hold a place of pride at Fortis and we boast of world class infrastructure and services. In recent years large CAPEX investment has been made to make available best in class equipment. To explore the vast realm of diagnostics and celebrate the remarkable shifts made by radiology, nuclear medicine, and lab medicine at Fortis, we bring this issue of Clinical Connect "Diagnostics – Radiology and Imaging, Nuclear Medicine and Lab medicine" to you. The theme resonates profoundly with me, both as a trained radiologist and as a proud member of Fortis' mission to provide exceptional patient care.

This is also an opportunity to acknowledge, appreciate, and applaud our colleagues from Diagnostic specialties who work tirelessly behind the scene to ensure timely and accurate inputs for informed clinical decision making and better patient care. We understand the significance of your contribution and encourage you to build on the great work being done by each one of you.

Best wishes and Happy Reading

THE EDITORIAL TEAM

Please send your comments, feedback and suggestions to clinical.connect@fortishealthcare.com

Radiology Specialty Council Members

Dr R K Gupta

Chair
Principal Director and Head - Radiology,
Fortis Memorial Research Institute,
Gurugram

Dr Pradeep Srinivasan

Director - Radiology and Fetal Medicine,
Fortis Hospitals, Bangalore

Dr Mona Bhatia

Director and Head - Radiology,
Fortis Escorts Heart Institute, Okhla

Dr Puneet Jain

Director and HOD - Radiology,
Fortis Hospital, Shalimar Bagh, New Delhi

Dr Abhishek Prasad

Director and Head - Radiology,
Fortis Hospital, Mohali

Dr Dinesh Kapoor

Director - Radiology,
Fortis Hospital, Noida

Dr Rajat Bhargav

Director and Head - Radiology
Fortis Hospital, Mulund

Dr Narayan Pendse

Convenor
Vice President - Medical Strategy and Operations,
Fortis Corporate

Neuro Radiology

Susceptibility-weighted Imaging: An Emerging Technique for Evaluation of the Spine and Spinal Cord

Scan QR Code for more

Dr R K Gupta
Principal Director and Head - Radiology, Fortis Memorial Research Institute, Gurugram

Dr Shalini Sharma
Consultant - Radiology, Fortis Memorial Research Institute, Gurugram

Abstract

We present the application of three-dimensional susceptibility-weighted imaging technique for evaluation of pathologies of the spine and spinal cord. This work focuses on the advantage of this imaging technique as an adjunct to the conventional imaging to evaluate various disorders of the spine and spinal cord like trauma, degenerative diseases, vascular malformations, and tumours, where susceptibility-weighted imaging may offer valuable harmonising evidence that may be helpful in the diagnosis and management of the patients with these pathologies.

Introduction

Susceptibility-weighted imaging (SWI) is a high resolution, three-dimensional (3D) radiofrequency (rf) spoiled gradient-echo technique that uses magnitude and filtered-phase information to enhance tissue susceptibility-based contrast.1 Until now, the use of SWI in clinical practice is largely restricted to brain for detecting micro-haemorrhages, calcification, iron, and deoxyhaemoglobin. Limited number of studies have explored its utility in imaging spine and epidural vasculature,2,3 gall bladder4 and female pelvis5 where it is found to be useful in improved pathological differentiation. Its use has not been extended to routine clinical practice in spine imaging, presumably, due to its limitations in spatial resolution and coverage, artefacts leading to suboptimal bone–tissue interfaces, and augmented noise. However, in this article, we show that with appropriate protocols at 3.0T, SWI provides additional information that could help in better diagnosis and management.

Conclusion

SWI provides high spatial resolution images along with excellent contrast-to-noise ratio in spine imaging, especially on the 3T system. The combination of phase and magnitude images provides useful information regarding the extravascular blood degradation products and calcium deposition. Presence of calcification in the discs and ligaments can be detected on SWI images, which helps in presurgical planning. Accurate identification of site and extent of haemorrhage in the spinal cord helps in better clinical management and formulation of rehabilitation plan. All the bony pathologies that require CT for better evaluation can be evaluated using 3D SWI. We recommend that SWI should be added to the routine imaging protocol of patients referred for evaluation of the pathology of the spine and the spinal cord.

Role of Intra-tumoral Vasculature Imaging Features on Susceptibility Weighted Imaging in Differentiating Primary Central Nervous System Lymphoma from Glioblastoma: A Multiparametric Comparison with Pathological Validation

Source : Bhattacharjee R, Gupta M, Singh T, Sharma S, Khanna G, Parvaze SP, Patir R, Vaishya S, Ahlawat S, Singh A, Gupta RK. Role of intra- tumoral vasculature imaging features on susceptibility weighted imaging in differentiating primary central nervous system lymphoma from glioblastoma: a multiparametric comparison with pathological validation. Neuroradiology. 2022 Sep;64(9):1801-1818. doi: 10.1007/s00234-022- 02946-5. Epub 2022 Apr 18. PMID: 35435463.

Scan QR Code for more

Dr R K Gupta
Principal Director and Head - Radiology,
Fortis Memorial Research Institute, Gurugram

Dr Shalini Sharma
Consultant - Radiology,
Fortis Memorial Research Institute, Gurugram

Abstract

Purpose Primary objective of this study was to retrospectively evaluate the potential of a range of qualitative and quantitative multi-parametric features assessed on T2, post-contrast T1, DWI, DCE-MRI, and susceptibility-weighted-imaging (SWI) in differentiating evenly sampled cohort of primary-central-nervous-system-lymphoma (PCNSL) vs glioblastoma (GB) with pathological validation.

Methods

The study included MRI-data of histo-pathologically confirmed ninety-five GB and PCNSL patients scanned at 3.0 T MRI. A total of six qualitative features (three from T2 and post-contrast T1, three from SWI: thin-linear-uninterrupted-intra-tumoral-vasculature, broken-intra-tumoral-microvasculature, haemorrhage was analysed by three independent radiologists. Ten quantitative features from DWI and DCE-MRI were computed using in-house-developed algorithms. For qualitative features, Cohen's Kappa-interrater-variability-analysis was performed. Z-test and independent t-tests were performed to find significant qualitative and quantitative features respectively. Logistic-regression (LR) classifiers were implemented for evaluating performance of individual and various combinations of features in differentiating PCNSL vs GB. Performance evaluation was done via ROC-analysis. Pathological validation was performed to verify disintegration of vessel walls in GB and rim of viable neoplastic lymphoid cells with angiocentric-pattern in PCNSL.

Results

Three qualitative SWI features and four quantitative DCE-MRI features (rCBVcorr, Kep, Ve, and necrosis-volume-percentage) were significantly different ($p < 0.05$) between PCNSL and GB. Best diagnostic performance was observed with LR classifier using SWI features (AUC-0.99). The inclusion of quantitative features with SWI feature did not improve the differentiation accuracy.

Conclusions

The combination of three qualitative SWI features using LR provided the highest accuracy in differentiating PCNSL and GB. Thin-linear-uninterrupted-intra- tumoral-vasculature in PCNSL and broken-intra-tumoral-microvasculature with haemorrhage in GB are the major contribtutors to the differentiation.

Keywords

Brain MRI • PCNSL • SWI • DCE-MRI • GB

Primary CNS Lymphoma Showing Open Ring Pattern of Enhancement on MR Imaging

Dr Abhishek Prasad
Director and Head - Radiology,
Fortis Hospital, Mohali

Dr Ritu Pankaj
Additional Director - Lab Medicine,
Fortis Hospital, Mohali

Case Report

A 55 years old female was referred for MRI of brain to our department with a history of headache and vomiting since 10 days. There was no history of seizures or focal neurological deficits.

MRI of the brain shows two well defined lesions showing open ring enhancement in the right frontoparietal lobes predominantly in the subcortical location. There was marked perilesional vasogenic edema with mass effect and midline shift to left side. They were few other small enhancing nodular foci adjacent to these lesions and in the left frontal lobe.

These lesions showed hypointense signal on T2w images with evidence of diffusion restriction with mean ADC values of 725 x 10-6mm2/s. On MRI perfusion the lesions were mildly hyper perfused with rCBV ranging from 2-3. The percentage signal recovery (PSR) obtained from DSC perfusion measurements were raised (142) and overshooting the base line. The lesions were hyperdense on CT. On PET CT the lesions were intensely hypermetabolic (SUV max: 65.73) with no other hypermetabolic extra cranial focus in rest of the body.

All these imaging features were in favour of and intracranial neoplastic lesion highly suggestive of lymphoma. Patient subsequently underwent right parietal craniotomy with subtotal excision and biopsy of the tumour. The histopathology reveals prominent perivascular lymphocytic cuffing by large atypical lymphoid cells which on immunostaining showed diffuse CD 20 positivity. Features were consistent with Non-Hodgkin lymphoma, B cell type.

Discussion

Open ring enhancement on contrast MRI are considered highly specific for tumefacien demyelination with specificity as high as 84.4-93.8 % for TDL diagnosis and a likelihood ratio of 5.2 for demyelination versus neoplasm in one study. (1). However open ring enhancement have been reported in GBM (2) and rarely in lymphoma (3).

We have reported multiple open ring enhancing lesions in an immunocompetent patient that turned out to be primary CNS lymphoma. The lesion however shows other imaging features which were suggestive of lymphoma. Even though open ring enhancement on MRI are highly specific for TDLs, other features of the lesion should be looked into to rule out neoplastic etiology. These features include T2w signal, diffusion restriction, relative perfusion, peak signal recovery and CT attenuation of the lesion.

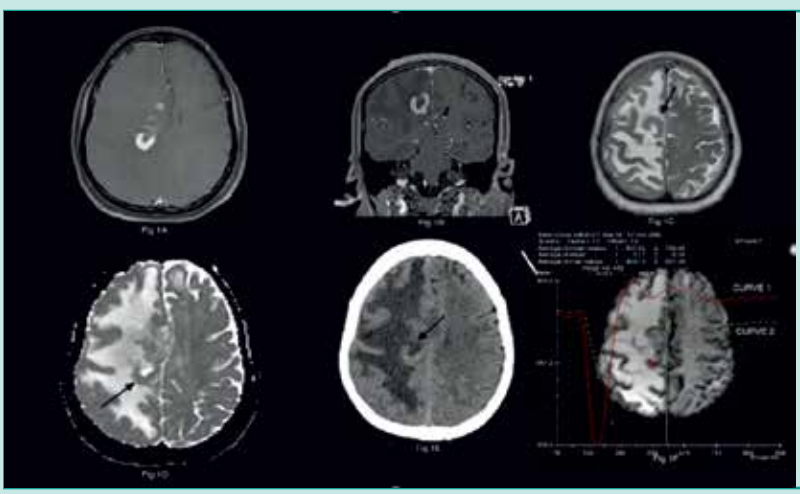

Figure 1: Fig 1A (Post contrast T1w fs axial) and Fig 1B (Post contrast T1w fs coronal) show open ring enhancing lesions in right frontoparietal lobe. Fig 1C (T2w axial) shows hypointense open ring lesions in right high frontal lobe. Fig 1D (ADC axial) shows diffusion restriction in the lesion. Fig 1E shows lesion to be hyperdense on plain CT head. Fig 1F shows peak signal recovery (PSR) curve obtained from the lesion (curve 1) shows increased PSR overshooting the baseline compared to normal measurement (curve 2).

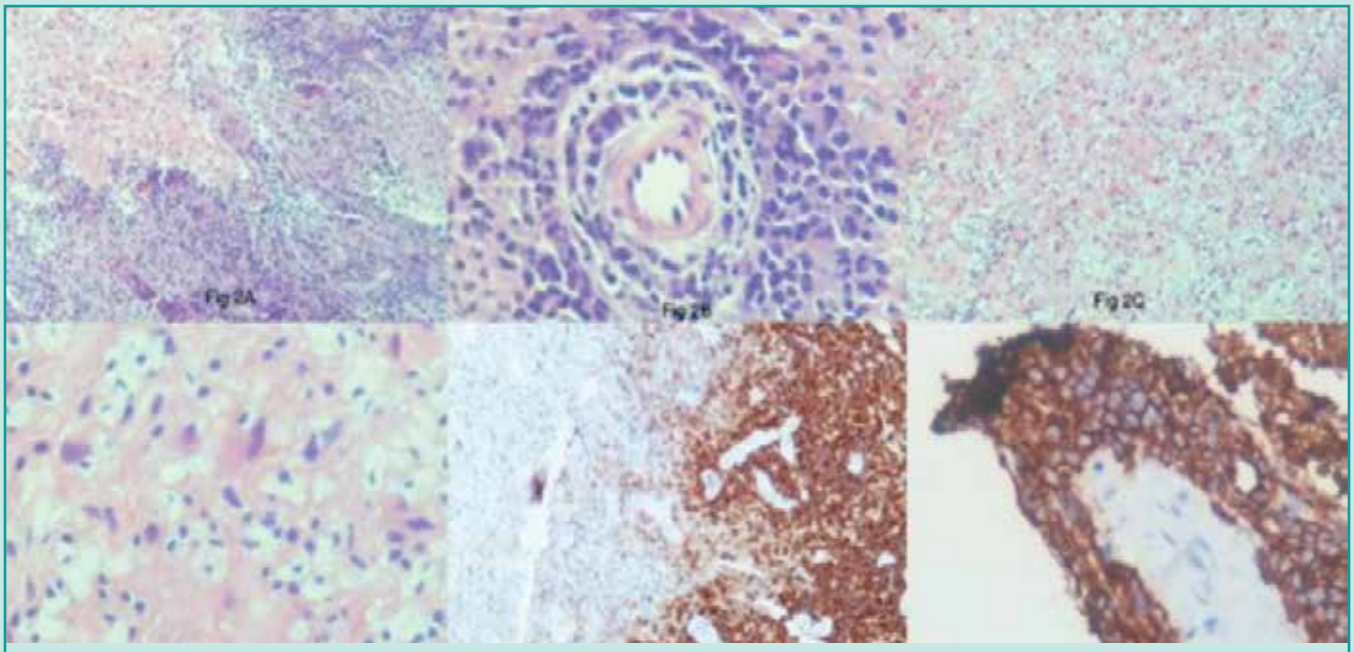

Figure 2: Fig. 2a (100x) shows tumour and brain interface. Fig. 2b (400x) shows perivascular cuffing by atypical lymphoid cells. Fig. 2c (100x) shows foamy macrophages. Fig. 2d (400x) shows high power magnification of foamy macrophages. Fig. 2e (100x) CD20 immunostain highlights tumour cells. Fig. 2f (400x) CD20 immunostain highlights perivascular tumour cells

References

1. Masdeu JC, Moreira J, Trasi S, Visintainer P, Cavaliere R, Grundman M. The open ring. A new imaging sign in demyelinating disease. J Neuroimag 1996;6:104-7
2. Kinon MD, Scoco A, Farinhas JM, Kobets A, Weidenheim KM, Yassari R, et al. Glioblastoma multiforme presenting with an open ring pattern of enhancement on MR imaging. Surg Neurol Int 2017;8:106
3. Zhang D, Liang-Bo Hu, Henning TD, Ravarani EM, Li-Guang Zou, Xiao-Yuan Feng, Wen-Xian Wang et al. MRI Findings of Primary CNS Lymphoma in 26 Immunocompetent Patients.Korean J Radiol 2010;11:269-277

Varied Imaging and Clinical Presentations of Acute Bacterial Cerebritis

Source: Sharma, S., Saini, J., Khanna, G. et al. Varied imaging and clinical presentations of acute bacterial cerebritis. Emerg Radiol 29, 791–799 (2022). https://doi.org/10.1007/s10140-022-02051-3

Scan QR Code for more

Dr R K Gupta
Principal Director and Head - Radiology,
Fortis Memorial Research Institute, Gurugram

Dr Shalini Sharma
Consultant - Radiology,
Fortis Memorial Research Institute, Gurugram

Abstract

Infectious diseases affecting the central nervous system remain an important cause of morbidity and mortality in developing countries and in immunocompromised patients. Cerebritis refers to pyogenic inflammation of the brain parenchyma that may lead to abscess formation if left untreated. Cerebritis is an uncommon diagnosis as patients are usually diagnosed at the stage of abscess formation. We present three cases of bacterial cerebritis with different clinical manifestations and varied appearances on MRI. To our knowledge, only few case reports of bacterial cerebritis have been published in the literature, and imaging findings are not fully elucidated. These cases of bacterial cerebritis add valuable information to the existing literature and would be helpful in making the appropriate diagnosis of this uncommon condition that can be medically managed if diagnosed appropriately. We recommend that cerebritis should be considered in the differential diagnosis of such lesions.

Radiomics Signature for Temporal Evolution and Recurrence Patterns of Glioblastoma using Multimodal Magnetic Resonance Imaging

Source: Sharma, S., Saini, J., Khanna, G. et al. Varied imaging and clinical presentations of acute bacterial cerebritis. Emerg Radiol 29, 791–799 (2022). https://doi.org/10.1007/s10140-022-02051-3

Dr R K Gupta
Principal Director and Head - Radiology,
Fortis Memorial Research Institute, Gurugram

Dr Sunita Ahlawat
Principal Consultant - Histopathology, Agilus,
Fortis Memorial Research Institute, Gurugram

Dr Rana Patir
Chairman - Neurosurgery,
Fortis Memorial Research Institute, Gurugram

Dr Sandeep Vaishya
Executive Director and Head - Neurosurgery,
Fortis Memorial Research Institute, Gurugram

Abstract

Glioblastoma is a highly infiltrative neoplasm with a high propensity of recurrence. The location of recurrence usually cannot be anticipated and depends on various factors, including the surgical resection margins. Currently, radiation planning utilizes the hyperintense signal from T2-FLAIR MRI and is delivered to a limited area defined by standardized guidelines. To this end, noninvasive early prediction and delineation of recurrence can aid in tailored targeted therapy, which may potentially delay the relapse, consequently improving overall survival. In this work, we hypothesize that radiomics-based phenotypic quantifiers may support the detection of recurrence before it is visualized on multimodal MRI. We employ retrospective longitudinal data from 29 subjects with a varying number of time points (three to 13) that includes glioblastoma recurrence. Voxelwise textural and intensity features are computed from multimodal MRI (T1-contrast enhanced [T1CE], FLAIR, and apparent diffusion coefficient), primarily to gain insights into longitudinal radiomic changes from preoperative MRI to recurrence and subsequently to predict the region of relapse from 143 ± 42 days before recurrence using machine learning. T1CE MRI first-order and gray-level co-occurrence matrix features are crucial in detecting local recurrence, while multimodal gray-level difference matrix and first-order features are highly predictive of the distant relapse, with a voxelwise test accuracy of 80.1% for distant recurrence and 71.4% for local recurrence. In summary, our work exemplifies a step forward in predicting glioblastoma recurrence using radiomics-based phenotypic changes that may potentially serve as MR-based biomarkers for customized therapeutic intervention.

F18-Fluorodeoxyglucose Positron Emission Tomography - Computed Tomography in Evaluation of Intracranial Space Occupying Lesions

SOURE: Junaid, S. (2022). 18F-FDG PET/CT IN THE EVALUATION OF ICSOLs. Pan Arab Journal of Neurosurgery, 17(2), 9-17. doi: 10.21608/pajn.2022.92073.1033

Scan QR Code for more

Dr Sayed Junaid
Consultant and Head -
Nuclear Medicine and Molecular Imaging,
Fortis Hospital, Mohali

Abstract

This current study was designed to appraise the diagnostic value of F-18 Fluorodeoxyglucose (18F-FDG) positron emission tomography (PET/CT) in evaluating and possible grading of intracranial space occupying lesions.

Materials & Methods

The study was performed on 27 patients referred from the department of Neurosurgery at a tertiary care institute of north India. Data was collected through history and clinical examination which was followed by baseline investigations and finally imaging. The study subjects were planned to be divided into four distinct groups: low grade tumours (n=7), high grade tumours (n=5), metastases (n=13), and other lesions (n=2). This division was based on the WHO classification post Clinico-histological diagnosis. The subjects underwent CECT, CEMRI and 18F-FDG PET/CT preoperatively. All were followed up postoperatively and histopathological reports were regarded as the gold standard for tumour grading.

Results

The results showed that high grade tumours (Grade III/IV & IV/IV according to the WHO classification) did not show a statistically significant SUV max or SUV max per unit volume indices when compared with low grade tumours or metastatic lesions.

Conclusions

The results of this study suggest that 18F-FDG PET/CT indices of SUV max or SUV max per unit volume of tumour by themselves are not reliable indices for differentiating high grade tumours from lower grade ones or metastases however PET-CT imaging could rule out metastases from primary CNS malignancies by evaluating the rest of the body.

Keywords

18F-FDG, PET/CT, ICSOLs, Grading, Brain tumour

Quantification of Radiomics Features of Peritumoral Vasogenic Edema Extracted from Fluid Attenuated Inversion Recovery Images in Glioblastoma and Isolated Brain Metastasis, Using T1-Dynamic Contrast-Enhanced Perfusion Analysis

Source: Parvaze PS, Bhattacharjee R, Verma YK, Singh RK, Yadav V, Singh A, Khanna G, Ahlawat S, Trivedi R, Patir R, Vaishya S, Shah TJ, Gupta RK. Quantification of Radiomics features of Peritumoral Vasogenic Edema extracted from fluid-attenuated inversion recovery images in glioblastoma and isolated brain metastasis, using T1-dynamic contrast-enhanced Perfusion analysis. NMR Biomed. 2023 May;36(5):e4884. doi: 10.1002/nbm.4884. Epub 2022 Dec 23. PMID: 36453877.

Scan QR Code for more

Dr R K Gupta
Principal Director and Head - Radiology,
Fortis Memorial Research Institute, Gurugram

Dr Sunita Ahlawat
Principal Consultant - Histopathology, Agilus,
Fortis Memorial Research Institute, Gurugram

Dr Rana Patir
Chairman - Neurosurgery,
Fortis Memorial Research Institute, Gurugram

Dr Sandeep Vaishya
Executive Director and Head - Neurosurgery,
Fortis Memorial Research Institute, Gurugram

Abstract

The peritumoral vasogenic edema (PVE) in brain Tumors exhibits varied characteristics. Brain metastasis (BM) and meningioma barely have Tumor cells in PVE, while glioblastoma (GB) show tumor cell infiltration in most subjects. The purpose of this study was to investigate the PVE of these three pathologies using radiomics features in FLAIR images, with the hypothesis that the tumor cells might influence textural variation. Ex vivo experimentation of radiomics analysis of T1-weighted images of the culture medium with and without suspended tumor cells was also attempted toinfer the possible influence of increasing tumor cells on radiomics features. This retrospective study involved magnetic resonance (MR) images acquired using a 3.0-T MR machine from 83 patients with 48 GB, 21 BM, and 14 meningioma. The 93 radiomics features were extracted from each subject's PVE mask from three pathologies using T1-dynamic contrast-enhanced MR imaging. Statistically significant (< 0.05, independent samples T-test) features were considered. Features maps were also computed for qualitative investigation. The same was carried out for T1-weighted cell line images but group comparison was carried out using one-way analysis of variance. Further, a random forest (RF)-based machine learning model was designed to classify the PVE of GB and BM. Texture-based variations, especially higher nonuniformity values, were observed in the PVE of GB. No significance was observed between BM and meningioma PVE. In cell line images, the culture medium had higher nonuniformity and was considerably reduced with increasing cell densities in four features. The RF model implemented with highly significant features provided improved area under the curve results. The possible infiltrative tumor cells in the PVE of the GB are likely influencing the texture values and are higher in comparison with BM PVE and may be of value in the differentiation of solitary metastasis from GB. However, the robustness of the features needs to be investigated with a larger cohort and across different scanners in the future.

Keywords

brain metastases, brain tumor, DCE perfusion MRI, glioblastoma, MRI, radiomicst

Recent Advancements in Technology at Fortis

Mr Tarun Deep Katyal
Deputy General Manager -
Medical Strategy and Operations Group,
Fortis Corporate Office

Mr Vipin Kumar Singh
Manager - Bio Medical Engineering,
Medical Strategy and Operations Group,
Fortis Corporate Office

MRI Machine 3T
(Magnetic Resonance Imaging)

Make : Philips **Model** : Elition X 3T
Location : Fortis Hospital, BG Road/Anandpur Bangalore

Digital PET CT Machine

Make : Siemens **Model:** Biograph Vision
Location : Fortis Memorial Reseach Institute, Gurgaon

SPECT CT Machine

Make : Siemens Healthcare
Model : Symbia Intevo 6
Location : Fortis Memorial Reseach Institute, Gurgaon

Digital X-Ray Machine

Make : Care Stream **Model:** DRX Compass 80KW
Location : Fortis Memorial Reseach Institute, Gurgaon

Digital Mammography Machine

Make : Fujifilm **Model** : Amulet Innovality
Location : Mohali/BG Road/Vadapalani

CT Scan Machine

Make : Siemens
Model : Somatom Go Top 128 Slice
Location : Fortis Hospital, Vashi

Cardiovascular Radiology

Coronary Artery Disease Reporting and Data System: A Comprehensive Review

Source : Kumar P, Bhatia M. Coronary Artery Disease Reporting and Data System: A Comprehensive Review. J Cardiovasc Imaging. 2022 Jan;30(1):1-24. doi: 10.4250/jcvi.2020.0195. Epub 2021 Mar 23. PMID: 34080334; PMCID: PMC8792723.

Scan QR Code for more

Dr Mona Bhatia
Director and Head - Radiology,
Fortis Escorts Heart Institute, Okhla, New Delhi

Abstract

The Coronary Artery Disease Reporting and Data System (CAD-RADS) is a standardized reporting method for coronary computed tomography angiography (CCTA). It summarizes the findings of CCTA in 6 categories ranging from CAD-RADS 0 (complete absence of coronary artery disease) to CAD-RADS 5 (total occlusion of at least one vessel). It is applied on per patient basis for the highest grade of the stenotic lesion. The CAD-RADS also provides category-specific treatment recommendations, helping patient management. The main objectives of the CAD-RADS are to improve the consistency in reporting, facilitate the communication between interpreting and referring clinicians, recommend the best course of patient management, and produce consistent data for quality improvement, research and education. However, CAD-RADS has many limitations, resulting into the misclassification of the observed findings, misinterpretation of the final category, and misguidance for the treatment based upon the single score. In this review, the authors discuss the CAD-RADS categories and modifiers, along with the strengths and limitations of this new classification system.

Keywords

Coronary artery; Coronary artery disease; Stenosis.

A Case of Anomalous Origin of Left Pulmonary Artery from Aorta

Dr Rajan Aggarwal
Consultant – Radiology,
Fortis Hospital, Mohali

Dr Abhishek Prasad
Director and Head – Radiology,
Fortis Hospital, Mohali

Abstract

8-year-old male, known case of tetralogy of Fallot presented with complaints of bluish discolouration of skin and dyspnoea. On examination, there was deep cyanosis. 2D-Echocardiography shows ventricular septal defect and pulmonary atresia. Hence, CT pulmonary angiogram was advised.

Case Report

Patient was referred to our Department of Radiodiagnosis, Fortis Hospital, Mohali for CT pulmonary angiography. Study was done on Siemens Somatom go Top128-Slice CT scanner. Case was analyzed on dedicated Syngo.via work station with VRT films. In the case, we observed that the left pulmonary artery is arising directly from the

ascending aorta at the level of T6 vertebra ~ 3.3 cm from sinus and shows normal contrast opacification. The main pulmonary artery is arising from right ventricle with infundibular stenosis and continuing as right pulmonary artery with normal contrast opacification. The branches of respective pulmonary arteries are unremarkable. Small MAPCAs also seen arising from the descending thoracic aorta. Ventricular septal defect with over-riding aorta was noted.

Discussion

Anomalous origin of left pulmonary artery is less common than the anomalous origin of right pulmonary artery from aorta. It is also called as Hemitruncus. Most cases of left-sided anomalous origin of pulmonary artery (AOPA) are always associated with tetralogy of Fallot and aortic arch anomalies, whereas right-sided is more commonly associated with a patent ductus arteriosus or aortopulmonary septal defect. The aortic origin of a branch pulmonary artery creates a large left-to-right shunt leading to pulmonary hypertension and eventually pulmonary oedema. Abnormal origin of one branch from the ascending aorta leads to symptoms in infancy due to pulmonary over circulation and pulmonary hypertension. This leads to very high mortality unless surgically corrected with re-implantation of aberrant branch[1,3].

On the left side, failure of fusion of left pulmonary artery with main pulmonary artery is due to failure of fusion of left sixth arch and presence of aortic sac from which left pulmonary artery arises. On right side, proximal form of anomalous origin of pulmonary artery (AOPA) due to incomplete migration of sixth aortic arch to the left [2].

Multi detector computed tomography (MDCT) is now preferred method of choice due to early diagnosis, increased efficacy and reliability. Computed tomography cardiac angiogram provides non-invasive accurate diagnosis with its advanced tools of like volume rendering (VR) techniques and virtual dissection techniques, allowing further delineation of the anatomy, relation between pulmonary artery with adjacent structures as well as to evaluate cardiac structures from various angles.

Given management, early diagnosis with early intervention, absence of other cardiac anomalies and patients with decreased to normal values of pulmonary systolic pressure have better prognosis. Failure of diagnosis of anomalous origin of pulmonary artery from aorta in a known case of tetralogy of Fallot leads to fatal consequences during the reparative surgery. Supportive management is not optimum for such cases because these types of congenital anomalies has high mortality due to the pulmonary hypertension and heart failure in non-surgically repaired patients[4].

References

1. Newman, B., & Alkhori, N. (2020). Congenital central pulmonary artery anomalies: Part 2. Pediatric Radiology. doi:10.1007/s00247-020-04703-3
2. Caudill DR, Helmsworth JA, Daoud G, Kaplan S. Anomalous origin of left pulmonary artery from ascending aorta. The Journal of Thoracic and Cardiovascular Surgery. 1969 Apr 1;57(4):493-506.
3. Garg P, Talwar S, Kothari SS, Saxena A, Juneja R, Choudhary SK. The anomalous origin of the branch pulmonary artery from the ascending aorta. Interact Cardiovasc Thoracic Surg 2012;15(1):86–92
4. Urbina-Vazquez, America; Lopez-Rodríguez, María del Carmen; Ortega-Silva, Susana; Criales-Vera, Sergio; Alexanderson-Rosas, Erick; Cano-Zarate, Roberto; Meave-Gonzalez, Aloha; Espinola-Zavaleta, Nilda (2018). Multimodality imaging of the anomalous origin of the right pulmonary artery anomalous origin from the ascending aorta in an adult (hemitruncus arteriosus). Journal of Cardiovascular Computed Tomography, (), S1934592518301795–. doi:10.1016/j.jcct.2018.09.002

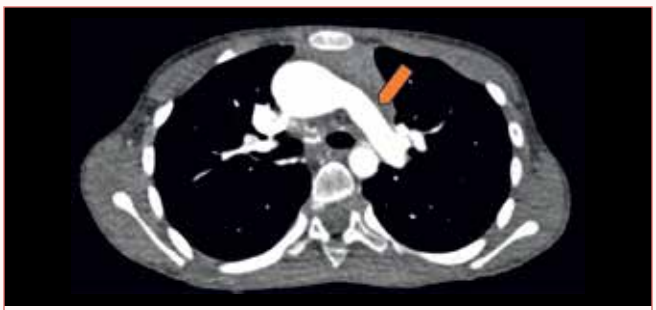

Figure 1: Origin of Left pulmonary artery from ascending aorta (Arrow)

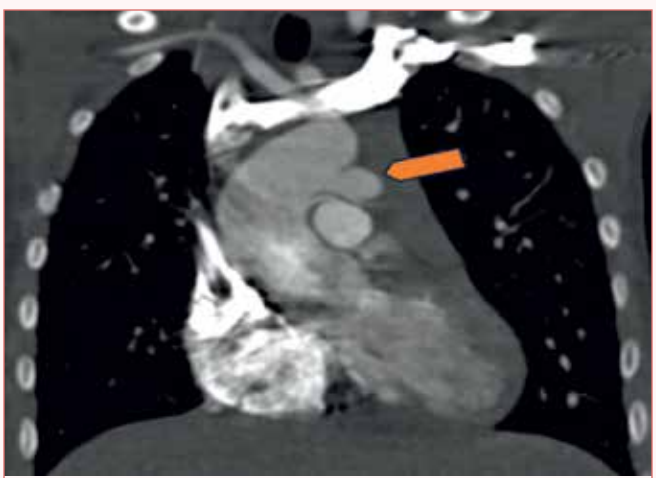

Figure 2: Origin of Left pulmonary artery from ascending aorta (Arrow)

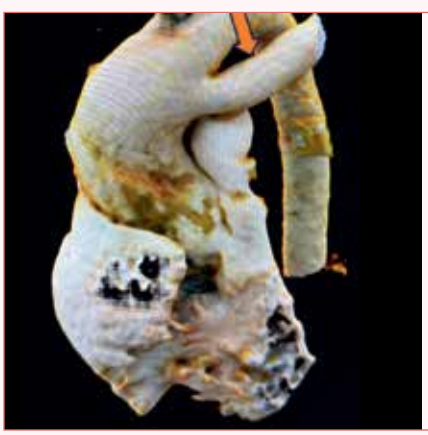

Figure 3:

Cinematic VRT showing origin of Left pulmonary artery from ascending aorta (Arrow)

Computed Tomography in the Evaluation of Fontan Circulation

Source: Kumar P, Bhatia M. Computed Tomography in the Evaluation of Fontan Circulation. J Cardiovasc Imaging. 2021 Apr;29(2):108-122. doi: 10.4250/jcvi.2020.0119. Epub 2020 Oct 27. PMID: 33605094; PMCID: PMC8099570.

Scan QR Code for more

Dr Mona Bhatia
Director and Head – Radiology,
Fortis Escorts Heart Institute, Okhla, New Delhi

Abstract

The Fontan procedure is a well-established surgical technique to improve survival in patients with univentricular heart disease. The procedure reroutes the systemic venous flow to the lungs, bypassing the right ventricle. The originally proposed method involved direct anastomosis of the right atrium to the pulmonary artery. Since then, several modifications have been made in the original technique leading to the modern Fontan, or total Cavo pulmonary connection. The modern Fontan technique has shown improved surgical outcomes and increased life expectancy in patients with univentricular disease. Due to the increased survival of these patients, long-term complications are becoming more prevalent. Common complications of Fontan procedure include right atrial dilatation and thrombosis; conduit stenosis and thrombosis; right-to-left and left-to-right shunts; hepatic congestion and cirrhosis; and lymph vascular. Computed tomography (CT) can reliably depict the normal Fontan anatomy and various postoperative complications. A fundamental understanding of the techniques of CT, including imaging protocols and common interpretive pitfalls, allows targeted imaging and precise reporting of clinically significant findings. Radiologists should be familiar with the multiple stages of single-ventricle palliation, normal Fontan anatomy, pathophysiology, and imaging features of common Fontan-related complications.

Keywords

Fontan circuit, Fontan circulation, Fontan operation, Fontan palliation, Computed tomography.

Agenesis of Right Common Carotid Artery Along with Very Low Intrathoracic Bifurcation of Left Common Carotid Artery- MRI and CT Demonstration

Dr Radha Krishan Verma
Additional Director - Radiology,
Fortis Memorial Research Institute, Gurugram

Dr R K Gupta
Principal Director and Head - Radiology,
Fortis Memorial Research Institute, Gurugram

Abstract

Variations of common carotid artery bifurcation are rare and include anomalies like absent common carotid artery with separate origins of internal and external carotid arteries from aortic arch, or low bifurcation of common carotid artery. Preoperative knowledge of these anatomical variations is important, since it may alter surgical manipulation and dissection techniques.

Introduction

Carotid arterial system shows a wide spectrum of variations which include aplasia, hypoplasia, anomalous origin, non-bifurcation and tortuous course [1]. Common carotid artery (CCA) usually bifurcates at the superior border of thyroid cartilage, corresponding to

the C3–4 junction, however bifurcation level usually varies around C2–C5 vertebrae [1]. Agenesis of common carotid artery with separate origins of left as well as right internal and external carotid arteries (ICA and ECA) from aortic arch is a rare anomaly [4]. Intrathoracic carotid bifurcation is also an extremely rare vascular anomaly and is found with and without Klippel–Feil syndrome [1, 10]. We present a case of combination of absent right common carotid artery with intrathoracic separate origins of right internal and external carotid arteries along with very low intrathoracic bifurcation of left common carotid artery demonstrated on MR angiography and CT angiography in a case with normal appearing cervical spine.

Case Report

A 78-year-old male presenting with complains of sudden onset right hemiparesis with gradual improvement of symptoms underwent emergent MRI brain with MRA of brain and neck vessels. On review of the imaging, patient did not have imaging evidence of acute stroke imaging. On neck MRA, he was found to have absent right common carotid artery with separate origins of right internal carotid artery and external carotid artery along with very low bifurcation of left common carotid artery within the intrathoracic region at D2 level. CT MRA confirmed the MRA neck findings (Fig 1).

Discussion

In radical neck surgeries and anterior cervical discectomy, CCAs are important landmarks for defining the dissection plane. Preoperative knowledge of anatomical variations like level of bifurcation is important, since it may alter surgical manipulation and dissection techniques [3, 6, 8]. High CCA bifurcation may render hypoglossal nerve more vulnerable and superior thyroid artery may arise from the CCA during neck surgeries[7]. Intrathoracic bifurcation of CCA can preclude carotid endarterectomy in cases with carotid stenosis. An alternative approach to re-establish distal ICA flow in such a case would be performing ICA to ECA transposition with ligation of the diseased proximal ICA[3].

Most bifurcation levels of common carotid arteries can be broadly categorized into high (between C2 and C3 or above C2), standard (at C4) and low (between C4 and C5 or below C5) with approximate rates of 31%, 58% and 11%, respectively [2].

Agenesis of right common carotid artery in itself is a rare congenital anomaly, which along with intrathoracic bifurcation of left common carotid artery forms an extremely rare combination anomaly. To the best of our knowledge, this combination has not been described in the English literature. We conclude that agenesis of right common carotid artery with concomitant very low intrathoracic bifurcation of left common carotid artery is an extremely rare combination congenital anomaly which has not been described in the literature and its prior knowledge may be useful in surgical and intravascular interventions.

References

1. Kandemirli SG (2020) Intrathoracic bifurcation of the left common carotid artery associated with rib fusion and Klippel-Feil syndrome. Surgical and Radiologic Anatomy 42:411-415
2. Hideshi I , Mataga I, Kageyama I, Kobayashi K (2006) Clinical anatomy in the neck region - the position of external and internal carotid arteries may be reversed. Okajimas Folia Anatomica Japan 82:157-167
3. Brown CR, Brown MR (2017) Treatment of a symptomatic intrathoracic internal carotid artery. J Vasc Surg Cases Innov Tech 3:171–174
4. Cakirer S, Karaarslan E, Kayabali M, Rozanes I (2002) Separate origins of the left internal and external carotid Arteries from the aortic arch: MR angiographic findings. Am J Neuroradiol 23:1600–1602
5. Elumalai G (2016) "Patent ductus caroticus" embryological basis and its clinical significance. Physiol Anat 98:42439–42442
6. Gulsen S, Caner H, Altinors N (2009) An anatomical variant: low-lying bifurcation of the common carotid artery, and its surgical implications in anterior cervical discectomy. J Korean Neurosurg Soc 45:32–34
7. Lo A, Oehley M, Bartlett A, Adams D, Blyth P, Al-Ali S (2006) Anatomical variations of the common carotid artery bifurcation. ANZ Journal of Surgery 76:970–972
8. Uzun L, Kokten N, Kilicaslan A, Tasel B, Kalcioglu MT, Tekin M (2013) Bilateral lower cervical bifurcation of the common carotid artery. Case Rep Otolaryngol 2013:894804:1–3 doi: 10.1155/2013/894804
9. Jerius JT, MD, Stevens SL, Freeman MB, Goldman MH, (1995) Vertebrobasilar syndrome associated with subclavian origin of the right internal carotid artery. J vascular surgery 21:855-861
10. Itabashi R, Yazawa Y, Shigehatake Y, Furui E.J (2018) A Case of Intrathoracic Carotid Bifurcation Without Klippel-Feil Syndrome. Stroke Cerebrovasc Dis 27(1):e15-e16.

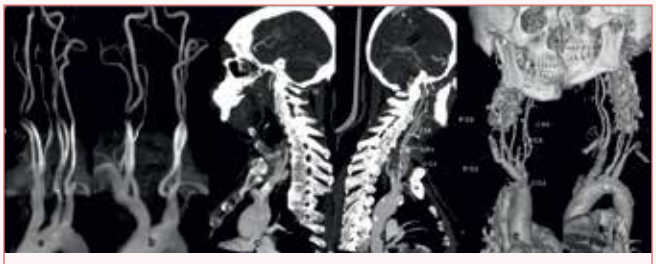

Figure 1 (a to f): Coronal sections of MRI of brain demonstrating maximum intensity projections of MRA of neck vessels demonstrating absent right CCA with separate origins of right ICA and ECA and very low bifurcation of left CCA (a, b). Maximum intensity projection CT images in curved MPR format showing separate origins of right ICA and ECA (c) and very low bifurcation of left CCA (d). Volume rendered CT images showing separate origins of right ICA and ECA and very low bifurcation of left CCA (e,f).

Solitary Fibrous Tumor of Internal Jugular Vein: An Extremely Rare Entity with Review of Literature

Source: Kumar K, Kumar P, Bhatia M, Garg A. Solitary Fibrous Tumor of Internal Jugular Vein: An Extremely Rare Entity with Review of Literature. Indian J Radiol Imaging. 2021 Apr;31(2):484-487. doi: 10.1055/s-0041-1734352. Epub 2021 Jul 27. PMID: 34556936; PMCID: PMC8448228.

Scan QR Code for more

Dr Mona Bhatia
Director and Head – Radiology,
Fortis Escorts Heart Institute, Okhla, New Delhi

Abstract

Solitary Fibrous Tumor (SFT) is an unusual spindle cell neoplasm that commonly arises from pleura. In the last decade, multiple case reports have described its diverse occurrence in extra pleural locations involving almost every anatomic site. Intravascular SFT is extremely rare and has been reported in inferior vena cava and renal vein only, to the best of our knowledge. SFT of the internal jugular vein has never been reported. We present a case of a SFT arising from internal jugular vein with extraluminal exophytic component extending into supraclavicular fossa. It should also be considered as a differential diagnosis for neoplasm arising from the internal jugular vein.

Keywords

Internal jugular vein; solitary fibrous Tumor; vascular.

Newer Imaging Techniques in CT and MRI in Cardiac Imaging

Dr Suman Singhal
Director - Cardiac Imaging,
Head - Radiology,
Mahajan Imaging,
Fortis Escorts Hospital,
Jaipur

Dr Rahul Singhal
Additional Director -
Cardiology and Cardiac
Electrophysiology,
Fortis Escorts Hospital,
Jaipur

Abstract

"The science of today is the technology of tomorrow" by Edward Teller is very apt quote in Cardiac imaging. In the past few decades Cardiac Imaging has undergone breath-taking advancements from single slice to multislice CT (MSCT) which started from 4-slice systems in 1998 to the latest 256-slice and 320-slice CT systems. CT Coronary angiography (CTCA) helps in detecting coronary calcium deposits, assessment of degree of coronary luminal stenosis, evaluation of stents, coronary bypass grafts and in prediction of disease outcomes. In addition to this, it has a potential to characterize atherosclerotic plaques,identify non-stenotic plaques (Fig-1), that may not be detected by invasive coronary angiography and in functional evaluation of coronary artery disease (CAD). Advances in radiation dose reduction techniques such as automatic tube current modulation, automatic tube current and voltage selection and several generations of reconstruction algorithms have ensured that high quality cardiac images can be obtained with minimal radiation.

Cardiovascular magnetic resonance (CMR) has undergone marked technical development and has become gold standard technique for evaluating myocardial function, quantifying myocardial volumes, and detecting myocardial scar. CMR has the unique ability to provide detailed tissue characterization, including assessment of edema, iron overload, and diffuse myocardial fibrosis. Parametric T1 mapping and T2 mapping (Fig-7) are routinely performed now a days along with T2*mapping for tissue characterization.

In this article we are discussing newer advancements in Cardiac CT - plaque imaging (Fig-2,3), functional evaluation of coronary artery disease-CT-FFR, 3D fusion imaging and 3D printing.

We are discussing role of artificial intelligence in Cardiac MRI along with a subset of evolving MRI techniques,

including 4D Flow MRI, advances in non-breath hold and non-ECG gated techniques, BOLD imaging and role of MR in molecular imaging. Non-invasive imaging techniques including CT, MRI and PET scanning can be used to differentiate stable from unstable atherosclerotic plaque, assess disease activity and thus can be used to improve risk stratification .

Artificial Intelligence In Cardiac MRI

New advances in Artificial Intelligence (AI) are working towards reducing scan time of Cardiac MRI from 90 minutes ischemia exam to just 15 minutes by automating more elements in image acquisition. The software helps in acquiring standard cardiac views in just 10 seconds by eliminating the need of breath hold and using artefact detection algorithm. Accelerated non-Cartesian 4 D flow is acquired in minutes providing more time for necessary calibrations prior to delayed contrast acquisition. The new advancements in this field are quantitative delayed enhancement for automated segmentation of myocardium, scar quantification and extent of enhancement on 17 segment heart model. It can help in assessing semi-quantitative perfusion including segmentation, identification and co-registration.

Figure1: CT features of plaque vulnerability. A. Curved reformatted image B. Volume rendered image and C. Axial sections showing low attenuation plaque (LAP) and positive remodeling (PR) in mid RCA. D. Curved reformatted image of LAD in another patient showing spotty calcification (<3mm)

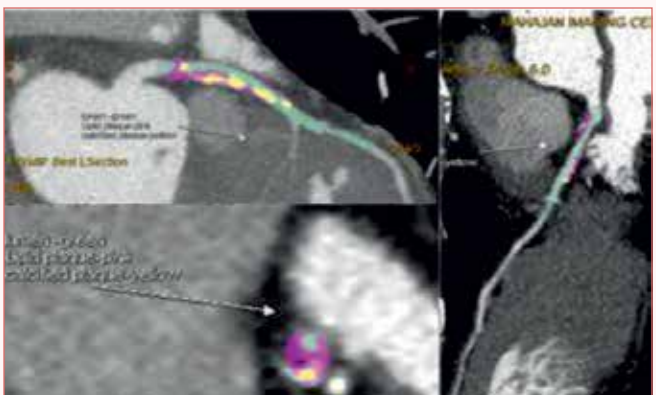

Figure 2: DECT (Gem stone spectral imaging technology) images with colour coding showing plaque composition. Lumen - green, Lipid plaque - pink and calcified plaque - yellow

Conclusion

Imaging will always be an integral part of clinical cardiovascular medicine. The past few decades have witnessed significant improvements in cardiovascular imaging, which is all to the benefit of better diagnosis, management, and early prevention of cardiovascular disease. With new realities in health care emphasizing quality and cost-effectiveness, future technologies in both CT and CMR will need to demonstrate value through greater efficiency and efficacy of care and/or patient outcomes.

Keywords

CT, CMR, Plaque, Advances, Artificial intelligence, Cardiac MRI

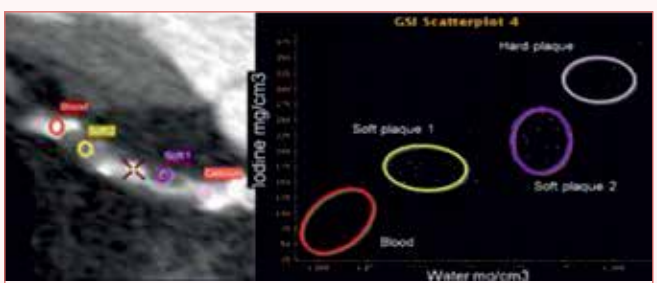

Figure 3: DECT (Gem stone spectral imaging technology) images showing plaque composition with GSI scatter plot.

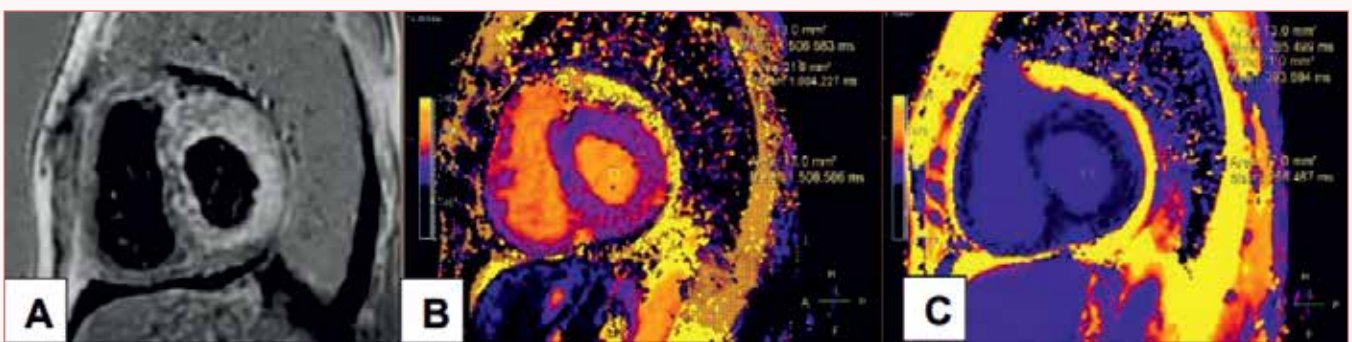

Figure 7: 57 years old female with LV hypertrophy, Bi-atrial enlargement and dilated IVC on echocardiography, mild bilateral pleural effusion and normal coronaries on CAG. Diffuse subendocardial enhancement in LV on LGE (A), Parametric mapping (B,C) with Native T1 of 1510-1950 ms, Post-contrast T1 of 285-340 ms and increased ECV fraction -45% led to diagnosis of Cardiac Amyloidosis.

Role of Computed Tomography in Postoperative Follow-up of Arterial Switch Operation

Source: Kumar P, Bhatia M. Role of Computed Tomography in Postoperative Follow-up of Arterial Switch Operation. J Cardiovasc Imaging. 2021 Jan;29(1):1-19. doi: 10.4250/jcvi.2020.0106. PMID: 33511796; PMCID: PMC7847786.

Scan QR Code for more

Dr Mona Bhatia
Director and Head – Radiology,
Fortis Escorts Heart Institute, Okhla, New Delhi

Abstract

An arterial switch operation (ASO) is the standard treatment for infants and children born with D-loop transposition of the great arteries. During the ASO, the great vessels are transacted from the native roots, switched and anastomosed with the opposite roots. This is accompanied by the relocation of the pulmonary artery anterior to the aorta by using the LeCompte manoeuvre and the translocation of coronary arteries to the neo-aorta. ASO has led to improved overall survival, and postoperative mortality is rare. Despite the improved outcomes, several postoperative sequelae may occur, and therefore patients require long-term follow-up. Computed tomography (CT) has emerged as a robust imaging modality in pre and postoperative evaluation of a variety of congenital heart disorders including ASO. Unlike echocardiography and cardiovascular magnetic resonance, CT is not hindered by a poor acoustic window, metallic devices or the need for sedation or general anaesthesia. CT with advanced three-dimensional postprocessing techniques, high pitch scanning, wider detector system, electrocardiogram-dependent modulation and dose-reduction strategies is invaluable in assessing the postoperative complications after ASO.

Keywords

Arterial switch procedure; Atrial switch operation; Atrial switch repair; Jatene procedure; Transposition of great vessels.

CT Coronary Angiography in 4 day Old Child with Complex Congenital Heart Disease

Dr Suman Singhal
Director - Cardiac Imaging, HOD
Mahajan Imaging, Department of Radiology,
Fortis Escorts Hospital, Jaipur

Dr Sunil Kaushal
Director and Head - Paediatric Cardiology
and Cardiac Surgery,
Fortis Escorts Hospital, Jaipur

Dr Sanjay Khatri
Additional Director - Paediatric Cardiology,
Fortis Escorts Hospital, Jaipur

Case Report

3-day old child came to emergency with respiratory distress during feeding and excessive crying. The child was referred to us from a peripheral hospital and was late preterm, low birth weight baby with complex congenital heart disease. On echocardiography there was situs solitus, Levocardia, concordant atrioventricular and ventriculo-arterial relations, dilated right atrium, right ventricle with severe pulmonary arterial hypertension. Fossa ovalis ASD measuring 5 x 6 mm was seen shunting bidirectionally. Dilated coronary sinus, normal and confluent pulmonary arteries with dilated left main coronary artery were seen. Aortic arch could not be profiled clearly and baby was sent for CT scan for further assessment of aorta and coronaries.

MDCT scan under 4D dynamic scanning (Virtual Helical shuttle) was performed with automated paediatric protocol using 5 mL of contrast, 79 mA a nd 80 kv.

CT scan images reveal Levocardia, situs solitus, concordant atrioventricular and ventriculoarterial connections. Cardiomegaly with dilated MPA, right atrium, right ventricle and ASD (Fig-2) were seen. Left sided aortic arch was seen with separate origin of left

vertebral artery from arch of aorta (Fig-2). Transverse arch of aorta measured 5.2 mm (z score -2.6) and distalarch measured 4.0 mm (Z score -2.2) suggestive of hypoplastic arch.

On evaluation of coronary arteries- RCA was ectatic, dilated left main trunk and left circumflex artery were seen with LCX communicating with dilated coronary sinus -suggesting coronary artery fistula with coronary sinus. LAD was normal in calibre. Dilated coronary sinus was draining into right atrium. PDA was dilated with significant narrowing distally. No significant aortopulmonary collaterals were seen, no pleural/ pericardial effusion, trachea- bronchi and spleen were normal.

Final diagnosis of Hypoplastic aortic arch, ASD, coronary fistula between LCX and coronary sinus, dilated PDA, dilated coronary sinus, pulmonary hypertension with dilated right atrium and right ventricle was made. Coronary arteriovenous fistulae are extremely rare and are classified by the site of drainage (i.e.-cardiac chamber, coronary sinus and its tributary veins, or great vessels. Rarely they drain into coronary sinus.

Family was explained about the high-risk surgery and child was taken up for coronary artery fistula ligation/repair plus PDA ligation.

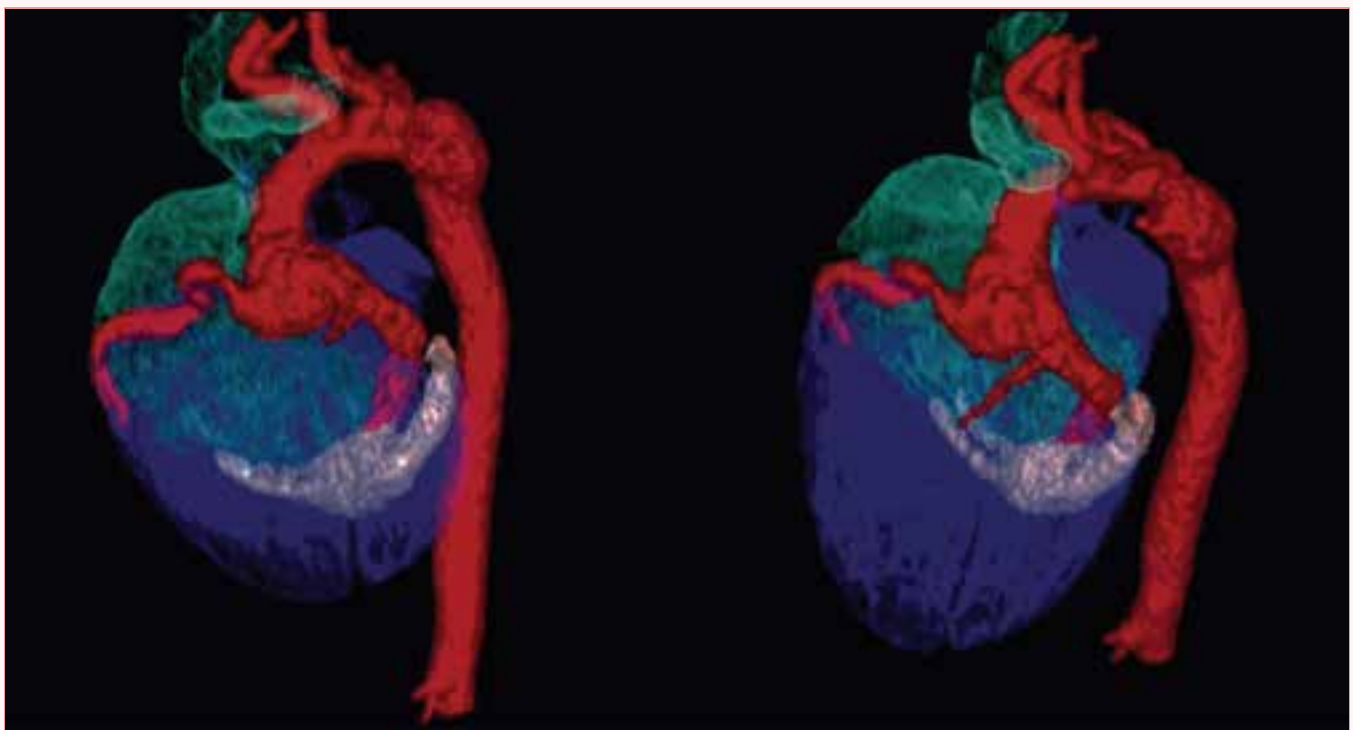

Figure1: Volume Rendered images in 4-day old child depicting hypoplastic aortic arch, ectatic RCA, dilated LMCA, normal LAD, dilated LCX with LCX – coronary sinus fistula.

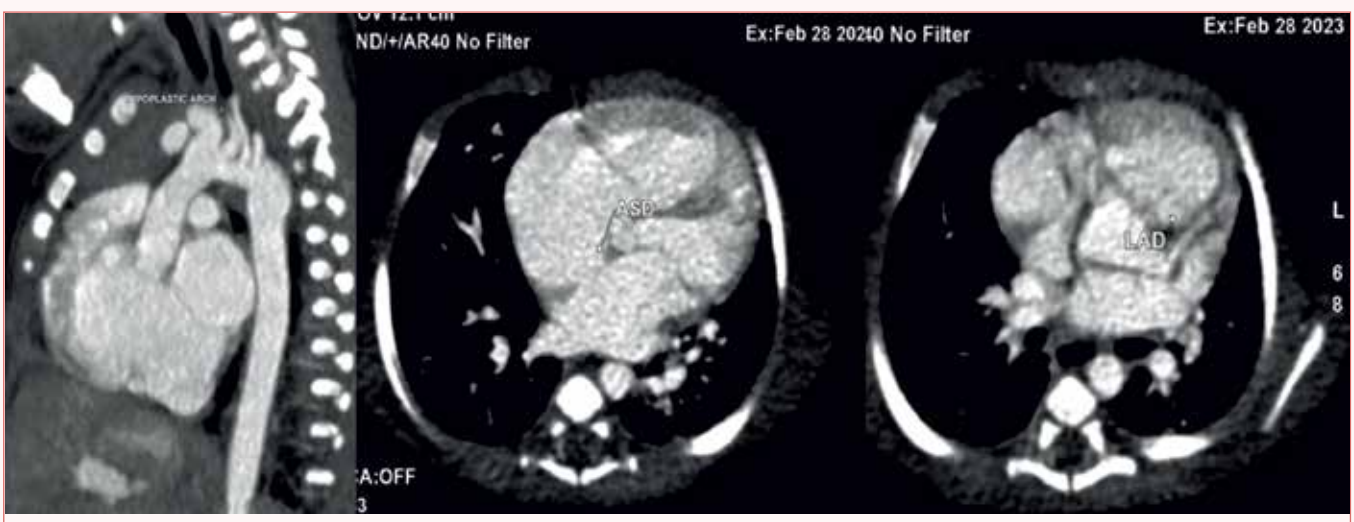

Figure 2: Axial and sagittal MIP images depicting cardiomegaly, ASD, hypoplastic aortic arch and **normal**

Gastrointestinal Radiology

Rare Case of Infected Omental Panniculitis Diagnosed with Imaging

Dr Lakshay Mehta
Consultant - Radiology,
Fortis Memorial Research Institute, Gurugram

Dr Raman Abhi
Director - Internal Medicine,
Fortis Memorial Research Institute, Gurugram

Dr R K Verma
Additional Director - Radiology,
Fortis Memorial Research Institute, Gurugram

Dr R K Gupta
Principal Director - Internal Medicine,
Fortis Memorial Research Institute, Gurugram

Abstract

45-year-old male with acute onset of pain abdomen, loose motion and fever with chills presented to the ER and was diagnosed to have bowel wall thickening on USG. MR enterography and CT Colonography demonstrated omental inflammation with abscess formation which was confirmed on USG guided FNAC. Patient was managed conservatively with antibiotics and anti-amoebic agents. Follow-up imaging done 20 days later confirmed complete resolution of disease without complications. The case highlights importance of intensive imaging in diagnosis and meticulous management of this rare entity.

Case Report

A 45-year-old male patient of Japanese origin presented to the Emergency with chief complaints of pain abdomen, loose motion and fever with chills since 3 days.

Patient was conscious, oriented with vital parameter within normal limits. Abdomen was soft, non-tender with normal bowel sounds. Rest of the systemic examination was within normal limits. USG abdomen was performed which revealed an ill-defined hypoechoic lesion along the wall of a large bowel loop in the supraumbilical region with internal vascularity (Figure 1A). Investigations are summarized in Table 1. Patient was admitted for evaluation.

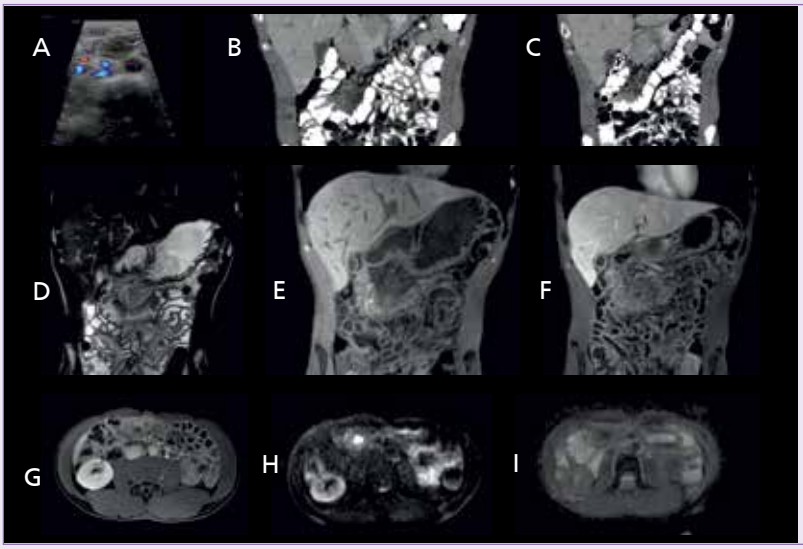

Figure 1: A. High resolution ultrasound image in the supraumbilical region shows an ill-defined hypoechoic lesion along the wall of a large bowel loop with internal vascularity.B. Coronal contrast enhanced CT image of the patient shows thickening of proximal transverse colon with an ill-defined enhancing omental lesion abutting transverse colon & stomach and ulcerations in the transverse colon (arrows in B) and adjacent extraluminal air foci(arrows in C). Coronal non-contrast BTFE image D shows ill-defined mass-like lesion in the transverse mesocolon with involvement of wall of transverse colon with hypointense signal on T1Wt image E. A peripherally enhancing area of flask-shaped micro-abscess is seen within (arrows in F & G) with diffusion restriction (H) and low ADC values in images (I)

Hemoglobin	14.5	13.0 - 17.0 g/dL
TLC	11.82	(4.0 - 10.0 thou/µL)
PLT	252	150 - 410 thou/µL
PCV	41.5	
Polymorphs/Lymphocytes	81/10	40-80 / 20-40 %
Absolute Neutrophil count	9.88	2-7 thou/µL
Liver function and renal function tests	Within normal limits	
Amylase 99	28 – 100 U/L	
CEA	1.5	Non- smokers < or = 3.8
CA 19-9	16.2	< 27 U/mL
Blood C/S	Sterile after 48 hrs	

Table 1

MR enterography and CT colonography (Figure 1 B-I) with rectal contrast was performed next day which displayed an ill-defined mass lesion (measuring approximately 6.8 x 3.0 cm) between the greater curvature of the stomach and transverse colon with internal area of diffusion restriction & low ADC values to suggest micro-abscess formation. The wall of transverse colon was involved and thickened. CT colonography demonstrated focal ulcerations and extra-luminal air foci within the lesion. In view of the findings, a diagnosis of infective panniculitis was suggested with possibility of amoebic etiology.

USG guided FNAC was performed from the lesion on Day 3, which showed mixed inflammatory cell infiltrates composed of neutrophils, histiocytes and lymphocytes. No definite organism was seen. The pus pocket could not be located on USG during the FNAC.

Patient was managed with intravenous antibiotics and anti-amoebic agents along with supportive therapy. Patient improved symptomatically and was discharged on Day 5 on oral antibiotics and anti-amoebic agents.

On follow-up, USG & MRI enterography were repeated which showed complete resolution of the disease process (Figure 2 A & B).

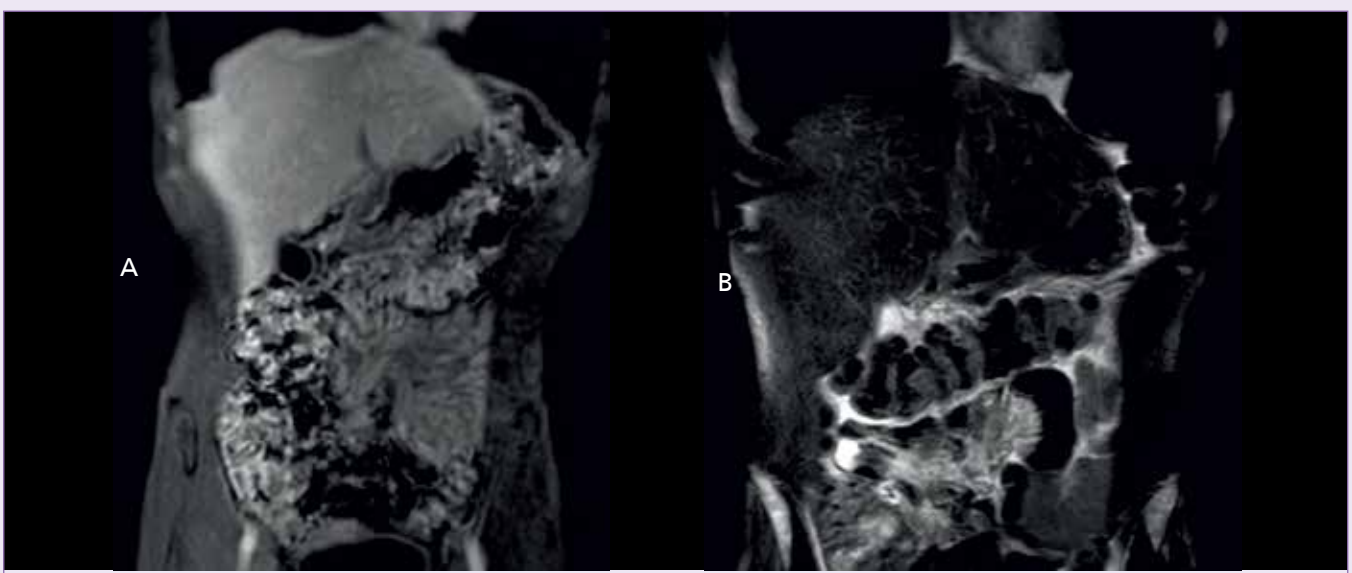

Figure 2: Coronal contrast enhanced mDIXON image A and coronal BTFE image of the patient B, approx 20 days after initiation of treatment shows complete resolution of previously noted mass-like lesion with normal wall thickness of the transverse colon.

Discussion

The case highlights the importance of detailed imaging in accurate diagnosis of acute abdominal infections. The mass effect and size of the lesion raised possibility of neoplasm, however the intralesional abscess formation evidenced by diffusion weighted imaging with low-ADC values and peripheral enhancement led to the diagnosis of infective / inflammatory pathology. CT Colonography was helpful in demonstrating the bowel wall involvement with ulcerations.

Infective etiologies involving the greater omentum are not uncommon and the spread is by either direct spread or hematogenous seeding. These infections can lead to focal abscess formation or to more diffuse involvement by such entities as peritoneal tuberculosis[1]. The role of the greater omentum in fighting infections also makes it more prone to be involved in these pathologies. The other possibility of omental infarction complicated by necrosis and superadded infection may also occur[2]. Idiopathic omental infarction is rare with only 5 such cases reported in literature[3-7].

References

1. Sompayrac SW, Mindelzun RE, Silverman PM, Sze R. The greater omentum. AJR Am J Roentgenol. 1997 Mar;168(3):683-7. doi: 10.2214/ajr.168.3.9057515. PMID: 9057515.
2. Balthazar EJ, Lefkowitz RA. Left-sided omental infarction with associated omental abscess: CT diagnosis. J Comput Assist Tomogr. 1993 May-Jun;17(3):379-81. doi: 10.1097/00004728-199305000-00007. PMID: 8491897.
3. Katz ME, Heiken JP, Glazer HS, Lee JK. Intraabdominal panniculitis: clinical, radiographic, and CT features. AJR Am J Roentgenol. 1985; 145:293–296.
4. Jeon EJ, Cho SM. Idiopathic isolated omental panniculitis confirmed by percutaneous CT-guided biopsy. Gut Liver. 2009; 3:321–324.
5. Rozin A, Bishara B, Ben-Izhak O, Fischer D, Carter A, Edoute Y. Fibrosing omental panniculitis and polyserositis associated with long-term treatment by paroxetine. Isr Med Assoc J. 2000; 2:714–716.
6. Hirono S, Sakaguchi S, Iwakura S, Masaki K, Tsuhada K, Yamaue H. Idiopathic isolated omental panniculitis. J Clin Gastroenterol. 2005; 39:79–80.
7. Lheureux P, Matos C, Charlier PH, Van Romphey A, Rickaert F, Van Gansbeke D, et al. Omental panniculitis: an unusual cause of acute appendiceal syndrome. Ann Emerg Med. 1987; 16:224–226.

Meckel Diverticulum with Ileoileal Intussception and Gangrene

Dr Aman Mamodia
Consultant - Radiologist, Fortis Hospital, Mahajan Imaging, Jaipur

Dr Lokesh Goyal
Consultant - GI and Minimal Access Surgeon, Fortis Escorts Hospital, Jaipur

Abstract

Meckel's Diverticulum is one of the uncommon congenital anomalies of the gastrointestinal tract. It may result in a number of complications including hemorrhage, intestinal obstruction, perforation secondary to diverticulitis and neoplasm.

Introduction

Meckel's diverticulum originates when the vitelline/ omphalomesenteric duct, which normally connects the primitive gut to the yolk sac, fails to obliterate around the seventh or eighth week of gestation. These are true diverticula containing all the layers of the small bowel wall, which are located on the antimesenteric border, and are found typically within 1 meter of the ileocecal valve.(1)

Obstruction of various types is the most common presenting symptom in the adult population. The correct diagnosis of complicated Meckel's diverticulum before surgery is challenging and imaging along with clinical correlation plays a major role. Delay in the diagnosis of a complicated Meckel's diverticulum can lead to significant morbidity and mortality.(2)

Here we describe a case report of patient with acute small bowel obstruction secondary to giant gangrenous Meckel's diverticulum along with ileoileal intussusception.

Case Report

A 53-year-old man was referred to gastro surgery department with a 24-hour history of pain abdomen, abdomen distension and obstipation. Pain was more localized in right iliac fossa. Laboratory examination demonstrated leucocytosis at 11,100/mcl and normal other blood parameters. A contrast-enhanced computed tomography (CT) scan was performed for further evaluation of pain abdomen.

On CT examination - There was a blind ended peripherally enhancing tubular structure seen in ileum along antimesenteric border measuring approx. 68 mm in length (Fig A, B) – likely Meckel's diverticulum. There was telescoping of this dilated tubular structure along with distal ileum (intussusceptum) into ileal loop (intussusceptions). Resultant proximal dilatation of proximal and mid ileal loops showing air fluid levels (Fig. A) were seen. The bowel loops revealed normal wall enhancement on CT scan. The cecum and appendix appeared to be normal. Subsequently, patient was taken up for surgery in view of non-resolving obstructive symptoms and clinical deterioration. Intraoperative findings confirmed ileo-ileal intussusception with dilated Meckel's diverticulum acting as lead point along with the ileal loop. Meckel's diverticulum was grossly dilated and revealed gangrenous changes. Adjacent ileum was also showing few pre-gangrenous patches, for which segmental resection of ileal loops was done with primary anastomosis. Patient stood the procedure well and was discharged uneventfully.

Discussion

The three most common complications of Meckel's diverticulum are bleeding, obstruction, and inflammation. Gastric heterotopias can be found in roughly 50% of cases and pancreatic, duodenal, colonic or biliary mucosa have rarely been reported. Haemorrhage is much less common in adults and is usually the result of heterotopic gastric or pancreatic mucosa causing ulceration.

Obstruction of various types is the most common presenting symptom in the adult population. The most common obstruction was intussusception or invagination, with the Meckel's diverticulum being the lead point as in our case study. Other causes of obstructions include volvulus around fibrous bands adherent to the umbilicus and inflammatory adhesions. Uncommon causes of obstruction include enteroliths being expulsed from the diverticulum forming a distal obstruction and loop formations with the end of an Meckel's diverticulum and adjacent mesentery constricting the distal ileum.(3) Axial torsion of an Meckel's diverticulum is a rare complication. (4)

References

1. Stone PA HMCJ et al. Meckel diverticulum: ten-year experience in adults. . South Med J. 2004;97:1038–41.
2. Akbulut S. YY. Giant Meckel's diverticulum: an exceptional cause of intestinal obstruction. . World J Gastroenterol. 2014;6:47–50.
3. Yahchouchy EK MAEJ et al. Meckel's diverticulum. . J Am Coll Surg. 2001;192:658–62.
4. Yamaguchi M TSAS. Meckel diverticulum. Investigation of 600 patients in the Japanese literature. Am J Surg . 1978;136:247–9.

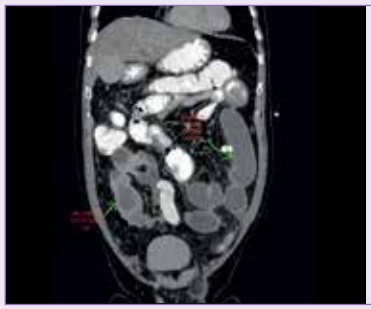

Figure A : CORONAL CT image showing dilated small bowel loops, large Meckel's Diverticulum telescoping into ileal loops.

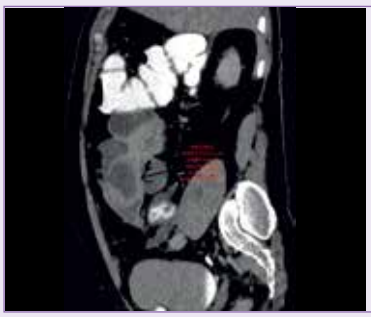

Figure B : SAGITTAL CT image showing Meckel's Diverticulum with wall thickening and intussusception.

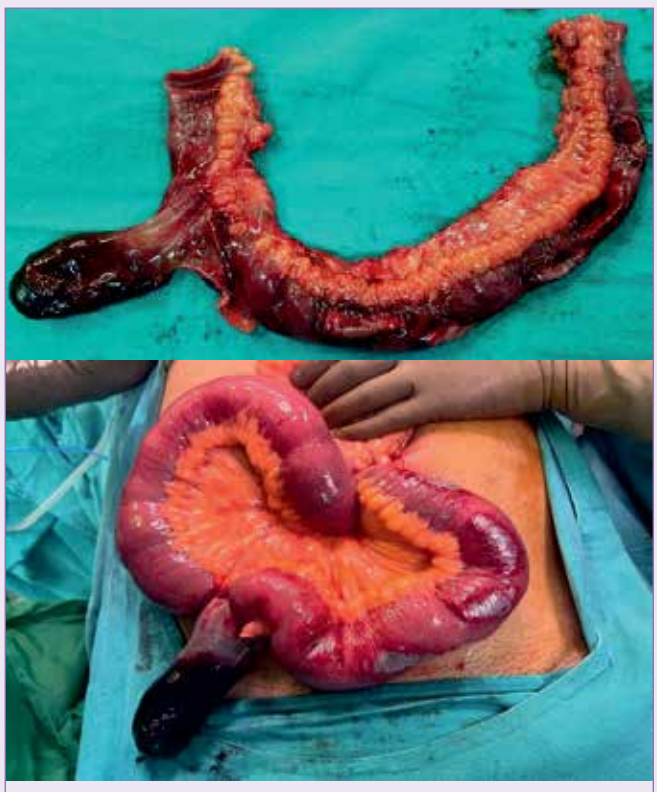

Figure 3,4. Surgical resected specimen depicting large Meckel's Diverticulum with gangrenous changes. Ileal segment with few pre- gangrenous patches.

Giant Myelolipoma of Adrenal Gland : Case Report

Dr Apra Kalra
Additional Director - Lab Medicine,
Fortis Hospital, Mohali

Dr Abhishek Prasad
Director and Head - Radiology,
Fortis Hospital, Mohali

Dr Ritu Pankaj
Additional Director - Lab Medicine,
Fortis Hospital, Mohali

Dr Jitender Rohila
Consultant Surgical Oncology GI Oncology,
Robotic and HIPEC,
Fortis Hospital, Mohali

Dr Shafira Garg
Assistant Consultant - Lab Medicine,
Fortis Hospital, Mohali

Introduction

Adrenal myelolipoma is a rare benign, nonfunctional lesion that is composed of macroscopic fat and mature hematopoietic tissue, resembling bone marrow. It is the second most common benign tumor in the adrenals following adrenocortical adenoma. It is usually an incidental finding on imaging (CT / MRI) or on autopsy.

Case Report

A 19 years old female presented in surgical OPD with dull aching pain in upper abdomen since one month. After clinical evaluation, CECT abdomen was planned which showed large mass in retroperitoneum measuring16x14x13cm. Possibility of retroperitoneal liposarcoma was suggested. PET CT was also done which showed similar findings and a likely possibility of low grade liposarcoma with no distant metastasis was suggested. After tumor board discussion and with a clinical impression of retroperitoneal liposarcoma, patient was planned for surgery. Exploratory laparotomy with enbloc removal of retroperitoneal mass with part of Gerota's fascia and renal capsule of left kidney with left adrenalectomy was performed Post-operative recovery was uneventful and she was discharged on post-operative day 4.

Radiological Findings

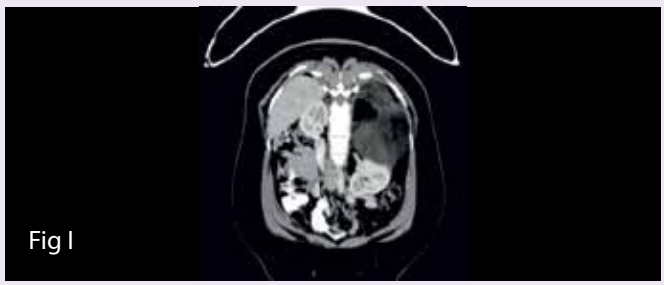

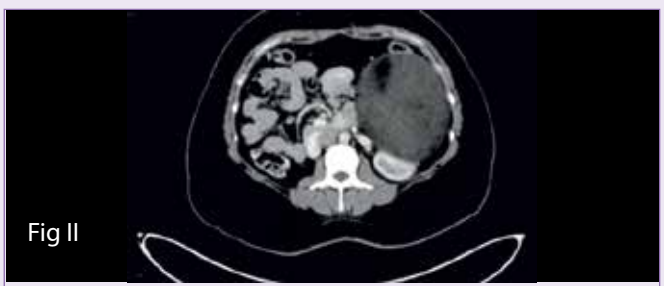

Figure i & ii: Contrast enhanced CT images show a large fairly well-circumscribed inhomogeneous soft tissue mass lesion with large fatty component in the suprarenal region inferiorly displacing the left kidney and superiorly displacing the pancreas.

Histopathological Findings

The specimen consisted of single globular soft tissue mass measuring 15x12x10 cm weighing 1.5Kg. Externally it was well encapsulated with smooth surface. Cut section was fatty with focal greyish tan areas.

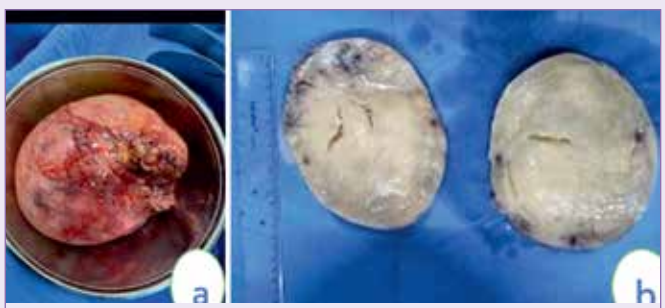

Figure1 (a) Surgical specimen -Fresh tissue showing large encapsulated tumor, After fixation (b) cut section is fatty with focal firm areas.

Light microscopy of haematoxylin and eosin (H&E) stained sections show circumscribed lesion composed predominantly of lobules of mature adipose tissue along with intermixed extramedullary trileange mature hemopoietic elements. Prominent megakaryocytes were noted. No lipoclastic features were seen.

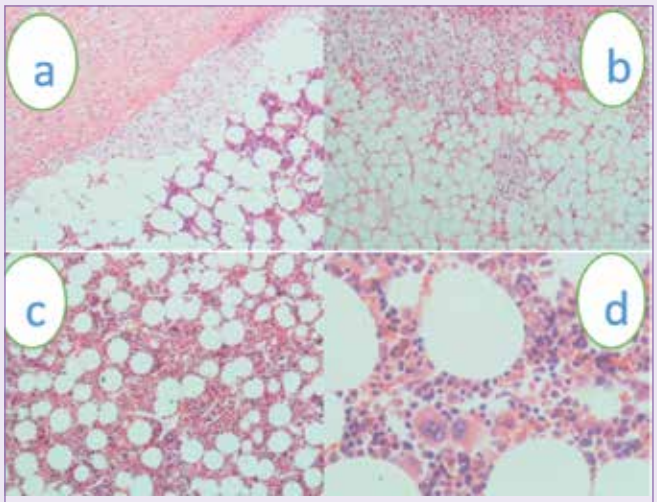

Figure 2 Microphotographs of H and E stained sections showing admixture of mature lipomatous and hemopoietic components (b and c). Compressed adrenal gland is identified at periphery of lesion in (a) while hematopoietic elements including megakaryocytes are seen in (d)

Discussion

Adrenal myelolipoma is a rare benign tumour with a prevalence of 0.08–0.2% that consists of mature adipose and hematopoietic tissue. Most of these present as adrenal incidentalomas and comprise 3·3–6·5% of all adrenal masses. Adrenal myelolipomas are usually unilateral (in 95% of cases), variable in size, most often found during midlife, and affect both sexes almost equally. Myelolipoma may rarely present with abdominal discomfort and pain due to necrosis, rupture, haemorrhage, or even haemorrhagic shock. The mean size at the time of diagnosis is ˜4 cm, while myelolipomas more than 10 cm in greatest diameter are defined as 'giant'.

This case had an unusual presentation as this patient was a young (19-year-old) female and the dimensions of the mass were quite large (approx. 15cm). The CECT and PET CT images raised concerns for malignancy suspecting a retroperitoneal soft tissue malignancy (? Liposarcoma). While the lesion is benign, surgery as a modality of treatment is used only symptomatic tumor or tumors larger than 6cm to reduce the risk of abdominal pain, rupture or haemorrhage. In this case, en-bloc removal of the mass with adrenalectomy was the best choice for alleviation of symptoms and to rule out any suspicion of malignancy.

Conclusion

Adrenal myelolipomas are uncommon benign tumors, most often asymptomatic with some presenting as large mass or pain. Rising use of CT and MRI has increased the rate of detection. Treatment varies depending on the size and symptoms. Smaller, asymptomatic myelolipomas can be observed expectantly. The indications for surgery are symptomatic patients and lesions bigger than 6 cm. Complete enbloc surgical removal should be ensured for good long-term outcome.

References

1. Lam AK. Lipomatous tumours in adrenal gland: WHO updates and clinical implications. Endocr Relat Cancer 2017;24:65–79.
2. Calissendorff J, Juhlin CC, Sundin A, Bancos I, Falhammar H. Adrenal myelolipomas. Lancet Diabetes Endocrinol 2021;9:767– 769
3. Iraklis E Katsoulis and others, A large adrenal myelolipoma: case report and review of the literature, Journal of Surgical Case Reports, Volume 2023, Issue 6, June 2023,
4. Ebbehoj A, Li D, Kaur RJ, et al. Epidemiology of adrenal tumours in Olmsted County, Minnesota, USA: a population-based cohort study. Lancet Diabetes Endocrinol 2020; 8(11): 894–902.

HBV Related Polyarteritis Nodosa Causing Sigmoid Colon Perforation

Dr Ashwini Joshi
Consultant - Radiology,
Fortis Hospital, Mulund, Mumbai

Dr Vishnu Sankar T S
DNB - Radiodiagnosis,
Fortis Hospital, Mulund, Mumbai

Abstract

Polyarteritis nodosa (PAN) is a rare multisystem vasculopathy which predominantly affects medium-sized muscular arteries. Kidneys are the most commonly involved internal organs (80–100%), followed by heart (~70%), gastrointestinal tract (50–70%), liver, spleen and pancreas.[2] Involvement of only the mesenteric vasculature, majorly inferior mesenteric artery (IMA) and causing subsequent large bowel perforation is a very uncommon manifestation of PAN.

We describe a 66-year-old male, known case of Hepatitis B virus (HBV) associated chronic liver disease (CLD) with portal hypertension (PHTN), who presented with intractable diarrhoea and generalized weakness, which progressed into severe abdominal pain. CT abdominal angiography performed showed multiple aneurysms coexisting with stenotic lesions, predominantly in the IMA and superior mesenteric artery (SMA) branches without involving renal vasculature, with mural stratification and overall poor enhancement of the colonic wall. A diagnosis of HBV associated PAN causing ischemic colitis of sigmoid colon and rectum was made on the basis of clinical presentation, laboratory workup and imaging findings. The case got complicated due to superimposed Clostridium difficile infection causing pseudomembranous colitis leading to delay in immunosuppressive treatment for PAN. Subsequently, sigmoid colon perforation was found for which exploratory laparotomy and sigmoid colectomy was done. Later the patient was started on steroids and had a favourable outcome.

Our case highlights the clinical importance of remaining cognizant to PAN as a differential for patients presenting with unexplained abdominal pain with imaging features suggestive of colitis and multiple mesenteric vasculature aneurysms, even in the absence of renal involvement, as delay in a timely diagnosis can lead to threatening consequences.

Keywords

Polyarteritis nodosa; vasculitis; HBV; inferior mesenteric artery; ischemic colitis; colonic perforation; sigmoid.

Case Description

A 66-year-old man, known case of HBV related CLD with PHT presented with loose stools, abdominal pain and fatigue since a week. CECT abdomen showed **(Image 1)** diffuse circumferential wall thickening involving sigmoid colon and rectum. Mural stratification with submucosal edema and overall poor enhancement of the colonic wall was seen associated with mild luminal narrowing. Peri colonic fat stranding and thickening of meso rectal fascia and adjacent peritoneum was also seen.

Hypertrophy of IMA and its branches supplying the sigmoid and rectum was seen showing beaded appearance and few aneurysmal dilatation (Image 2). There was poor opacification of the distal most part of the vasa recta supplying the colonic wall (Image 3). Few of the hypertrophied vasa recta showed transmural course predominantly in the region of proximal sigmoid colon.

The branches of SMA including the inferior pancreaticoduodenal and ileocolic branches also showed beaded appearance with aneurysmal dilatations (Image 2). Both renal arteries were found to be normal in calibre and contrast opacification.

Imaging findings overall was in favour of HBV associated PAN with resultant ischemic colitis involving the sigmoid colon and rectum.

Subsequently he was tested positive for Clostridium difficile infection. His ANCA workup came out negative. Sigmoidoscopy showed multiple ulcers and erythema with pseudo membrane in rectum and sigmoid colon.

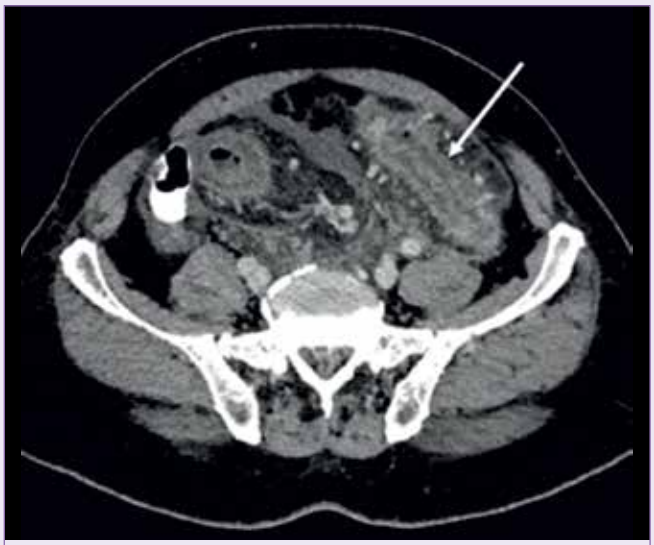

Image 1. Long white arrow showing diffuse circumferential wall thickening involving the sigmoid colon with submucosal edema and mural stratification.

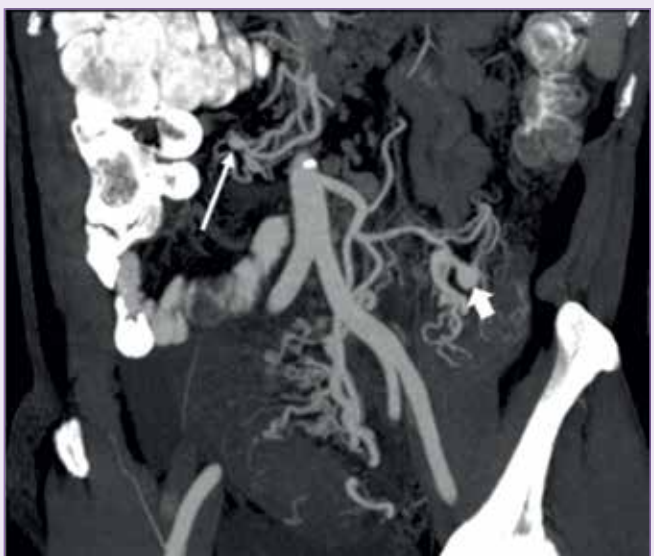

Image 2. Short white arrow showing aneurysmal dilatation of SMA branches and white arrowhead showing aneurysmal dilatation of IMA branches.

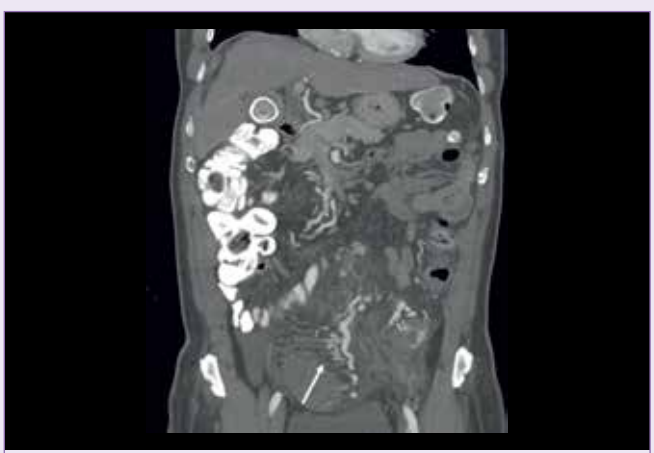

Image 3. White arrow showing poor opacification of the distal most part of the vasa recta supplying the colonic wall.

Three weeks later, he developed severe abdominal pain and distension. An emergency contrast CT scan was done to rule out intestinal obstruction. Imaging findings were suggestive of ischemic colitis with perforation of the proximal sigmoid colon. It showed evidence of pneumoperitoneum in the form of focal collection of air locules adjacent to the proximal sigmoid colon and the dependent portion of the ascitic fluid [Images 4(a) and 4(b)]. Diffuse circumferential thickening of sigmoid colon and rectum with mural stratification and focal non-enhancing segment in the proximal sigmoid were persistent.

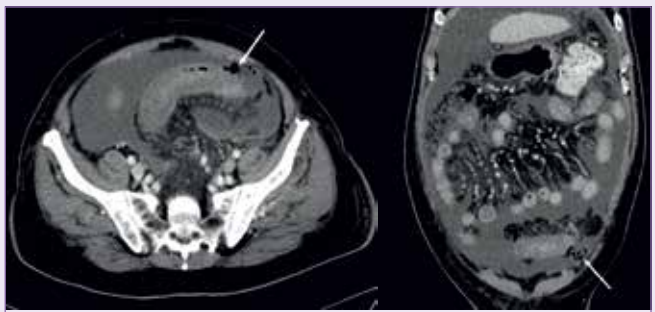

Image 4(a) and (b). CECT coronal and axial images showing focal collection of air locules adjacent to the proximal sigmoid colon (white arrow) suggesting pneumoperitoneum secondary to perforation.

He was taken for emergency exploratory laparotomy. On table (Image 5), sigmoid perforation was identified with evidence of faecal peritonitis. Sigmoid colon was noted to have thickened mucosa with surrounding fat stranding and thickened oedematous mesentery. Sigmoid colectomy was performed with end to end anastomosis and diversion loop ileostomy done. Around 3 litres of ascitic fluid was aspirated. Patient was maintained on steroids and was shifted to ward.

Image 5. Intra-operative on table examination showing ischemic and gangrenous changes of sigmoid colon.

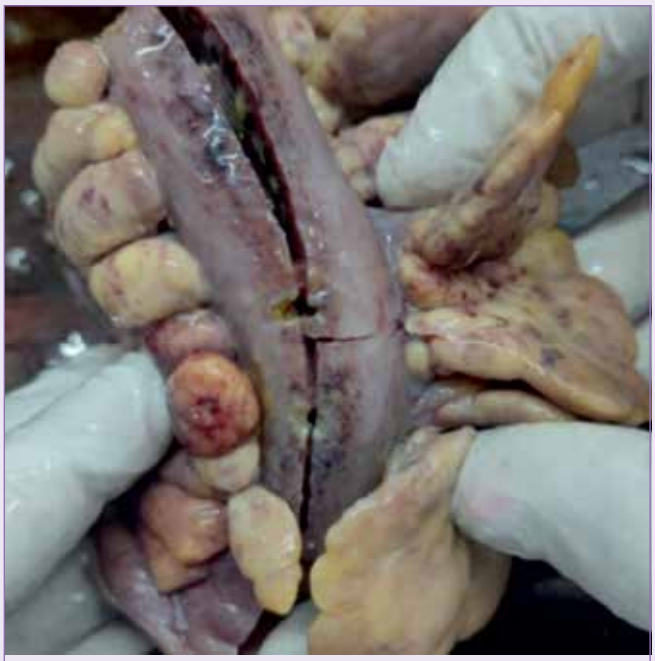

Image 6. Resected gangrenous segment of sigmoid colon.

Histopathological examination (HPE) findings

Image 7. Gangrenous changes in mucosa, submucosa and inner muscle layer with congested and neovascularised blood vessels

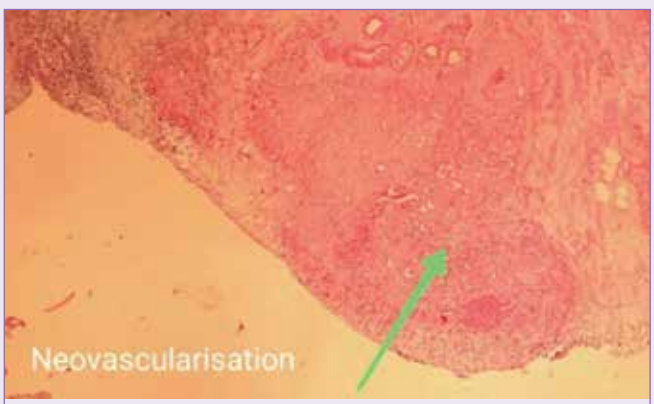

Image 8. Gangrenous changes in mucosa, submucosa and inner muscle layer with congested and neovascularised blood vessels

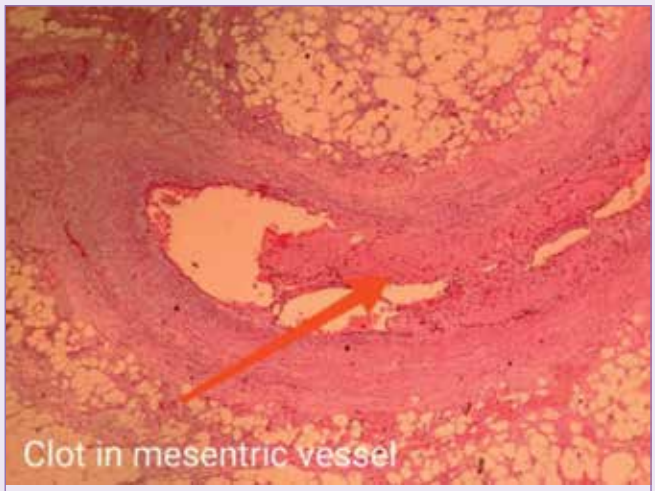

Image 9. Gangrenous perforation was seen secondary to chronic ischemia due to underlying thrombosis of mesenteric vessels.

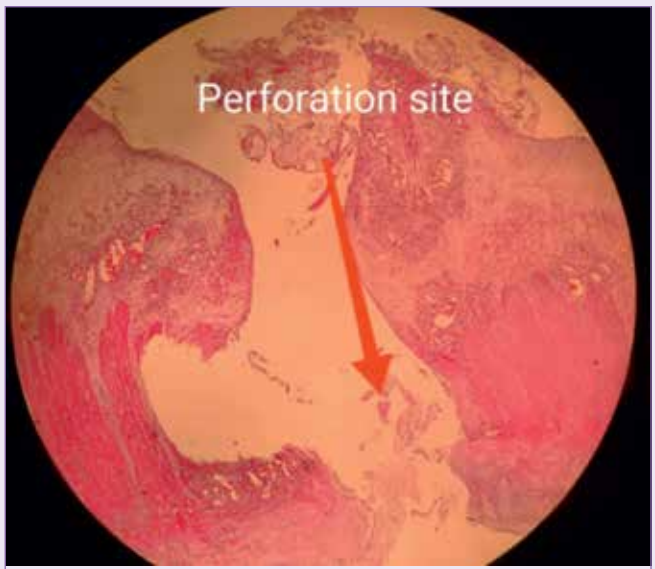

Image 10. Mesenteric veins with Perforation at two places with serositis. Cut margins showing early gangrenous change

Discussion

PAN is a rare systemic necrotizing vasculitis involving medium-sized muscular arteries. Historically, PAN is commonly associated with prior HBV infection.[3] PAN, although frequently has gastrointestinal manifestation (40-60%)[4], large bowel involvement in PAN is rare, with colonic perforation even rarer. Large retrospective studies done on PAN have revealed only a few cases of isolated colonic perforation.[4,5] Large bowel involvement in PAN ranges from colitis, colonic ulcer, ischemia and perforation.[4,6,7] Kronzer et al. has described 20 cases of GI perforation with vasculitis from 1998 to 2017 at the Mayo Clinic, but only one patient with PAN had isolated sigmoid perforation[6]. Pragnoux et al. has described 12 cases of PAN with acute surgical abdomen in France from 1981 to 2002, of which 2 had colonic involvement, but none had colonic perforation[4].

Diagnosis of PAN theoretically requires histological proof showing segmental fibrinoid necrosis of medium sized vessels. However, the diagnosis can be reached based on a combination of clinical, immunologic, and radiological findings.[8] Antineutrophil cytoplasmic antibodies negativity and angiographic features are useful for diagnosis.[8]

Angiography of the viscera (especially renal, abdominal, or coronary arteries) can be performed when PAN is suspected and biopsy cannot be achieved.[11] Typical lesions show multiple aneurysms (1–5 mm in diameter), usually coexisting with stenotic lesions, predominantly in kidney, mesenteric, and hepatic artery branches. [11][9] Less invasive arteriography techniques, such as CT and MRI can also be used. If histopathology cannot be obtained, diagnosis of PAN can be established in presence of typical imaging abnormalities.[10] Angiographic findings, including microaneurysms (1 to 5mm diameter), ectasia or occlusive disease in celio mesenteric and renal arteries are present in ≈40%-90% of patients at the time of symptom onset.[8] These techniques can establish the extent of disease in PAN and can be used for prognosis and treatment response.

Our patient's abdominal CT angiography showed multiple aneurysms, leading us to work up vasculitis as an etiology for his colitis. In view of background comorbidity of HBV related CLD and multiple mesenteric aneurysms with co-existing stenotic lesions on angiographic imaging, PAN was placed high among the differential diagnosis.

Conclusion

This case highlights the clinical difficulty of diagnosing PAN, with minimal assistance from laboratory and endoscopy results. Due to the threatening consequences of untreated PAN, all radiologists must remain cognizant to PAN on a differential for unexplained abdominal pain with imaging features suggestive of colitis and multiple mesenteric vasculature aneurysms, even in the absence of involvement of renal vasculature.

References

1. Polyarteritis nodosa: a case report of isolated large bowel involvement and surgical intervention;Georgina E Sellyneyal, Journal of Surgical Case Reports, Volume 2023, Issue 4, April 2023.
2. Radiologic Findings of Abdominal Polyarteritis Nodosa; KeumJee et al, American Journal of Radiology:174, June 2000
3. Colonic Perforation in Polyarteritis Nodosa With Concurrent Perforated Sigmoid Diverticulitis; Leung C, Zahid A (January 23, 2022) Cureus 14(1)
4. Presentation and outcome of gastrointestinal involvement in systemic necrotizing vasculitides: analysis of 62 patients with polyarteritis nodosa, microscopic polyangiitis, Wegener granulomatosis, Churg-Strauss syndrome, or rheumatoid arthritis-associated vasculitis. Pagnoux C et al. Medicine (Baltimore) 2005;84:115–128.
5. Gastrointestinal involvement in polyarteritis nodosa (1986-2000): presentation and outcomes in 24 patients. Levine SM et al, Am J Med. 2002;112:386–391
6. Occurrence and aetiology of gastrointestinal perforation in patients with vasculitis. Kronzer VL et al, Clin Exp Rheumatol. 2019;37:32–39.
7. Polyarteritis nodosa of the descending colon. case report. Gullichsen Rey al.Eur J Surg= Acta chirurgica. 1991;157:421–422.
8. Medium- and Large-Vessel Vasculitis; David Saadounand et al, Circulation. 2021;143:267–282
9. Diagnosis and classification of polyarteritis nodosa; Jose Hernandez-Rodriquez and et al, Journal of Autoimmunity, Vol 48-49, Feb-Mar 2014
10. Development and validation of a consensus methodology for the classification of the ANCA-associated vasculitides and PAN for epidemiological studies. ANN Rheum Dis 2007;66(2):222-7. Watts R and et al.
11. Polyarteritis nodosa; Lindsy Forbess et al, Rheum Dis Clin N Am 41 (2015).

Gallstone Ileus- Lessons from Missed Diagnosis

Source : DOI: 10.1055/s-0042-1754327

Scan QR Code for more

Dr Rajat Bhargav
Director and Head - Radiology
Fortis Hospital, Mulund

Abstract

Gall stone ileus is an uncommon presentation among acute surgical patients. Its diagnosis and treatment is often delayed due to its non-specific clinical presentation. Presence of gall stone in ileum can be difficult to detect on CT as they are mostly lucent. We report the case of a 66-year-old man with one day history of vomiting and bloating. Initial CT could not identify the obstructing gall stone. On the follow-up CT, there was a distal shift of obstruction site in the intestine raising suspicion of a gall stone. We discuss the imaging findings on CT and the clues to diagnose gall stone ileus.

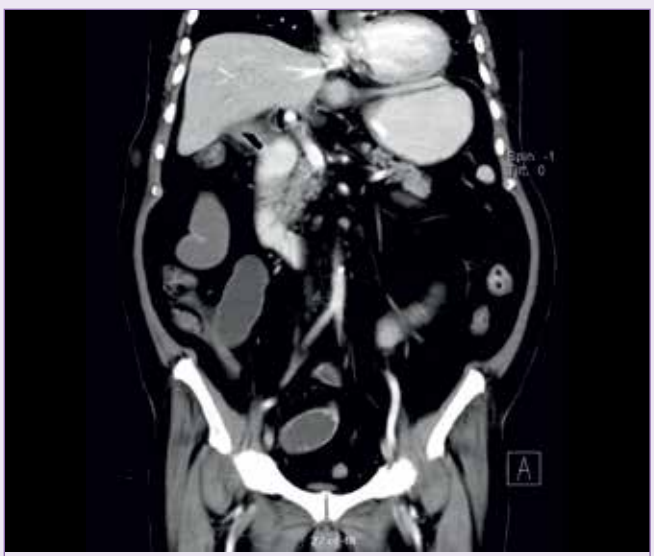

Figure 1: Coronal section of contrast enhanced follow-up CT scan shows increased air pocket in the gallbladder lumen (thin blue arrow) which was missed in the first CT. It also shows the obstructed gallstone in the pelvic region which is radiolucent with a few calcific specks in periphery (thick blue arrow). Note that its contour is conforming with the lumen of the ileal wall.

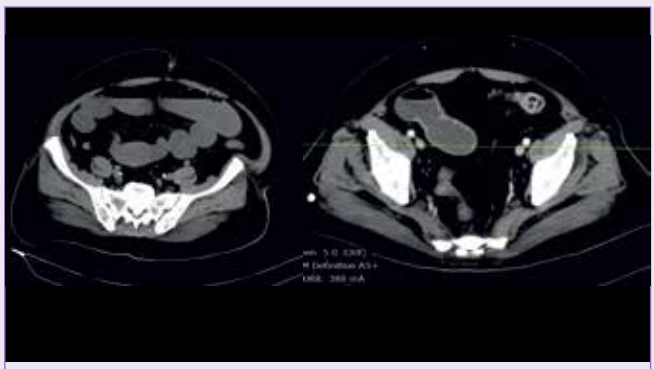

Figure 2: A)Initial CT and B) Followup CT show intestinal obstruction, gall stone with calcific specks and migration of gall stone from proximal to distal ileum in the follow-up CT after 4 days

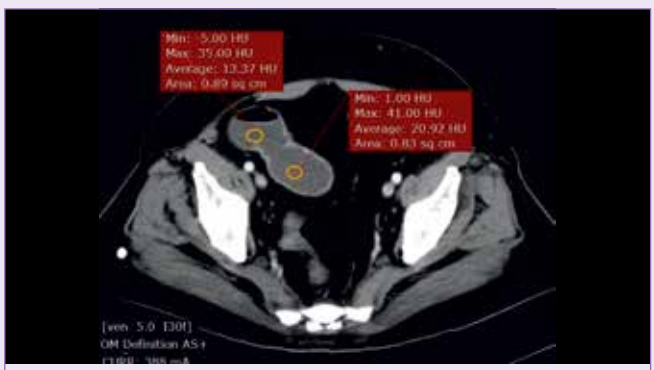

Figure 3: Axial section of follow-up enhanced CT which shows that the density of the gallstone (straight blue arrow) and the adjacent fluid (curved blue arrow) within the bowel lumen is almost similar thus making it difficult to identify

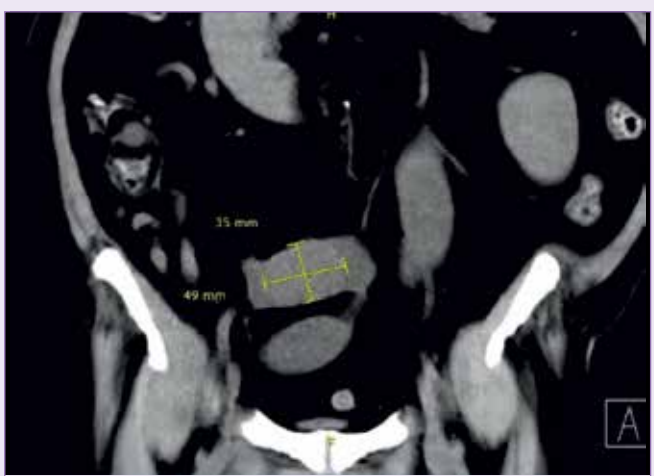

Figure 4: Coronal section of unenhanced CT. The gallstone is better visualised after the narrowing the window settings and its size can be measured.

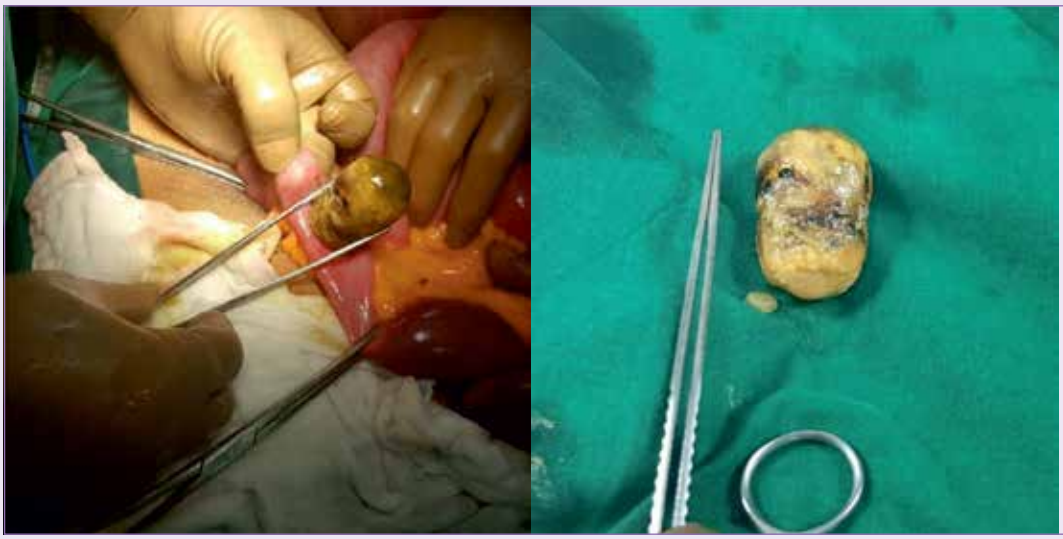

Figure 5:
Intra-operative image of removal of obstructed gallstone from the ileum.

Gallstone Coleus

Dr Puneet Jain
Director and HOD - Radiology,
Fortis Hospital, Shalimar Bagh, New Delhi

Dr Vibha Mital
Senior Consultant - Radiology,
Fortis Hospital, Shalimar Bagh, New Delhi

Dr Alisha Jagga
Junior Consultant - Radiology,
Fortis Hospital, Shalimar Bagh, New Delhi

Dr Rounak Bagga
Attending Consultant - Radiology,
Fortis Hospital, Shalimar Bagh, New Delhi

Dr Anushka Jain
DNB Resident - Radiology,
Fortis Hospital, Shalimar Bagh, New Delhi

Dr Shweta Prasad
DNB Resident - Radiology,
Fortis Hospital, Shalimar Bagh, New Delhi

Gall stone lieus is rare, gall stone coleus is even rarer!

Introduction

A rare cause of intestinal obstruction, gall stone coleus is one of the subsets of gallstone ileus which itself is an uncommon sequela of cholelithiasis. This pathology occurs as a result of a bilioenteric fistula formation due to erosion by the migrated gall bladder stone. It has a high rate of morbidity and mortality often due to delayed or misdiagnosed intestinal obstruction and increased incidence in the elderly. Diagnosis can be made by CT imaging which is then followed by surgical intervention for relieving the obstruction, with or without the fistula excision.

Case presentation

An 87 years old woman came to the emergency department with a history of abdominal pain, vomiting, and constipation for the last 2 days. On physical examination abdomen was soft, non-tender and bowel sounds could be auscultated. The supine abdominal plain film showed dilated bowel loops, however due to patient condition, an erect film could not be taken. Lab investigations revealed increased leucocytosis, increased neutrophil count and mildly raised bilirubin. LFTs and KFTs: unremarkable.

On computed tomography scan, a large rounded calcific shadow measuring 30 x 23 mm with lamellated appearance was seen lodged in the sigmoid colon-raising the possibility of ectopic gallstone / faecolith. On post rectal contrast imaging, a segment of narrowing was noted in the sigmoid colon just distal to the impacted calculus. Multiple diverticulae were seen in the sigmoid colon. Air focus was noted in the gall bladder lumen as a result of fistula formation, with no definite intraluminal calculus. These findings, along with the presence of intestinal obstruction, are consistent with the diagnosis of gall stone coleus.

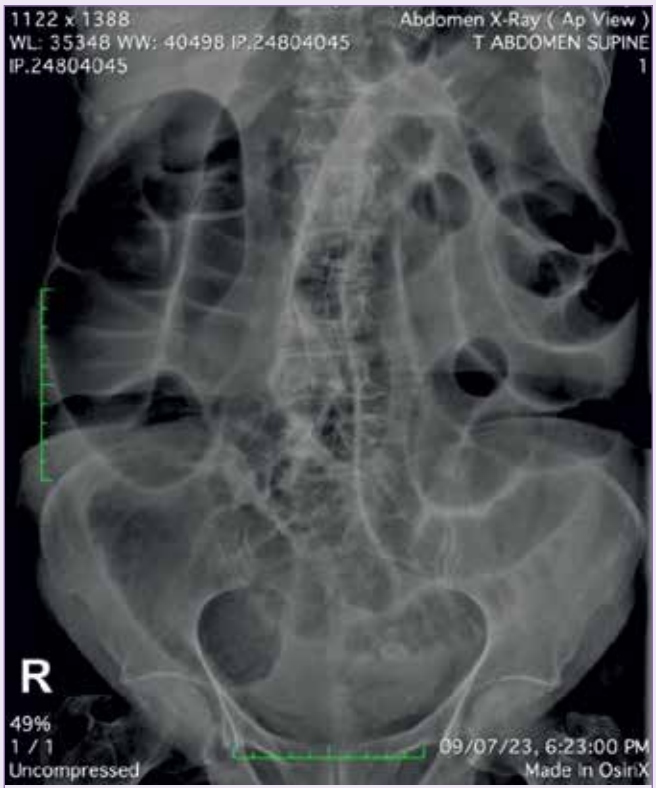

Figure: Plain supine abdominal radiograph film showing dilated bowel loops and a radiodense shadow in the pelvic region on the left side

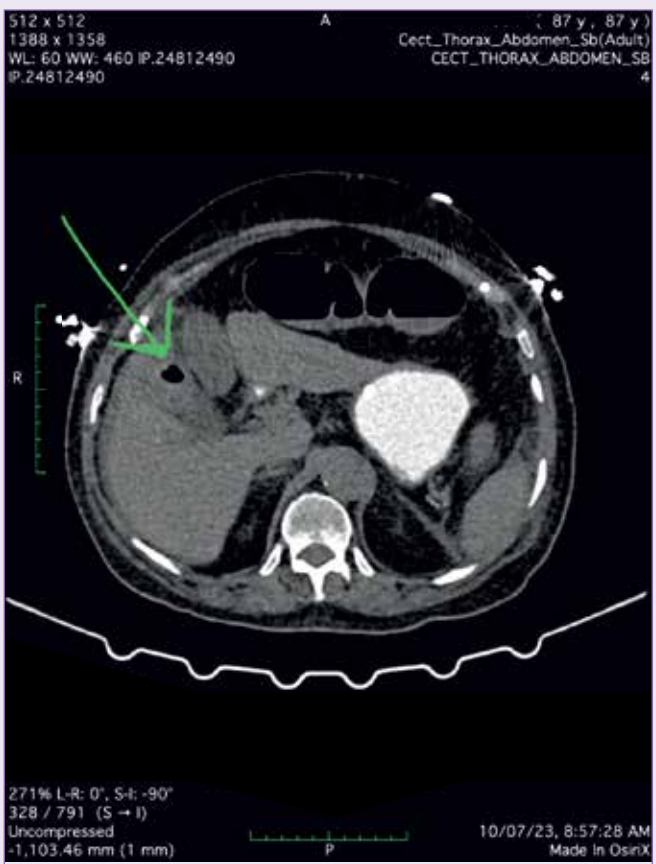

Figure a: Inflamed gall bladder with air in its lumen, raising the suspicion of cholecystoenteric fistula.

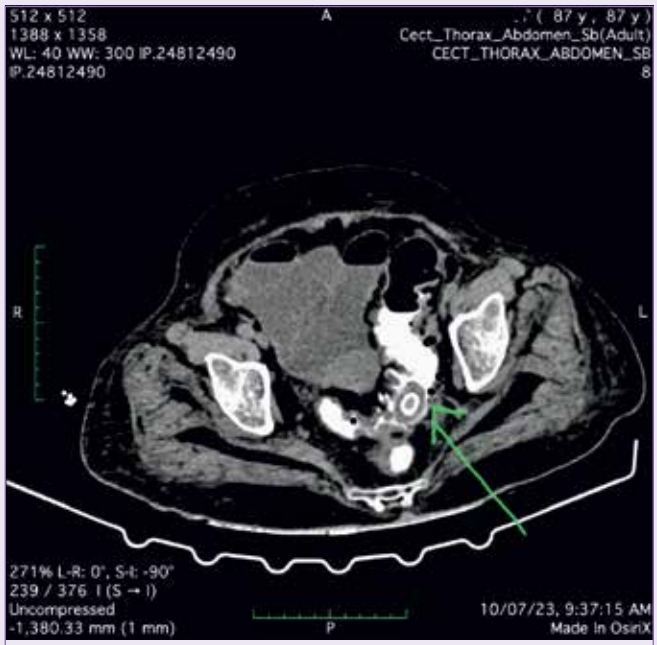

Figure b: Dilated bowel loops with a lamellated calculus in the sigmoid colon.

Retrospectively, ultrasonography showed dilated fluid filled bowel loops closely abutting the gall bladder wall and a doubtful cholecystoenteric fistula was also demonstrated.

The patient was first resuscitated with intravenous fluid and antibiotics were administered. Consent was taken for the the surgical removal of the gall stone. The post-operative recovery of the patient was uncomplicated. There was no requirement of any ventilatory support and the patient was discharged subsequently.

Discussion

Gall stone resulting in mechanical obstruction of the bowel loop is a rare manifestation which occurs in 0.3-1.5 % of patients with cholelithiasis. Gall stone ileus itself accounts for 1-4% of all the cases of intestinal obstruction and gall stone coleus being rarer would result in only a handful of cases. In a study done by Francesco Lassandro et al, 2004, on 27 patients (23 women and 4 men) aged between 58-96 years: the following findings were noted.

Plain abdominal films showed: air-fluid levels (77.78% of cases), bowel loops dilatation (88.89%), site of obstruction (44.4%), pneumobilia (37.04%), air in gallbladder (3.70%), ectopic stone (33.33%).

Abdominal sonography demonstrated bowel loops dilatation (44.44%), extraluminal fluid (14.81%), ectopic stones (14.81%), gallbladder abnormalities, (37.04%), pneumobilia (55.56%).

CT findings retrospectively observed were: bowel loops dilatation (92.59%), air-fluid levels (37.04%), bilio-digestive fistula (14.81%), pneumobilia (88.89%), ectopic stone (81.48%), extraluminal fluid (22.22%). The Rigler's triad, that is pneumobilia, bowel mechanical obstruction and ectopic stone detection was observed 4 times with RX (14.81%), 3 times with US (11.11%) and 21 times with CT (77.78%).

The associated mortality with gall stone lieus and its subsets is around 30% if not diagnosed on time, making early diagnosis a cornerstone for further management.

This disease majorly affects elderly females of over 70 years with a female to male ratio of 3:1. Patients generally have a history of gall stones but 25-72% cases were diagnosed for the first time without any evidence of cholelithiasis earlier.

Plain abdominal radiography is the first line of investigation when a patient presents with acute abdomen, but it has a low sensitivity of around 40-70% for detecting gallstones. CT scan has a sensitivity of around 93% which makes it the modality of choice.

Cholelithiasis can lead to inflammation of the gall bladder wall causing pressure erosion which results in fistula formation between the gallbladder and the adherent segment of the gastrointestinal tract, allowing the gallstone to pass through. The gall stone moves further and can get lodged in any part of the tract resulting in obstruction of the segments proximal to it.

Conclusion

This study focuses on a rare development of gall stone coleus in an elderly female who happened to be a beneficiary of early detection by radiological modalities. Plain abdominal radiograph showed dilated bowel loops and a radiodense shadow which enabled us to identify the sign of obstruction. Ultrasonography detected a cholecystoenteric fistula with increased bowel loop diameter. Computed tomography scan further demonstrated pneumobilia and the exact location of the gall stone in the sigmoid colon which was then surgically removed.

References

1. Lassandro R, Gagliardi N, Scuderi M, Pinto A, Gatta G, Mazzeo F. Gallstone ileus: analysis of radiological findings in 27 patients. Eur J Radiol 2004; 50:23–29
2. Abdihamid Mohamed Ali, Sadettin ER, Gallstone ileus: Unusual complication of cholelithiasis: A case report, Annals of Medicine and Surgery, Volume 75,2022,103476, ISSN 2049-0801. https://doi.org/10.1016/j.amsu.2022.103476. (https://www.sciencedirect.com/science/article/pii/S2049080122002369)
3. Jaffar Hussain, Asmaa M. Alrashed, Talal Alkhadher, Sarah Wood, Abdullah D. Behbehani, Salah Termos, Gall stone ileus: Unfamiliar cause of bowel obstruction. Case report and literature review, International Journal of Surgery Case Reports, Volume 49,2018, Pages 44-50, ISSN 2210-2612,

   https://doi.org/10.1016/j.ijscr.2018.06.010. (https://www.sciencedirect.com/science/article/pii/S2210261218302128)
4. Sena Park, Janaka Balasooriya, Thembi Ncube, "A Rare Case of Gallstone Ileus: Bouveret Syndrome Presenting with Concurrent Gallstone Coleus", Case Reports in Surgery, vol. 2020, Article ID8844199, 5 pages, 2020. https://doi.org/10.1155/2020/8844199
5. Furukawa A, Yamasaki M, Furuichi K, et al. Helical CT in the diagnosis of small bowel obstruction. RadioGraphics 2001; 21:341 –355

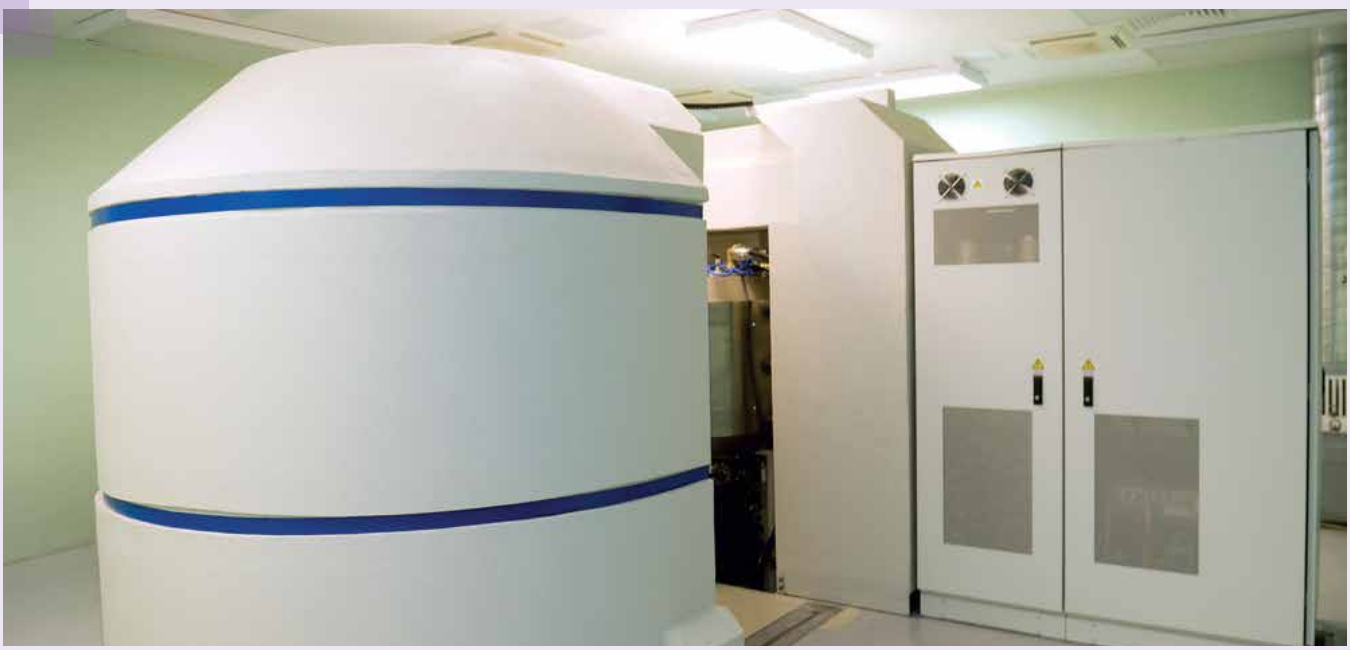

Gynecologic Radiology

Imaging Diagnosis of Accessory and Cavitated Uterine Mass – ACUM - A Rare Mullerian Duct Anomaly

Dr Kamaljeet Singh Randhawa
Consultant - Radiology,
Fortis Hospital, Mohali

Dr Akshat Chauhan
Consultant - Radiology,
Fortis Hospital, Mohali

Dr Abhishek Prasad
Director and Head - Radiology,
Fortis Hospital, Mohali

Introduction

Accessory and Cavitated Uterine Mass (ACUM) is an accessory cavity lined by functional endometrium within an otherwise normal uterine cavity. It bears uterus-like histological organization. The entity needs expertise to diagnose as it is a rare but treatable cause of severe dysmenorrhea and chronic pelvic pain in young females.

Case Report

A 20-year-old unmarried female presented with severe dysmenorrhea and chronic pelvic pain since menarche, which aggravated 2 months prior to presentation. Previous USG reports done outside revealed a 2x2.0 cm, solid left adnexal mass between uterus and left ovary.

MRI pelvis was done to further characterize the adnexal mass. On MRI, the uterus appeared normal with a well-defined, rounded, non-communicating cystic lesion measuring 2.3x2.0cm noted on left side along the site of attachment of round ligament with haemorrhagic contents within, which appeared hyperintense on T1 and hypointense on T2W images (Figure 1a, 1b, 1c, 1d) . The junctional zone of the cavity was thickened and endo-myometrial interface was indistinct. The main uterine cavity was normal in shape and size, and both the cornua were visualized normally [Figure 2, 3, 4]. The junctional zone, end myometrial interface, and myometrial signal intensity of the main uterine cavity were normal. Based on the above findings, a diagnosis of ACUM was considered. Histopathology revealed a cavitated mass lined by functional endometrium with glands and stroma surrounded by irregularly arranged smooth muscle cells.

Discussion

Uterus develops from embryonic fusion of two Mullerian ducts. Seven classes of Mullerian anomalies have been described.(1) Uterus-like mass (ULM) is an uncommon distinct entity described in literature which represents cavitated mass lined by endometrial glands and stroma.(2) ACUM is a non-communicating ULM arising in the uterus itself. The entity needs to be classified separately as the uterine cavity is otherwise normal unlike other Mullerian anomalies. It characteristically presents at a younger age, usually <30 years, with severe dysmenorrhea and chronic pelvic pain due to distention of the cavity caused by repeated bleeding. Various authors have previously described such masses with different names such as juvenile cystic adenomyoma (JCA), cavitated adenomyoma, accessory cavitated masses, etc., essentially representing the same entity now termed as ACUM. (3)

The criteria (4) for diagnosing ACUM are: an isolated accessory cavitated mass, normal uterus and adnexa , excised mass and pathological examination, accessory cavity lined by endometrial epithelium with glands and stroma, chocolate brown coloured fluid contents, no adenomyosis in the uterus.

USG is the initial imaging modality that can identify them as solid isoechoic to predominantly cystic masses resembling endometrioma arising within the uterus, visualized separately from the ovaries. MRI is the imaging modality of choice as it non-invasive and, hence, preferred over HSG in young unmarried females. It clearly shows the pelvic anatomy; cavitated mass with hemorrhagic contents; and the uterus, myometrium,

and endo-myometrial interface. Hence, adenomyosis and pelvic endometriosis are best appreciated with MRI. Thin sections (3 mm) should be used as it will also help in ruling out Mullerian anomaly by demonstrating both cornua clearly. The entity closely mimics obstructed cavitated rudimentary horn (5) with unicornuate uterus and differentiation may be difficult. Regarding therapeutic management, most recent publications have included laparoscopic excision of the mass.

Conclusion

ACUM, a rare mullerian anomaly related to dysfunction of gubernaculum, is a treatable cause of severe dysmenorrhea in young females. The entity is not as rare as thought previously. MRI is highly accurate in making the diagnosis. The MRI findings of an accessory cavitated ULM located below the attachment of round ligament usually with hemorrhagic contents, an otherwise normal-shaped uterus with both cornua identified normally, without any evidence of adenomyosis, and bilateral normal tubes and ovaries should suggest the diagnosis of ACUM pre-operatively

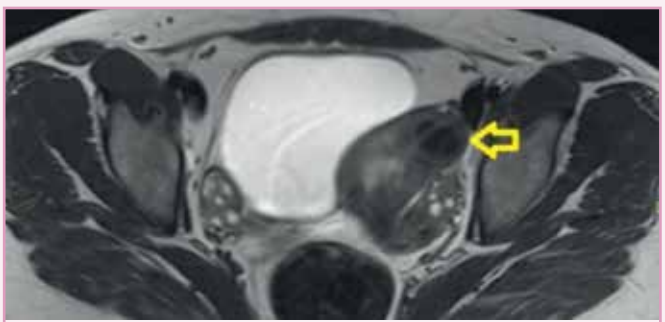

Figure 1a: T2 Axial Image showing T2 isointense periphery with T2 hypointense internal contents in left side of uterus

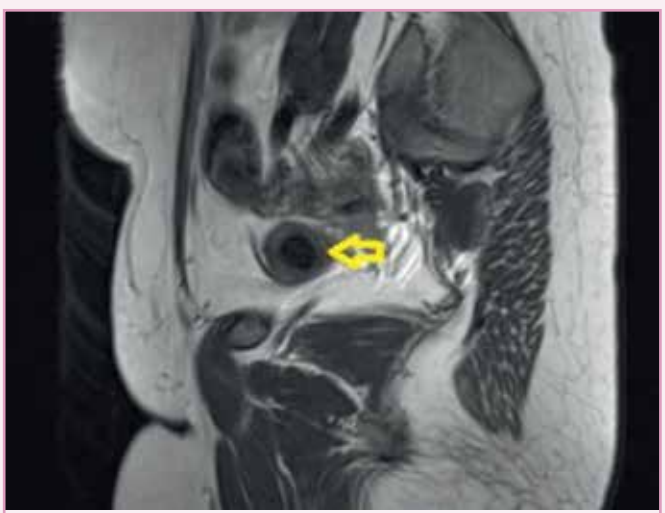

Figure 1b: T2 Sagittal Image showing T2 isointense periphery with T2 hypointense internal contents

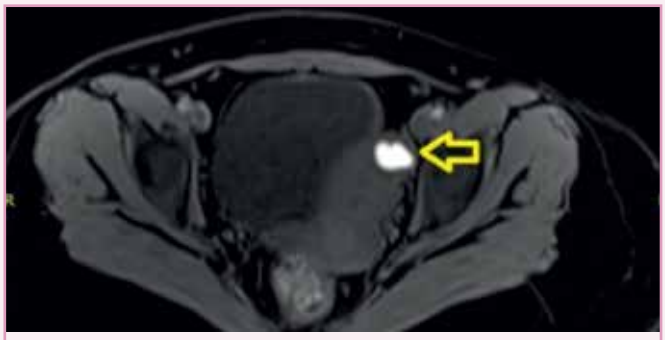

Figure 1c: T1FS Axial Image showing T1 isointense periphery with T1 hyperintense internal contents in left side of uterus

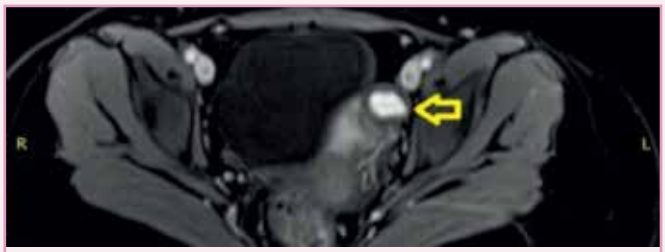

Figure 1d: T1FS Post contrast Axial Image showing T1 isointense periphery with T1 hyperintense internal contents in left side of uterus with no enhancement

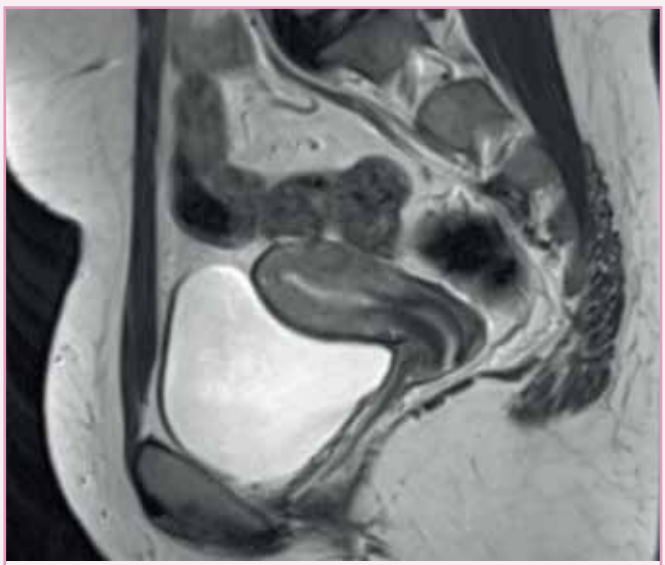

Figure 2: T2 Sagittal Image showing normal appearing uterine cavity and junctional zone.

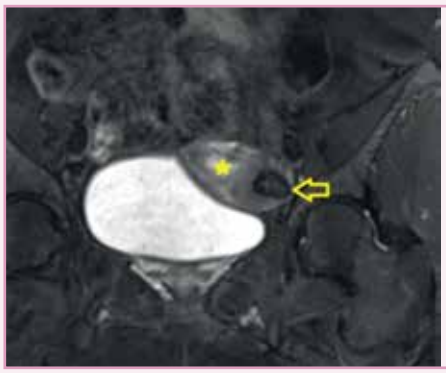

Figure 3a: STIR Coronal Image showing isointense periphery with hypointense internal contents in left side of uterus. Normal appearing endometrium.

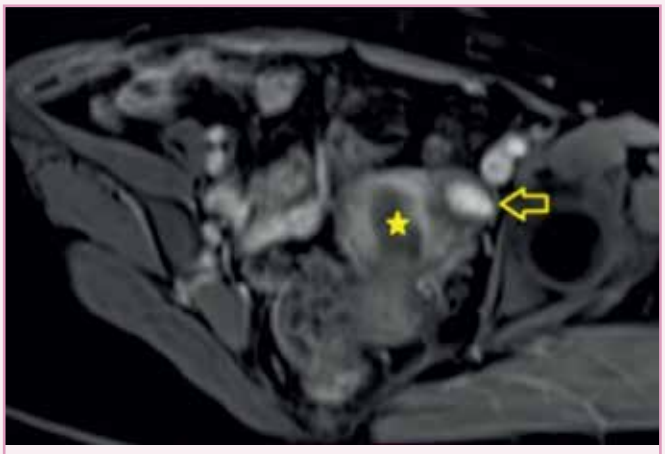

Figure 3b: T1FS Post contrast Oblique Axial Image showing T1 isointense periphery with T1 hyperintense internal contents in left side of uterus with no enhancement and no communication to the uterine cavity.

References

1. The American Fertility Society classifications of adnexal adhesions, distal tubal occlusion, tubal occlusion secondary to tubal ligation, tubal pregnancies, müllerian anomalies and intrauterine adhesions. Fertil Steril. 1988 Jun;49(6):944–55.
2. Na KY, Kim GY, Won KY, Kim HS, Kim SW, Lee CH, et al. Extrapelvic Uterus-like Masses Presenting as Colonic Submucosal Tumor: A Case Study and Review of Literature. Korean J Pathol. 2013 Apr;47(2):177–81.
3. Jain N, Verma R. Imaging diagnosis of accessory and cavitated uterine mass, a rare mullerian anomaly. Indian J Radiol Imaging. 2014 Apr;24(2):178–81.
4. Acién P, Acién M, Fernández F, José Mayol M, Aranda I. The cavitated accessory uterine mass: a Müllerian anomaly in women with an otherwise normal uterus. Obstet Gynecol. 2010 Nov;116(5):1101–9.
5. Jain N, Goel S. Cystic Adenomyoma simulates uterine malformation: A diagnostic dilemma: Case report of two unusual cases. J Hum Reprod Sci. 2012 Sep;5(3):285–8.

Imaging in Uterine Artery Pseudoaneurysm: A Rare, Potentially Fatal Cause of Secondary Post-partum Haemorrhage

Scan QR Code for more

Dr Sanjota Satish Nair
Consultant - Radiodiagnosis,
Fortis Hospitals, Mulund

Abstract

Secondary postpartum haemorrhage is one of the important causes of postpartum morbidity and mortality. Uterine artery pseudoaneurysm is a rare, potentially fatal but treatable cause of secondary post-partum haemorrhage. If not diagnosed timely, it can lead to life-threatening haemorrhage. We report the case of a 41-year-old woman who presented with profuse vaginal bleeding on 32nd day of caesarean section. On imaging a left uterine artery pseudoaneurysm was found in the uterine wall with blood clots in the uterine cavity. Patient was managed with aggressive fluid resuscitation and immediate interventional radiology procedure of selective embolization of pseudoaneurysm. High index of suspicion is needed to search for rare vascular causes like pseudoaneurysm.

Keywords

uterine artery pseudoaneurysm, Yin-yang sign, secondary postpartum haemorrhage, caesarean section.

Endometrial Stromal Sarcoma: A Challenge for Diagnosis And For Treating : A Case Report

Source : DOI: 10.1055/s-0042-1754327

Dr Sunita Ahlawat
Principal Consultant - Histopathology,
Agilus, Fortis Memorial Research Institute, Gurugram

Dr Rama Joshi
Principal Director - Gynae-oncology,
Fortis Memorial Research Institute, Gurugram

Dr Nitesh Rohatgi
Senior Director - Medical Oncology,
Fortis Memorial Research Institute, Gurugram

Dr Ishita Sen
Senior Director - Nuclear Medicine,
Fortis Memorial Research Institute, Gurugram

Dr Mala Sinha
Fellow in Gynae - Oncology,
Fortis Memorial Research Institute, Gurugram

Dr Pavitra Vijaya Raghavan
Senior Resident - Medical Oncology,
Fortis Memorial Research Institute, Gurugram

Abstract

Endometrial stromal sarcoma (ESS) in extrauterine locations presents diagnostic and management challenges due to their heterogeneous morphological, immunoprofile, and genetic features. This article discusses a challenging case of a 62-year-old woman with a unique ESS tumor, emphasizing the role of molecular profiling in diagnosis, grading, and guiding patient management.

Introduction

Endometrial stromal sarcoma (ESS) is an uncommon tumor, accounting for less than 1% of uterine tumors and 10% of uterine mesenchymal sarcomas1. The heterogeneity in morphological, immunoprofile, and genetic features complicates diagnosis and grading, which are crucial for treatment decisions.

Case Report

A 65-year-old postmenopausal woman presented with a six-month history of bloating and a one-month history of a palpable abdominal mass. Initial evaluation revealed a massive abdominal mass extending from the pelvis to the xiphisternum, with a serum CA 125 level of 217U/ml. Imaging confirmed a large, solid-cystic mass measuring 24x17x16 cms with necrosis, haemorrhage and diffusion restriction. (Figure 1). PET CT showed a large FDG avid mass 14.9x16x23.7 cm. (Figure 2)

Exploratory laparotomy and excision were performed, leading to the discovery of a 6.5 kg cystic mass. (Figure 3) Pathological analysis revealed ambiguous morphology, low and high-grade features, and immunohistochemistry indicated both low-grade and high-grade ESS markers. Molecular profiling identified a

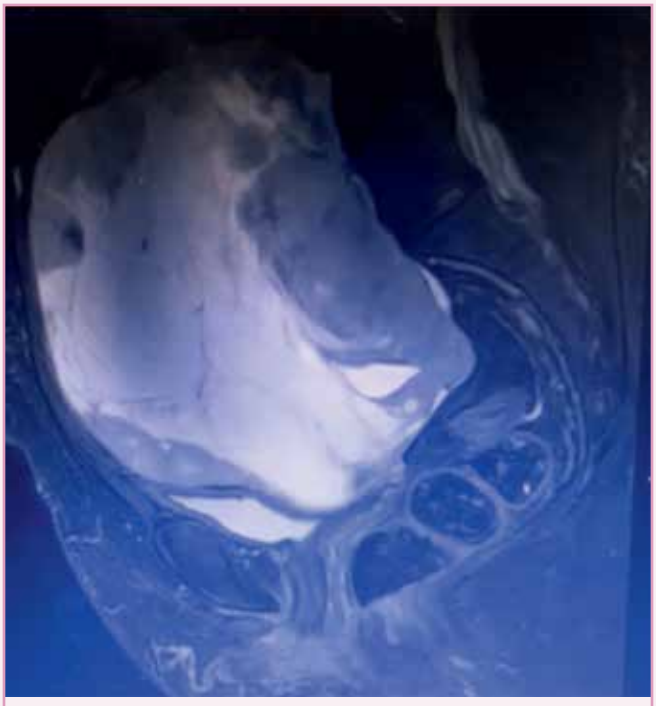

Figure 1: MRI whole abdomen - Large well defined solid cystic mass ~24x17x16cm, extending to abdomen with necrosis, hemorrhage and diffusion restriction. Right ovary small and pushed posteriorly, left ovary not visualised. Minimal ascites.

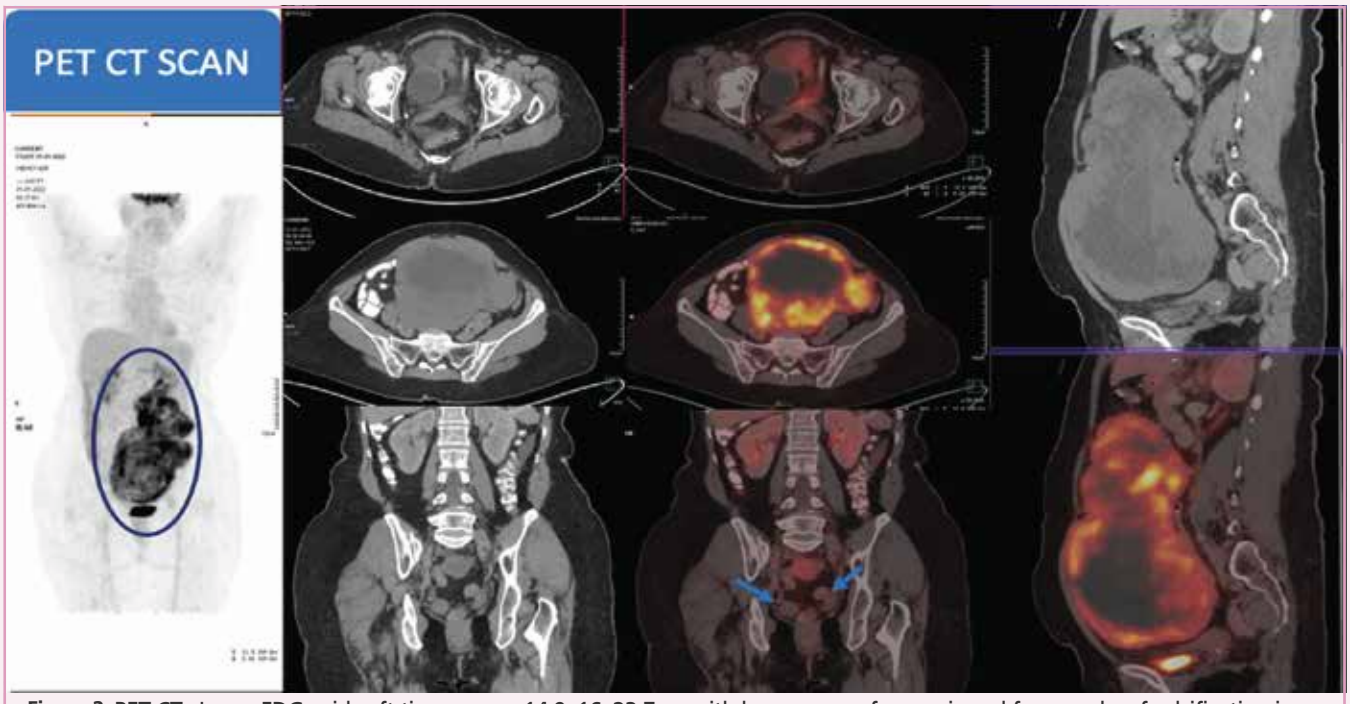

Figure 2: PET CT—Large FDG avid soft tissue mass ~14.9x16x23.7cm with large areas of necrosis and few specks of calcification in left side of pelvis. Bilateral ovaries not visualised separately.Mild ascites.

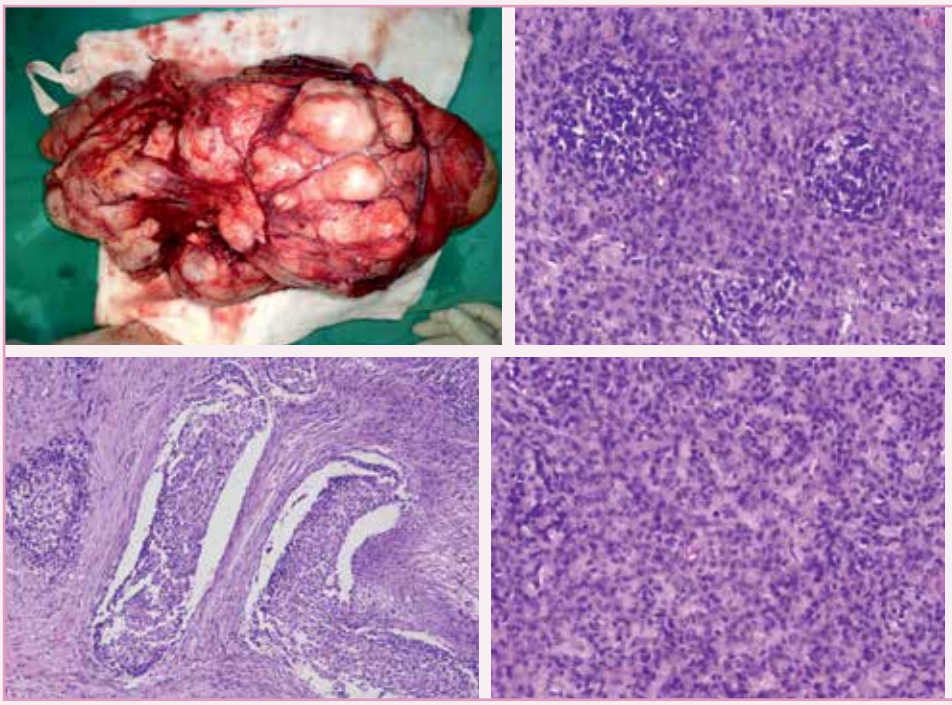

Figure 3:

A: Large bosalated mass 6.5 kg in weight and measuring 25x20x16 cm with grossly normal both tubes and ovaries.

B: Tumour shows perivascular whorls of ovoid cells (H&E stainX100X)

C: Left fallopian tube with lymphovascular emboli

D: Tumour showing few tubule formation with (Inset area of necrosis)

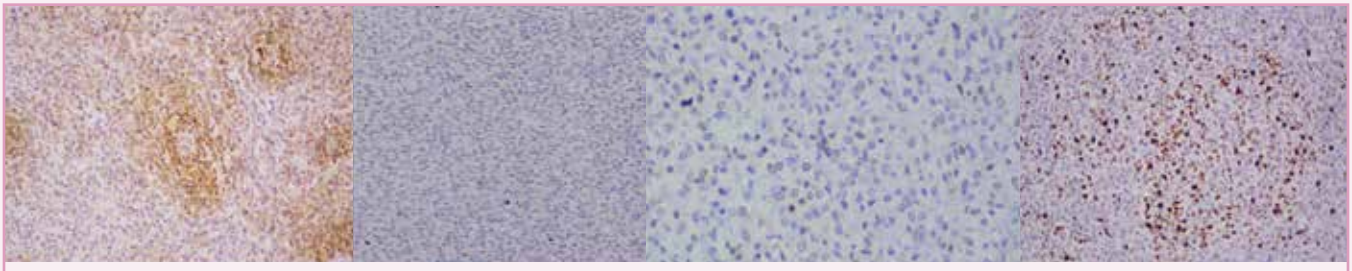

Figure 4: Tumour cells showing positive CD10 staining ER: very weak patchy expression of oestrogen receptor Cyclin D1 very focal expression is seen KI67 labelling is seen in about 35% of nuclei.

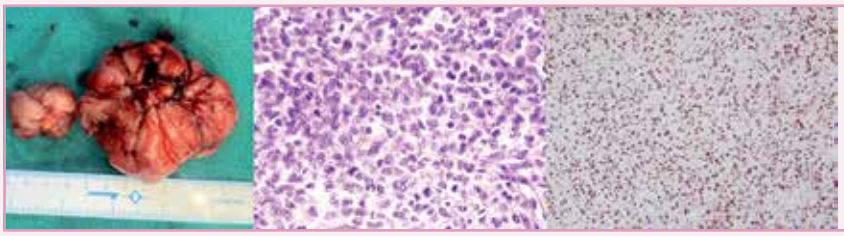

Figure 5: A: Recurrent tumour in sigmoid epiploicae ~ 10x9 cm

B: Foci showing nuclear atypic with brisk mitosis

C: Ki67 labelling index shows a high labelling index of 70%

JAZF1-PHF1 fusion, suggesting early transformation into high-grade ESS. Adjuvant therapy was initiated, including Gemcitabine and Docetaxel but the patient suffered a recurrence, presenting as a 10 cm pelvic mass on the right side. Surgical removal of the mass revealed a Tumor with a similar immunoprofile, but distinct high cellularity regions characterized by nuclear atypia and brisk mitotic activity, as evidenced by a Ki67 labelling index of 70% (Figure 5). Subsequent molecular analysis identified the presence of a PIK3CA mutation. Following her second surgery, she underwent six cycles of adjuvant chemotherapy followed by radiotherapy. Her treatment was successfully completed in early August 2023, and as of her last follow-up, she remains free of the disease.

Discussion

ESS is a rare Tumor, classified into three types: Low grade (LG-ESS), high grade (HG-ESS), and undifferentiated uterine sarcoma, based on their appearance and immunohistochemistry (1). Tumor grade is crucial for treatment decisions (2). LG-ESS is primarily treated with surgery, possibly with aromatase inhibitors. HG-ESS usually requires adjuvant chemotherapy and sometimes radiotherapy (2,3). Grading ESS typically relies on morphology and immunohistochemistry (1). Some cases have unclear features, and molecular profiling aids in precise diagnosis. LG-ESS is linked to JAZF1-SUZ12 fusion, while HG-ESS is associated with YWHAE-NUTM2 fusion (4,5). In our discussed case, JAZF1-PHF1 fusion suggests LG-ESS, especially when it exhibits sex cord differentiation. Most cases are graded using morphology and immunohistochemistry, but ambiguous cases benefit from molecular profiling. LG-ESS often exhibits JAZF1-SUZ12 fusion, while HG-ESS is associated with YWHAE-NUTM2 fusion. In this case, JAZF1-PHF1 fusion indicated LG-ESS, but with aggressive behaviour due to additional genetic alterations.

In this case, the tumor displayed mixed characteristics, including low-grade morphology with perivascular whorls and CD10 expression, alongside the absence of estrogen receptor expression. Additionally, there were focal areas with high cellularity, nuclear changes, brisk mitosis, and necrosis. Cyclin D1, a high-grade marker, was not broadly expressed, as seen in HG-ESS. The Ki67 labeling index was notably high. Molecular analysis identified a JAZF1-PHF1 fusion, typically associated with LG-ESS. However, considering the overall features, the diagnosis was endometrial stromal sarcoma with early transformation to high grade. Adjuvant chemotherapy was administered, but recurrence occurred during treatment.

Brahmi et al. (6) demonstrated that ESS encompasses heterogeneous tumors, with some LG-ESS cases exhibiting aggressive behavior despite their molecular profile. These alterations, often missed by routine molecular techniques, may require additional testing for potential targeted treatments. Upon examination of the recurrent tumor, it was found to harbor both JAZF1-PHF1 fusion and a PIK3CA mutation, likely contributing to its aggressive behavior.

Conclusion

ESS represent a heterogenous group of tumours, in terms of clinical behaviour, pathology and genetics with the help of detailed molecular analysis new targets for treatment can be identified which may help in understanding the behaviour of tumour better.

References

1. WHO Classification of Tumours 5th Edition, Female Genital Tract, 2019.
2. Meurer, M. et al. (2019). Localized high-grade endometrial stromal sarcoma and localized undifferentiated uterine sarcoma: A retrospective series of the French Sarcoma Group. International Journal of Gynecological Cancer, 29(5), 691–698.
3. Casali, P.G. et al. (2018). Soft tissue and visceral sarcomas: ESMO-EURACAN Clinical Practice Guidelines for diagnosis, treatment and follow-up. Annals of Oncology, 29(Suppl. 4), iv51–iv67.
4. Pautier, P. et al. (2014). Gynecologic Cancer InterGroup (GCIG) consensus review for high-grade undifferentiated sarcomas of the uterus. International Journal of Gynecological Cancer, 24(Suppl. 3), S73–S77.
5. Aisagbonhi, O. et al. (2018). YWHAE Rearrangement in a Purely Conventional Low-grade Endometrial Stromal Sarcoma that Transformed Over Time to High-grade Sarcoma: Importance of Molecular Testing. International Journal of Gynecological Pathology, 37(5), 441–447.
6. Brahmi, M. et al. (2020). Molecular Classification of Endometrial Stromal Sarcomas Using RNA Sequencing Defines Nosological and Prognostic Subgroups with Different Natural History. Cancers (Basel), 12(9), 2604. doi: 10.3390/cancers12092604.

Fetal Medicine

Radiology of Abortus

Dr Pradeep Srinivasan
Director - Radiology,
Fortis Hospitals, Bangalore

Abstract

The role of a radiologist in Obstetric imaging and diagnosis of various fetal aneuploidies and congenital anomalies is well known. It does not end with diagnosis alone and there is a bigger role as a research scientist when he performs the next logical step called 'RADIOLOGY OF ABORTUS AND AUTOPSY".

Over the years X rays have been used to image the abortuses with various skeletal dysplasia for confirmation of antenatal findings and for detection of additional findings. Over the years, autopsies have been performed on abortuses to confirm antenatal findings and to detect more undiagnosed abnormalities. In the last 15 years I have used sonography and CT scan with a novel technique called LUMINIGRAPHY. This technique involves injection of Iodinated contrast or air into Cardiac chambers, trachea, esophagus, urinary bladder and anal canal according to the clinical congenital anomaly detected antenatally.

Abortuses with cardiac anomalies were assessed in following manner. Plain CT was done. The chamber of interest with anomaly was selected and a 24-gauge needle was place trans thoracically under CT guidance. Tip of needle was placed within the chamber and checked by plain CT. Diluted contrast was gently injected, Volume of injection was 1 to 3cc. Subsequent axial multislice CT was done and after seeing the CT if needed needle tip adjustment was made and reinjection was done. The contrast filled chamber and its outlet were studied with egresses of contrast into other chambers or inlets and outlets or septal defects. Subsequently, MPR, MIP, VRT etc were used for post processing in 2D and 3D. Sonography was performed and 2D images of the cardiac anatomy were obtained. Finally, dissection and autopsy were done.

Abortuses with gastrointestinal anomalies were imaged in the following way. Plain CT was done. Air or iodinated contrast was injected into the oral cavity and the esophagus, stomach and intestines with contrast and imaged by axial CT. Further coronal and sagittal reformations were done. MIP and VRT were used to render a barium meal like picture. Finally, dissection and autopsy was done.

Abortuses with respiratory tract anomalies were assessed in the following manner. Plain CT was done. Subsequently air or iodinated contrast was injected into the trachea and axial CT scans were done. Subsequently MIP was used in coronal view to demonstrate the tracheobronchial anomalies. Finally, dissection and autopsy was done.

Abortuses with genitourinary anomalies were assessed in the following manner. Plain CT was done. Subsequently, iodinated contrast was injected into the urinary bladder percutaneously and axial CT scans were done. MIP, coronal and sagittal reconstructions of the kidneys and ureters and urinary bladder were obtained. Sonography was performed to demonstrate the anomalies. Finally, dissection and autopsy was done.

Abortuses with skeletal anomalies, facial anomalies were assessed in the following manner.

Plain x rays were done AP and lateral views. Plain CT was done. Sagittal and coronal reconstructions were done to demonstrate the anomalies.3d reconstructions were done to show facial anomalies. Sonography was performed with abortus immersed in a water bath and transducer was immersed into the water.

14 cases with congenital anomalies were terminated and the abortuses were subjected to Sonography and Various Types of CT Contrast Luminographies.

Subsequent Autopsy Correlations were done.

Case 1

16 weeks fetus had antenatal findings of Unossified nasal bone and thickened nuchal fold. Amniocentesis confirmed Trisomy 21. Post termination abortus was immersed in a water bath.Sonography of face was done in mid sagittal plane which showed presence of unossifiednasal bone and increased pre-nasal thickness. Sonography of neck in axial plane showed thickened soft tissues with edema of neck behind the cervical spine. Sagittal view of the back of neck and upper chest showed thickened soft tissues and edema of subcutaneous tissues.

Screening of chest showed abortus to be still alive with bradycardia. Abortus died in few seconds. Photographs of face showed low set ears. This case used Sonography to validate antenatal findings

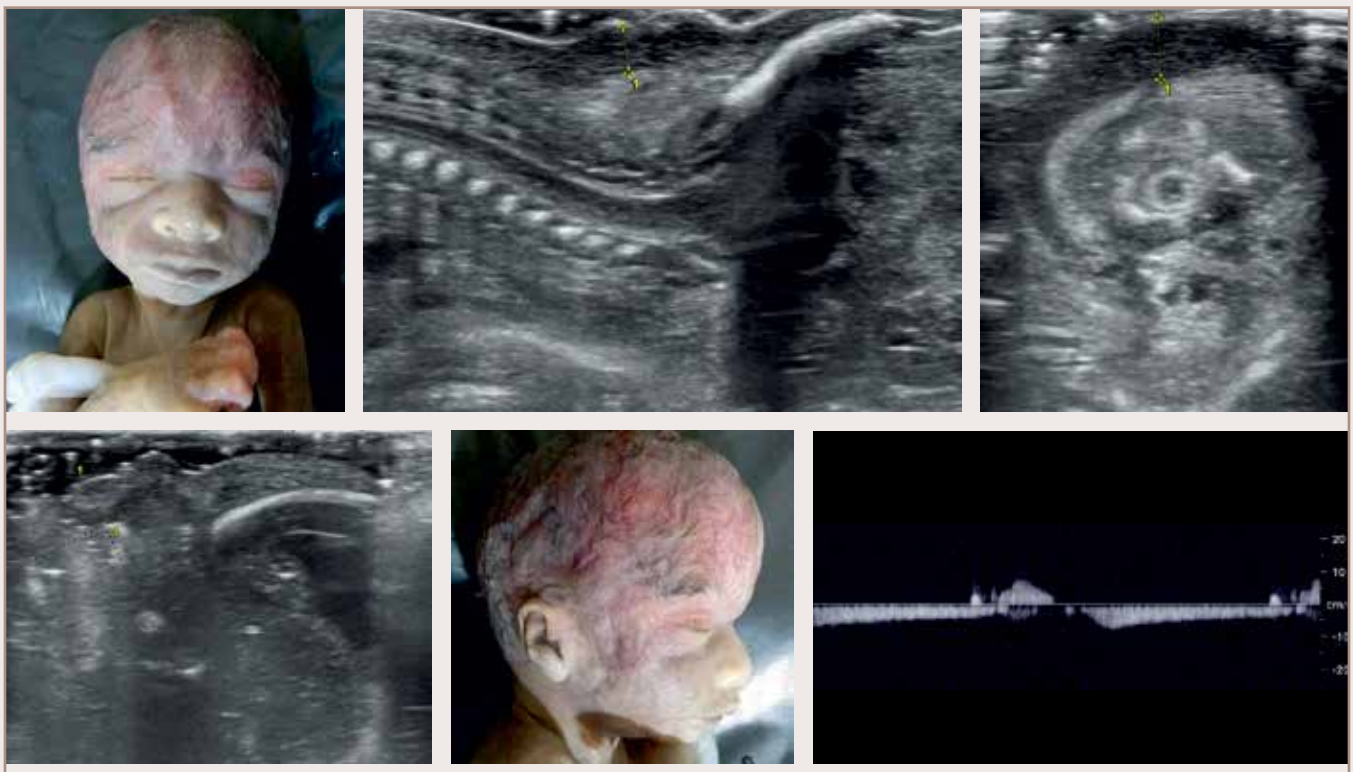

Figure : Down's Abortus: Abortus Sonography Shows Thick NT In Sagittal and Axial Scans / Unossified Nasal Bone and Bradycardia

Case 2

18-week fetus showed antenatal findings of Unossified nasal bone, Echogenic intracardiac focus, ventriculomegaly. Amniocentesis confirmed Trisomy 21. Post termination the abortus was imaged using sonography water bath. Upper row shows antenatal pictures of Unossified nasal bone, echogenic intracardiac focus and ventriculomegaly. Lower row shows abortus sonograms validating the same findings.

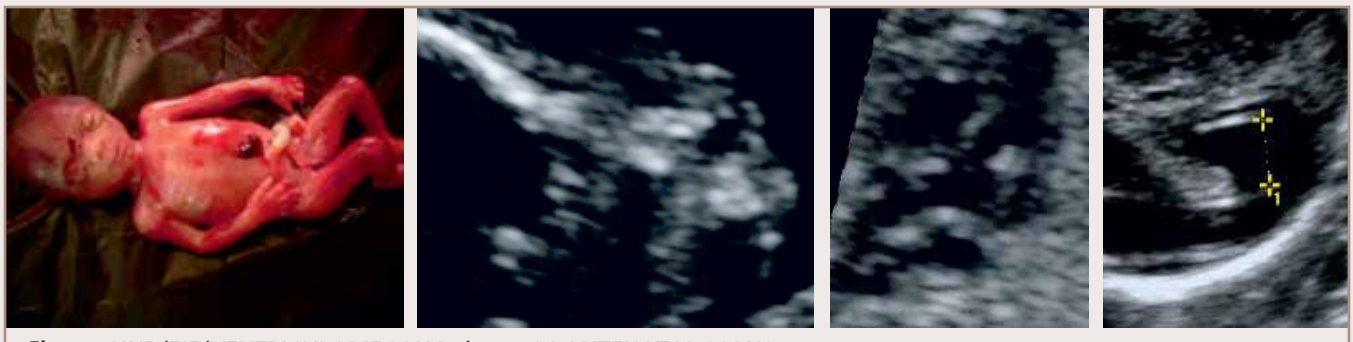

Figure : UNB/EIF/VENTRICULOMEGALY-trisomy 21 ANTENATAL SCANS

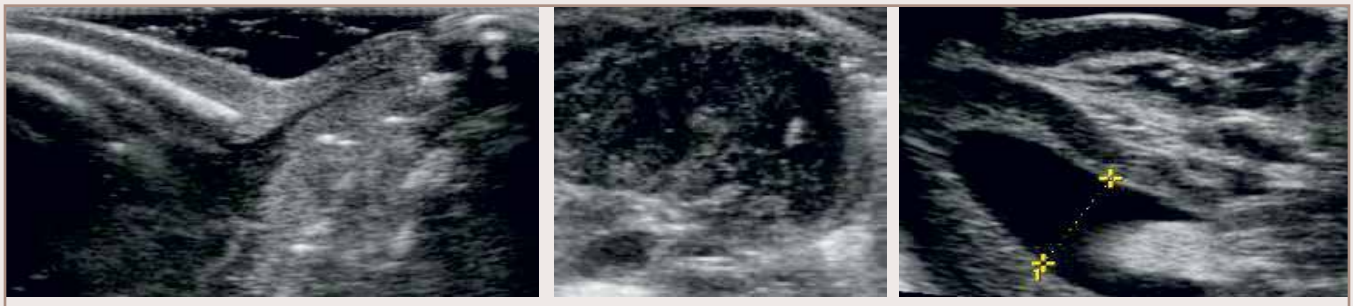

Figure : Abortus Scans

Case 3

Antenatal diagnosis was Hypoplastic left heart with no Left ventricular cavity and no ascending aorta. Distal arch showed reversed flow from ductus arteriosus. Post termination Plain CT and contrast CT VENTRICULOGRAPHY showed Right atrium and right ventricle and arch of aorta with descending aorta. Left ventricle, ascending aorta showed no contrast and are absent in the coronal thick slab MIP. Axial CT at the level of cardiac chambers show Right ventricle filled with contrast but there is no contrast in the left ventricle. Axial CT at the level of 3 vessels shows only 2 contrast filled vessels, namely SVC and Ductal arch. The aortic arch is absent. Autopsy showed a normal sized RV cavity and an absent LV cavity.

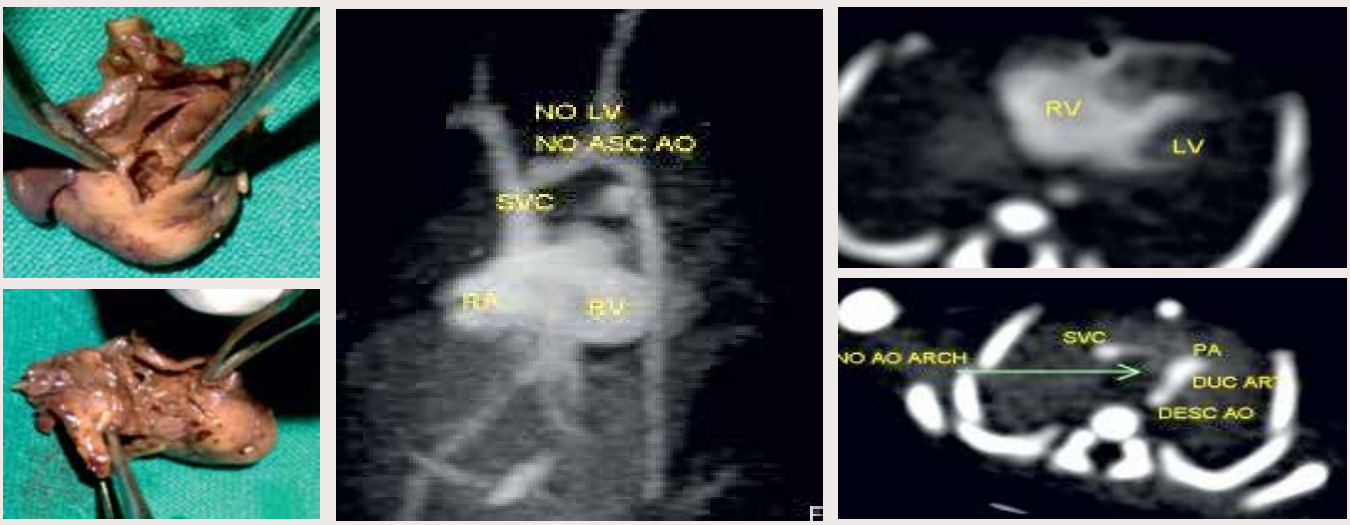

Case 4

Antenatal diagnosis at 20 weeks was short nasal bone, bilateral pelviectasia and thickened aortic valve. 4 chamber cardiac view showed a small inlet VSD. Colour doppler shows abnormal shunt across the VSD. LVOT view shows persistence of visibility of aortic valve during systole. Amniocentesis revealed a supernumerary chromosome. Post termination autopsy showed bicuspid aortic valve and bovine aortic arch.

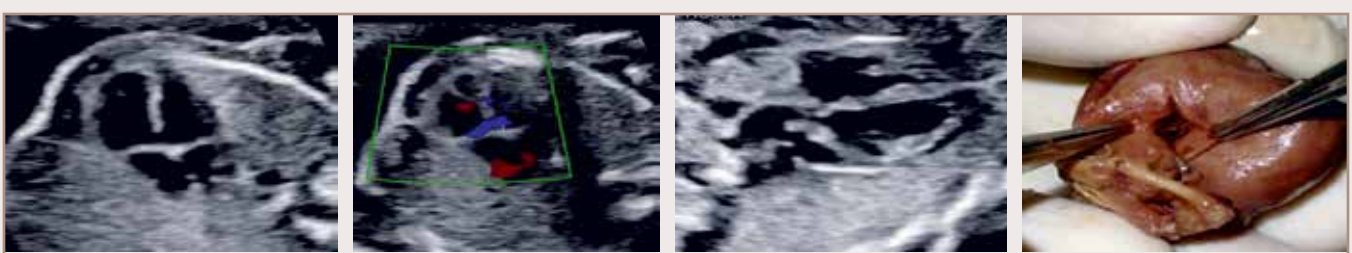

Figure : Antenatal Sonography Shows VSD In 2d and Colour Four Chamber Views and Thick Aortic Valvein LVOT View /autopsy Shows Bicuspid Aortic Valve

Case 5

Antenatal diagnosis of double outlet right ventricle was made with transposed great vessels. Right ventricle which is the anterior chamber gives rise to anterior aorta in first picture and to posteriorly placed pulmonary artery in the second picture.

Post termination CT was done by injecting iodinated contrast into the right ventricle. Accidental injection into pericardial sac resulted in contrast in the pericardium. Reinjection into Right ventricle resulted in filling of both aorta and pulmonary artery from right ventricle. Autopsy pictures show right ventricle giving rise to anterior aorta and posterior pulmonary artery.

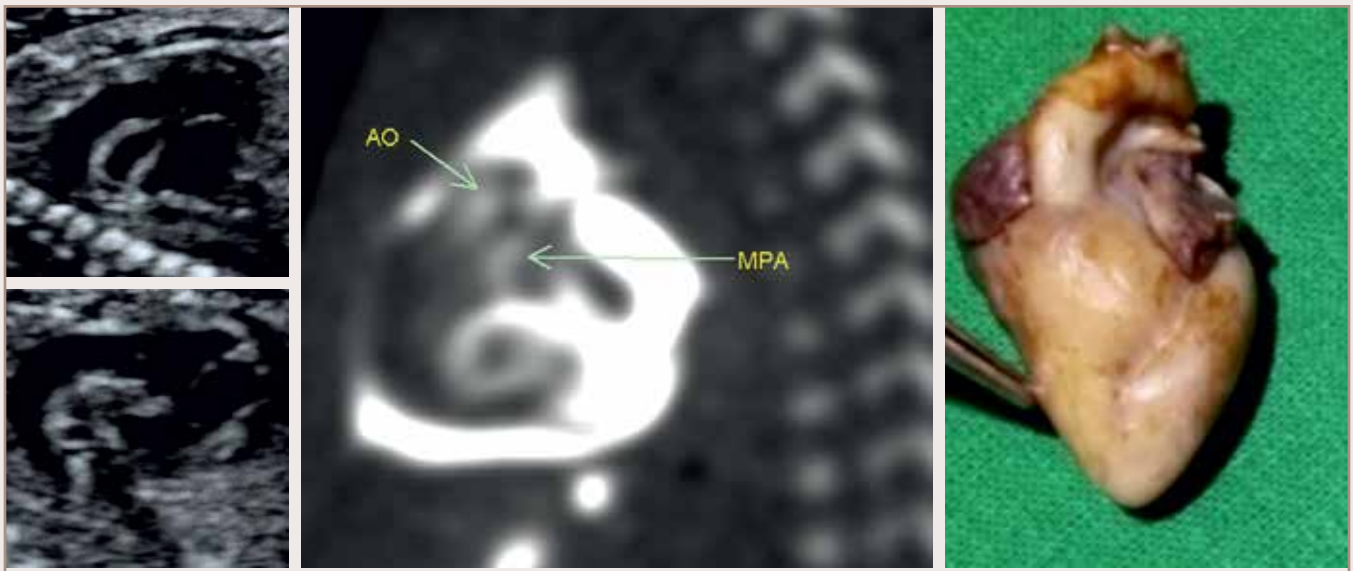

Figure : Antenatal sonography showing RV giving anterior aorta and posterior MPA abortus CT ventriculography shows accidental contrast injection into pericardial sac/anterior aorta and posterior MPA/autopsy shows RV giving rise to anterior aorta and posterior main pulmonary artery-DORV with TGA

Case 6

Antenatal diagnosis of LEFT ATRIAL ISOMERISM was made with multiple findings. There was Interruption of IVC, Hemiazygos continuation, Left SVC, VSD, Small ascending aorta. Hammock view showed absent IVC in the upper right picture. 4 chamber view showed Inlet VSD in upper left picture. LVOT view showed hypoplastic aorta in lower right picture. Axial view in colour showed absent IVC and hemiazygous vein in blue to right of aorta in red by its side at the same plane. Termination was done. Sonography of abortus showed, absent IVC and an additional small vessel to the right of aorta at the same plane.

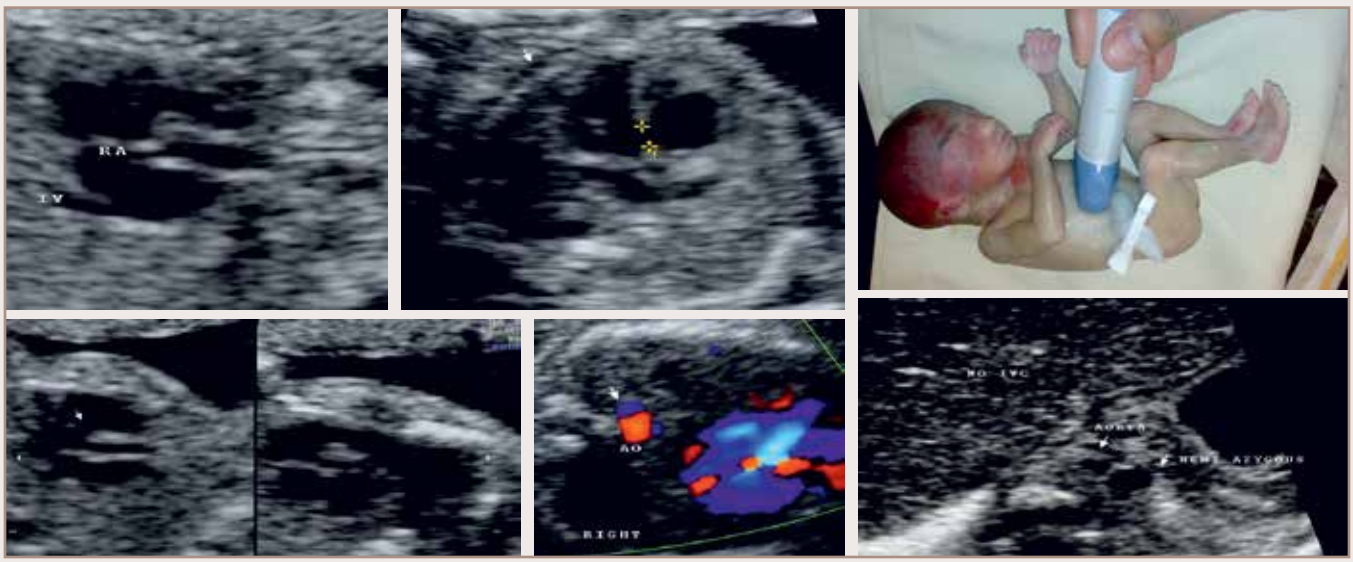

Case 7

Antenatal diagnosis of RIGHT ATRIAL ISOMERISM was made with following findings. Double SVC, DORV, ASD, VSD, Tracheal Atresia, Esophageal Atresia, Central liver. Origin of both aorta and pulmonary artery are seen in blue color parallel to each other arising from right ventricle in upper right picture. 4 chamber cardiac view shows ASD and VSD as communications across both atrium and both ventricles in upper mid picture. RV gives rise to aorta in upper left picture. RV gives rise to pulmonary artery in lower mid picture. Central large liver seen in lower mid picture. Hyperinflated echogenic lungs seen in lower left picture. Termination was done. Abortus CT reconstructions showed Contrast in obstructed upper esophagus in lower right picture and contrast in obstructed trachea in lower left picture. Right ventricle injection showed both aorta and pulmonary artery filling from RV and they were transposed as seen in upper left picture. Right atrial injection showed Double SVC as seen in lower left picture. Autopsy showed validation of cardiac, tracheal and Esophageal findings and showed central liver and asplenia.

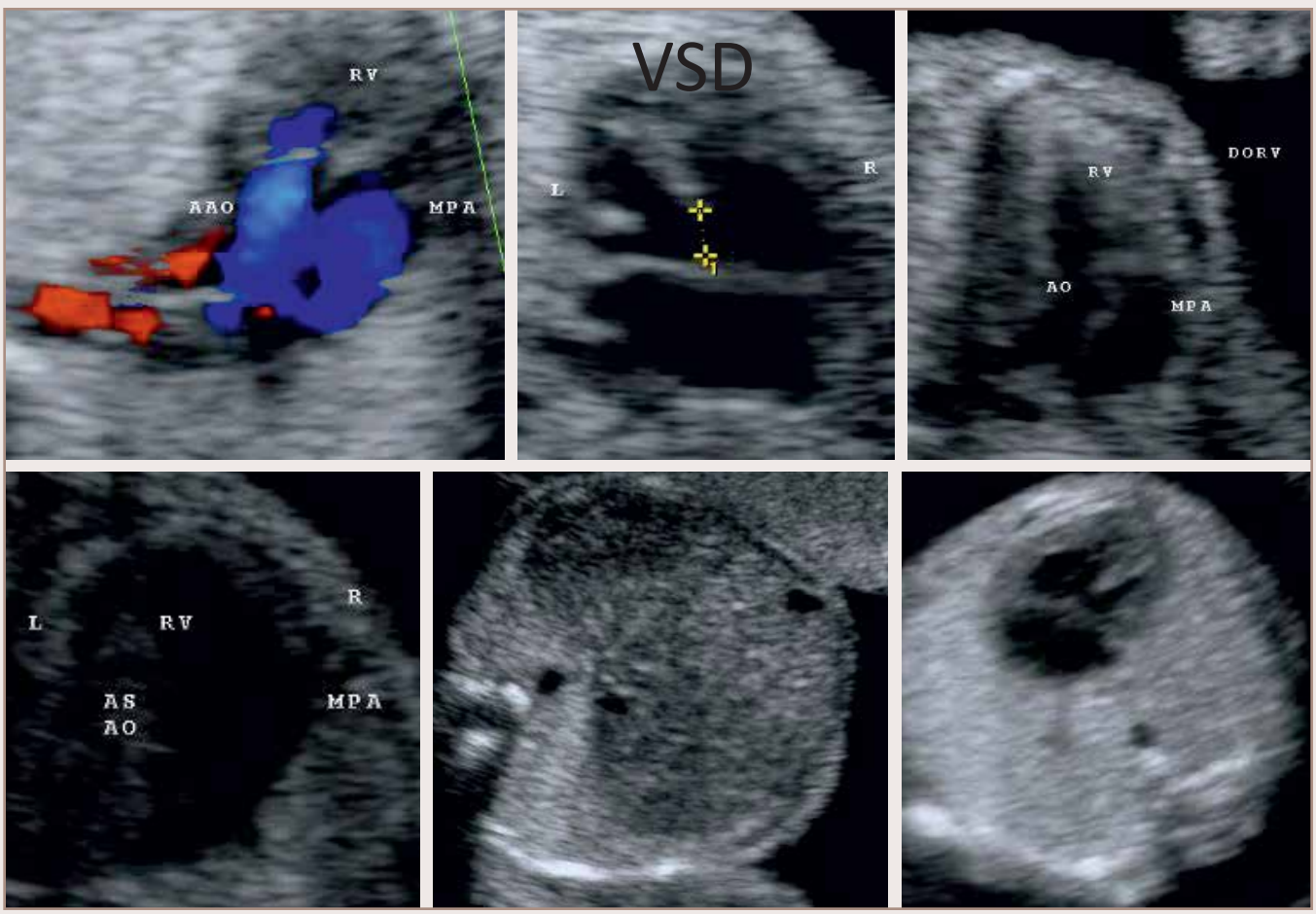

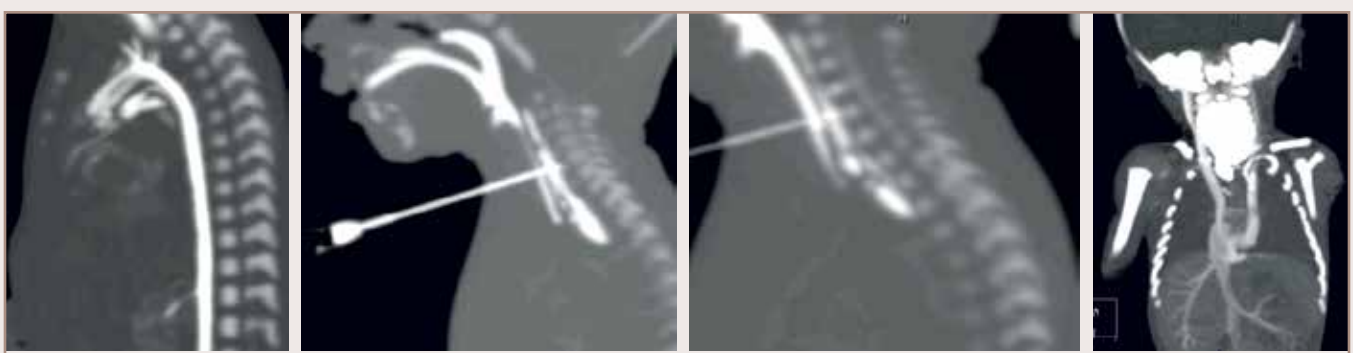

Figure : CT Trachogram, CT Esophagogram of Abortus-Tracheal and Esophageal Atresia
CT Angiogram-Dorv with Transposition/Bilateral SVC

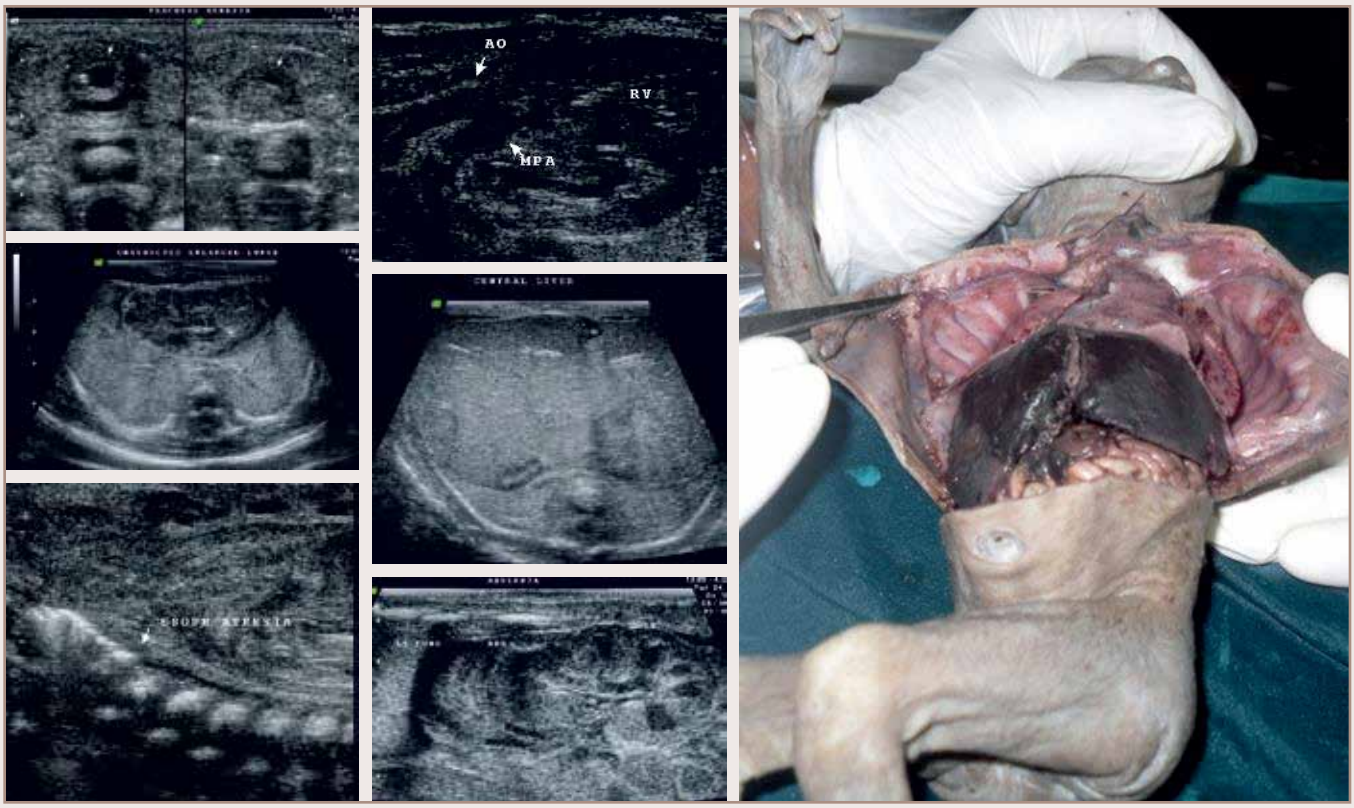

Case 8

Antenatal diagnosis of TRUNCUS ARTERIOSUS was made. Antenatal fetal echo Cardiac outlet view in colour showed a single outlet from both ventricles and this vessel showed a large regurgitation as shown. 2D scan showed single cardiac outlet giving rise to both aorta and pulmonary arteries. Single umbilical artery was seen. Doppler showed regurgitation across the cardiac valves suggestive of cardiac failure. Termination was done. Abortus CT was done by injecting iodinated contrast into the left ventricle which showed single outlet from which aorta and both pulmonary arteries arised as shown. 3D reconstruction and Volume rendering showed a dilated globular cardia with single outlet giving rise to aorta and both pulmonary arteries. Sonography of the abortus showed Bilateral pleural effusions, pericardial effusion, ascites and single umbilical artery in umbilical cord.

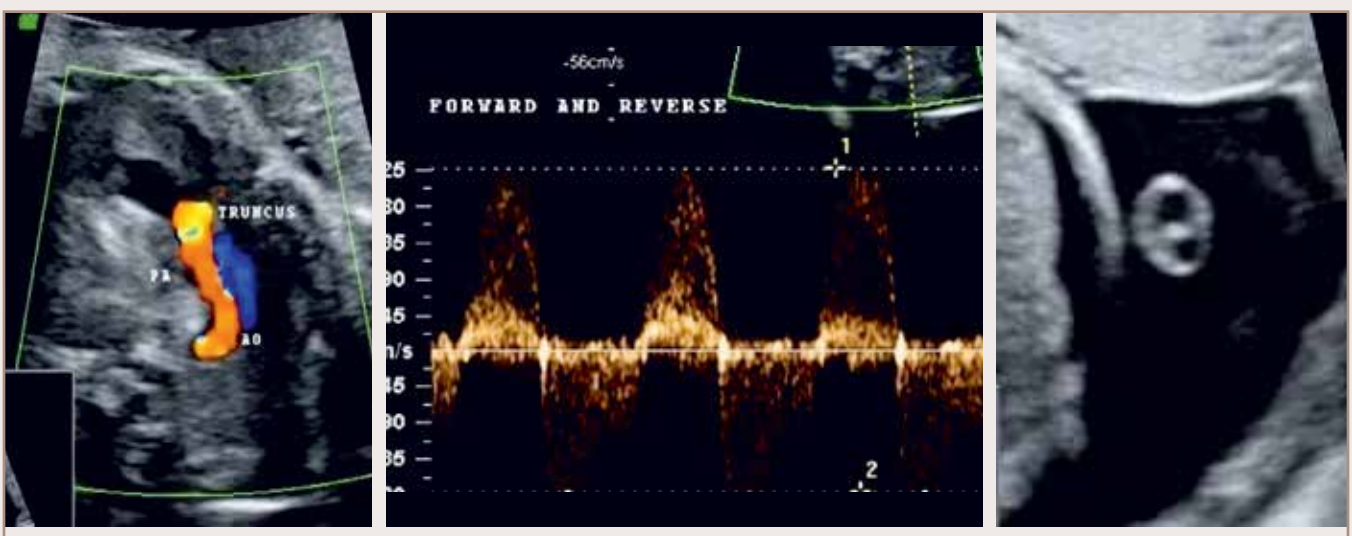

Figure : Antenatal Sonography Shows Truncus in Colour with Forward and Reversed Flows /in 2D/Single Umbilicl Artery

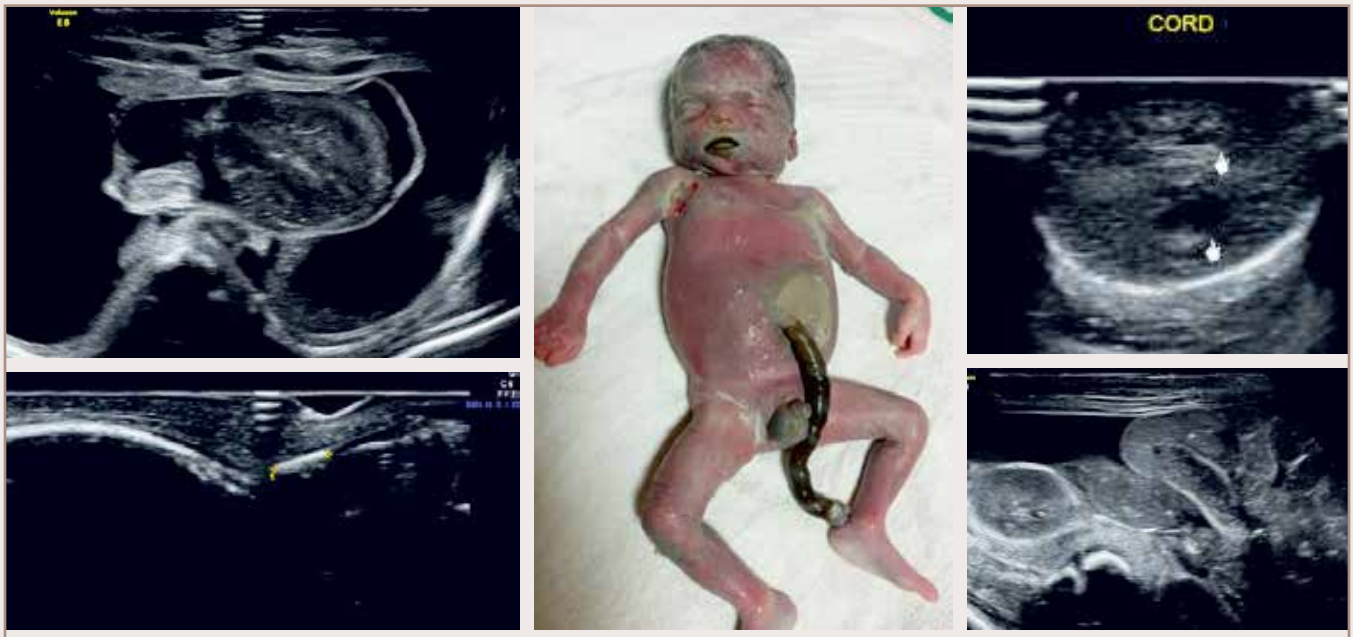

Figure : Abortus Sonography SHWS Bilateral Pleural Short Nasal Boneeffusion/pericardial Effusion/Single Umbilical Artery/Ascites/Nasal Bone

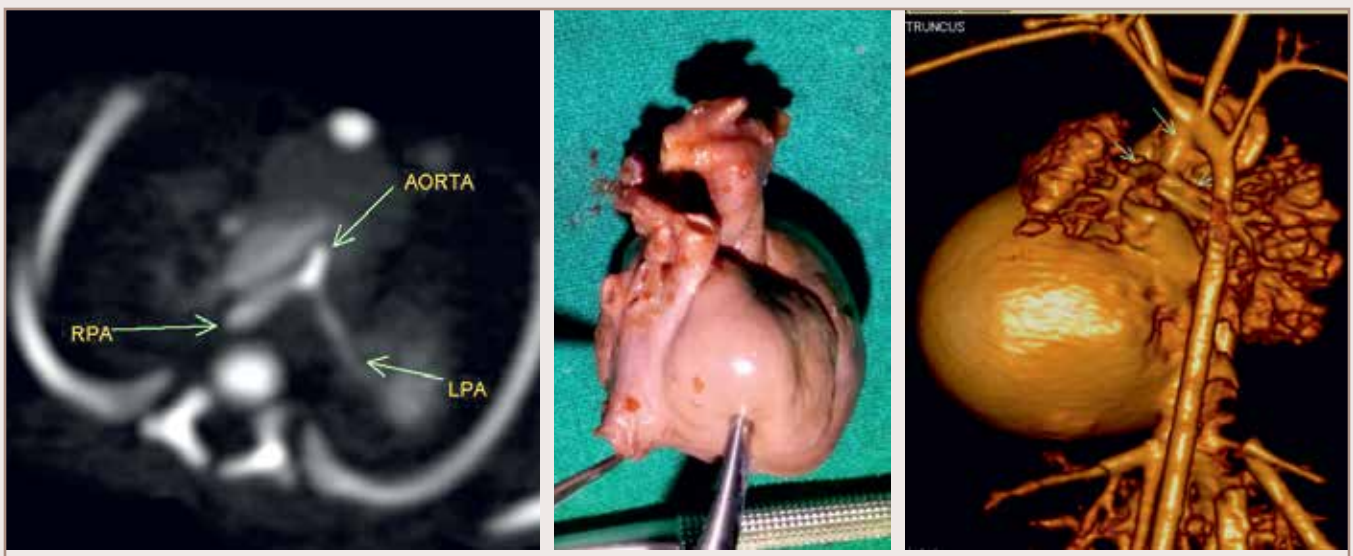

Figure : Abortus Contrast CT in Axial Shows Aorta And Both Pulmonary Arteries Arisisng From Single Outlet by Left Ventricular Injection/VRT in Colour Shows Dilated Cardiomegaly Single Outlet Giving Aorta and Both Pulmonary Arteries-Truncus Arteriosus

Case 9

Antenatal diagnosis of Posterior urethral valve with dilated urinary bladder, bilateral dilated ureters, bilateral hydronephrosis, bilateral echogenic kidneys. Pericardial effusion, echogenic intracardiac focus, talipes was made. Termination was done. Abortus sonography showed echogenic kidneys, multiple tiny cysts in kidneys, bilateral hydroureters, dilated urinary bladder, dilated posterior urethra. CT Cystogram was done by injecting iodinated contrast into urinary bladder.

Severely dilated urinary bladder, dilated posterior urethra, bilateral dilated ureters with reflux, bilateral dilated pelvicalyceal systems were shown on axial CT and coronal MIP.

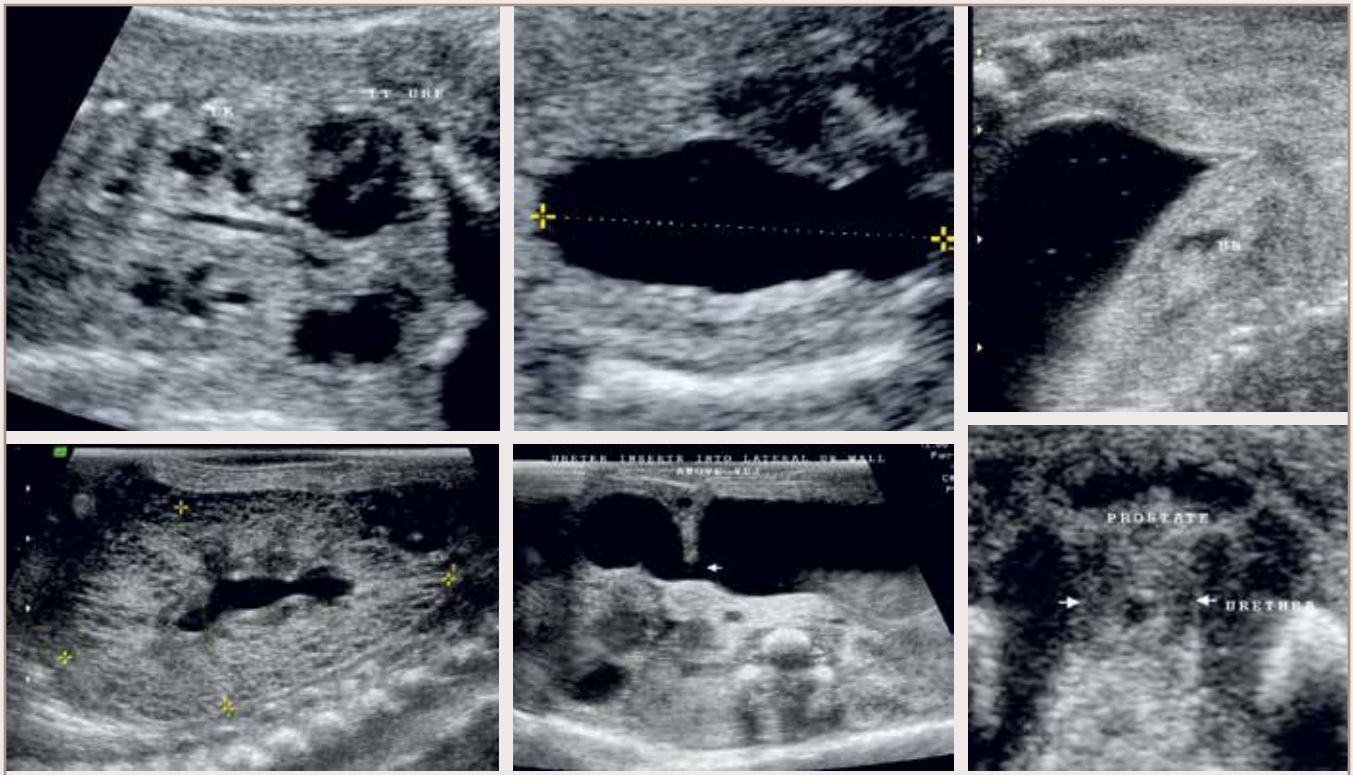

Figure : Antenatal Sonography Shows Bilateral Echogenic Kidneys With Hydroureteronephrosis And Dilated Urinary Bladder/ Abortus Sonography Shows Echogenic Kidney With Multiple Tiny Cysts and Dilate Ureter And Dilated Urinary Bladder Abortus Sonography Shows Dilated Urinary Bladder And Dilated Posterior Urethra

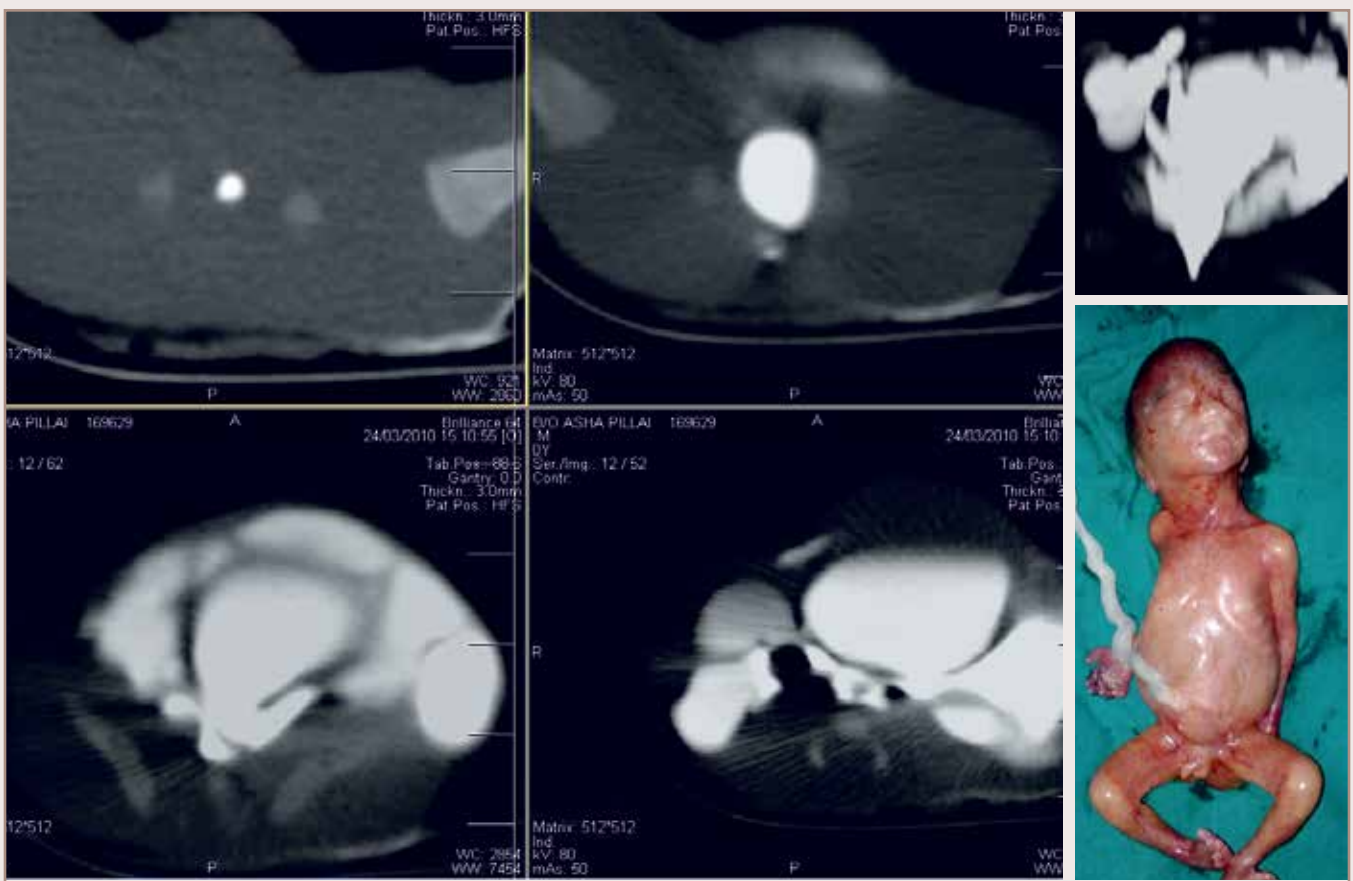

Figure :
Abortus Ct Cystogram Shows Dilated Posterior Urethra,dilated Urinary Bladder,dilated Ureters Due To Reflux of Contrast

Case 10

Antenatal diagnosis of Right atrial isomerism was done on the basis of dextrocardia with cardiac apex pointing to right, Absent pulmonary vein to Left atrium confluence-TAPVC, central liver, central stomach. Termination was done. Abortus CT Ventriculography was done. Contrast was injected into cardiac left atrium. No reflux of contrast was seen into pulmonary veins proving TAPVC. Cardiac apex was pointing to the right showing Dextrocardia, Liver was broad and central. Contrast filled IVC was seen in midline anterior to contrast filled aorta. Contrast was injected into mouth of abortus. CT gastro enterography was done. Contrast filled stomach was very small and was centrally placed. Gastroesophageal junction was abnormal. Gastroduodenal junction was abnormal and central. C Loop was straight and central. D J flexure was abnormal and central. Jejunal loops were abnormal and malrotated and central. Axial CT and coronal MIP were done.

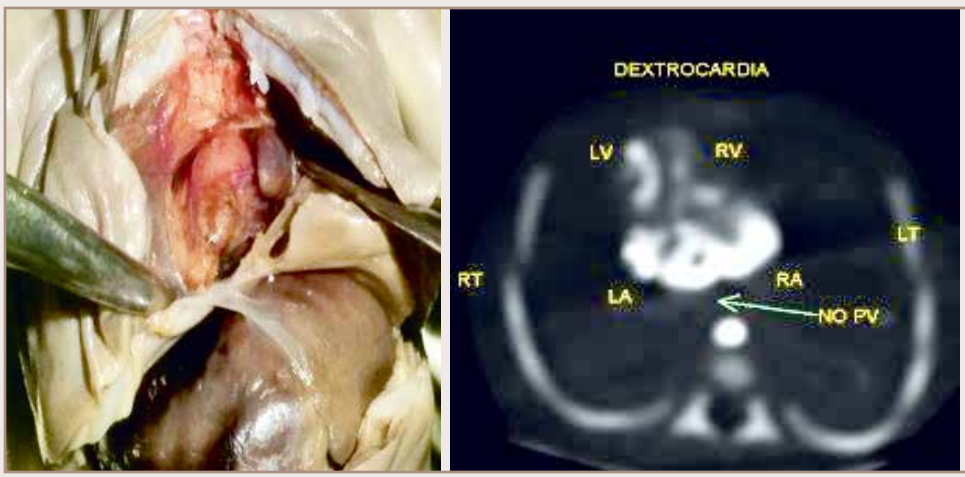

Figure :
Autopsy Shows Dextrocardia/Abortus CT Ventriculogram Shows Cardiac Apex Pointing to the Right/ absent Pulmonary Veins with Smooth Posterior Walls of Left Atrium-Tapvc

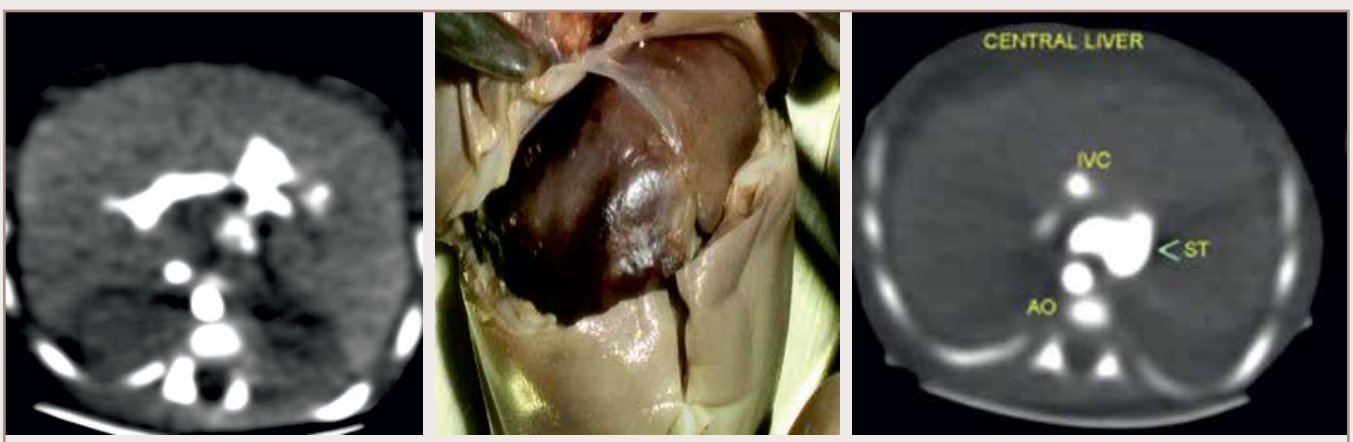

Figure : Abortus Axial CT Showing Central Liver/ Autopsy Showing Central Liver CT Gastrography Showing Central Stomach/central Liver And IVC Anterior to Aorta Seen

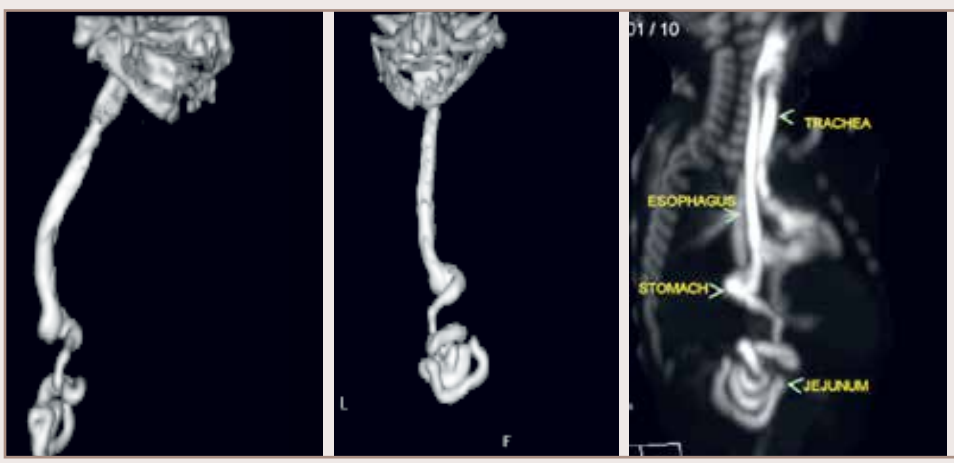

Figure :
Abortus CT Gastrogram-normal Esophagus/ Midline Gastro Esophageal Junction/small Midline Stomach and Duodenum/abnormal D J Junction/malrotated Jejunum/midline Stomach and Midgut Malrotation

Case 11

Antenatal diagnosis of Double outlet left ventricle was done. Abortus CT Ventriculogram was done by injection iodinated contrast into left ventricle. Both Aorta and pulmonary artery are seen to arise from left ventricle and are transposed with anterior aorta and posterior pulmonary artery. Axial CT, Sagittal MIP, Autopsy and VRT done.

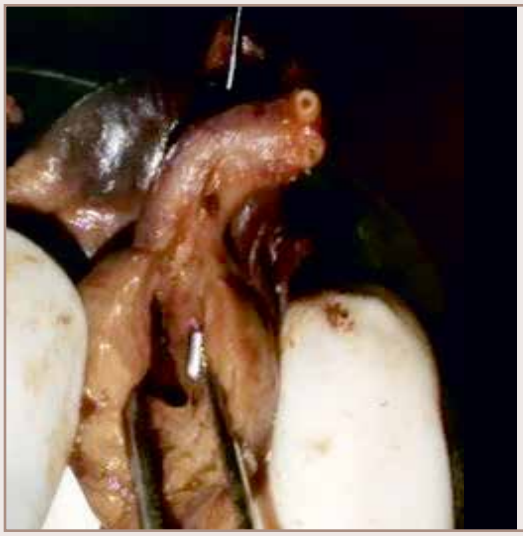

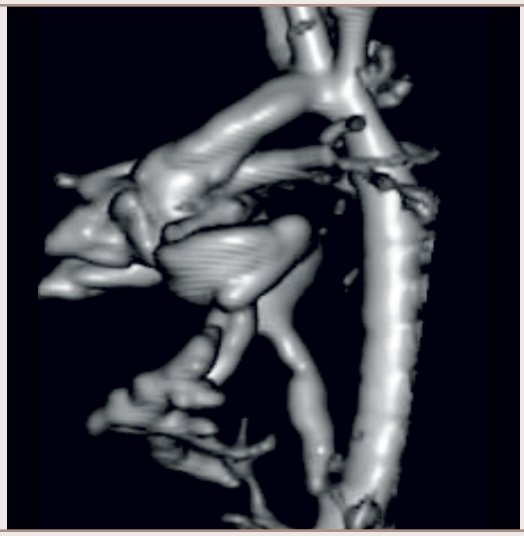

Figure :
Autopsy Shows Probe From PA Going Into LV Which Gives Rise to Aorta/

Ct Contrast Ventriculogram VRT Showing Anterior Aorta and Posterior MPA /both Arise From LV Injection-dolv

Case 12

Antenatal diagnosis of LEFT ISOMERISM was made by detection of Interrupted IVC, Azygous continuation with its presence to right of aorta at same coronal level-DOUBLE BUBBLE SIGN, right sided stomach, central liver. Termination was done. Autopsy was done which showed Bilobed right lung, interrupted IVC, Azygous continuation, Central liver, right sided stomach and right duodenum, malrotated small bowel, normal colon.

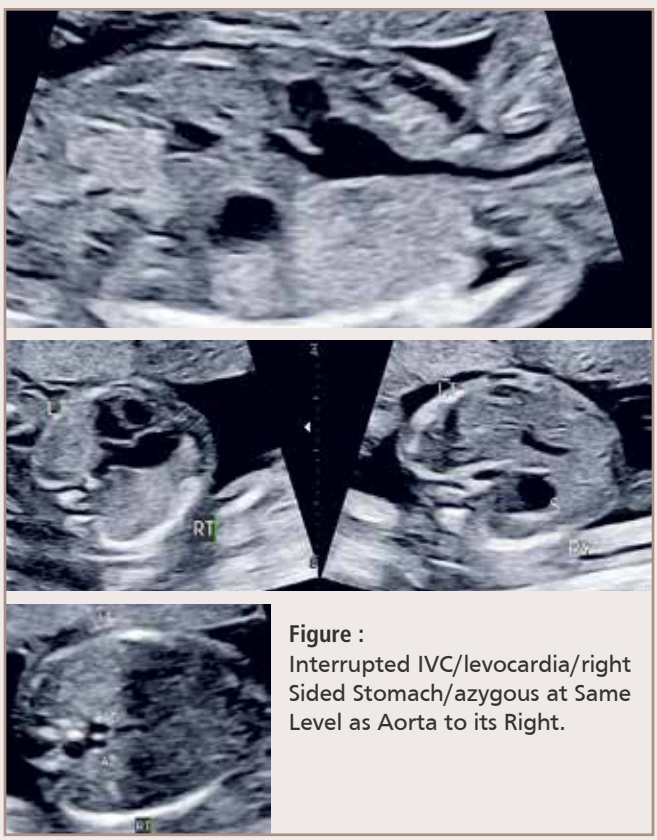

Figure :
Interrupted IVC/levocardia/right Sided Stomach/azygous at Same Level as Aorta to its Right.

Figure :

Right Stomach
Right Duodenum
Small Bowel Malrotation
Normal Colon
Central Liver
Bilobed Right Lung
Normal Heart

Case 13

Antenatal diagnosis of semi-lobar holoprosencephaly was made by detecting Intracranial severely dilated cerebral lateral ventricles, dorsal cyst, fused thalami, Facial midline cleft lip, cleft-palate, hypotelorism, orbital hypoplasia. Termination was done. Abortus CT showed severely dilated cerebral lateral ventricles, dorsal cyst, fused thalami, cleft lip cleft palate, flat face. Axial CT, coronal and sagittal reformation, SSD, VRT done.

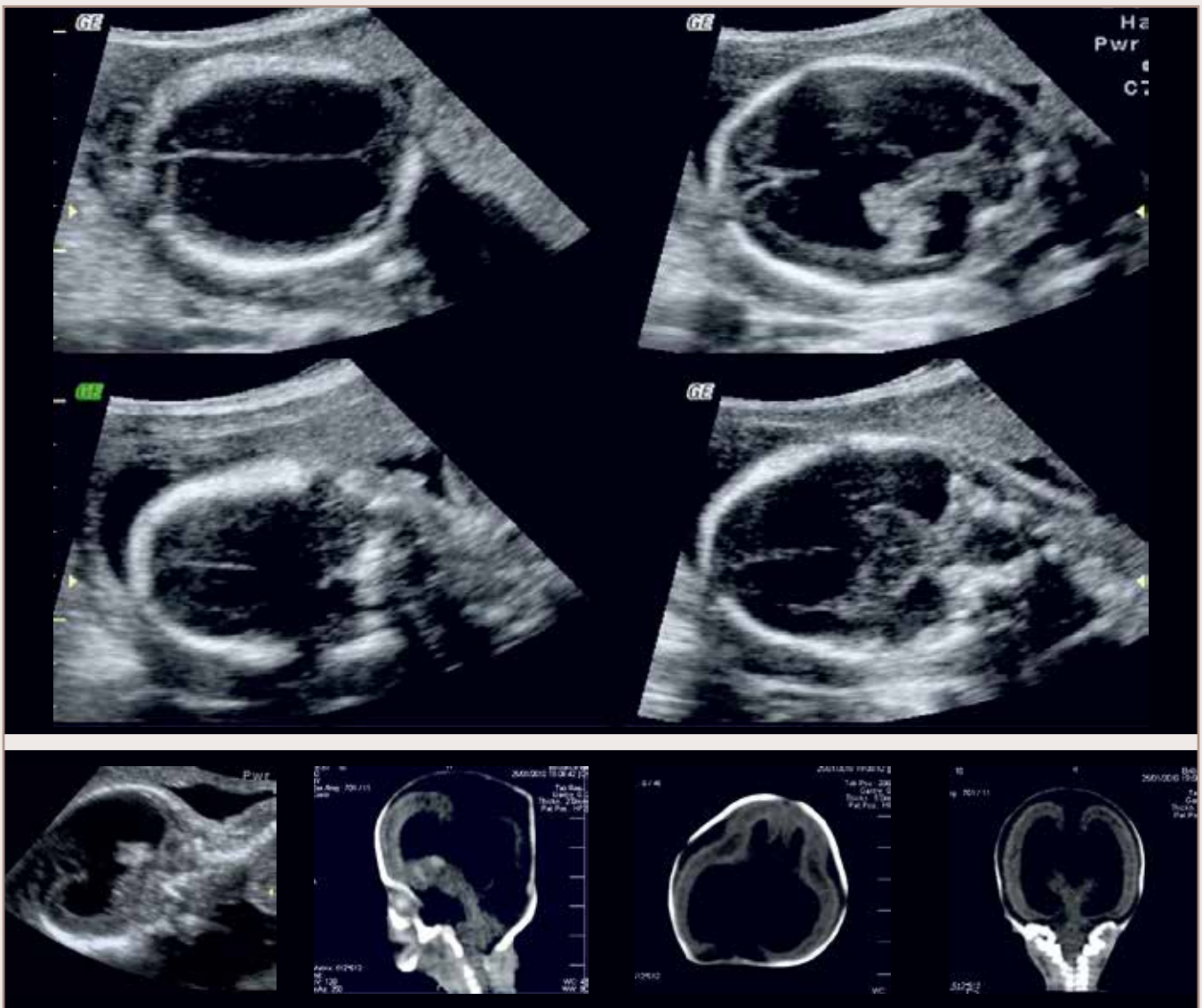

Figure : Antenatal Ultrasound Shows Dilated Ventricles, dorsal Cyst,fused Thalami Abortus CT in Axial Coronal and Sagittal Recons Show Semilobar Holoprocencephaly

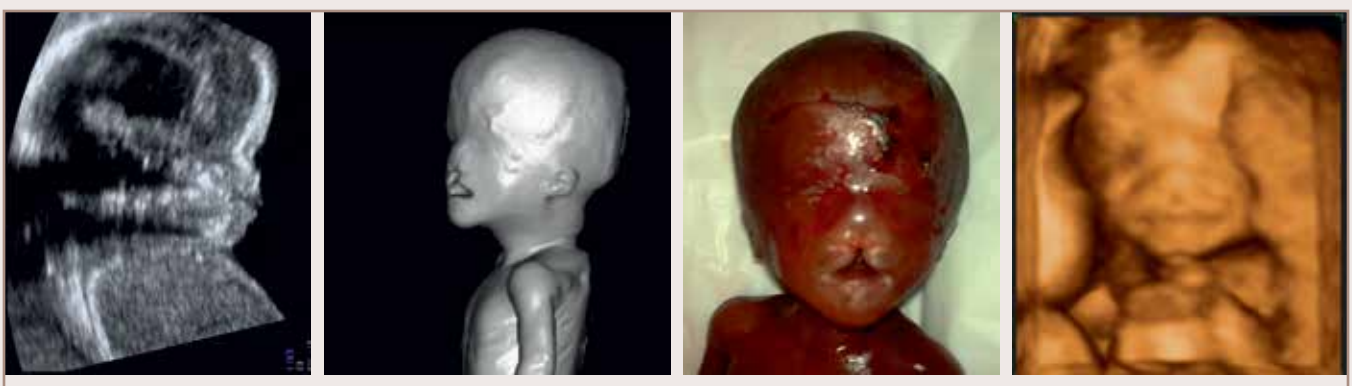

Figure : Aortus Sonography/CT,autopsy and Antenatal 3D Show Facial Cleft and Flat Face

Case 14

13-week foetus was antenatally diagnosed with Aortic atresia, hypoplastic left heart, cleft lip, single umbilical artery, unossified nasal bone and cystic hygroma and Ductus venosus A wave reversal. Termination was done. Abortus sonography showed Cleft lip, unossified nasal bone, cystic hygroma. Autopsy showed hypoplastic left heart, aortic atresia, cleft lip single umbilical artery. Antenatally undiagnosed small polydactyly was seen.

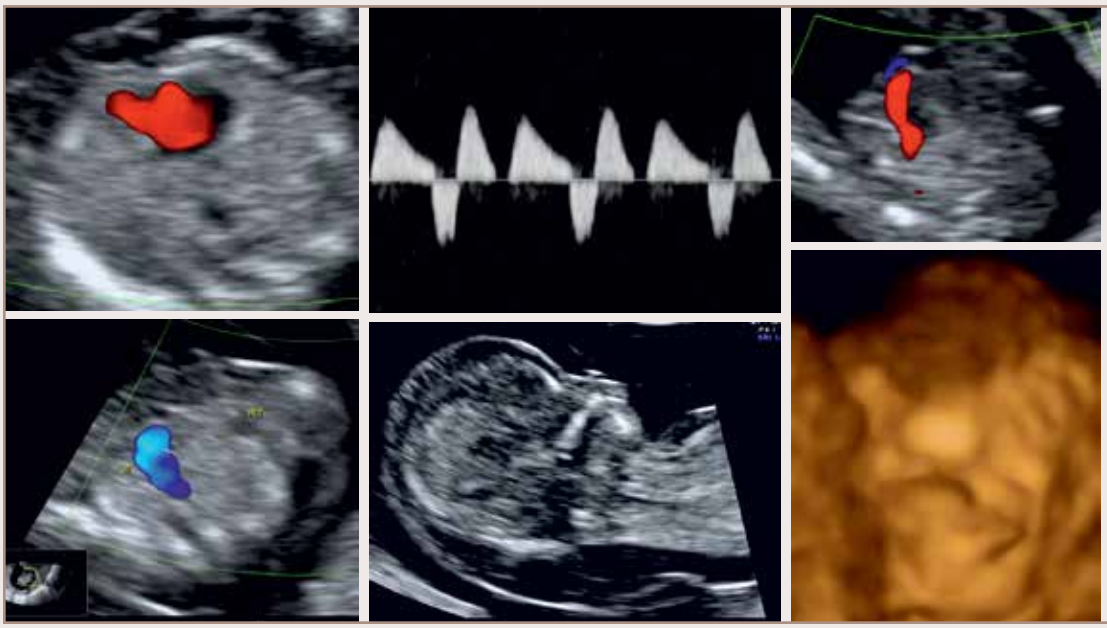

Figure : 12 Week Fetus Small Left Ventricle in 4 Chamber View/Absent Aorta in 3VTV/Cystic Hygroma/unossified NB/single Umbilical Artery/Cleft Lip in 3D

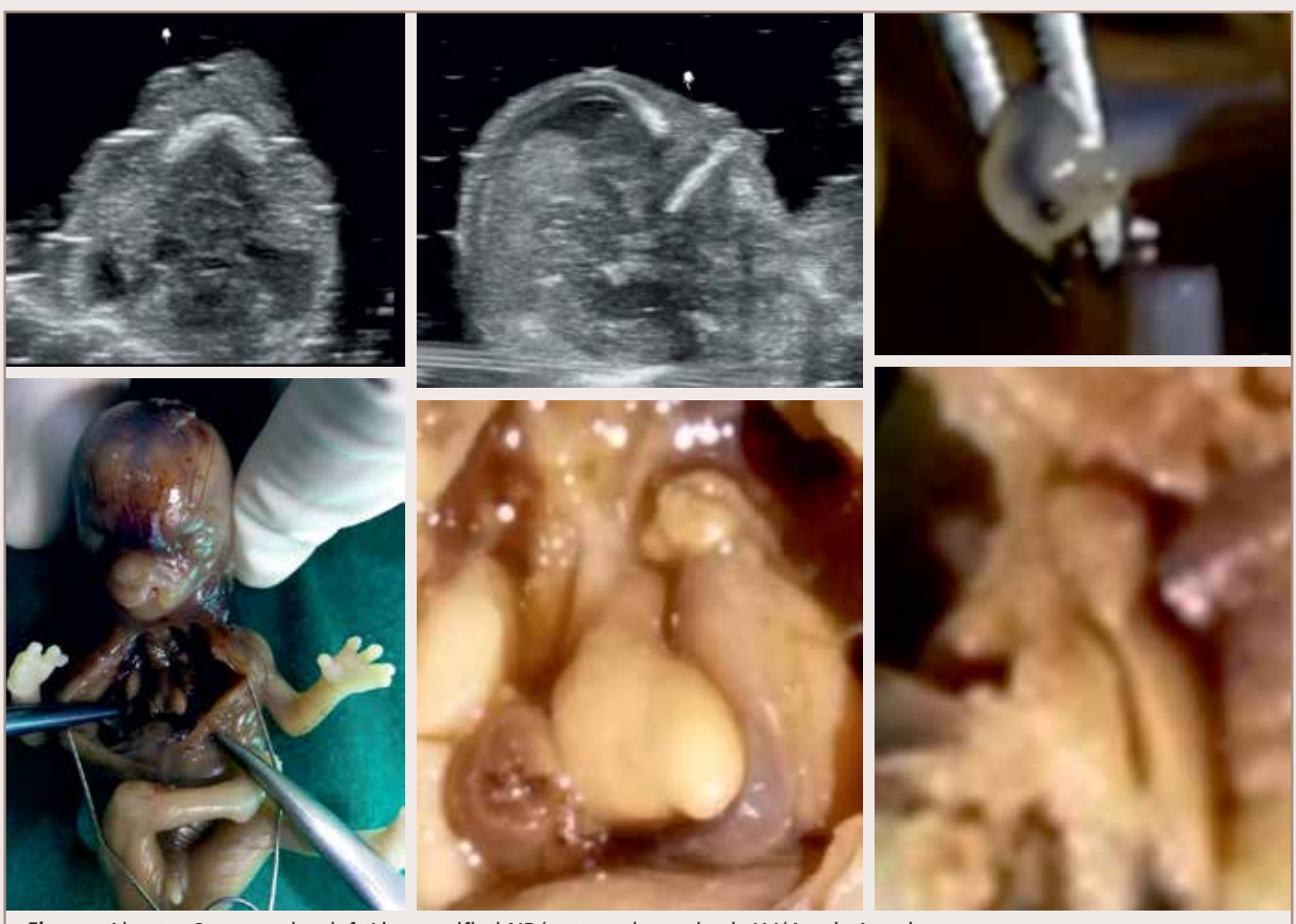

Figure : Abortus Sonography-cleft Lipunossified NB/autopsy-hypoplastic LV/Aortic Atresia

Spectrum of Fetal Limb Anomalies

Source: Source: Thakur S, Chaddha V, Gupta R, Singh C, Dagar S, Shastri A, Tiwari B, Kavitha, Sethia V, Malik M, Jain P, Kapoor A, Kapoor A, Kapoor T, Kapoor A, Kapoor R, Kumar M, Uppal R. Spectrum of fetal limb anomalies. J Clin Ultrasound. 2023 Jan;51(1):96-106. doi: 10.1002/jcu.23273. Epub 2022 Aug 10. PMID: 36639848.

Scan QR Code for more

Dr Puneet Jain
Director - Radiology,
Fortis Hospital,
Shalimar Bagh

Dr Seema Thakur
Senior Consultant - Radiology,
Fortis La Femme, GK-II,
New Delhi

Abstract

Purpose: Antenatal detection of limb anomalies is not uncommon, and pregnancies are usually terminated in view of the expected physical handicap. The aim of this retrospective observational study is to delineate the spectrum of fetal limb anomalies and provide evidence in support of complete postnatal evaluation in establishing recurrence risk.

Methods

We present 54 cases of limb malformations detected antenatally and discuss the spectrum of abnormalities, the utility of fetal autopsy, and genetic testing to establish recurrence risk in subsequent pregnancies.

Results: 16/54 cases were isolated radial ray anomalies. There were five cases of amniotic band syndrome, five limb body wall complex cases, three VACTERL (vertebral defects, anal atresia, cardiac defects, tracheoesophageal fistula, renal anomalies, and limb abnormalities) associations, one case of sirenomelia, two cases of limb pelvis hypoplasia, and one case of OEIS (Omphalocele Exstrophy Imperforate anus and spinal defects). Four foetuses with non-isolated radial ray anomaly had trisomy 18. One case with bilateral radial ray defect had a mutation in the FANC-E gene confirming Fanconi anemia. Twelve cases were unclassified.

Conclusion

Autopsy is the most important investigation in foetuses with limb anomalies. We suggest chromosomal microarray (CMA) as a first-tier test after autopsy. However, in cases of bilaterally symmetrical limb anomalies, in case of previous similarly affected child, or history of consanguinity, whole exome sequencing (WES) can be offered as the primary investigation, followed by CMA if WES is normal.

Keywords

Amniotic band defects, autopsy, limb anomaly, microarray, radial ray defect, Robert syndrome,VACTERL

Comprehensive Textbook of Clinical Radiology (Vol-V: Obstetrics and Breast) - Intermediate and High-Risk Lesions

Dr Vaneeta Kapur
Senior Consultant - Radiology,
Fortis Hospital, La Femme, GK-II, New Delhi

Phyllodes Tumour

First described in 1838 by Miller and was termed 'cystosarcoma phyllodes' because of its leaflike pattern. Miller believed it to be benign. The first case of malignant phyllodes tumour was described in 1931. Phyllodes tumours are rare and account for less than 1% of all mammary tumours.

Only 2%–3% of fibroepithelial neoplasms of the breast. Phyllodes tumours, like fibroadenomas, are composed of epithelial tissue and connective tissue stroma but have higher stromal cellularity since they develop

primarily from periductal stroma. Lobular elements are sparse. The tumour cells are spindle-shaped, with varying degree of nuclear atypia and mitotic activity. The tumour does not have a true capsule. Typical clefts seen in the tumour are due to hypercellular overgrowth, in convoluted pattern.

Clinical Presentation

Phyllodes tumours present as clinically palpable firm-to-hard round masses of reasonably large size, not felt earlier or showing a recent or rapid increase in size. Presenting at any age (phyllodes present between 15 and 65 years of age), they are commonly found in women between 30–50 years, with highest incidence between 40 and 50 years for both benign and malignant phyllodes. Phyllodes may be categorized as benign, borderline or malignant or as low grade or high grade. The latter classification is gaining favour, as all have to be excised. The histopathological features, such as the degree of atypia, number of mitotic figures and infiltration of margins, are of significance. There is no known genetic predisposition, nor lifestyle choices that seem to affect the development of this tumour.

Imaging Features

Mammographic and sonographic features of low/high-grade, benign/malignant phyllodes tumours overlap.

Mammography

Phyllodes tumours appear as round to oval-shaped masses in older women, with circumscribed margins or slightly ill-defined margins at close inspection (Fig.Ai & Aii). Sometimes, margins are obscured due to surrounding parenchyma. The mass is of equal, high or low density. Spiculations are not a feature. Calcification may or may not be present; however, microcalcifications are not seen.

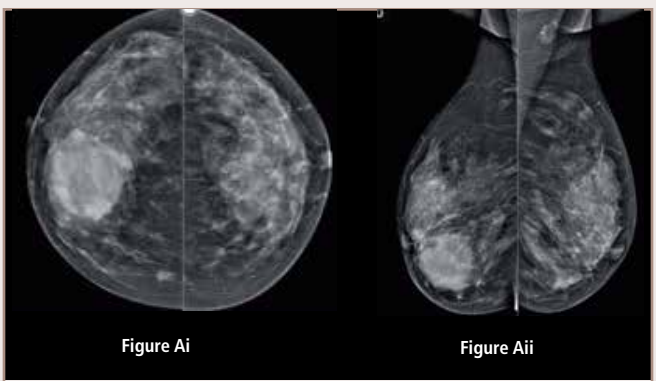

Figure : Craniocaudal (CC) and mediolateral oblique (MLO) views of bilateral mammogram show a round hyperdense mass with partially indistinct margins in the anterior and mid-depth in the retroareolar region in the right breast.

Ultrasonography

The mass is round or oval, to hypoechoic in echotexture and has circumscribed or indistinct margins. Posterior acoustic enhancement is present. Phyllodes tumour is difficult to distinguish from a fibroadenoma, except the presence of clefts (Fig. Bi, Bii, Biii&Biv)). Vascularity, both central and peripheral, is a classic feature.

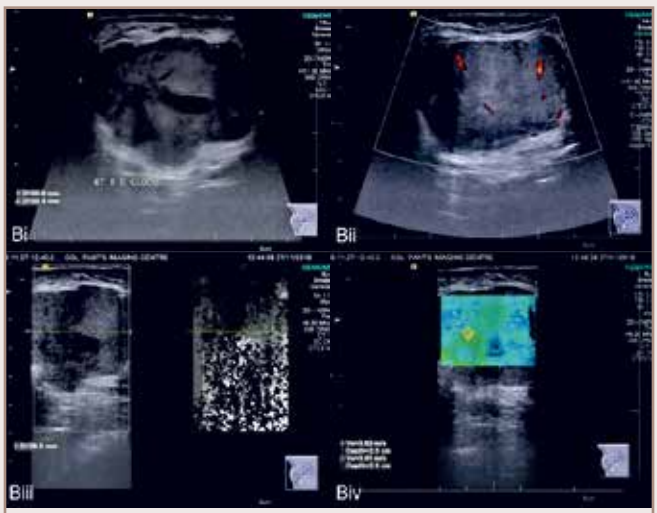

Figure : US scan shows a round hypoechoic mass, with indistinct margins, in a parallel orientation, with large anechoic clefts within, located at the 6 o'clock axis, close to the nipple. It measures 51 x 35 mm. The mass shows increased central and peripheral vascularity. Strain elastography reveals it to be intermediate. Quantitative elastography (VTIQ) is 3.91 m/s

Elastography

The role of elastography is still being researched in differentiating phyllodes from fibroadenoma. However, it does appear to have future potential. Strain elastography provide additional information and has a significant potential in improving specificity. Fibroadenomas have lower stiffness than phyllodes tumours.

MRI

Benign phyllodes are round or lobulated mass with smooth margins and a heterogeneous internal structure suggestive of occasional cystic changes or internal septations. They appear hypointense on T1-weighted (T1W) and T2-weighted (T2W) images, with hypointense appearance of the surrounding tissues on T2W images and gradual to rapid enhancement on dynamic contrast images.

Malignant phyllodes ((Fig. Ci, Cii,&Ciii)). The mass shows cystic changes, irregular walls with high signal intensity on T1W images, low signal intensity on T2W images with or without low apparent diffusion coefficient (ADC) on diffusion- weighted imaging (DWI).

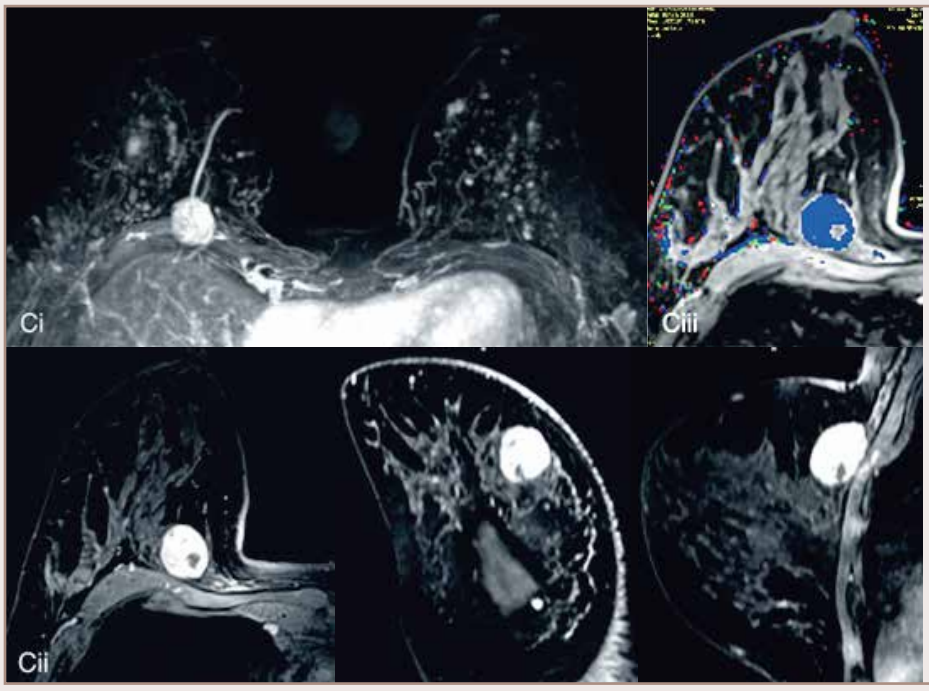

Figure : Pathology was inconclusive. MR enclinch the diagnosis. MRI mimic subtraction MIP (minimum intensity projection) image shows an enhancing mass in the right breast along with multipic enhancing, foes in both beasts. MRI, axial, coronal and sagitial reformaited dynamic posiconirast fat suppressed GR image of the right breast shows a circumscribed fairly homogeneously enhancing mass at the 2:30' clock axis in the posterior depth close in the chest wall. Corresponding computer aided design (CAD) image: shines persistent kinetics depicted as blue color on the color code CAD map. Source: Image Courtesy: De Sangeeta Taneja, Indraprastha Apollo Hospital, Delhi).

Management

In all cases, wide local excision with more than 1-cm margin is recommended. If there is a clinical suspicion core needle biopsy (CNB) is performed. If on CNB the diagnosis is fibroadenoma, a close clinical follow-up is advised if the mass is large and there is a strong radiological suspicion of phyllodes. Differentiating juvenile fibroadenoma from phyllodes can be challenging. On CNB, regardless of whether the phyllodes is benign or borderline malignant, wide excision without axillary staging is done. Malignant phyllodes tumour may spread haematogenously. Lymph node spread is unusual and has rarely been reported. For large malignant masses, even mastectomy with radiotherapy and chemotherapy are considered.

Prognosis

The survival rate depends on malignant potential and the extent of surgical resection and resection of margins. The overall 5-year survival rate is 90%. In high-grade phyllodes, the 5-year survival is 65%.

Differential Diagnosis

The most common D/D is the fibroadenoma, which is usually discovered at a younger age and does not show such a rapid increase in size or the presence of clefts. There is often a diagnostic dilemma in patients who have multiple coexisting fibroadenomas

Metaplastic carcinoma is another mass that mimics it. Mammogram reveals a large oval to round mass with margins, which may be slightly irregular. On USG, the mass is hypoechoic irregular margins is parallel in orientation.

Bibliography

1. Liberman L, Bonaccio E, Hamele-Bena D, Abramson A F, Cohen M A, DershawD D: Benign and malignant phyllodes tumors : mammographic and sonographic findings. Radiology 1996; 198:121-124
2. GoelNeeti B., KnightThomas E. ,PandeyShilpa, et al: Fibrous Lesions of the Breast: Imaging-Pathologic Correlation. RadioGraphics 2005; 25:1547–1559:
3. FederJay M., de Paredes Ellen Shaw, Hogge Jacquelyn P., WilkenJennifer J. :Unusual Breast Lesions: Radiologic-Pathologic Correlation. Radio Graphics 1999; 19:S11-S26
4. HarveyJennifer A.Unusual Breast Cancers: Useful Clues to Expanding the Differential Diagnosis. Radiology: Volume 242: Number 3—March 2007
5. AdamietzB R, Kahmann L, FaschingP A,et al Differentiation Between Phyllodes Tumor and Fibroadenoma Using Real Time Elastography. Ultraschall Med. 2011 Dec;32Suppl 2:E75-9.

Miscellaneous

Severe Pulmonary Manifestations of Leptospirosis

Dr Narayan Solanki
Consultant- Radiology,
Mahajan Imaging, Fortis Escorts Hospital, Jaipur

Abstract

Leptospirosis is a common zoonosis in tropical countries with hepatic, renal, pulmonary CNS and skeletal muscle manifestations. The pulmonary manifestations are usually mild. However, features of severe disease such as pulmonary hemorrhage and acute respiratory distress syndrome, can present as a diagnostic dilemma and can cause delayed diagnosis, thus resulting in delay in optimal treatment.

Introduction

Leptospirosis is typically a biphasic illness. It can also present as a fulminant monophasic illness which rapidly progresses to refractory shock, jaundice, renal failure and pulmonary hemorrhage. The diagnosis is usually made by clinical and laboratory features. The association of leptospirosis with pulmonary involvement is not easily detected even in endemic areas. Due to multi-system involvement and changing nature of illness, its diagnosis is often delayed and can be misdiagnosed even in areas of high prevalence. We present two cases showing imaging findings in severe pulmonary manifestations.

Case 1

A 74-year-old male presented with fever, breathlessness, cough with hemoptysis and chest pain with known history of hypertension. Laboratory investigations tested positive for leptospira IgM Antibody. Chest radiographs showed bilateral diffuse patchy infiltrates. HRCT imaging revealed confluent hilar-parahilar ground glass opacities and consolidations associated with bilateral pleural effusion.The management included intravenous antibiotics (including doxycycline), steroids, oxygenation, plasmapheresis and intravenous immunoglobulin. The patient made gradual recovery and was weaned off of oxygen. Repeat HRCT chest revealed significant resolution of bilateral consolidations.

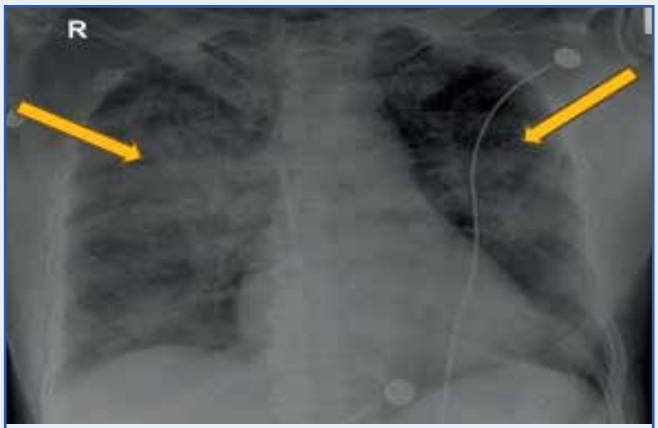

Figure A : Chest Radiograph AP bilateral diffuse patchy infiltrates (yellow arrows)

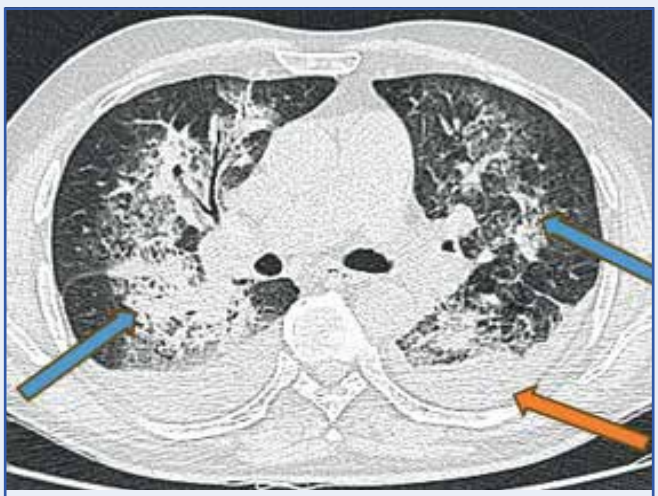

Figure B : HRCT chest axial image confluent hilar-parahilar ground glass opacities and consolidations (blue arrows) with bilateral pleural effusion (orange arrow)

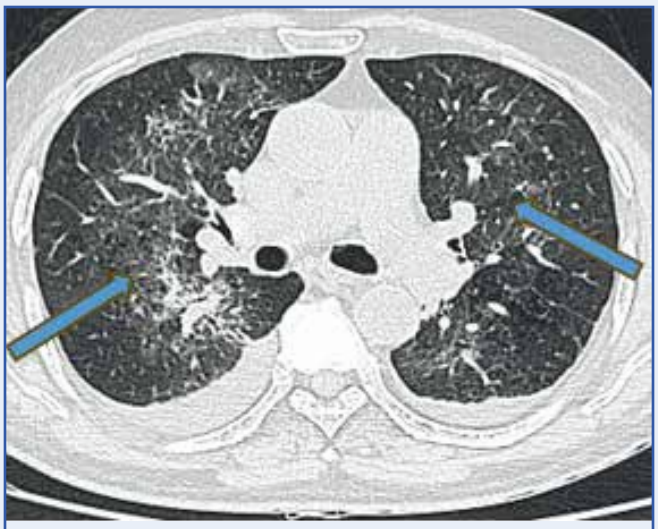

Figure C : HRCT chest axial image significant resolution of bilateral consolidations (blue arrows)

Case 2

A 29-year-old female presented with fever with skin rashes involving all four limbs, abdominal pain, loose motions and shortness of breath. Laboratory investigations tested positive for leptospira IgM Antibody.Chest radiograph showed bilateral diffuse confluent infiltrates with obliteration of bilateral costophrenic angles. HRCT imaging revealed large confluent hilar-parahilar consolidations with ground glass opacities and bilateral pleural effusion with features of ARDS.The management included achieving hemodynamic stability, broad spectrum antibiotics including doxycycline, supportive medications, FFP in view of thrombocytopenia and intubation with ventilator support.

Discussion

Chest radiograph and HRCT chest are helpful to find out involvement and severity in patients of leptospirosis. Even though manifestations on chest radiographs may mimic viral pneumonia, bronchopneumonia, tuberculosis, other causes of pulmonary hemorrhage or adult respiratory distress syndrome; patterns of rapidly evolving, diffuse nodular or confluent pulmonary lesions along with fever and appropriate clinical settings, could reasonably direct towards diagnosis of leptospirosis.

Radiological severity correlates with severity of pulmonary symptoms. Recently, an increasing number of cases have been reported with pulmonary hemorrhage as a prominent feature, preceding all other manifestation of leptospirosis such as jaundice and acute renal failure. Severe pulmonary form of leptospirosis is considered distinct from Weil's disease because pulmonary presentation has been found to occur independently without renal and hepatic impairment. Manifestations of these severe pulmonary forms, including respiratory distress or pulmonary hemorrhage, are usually massive, potentially leading to ARDS, have a rapid and severe course with high mortality rates.

As chest radiograph typically shows abnormality in initial stages, it can often allow an early diagnosis and proper guide to management before serologic tests for Leptospira become positive. Also, effectiveness of treatment and improvement can be assessed by follow-up with these investigations. A high index of suspicion with adjunct radiological & serological findings, appropriate treatment and supportive therapy, can facilitate optimum management especially in severe respiratory failure.

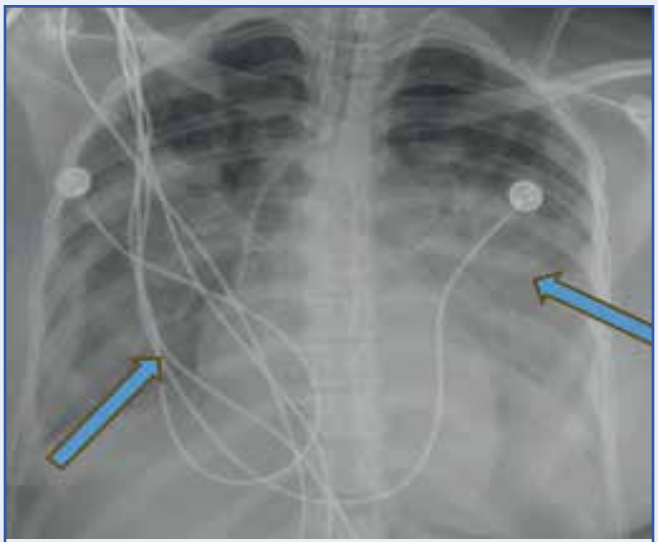

Figure A : Chest Radiograph AP bilateral diffuse confluent infiltrates (blue arrows)

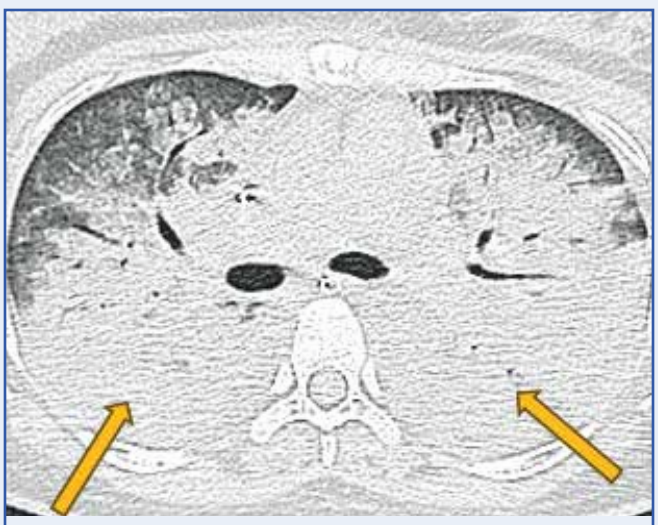

Figure B : HRCT chest axial image large confluent hilar-parahilar consolidations and surrounding ground glass opacities and (yellow arrows)

Safety and Diagnostic Yield of Transbronchial Lung Cryobiopsy by Flexible Bronchoscopy using Laryngeal Mask Airway in Diffuse and Localized Peripheral Lung Diseases: A Single-centre Retrospective Analysis of 326 Cases

Dr Sunita Ahlawat
Principal Consultant - Histopathology, Agilus Fortis Memorial Research Institute, Gurugram

Dr Priti Jain
Principal Consultant - Histopathology, Fortis Memorial Research Institute, Gurugram

Dr R K Verma
Additional Director – Radiology, Fortis Memorial Research Institute, Gurugram

Dr Balkar Singh
Principal Director – Anaesthesiology, Fortis Memorial Research Institute, Gurugram

Dr Ajay Kumar
Additional Director – Pulmonology and Sleep Medicine, Fortis Memorial Research Institute, Gurugram

Dr Manoj Kumar Goel
Director and Head – Pulmonology and Sleep Medicine, Fortis Memorial Research Institute, Gurugram

Dr Gargi Maitra
Consultant – Pulmonology, Fortis Memorial Research Institute, Gurugram

Abstract

Background: Intubation with either an endotracheal tube or a rigid bronchoscope is generally preferred to provide airway protection as well as to manage unpredictable complications during transbronchial lung Cryobiopsy (TBLC). The laryngeal mask airway has been described as a safe and convenient tool for airway control during bronchoscopy. Aims and Objectives: In this study, we evaluated the safety and outcome of using a laryngeal mask airway (LMA) as a conduit for performing TBLC by flexible video bronchoscopy (FB). Methods: We retrospectively analysed the database of the patients who underwent TBLC between November 2015 and September 2019. The procedure was performed using FB through LMA under general anaesthesia. Prophylactic occlusion balloon was routinely used starting January 2017 onwards. Radial endobronchial ultrasound (R-EBUS) guidance was used for TBLC in the localized lung lesions when deemed necessary. Multidisciplinary consensus diagnostic yield was determined and periprocedural complications were recorded. Results: A total of 326 patients were analysed. The overall diagnostic yield was 81.60% (266/326) which included a positive yield of 82.98% (161/194) in patients with diffuse lung disease and 79.54% (105/132) in patients with localized disease. Serious bleeding complication occurred in 3 (0.92%) cases. Pneumothorax was encountered in 8 (2.45%) cases. A total of 9 (2.76%) cases had at least 1 major complication. Conclusion: This study demonstrates that the use of LMA during TBLC by flexible bronchoscopy allows for a convenient port of entry, adequate airway support and effective endoscopic management of intrabronchial haemorrhage especially with the use of occlusion balloon.

Key Words

Cryobiopsy, interstitial lung disease, radial endobronchial ultrasound, transbronchial biopsyt

Novel Procedure: Image Guided ACL Debridement

Dr Rajat Bhargava
Director and Head – Radiology,
Fortis Hospital, Mulund

Abstract

We present a novel procedure of image guided debridement of mucoid degeneration of ACL. Mucoid degeneration of ACL is a less commonly reported density, however, is increasingly being recognized as a common cause of knee pain, with a reported incidence of 0.7-5.3% on the knee MRIs. The pain is typically located posteriorly with an associated restriction of knee flexion.

Mucoid ACL degeneration is characterized by thickening of the ACL by mucinous material with a spectrum ranging from mucoid degeneration to ganglion cyst formation. The etiology is disputed with two most common theories of origin being, degenerative and synovial insinuation (3,4,5) various studies have proposed different causes for pain which include neurotendinous nociceptor irritation during flexion and a mechanical impingement on the posterior cruciate ligament / posterior capsule (3, 9)

The preferred modality for diagnosis of mucoid degeneration of ACL is MRI. It reveals a spectrum of findings ranging from mucoid degeneration, giving a classic celery stalk appearance which may or may not be associated with ganglion cyst (Fig1). The ganglion cyst may be confined to the ligament, extend into the intercondylar notch, near the tibial footprint and reduced varying degrees of bone marrow edema and cystic change at the femoral and tibial attachments (4, 5)

In refractory cases to conservative management, surgical an arthroscopic debulking and decompression of the mucinous material from the ACL are considered the preferred line of management with or without notch plasty (3, 11, 12). Over debridement has an associated risk of instability and may require ACL reconstruction surgery in the future (13) lobe. Very few case reports of the image guided mucoid ACL debridement are available.

We performed this procedure on 26 symptomatic patients with knee pain with MRI confirmation of mucoid degeneration. We use the CT guidance for needle placement. Patient was placed prone and needle was placed into the cystic and swollen portion of the ACL (Fig2). An attempt to aspirate the thick gelatinous fluid was made and subsequently several ligament fenestrations were performed with a needle. After withdrawing the needle from the ligament, a 2ml mix of Bupivacaine and, 40mg Triamcinolone was injected into joint. All patients reported immediate pain relief with average pain scores improving from 7.7 to 2.4 (Fig3) The knee flexion angle improved from 95° to 120° (Fig4). Patient were followed for a variable time period of 6 months to 12 months. 81% of patients reported excellent 19% reported average and 0% patients reported poor Satisfaction scores

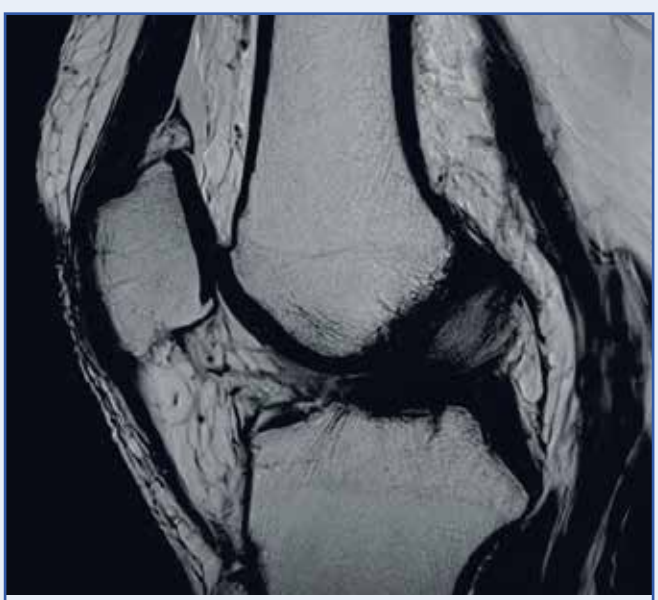

Figure 1 : MRI PD sagittal image showing swollen hyperintense ACL suggesting mucoid degeneration

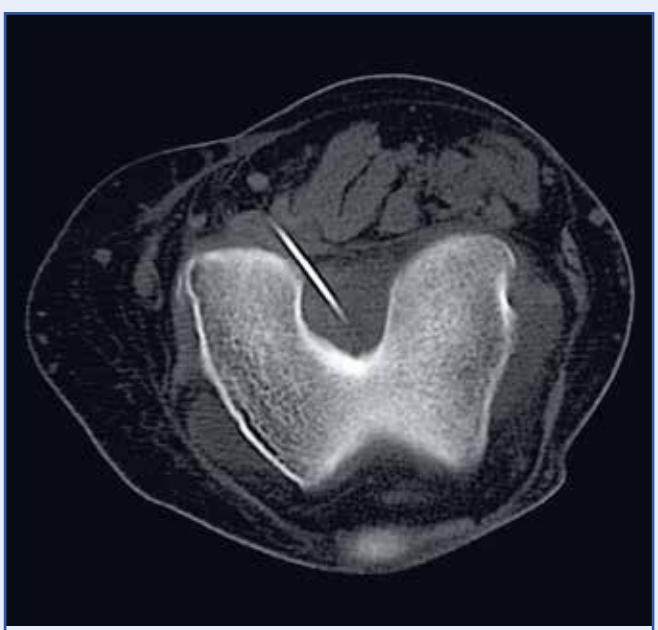

Figure 2 : CT image showing needle placed in the ACL in intercondylar notch

Figure 3: Mean VAS score at various assessed time-points

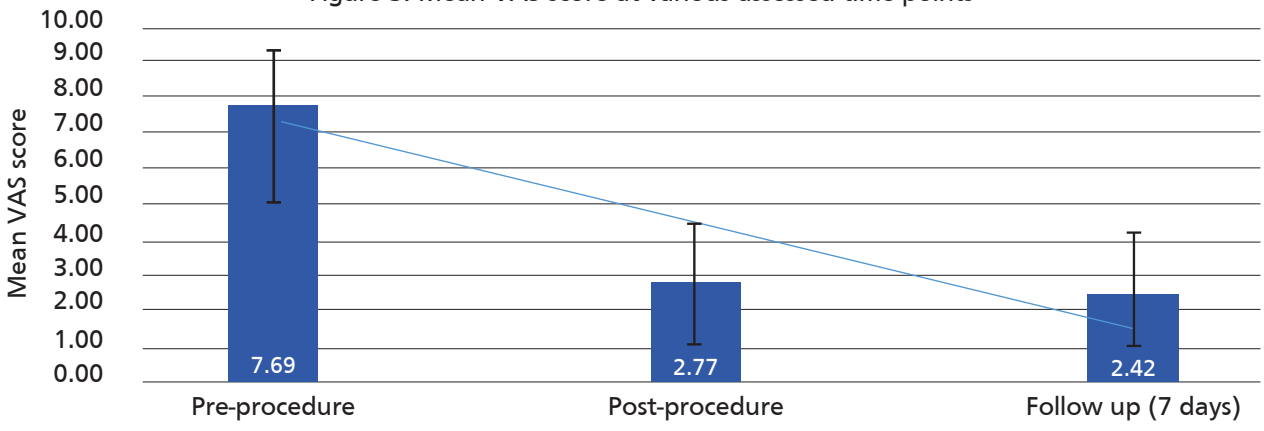

Figure 4: Mean flexion at various assessed time-points

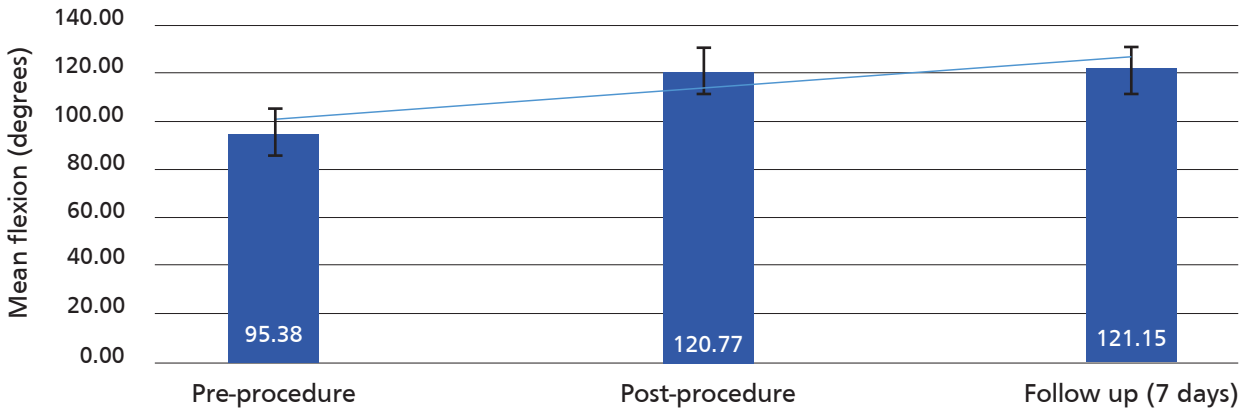

VAS Score-Based Patient Distribution			
VAS score range	Pre-procedure	Post-procedure	Follow-up (7 days)
0 to 3	0	19 (73.08%)	21 (80.77%)
4 to 6	2 (7.70%)	7 (26.92%)	5 (19.23%)
7 to 10	24 (92.3%)	0	0

None of our patient has complained of post-procedure instability which is a potential complication of surgical debulking. There were no neurovascular complications and only 2 patient's complaint of post-procedure pain which resolved within 24 hours with oral pain medications. These reinforced versatility and CT features. Image guided ACL mucoid degeneration decompression appears to be safe, simple technique which shows promising results in the short and long-term.

Bibliography

1. Ahuja, Ankita etal (2021). Role of ultrasound-guided decompression in management of mucoid degeneration of the anterior cruciate ligament. Skeletal Radiology. 50. 10.1007/s00256-021-03750-7.
2. Matrawy KA, etal. Mucoid degeneration of the anterior cruciate ligament: frequently underdiagnosed entity in MRI. Egypt J Radiol Nucl Med. 2012;43(2):c227–33

The Beauty of Radiopharmaceutical Specificity in Positron Emission Tomography

Dr Sayed Junaid
Consultant and Head -
Nuclear Medicine and Molecular Imaging,
Fortis Hospital, Mohali

Positron Emission tomography involves the tagging of biomolecules by positron-emitting radiopharmaceutical helping researchers and clinicians to visualize complex biological processes depending on the pharmacokinetics of the biomolecule and its receptor which can be detected by visualizing the emitted positrons from the radiotracer.

F-18 fluorodeoxyglucose is the most widely used radiopharmaceutical as it depicts glucose metabolism within the body. Glucose metabolism is high in most tumors due to the upregulation of GLUT receptors and enzyme hexokinase (especially GLUT 1 and HK2) which transport the F-18 FDG molecule within tumor cells. The FDG is phosphorylated to FDG-6-phosphate which gets trapped in the tumor cells as the subsequent enzyme isomerase cannot act due to the presence of an electronegative fluorine atom at the second carbon of the FDG molecule. This molecule is essential in detecting areas of high glucose metabolism within the tumors.

Despite being such a good radiopharmaceutical FDG too has its pitfalls in tumors which display poor glucose metabolism like the case we will be discussing subsequently.

The current case is of a 92-year-old gentleman presenting to a urologist clinic with hematuria. On cystoscopy, a mass was visualized within the bladder wall and a biopsy was performed which turned out to be transitional cell carcinoma.

The patient was sent to our molecular imaging department to evaluate the stage of the tumor using F-18 FDG PET-CT. The whole body can of the patient shows subtly hypermetabolic nodes within the pelvic cavity with two non-hypermetabolic to subtly hypermetabolic sclerotic lesions in a thoracic vertebra and right iliac bone. The dual time point imaging of the distended bladder showed a hypermetabolic thickening along the left posterolateral aspect of the bladder collaborating with the history of a bladder tumor. The SUVmax values of the bladder lesion were significantly higher than the pelvic nodes as well as the sclerotic bone lesions.

On close evaluation of the base of the bladder, a suspicious hypermetabolic focus was noted in the peripheral zone of the prostate along the left posterolateral aspect which led to a suspicion of a possible second primary within the prostate. The patient was advised to undergo an evaluation of serum PSA levels as well as a multiparametric MRI of the prostate.

The clinician again called us in to perform a prostate membrane specific antigen (PSMA) PET-CT scan of the patient to determine the primary as well as the status of the metastatic lesions.

A subsequent Ga-68 PET-CT showed intense uptake of PSMA within the lesion in the peripheral zone of the prostate with no uptake in the contrast-enhancing thickening within the urinary bladder.

In addition, both the pelvic lymph nodes as well as the sclerotic bony metastases displayed PSMA uptake prompting the diagnosis of an early bladder tumor with stage IV prostatic malignancy (which has a far better prognosis and can be managed conservatively on hormonal therapy at his age).

The subsequent TRUS-guided biopsy confirmed our observations and the patient is doing well with surgery (transurethral resection of bladder tumor, TURBT and intravesical BCG instillation) and hormonal therapy/ bisphosphonates for stage IV carcinoma prostate with subsequent fall of serum PSA levels.

This case distinguishes how specific radiopharmaceutical can clear the fog of multiple malignancies in a single patient, their accurate staging and even the best sites for a tissue biopsy thereby holistically approaching the desired goals.

Prostate-specific membrane antigen (PSMA) is a 100 kD, 750 amino acid (AA) long type II transmembrane glycoprotein whose expression, is significantly up-regulated in prostate carcinoma and has been used in targeted therapy of diffuse PSMA expressing metastases using either Lutetium or Alpha therapies.

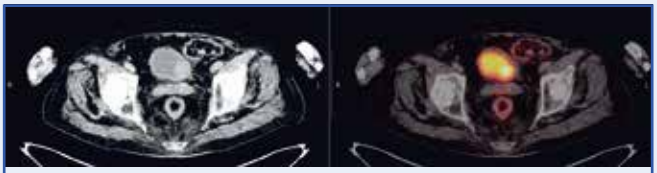

Figure 1 : FDG PET CT displaying FDG avid thickening along the left posterolateral aspect of the urinary bladder, subsequently found to be the cause of hematuria (transitional cell carcinoma).

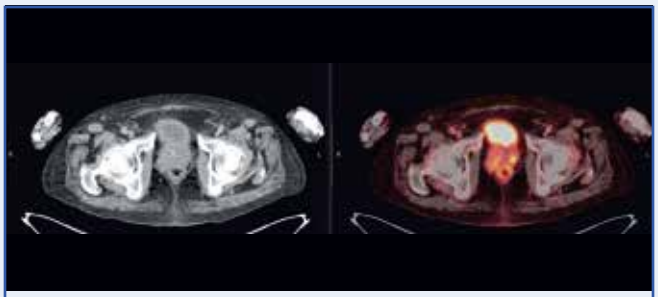

Figure 2 : FDG PET CT displaying a subtly FDG avid nodule in the peripheral zone of the prostate along the left posterolateral aspect, suspicious of a second primary (carcinoma prostate).

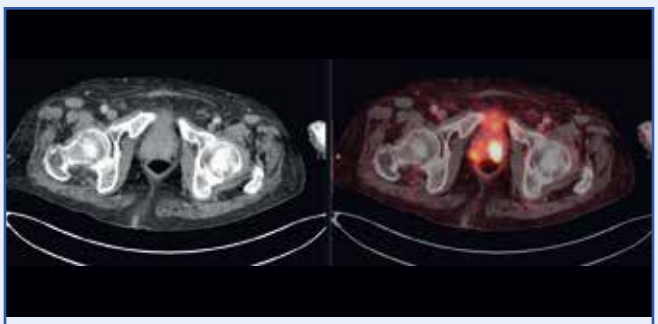

Figure 3 : Ga-68 PSMA PET-CT distinctly displays a PSMA expressing nodule within the prostatic parenchyma confirming a second primary within the prostate which later on was deemed to be an adenocarcinoma.

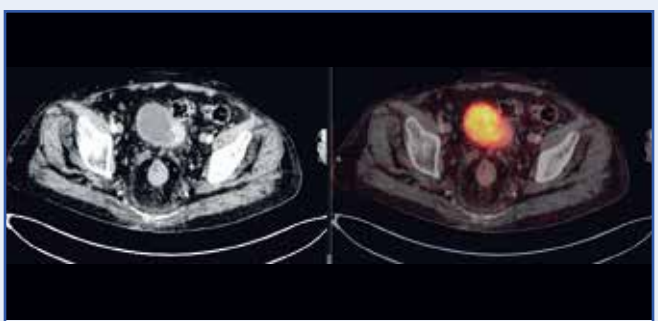

Figure 4 : Ga-68 PSMA PET-CT distinctly displays no PSMA uptake in the contrast-enhanced thickening within the bladder distinguishing its alternate histopathological nature (transitional cell carcinoma in this case).

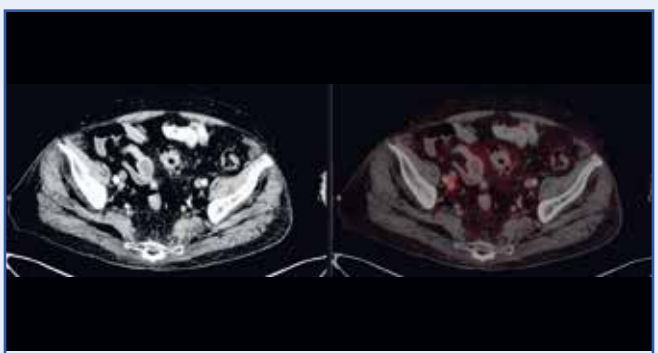

Figure 5 : Ga-68 PSMA PET-CT distinctly displays mild to moderate PSMA uptake in the right iliac node.

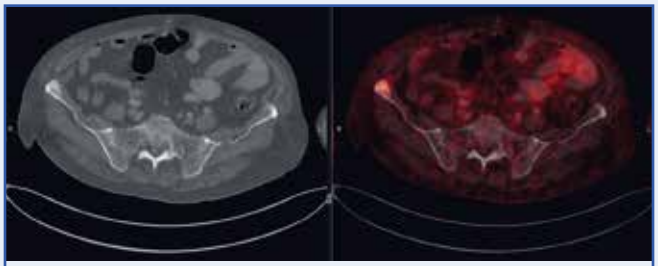

Figure 6&7 : Ga-68 PSMA PET-CT distinctly displays moderate PSMA uptake in the right iliac bone and D8 vertebral lesions determining that the metastases are from the prostatic second primary rather than the bladder tumor.

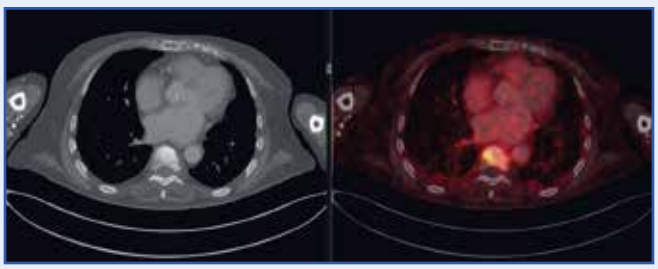

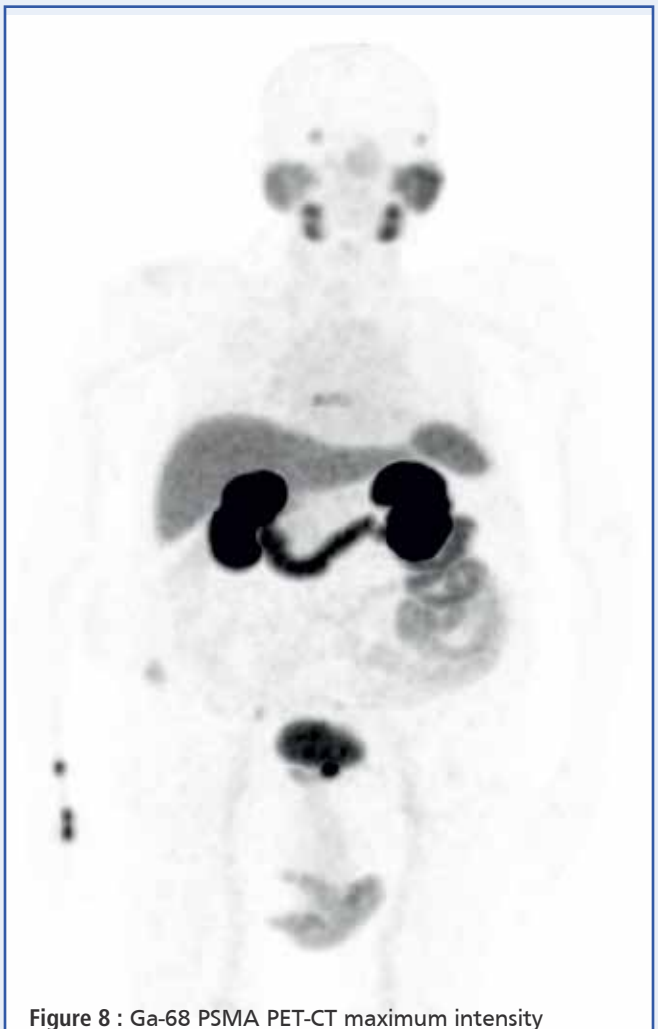

Figure 8 : Ga-68 PSMA PET-CT maximum intensity projection (MIP) distinctly displays PSMA expressing primary in the prostate, faintly visualized lymphatic and skeletal metastases

Ancient Schwannoma of Parapharynx- An Unusual Location of a Rare Tumor

Dr Irneet Mundi
Associate Consultant - Lab Medicine,
Fortis Hospital, Mohali

Dr Abhishek Prasad
Director and Head - Radiology,
Fortis Hospital, Mohali

Dr Ritu Pankaj
Additional Director - Lab Medicine,
Fortis Hospital, Mohali

Introduction

Parapharyngeal space tumor's are very rare and account for only 0.5% of all head and neck Tumors [1]. Although head and neck region account for 25–40% of the schwannomas, it is extremely rare to develop an ancient schwannoma in the parapharyngeal region. The term 'ancient schwannoma' was first coined by Ackerman and Taylor for schwannomas undergoing degenerative changes [2]. We report a case of ancient schwannoma in the parapharyngeal region which was diagnosed on histopathological examination.

Case Report

A 15-year old male presented in ENT department with the complaints of swelling over left side of the upper neck since one month. The swelling was painless, slowly increasing in size and was not causing any difficulty in swallowing, change of voice or difficulty in breathing. Clinical examination revealed a 5x4cm swelling along the anterior border of sternocleidomastoid. Indirect laryngoscopy was normal.

Contrast enhanced MRI of the neck revealed a well-defined ovoid heterogeneously enhancing, centrally cystic lesion in the left parapharyngeal space (Figure 1a). USG guided FNAC was performed which yielded 2ml haemorrhagic fluid smears from which showed only an occasional macrophage. The patient was taken up for surgery. The Tumor was completely removed and sent for histopathological examination.

Histopathological Findings

The specimen consisted of an irregular globular encapsulated soft tissue mass measuring 6x5x1.8cm. Cut section was partially cystic filled with blood clot. Rest of the lesion was solid grayish white and soft to firm. Haematoxylin and eosin (H&E) stained sections revealed a Tumor comprising of hypercellular and hypocellular myxoid areas. The cells were spindle shaped and arranged in fascicles and vague palisade pattern forming Verocay bodies (Figure 1b). Degenerative changes in form of cystic change, thick walled blood vessels, areas of hyalinization and calcification (Figure 1c) were seen. In some areas the cells showed nuclear atypia in form of enlargement and hyperchromasia (Figure 1d). On immunohistochemistry, the spindle cells were immunoreactive to S100 immunostain (Figure 1d inset).

Based on histopathology and immunohistochemistry findings the lesion was diagnosed as ancient schwannoma. Post-operative course was uneventful. Patient is on regular follow up and is doing fine with no evidence of recurrence.

Discussion

The parapharyngeal space is a potential site reported to house spectrum of benign and malignant tumors. Tumors of salivary gland origin are commonest (50%) followed by neurogenic origin (20%). Amongst the neurogenic tumors, schwannoma is the commonest[1].

Schwannomas also called neurilemmomas are typically benign, slow growing tumors derived from Schwann cells of the nerve sheath. These tumors may remain undetected for long periods of time until they become large enough to displace and compress nearby structures. The symptoms depend on the anatomical location of the tumor and nerve of origin. Pain and paraesthesia has been reported in up to 50% of cases. Other symptoms can include dysphagia, difficulty in breathing and hoarseness[3].

These tumors present as a cystic mass in the neck and the differential diagnoses to be considered are lymphadenitis (reactive / tuberculous / metastatic), lipoma, cystic hygroma, second branchial cleft cyst, carotid body tumor and laryngocoele[2]. Histopathology establishes the diagnosis.

Schwannomas have been classified histopathologically into five types: common, plexiform, cellular, epithelioid and ancient[2]. Among these ancient schwannoma of parapharyngeal space is exceedingly rare[4]. The term 'ancient schwannoma' was first coined by Ackerman and Taylor for benign tumor that display degenerative features attributed to the growth and "aging" of the tumor[2].

Schwannomas exhibit characteristic histological features of an encapsulated lesion showing biphasic pattern. Antoni A lesions are characterized by broad interlacing ribbons of spindle cells with elongated nuclei. On cross section, these cells produce a palisading pattern of nuclei about a central mass of cytoplasm called a Verocay body. Antoni B pattern is made up of very loose tissue and is thought to be a degenerative form of Type A with a looser texture and polymorphism of cells separated by abundant myxoid, often microcystic matrix. Immunostaining for S-100 is required to establish the neural origin of the tumor[5].

Degenerative 'ancient' changes include large cystic/ myxoid areas with hyalinization and calcification and occasional bizarre spindle cells and even a few mitoses[2].

Schwannomas with these degenerative changes can be misdiagnosed as sarcomas. Absence of necrosis, mitosis, and invasiveness, as well as absence of abrupt transition between typical schwannoma areas and cellular foci of atypical large cells, supports the diagnosis of ancient schwannoma[6].

Ancient schwannomas behave similar to the usual schwannomas. The treatment of choice for parapharyngeal space schwannoma is surgical enucleation. The encapsulated form can be easily enucleated and recurrence rates are extremely low. Radiotherapy should only be considered for palliation in cases of inoperable tumors[3].

Conclusion

Ancient schwannomas are rare tumors of the parapharyngal space and should be kept in the differential diagnosis of cystic masses of the neck. On histopathology degenerative changes like nuclear atypia should not be misinterpreted as malignancy.

References

1. Giraddi G, Vanaki SS, Puranik RS. Schwannoma of parapharyngeal space. J Maxillofac Oral Surg. 2010; 9(2): 182-185.
2. Sayed S, Rane P, Deshmukh A, Chaukar D, Menon S, Arya S, D'cruz AK. Ancient schwannoma of the parapharynx causing dysphagia: a rare entity. Ann R Coll Surg Engl. 2012; 94(7):e217-e220.
3. Carrol C, Jagatiya M, Kamel D, Siddiqi J. A parapharyngeal space schwannoma arising from the vagus nerve: A case report. Int J Surg Case Rep. 2017;41:22-25.
4. Walther LE, Mentzel T, Sens A, Beleites E. Degenerative changes in parapharyngeal schwannoma 'ancient schwannoma'. Case report and review of the literature. HNO. 2001; 49: 54–58.
5. Serhrouchni KI, Chbani L, Hammas N, Kamal D, Fatemi H El, Harmouch T, etal. Two rare schwannomas of head and neck. Diagn Pathol. 2014; 9-27.
6. Bindra R, Gupta S, Gupta N, Asotra S, Sharma A. Ancient schwannoma of the neck mimicking soft tissue sarcoma. J Cancer Res Ther. 2010 Apr-Jun;6 (2):234-5.

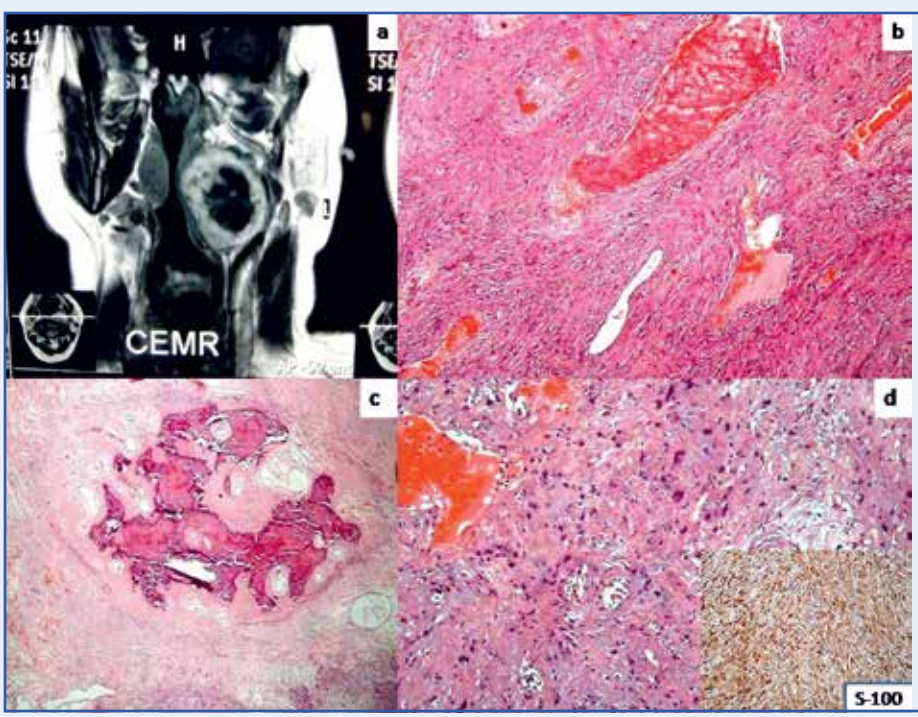

Figure 1 :

A: Post contrast T1w imageshowing a well defined peripherally enhancing lesion in left parapharyngeal space compressing over the oropharynx

B: Microphotograph showing a spindle cell tumor arranged in fascicles and vague palisade pattern along with thick walled blood vessels (H&E,400x)

c: Microphotograph showing degenerative changes within the tumor including areas of hyalinisation and calcification (H&E,100x)

d: Tumor cells showing nuclear atypia representing degenerative changes (H&E,400x)

d (Inset): Microphotograph showing S100 positivity of the tumor cells (S100, 100x)

A Rare Case of Invasive Lobular Carcinoma of Breast Presenting with Gastric and Uterine Metastases Demonstrated on F-18 FDG PET CT

Dr Shankar Murthy Gayana
Consultant -
Nuclear Medicine,
Fortis Hospital,
Bannerghatta Road,
Bangalore

Dr Vivek Belathur
Senior Consultant -
Medical Oncology,
Fortis Hospital,
Bannerghatta Road,
Bangalore

Dr Ravindra B S
Director - Gastroenterology and Hepatology,
Fortis Hospital, Bannerghatta Road,
Bangalore

Abstract

Invasive lobular carcinoma (ILC) breast is distinct from other pathologies in that it has unique sites of metastases, with involvement of liver, genital tract and the gastro-intestinal tracts. ILC being low-grade FDG avid, the role of F-18 FDG PET CT in these special subtypes of breast cancer is not extensively studied. We present a rare case of ILC of the right breast presenting with gastric and uterine metastases detected on F-18 FDG PET CT.

Key words

Invasive lobular carcinoma breast (ILC), F-18 FDG PET CT, gastric metastases Upper GI endoscopy performed revealed circumferential thickened, erythematous gastric mucosa with loss of rugosity and poor distensibility involving the entire stomach except pylorus(B). Upper GI endoscopy guided biopsy specimen stained with hematoxylin and eosin demonstrating tumour cells invading into the gastric stroma (C) and positive for GATA 3 (D). ILC of the breast forms the second most common type of invasive breast cancer constituting 10-15% of all breast cancers and is the most common of special types of breast cancer 1. Among epithelial neoplasms, GATA3 is expressed in >90% of primary and metastatic ductal and ILC2. GATA3 serves as one of the specific markers for breast cancer even when ER, PR and HER-2/neu are negative3. A diagnosis of ILC with gastric, uterine, pleural, peritoneal and skeletal metastases was made. The patient was started on chemotherapy with nabpaclitaxel and carboplatin. Breast cancer is the second most common primary neoplasm with GIT as the site of metastases with melanoma being the most common primary4. ILC has propensity for transcoelomic spread with skip metastases5.

ILC is known to have low grade FDG avidity, however, it serves as a prognostic indicator and helps in identifying rare sites of metastases6-9. Gastric metastases of ILC are rare, with a reported incidence between 2.8% and 27%10. ILC presenting with gastric and uterine metastases is extremely uncommon. F-18 FDG PET is a useful tool in determining rare unsuspected sites of metastases.

References

1. McCart Reed AE, Kalinowski L, Simpson PT, et al. Invasive lobular carcinoma of the breast: the increasing importance of this special subtype. Breast Cancer Research. 2021 Dec;23:1-6.
2. Voduc D, Cheang M, Nielsen T. GATA-3 expression in breast cancer has a strong association with estrogen receptor but lacks independent prognostic value. Cancer Epidemiol Biomarkers Prev. 2008;17:365-73.
3. Miettinen M, McCue PA, Sarlomo-Rikala M, et al. GATA3: a multispecific but potentially useful marker in surgical pathology: a systematic analysis of 2500 epithelial and nonepithelial tumors. Am J Surg Pathol. 2014 Jan;38:13-22.
4. Bo J, Yan-ping L, Hai-jiang W. Clinical characteristics of metastatic gastric tumors: a report of 8 cases in a single hospital. J Case Rep Stud. 2014;2:203.
5. Hanby AM, Hughes TA. In situ and invasive lobular neoplasia of the breast. Histopathology. 2008 Jan;52:58-66.

6. Fujii T, Yajima R, Kurozumi S, et al. Clinical Significance of 18F-FDG-PET in Invasive Lobular Carcinoma. Anticancer Res. 2016;36:5481-5485.
7. Jung NY, Kim SH, Choi BB, Kim SH, et al. Associations between the standardized uptake value of 18F-FDG PET/CT and the prognostic factors of invasive lobular carcinoma: in comparison with invasive ductal carcinoma. World J Surg Oncol. 2015 Mar 15;13:113.
8. Hogan MP, Goldman DA, Dashevsky B, et al. Comparison of 18F-FDG PET/CT for
   a. Systemic Staging of Newly Diagnosed Invasive Lobular Carcinoma Versus Invasive
   b. Ductal Carcinoma. J Nucl Med. 2015 Nov;56:1674-80.
9. D'Souza MM, Sharma R, Tripathi M, et al. Cervical and Uterine Metastasis from
   a. Carcinoma of Breast Diagnosed by PET/CT: An Unusual Presentation. Clin Nucl
   b. Med. 2010;35:820-823.

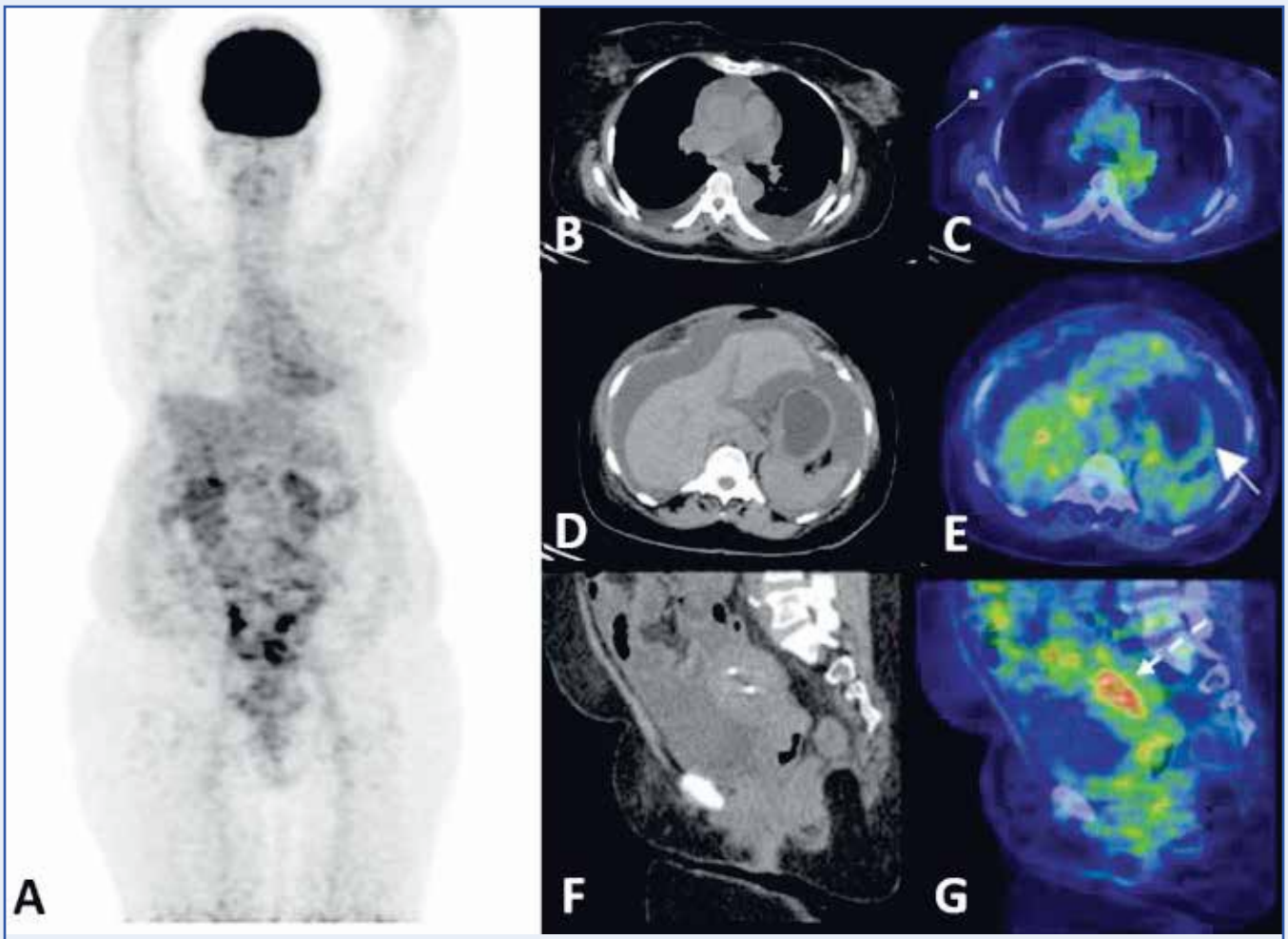

Figure 1 : A 71-year-old lady presented with complaints of fatigue, loss of weight and pain abdomen. Blood investigations revealed elevated CA 125 (128.0 units/mL) and CA 19-9 (170.00 units/mL) levels. Ascitic fluid was positive for malignant cells. F-18 FDG PET-CT was performed to evaluate malignancy of unknown origin. Maximum intensity projection image of the staging PET-CT study (A), axial CT (B and D), fused axial PET CT (C and E), show metabolically active lesion in the right breast (arrow with diamond head), pleural effusion, pericardial effusion, stomach wall thickening (solid arrow), metabolically active thickening in the uterine endometrium-cervix (F and G, dotted arrow), ascites, peritoneal deposits and skeletal lesions. These findings posed a diagnostic dilemma as all the rare sites of metastases from ILC was seen in a single case at presentation.

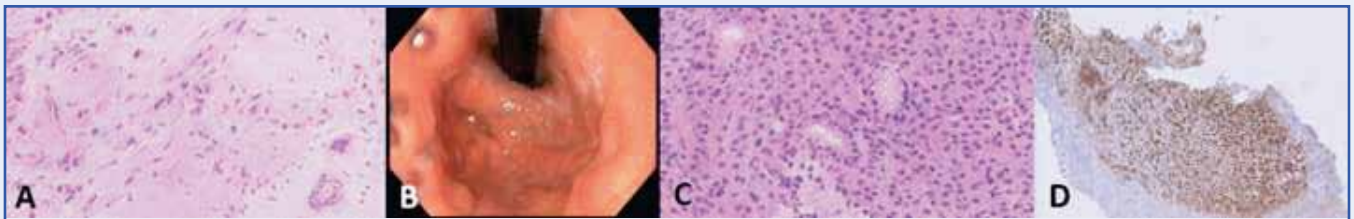

Figure 2 : Biopsy sample of right breast lesion stained with haematoxylin and eosin demonstrating disclosive tumour cells permeating the intraductal stroma (A) suggestive of ILC.

Early Identification of Osteomyelitis by 18F-FDG-PET/CT with an Example of Melioidotic Osteomyelitis.

Dr Mary Anne Joseph
Consult and Head -
PET-CT and Nuclear Medicine Department,
Fortis Hospital, Mulund

Dr Sachin Bhonsle
Senior Consultant - Orthopaedics - Joint Replacement,
Fortis Hospital, Mulund

Dr Kirti Sabnis
Consultant - Infectious Diseases,
Fortis Hospital, Mulund

Introduction

Fluorine18-fluoro-2-deoxyglucose (^{18}F-FDG) positron emission tomography with hybrid computerized tomography imaging (^{18}F-FDG PET/CT) is an established functional biomarker for the diagnostic assessment in bone & joint imaging. Activated inflammatory cells show increased intracellular concentration of ^{18}F-FDG via higher expression of the glucose membrane transporters leading to high sensitivity for detection of infection / inflammation. However, despite its high sensitivity, the low specificity of ^{18}F-FDG-PET poses a limitation, hence, Magnetic Resonance Imaging (MRI) is the imaging modality of choice for the diagnosis of osteomyelitis as it is both sensitive & specific and provides a detailed anatomy.

Nonetheless, atypical presentations of osteomyelitis do occur, which include: patients with negative radiographs, and negative or non-specific MRIs and patients with no characteristic clinical symptoms.

Case Description

As an example, we present the case of a 50-year-old diabetic gentleman, construction worker, who presented with worsening joint pain and restriction of movements in right shoulder and right knee, with high grade fever (101 oF), elevated white blood cell count (12,340 µL), and C-reactive protein levels (300 mg/dl).

Blood cultures drawn grew *Burkholdera Pseudomallei,* the causative pathogen for Meliodosis.

Although treatment was initiated with high dose antibiotics (Ceftazidime with Cotrimazaxole), he continued to have fever with no improvement of inflammatory markers and persistent bacteraemia. There was also worsening of pain in right knee and shoulder despite inflammatory and analgesic therapy.

MRI scans done at external center showed non-specific serpiginous signal abnormalities in the metadiaphyseal region of the right humerus with extensive periarticular edema. Only periarticular edema was reported in the right knee and no signal abnormalities in the marrow.

Plain radiographs of right knee at our center, showed no bony abnormalities (Figures 1A & 1B).

Figure 1a, 1b, 1c : Radiograph of knee at presentation showing no bony abnormality

In absence of radiographically or clinically demonstrable collection to aspirate or debride, ^{18}F-FDG-PET /CT was performed which showed (Figure 2):

1. Increased intramedullary radiotracer uptake noted in the proximal metadiaphysis of the right humerus. No cortical or periosteal changes were identified. (Fig. 3A – 3I).

2. Increased radiotracer uptake along cortex of distal metadiaphysis with multiple focal intra-medullary hot-spots in lower end of right femur with no cortical or periosteal changes on the CT images (Fig 4A – 4 I).
3. No collections or abscesses were identified at either site.

Debridement of the right humerus & right femur were performed (Fig 5A and 5B).

Pus was drained from both sites and cultures also grew same strain of B. Pseudomallei. He was continued on the antibiotic therapy and became afebrile after 5 days of debridement with progressive reduction in pain scores, his inflammatory markers, steady improvement in joint mobility. On 6-weekly follow up, he was found to be doing well and had already resumed normal activities

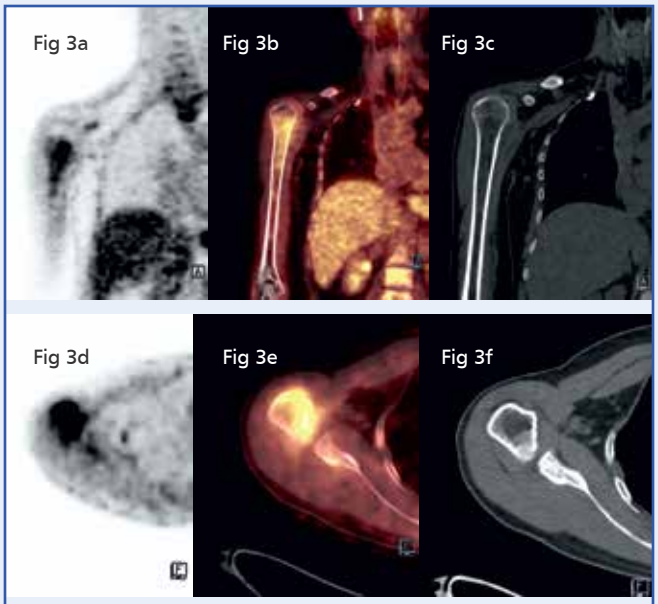

Figure 3 : Increased intramedullary 18F-FDG uptake in right humerus with no significant changes on CT

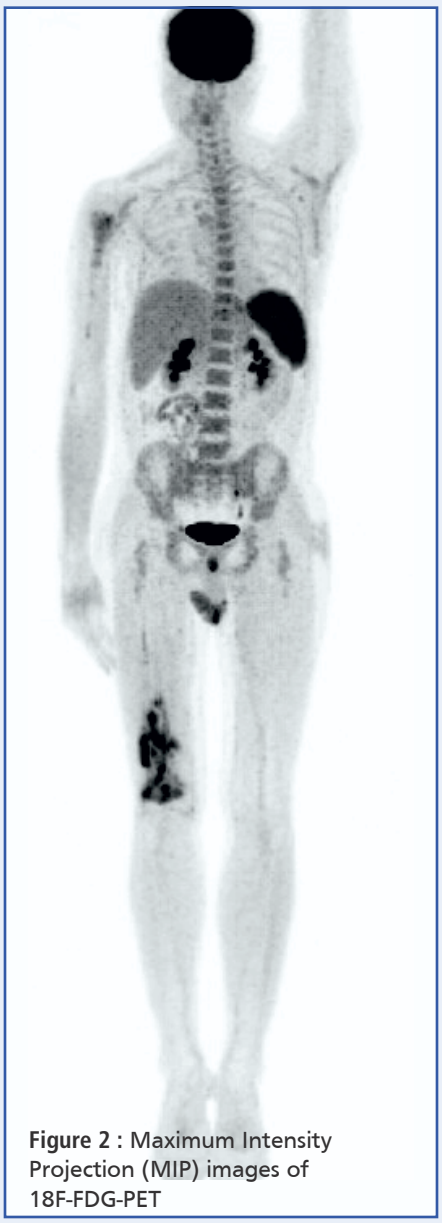

Figure 2 : Maximum Intensity Projection (MIP) images of 18F-FDG-PET

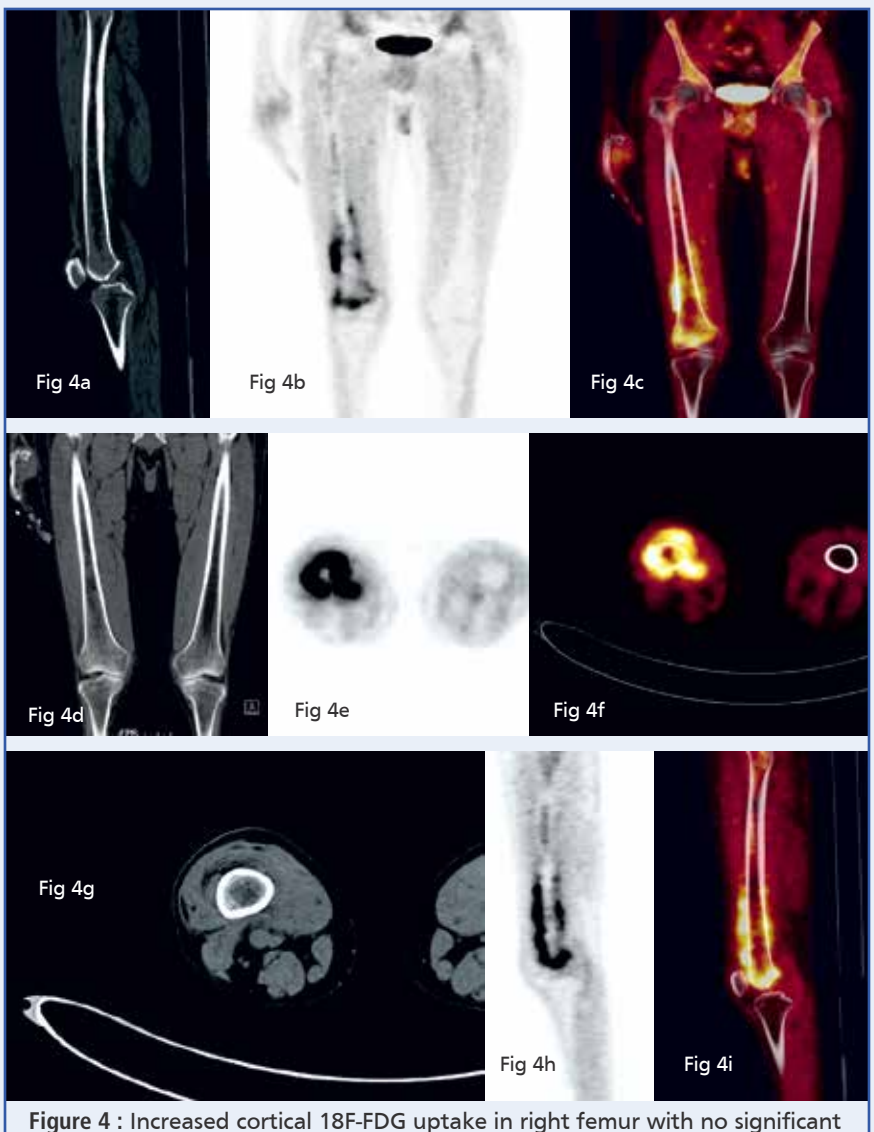

Figure 4 : Increased cortical 18F-FDG uptake in right femur with no significant changes on CT

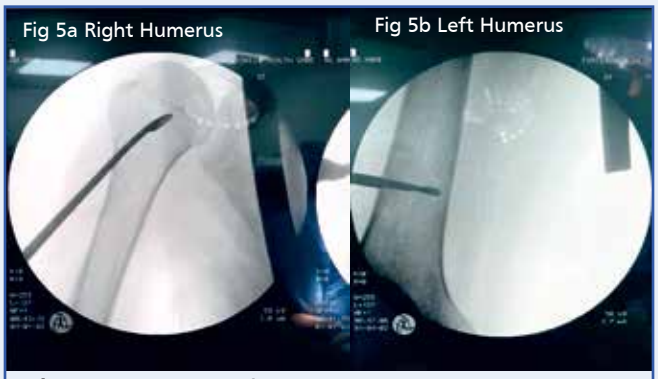

Figure 5 : Intraoperative Images

Discussion

Considering the natural history of osteomyelitis, we know that infection of the bone occurs via hematogenous route of infection through bacteremic seeding, starting primarily in the medullary cavity. Stage 1 of Cierny and Mader classification of osteomyelitis is described as medullary osteomyelitis - implying infection confined to the intramedullary surfaces of the bone. Hematogenous osteomyelitis and infected intramedullary rods are examples.

It is at this early stage, that MRI scans may be not be conclusive. When pus formation causes increased intramedullary pressure, the inflammatory exudate can rupture through the cortex to the periosteum if left unchecked, at which stage MRI scans tend to become pathognomic.

In our patient, increased ^{18}F-FDG uptake was noted within the medullary cavity of the right humerus with no bony changes - suggesting that the infection was at the medullary stage. Where as in the right femur, the activity was also seen along the cortex despite no unequivocal CT evidence – suggestive that there was early (metabolic) involvement of the cortex.

Bone and joint involvement of various pathogens can be indistinguishable from different forms of osteomyelitis, septic arthritis, infections and rheumatoid disorders. Lack of awareness, limited laboratory resources to isolate organisms, and confusion with more common infectious pathogens such as *Mycobacterium tuberculosis,* may lead to the misdiagnosis of bugs like *B. pseudomallei.* Sole dependence on MRI features would be result in unnecessary delay in critical interventions like debridement.

All the more, impact of poor and delayed localization of osteomyelitis would be devastating. Prolonged morbidity, longer treatment duration and high recurrence of local infection notwithstanding, higher rates of systemic relapse would be likely, which are documented in the literature with *B. pseudomallei.* Bias by radiological changes in the bone, can lead to over-resection or under-resection would and mandate more future and complex surgeries, negatively affecting the patients in all aspects.

Because, *B. pseudomallei* is a highly resistant pathogen with innate resistance to a large number of antibiotics including colistin & gentamicin, timely diagnosis and initiation and completion of antibiotic therapy in our patient was paramount. Insight and awareness of utility of ^{18}F-FDG-PET /CT in bone and joint infections by the infectious disease specialist and the orthopaedic surgeon resulted in earlier diagnosis of osteomyelitis in our patient, leading to early intervention, leading to a complete recovery with no relapse. An additional advantage of the whole-body PET scan was the ease of visualization of simultaneous multiple infective foci and permitting identification of the appropriate sites for aspiration and debridement.

Misinterpretation of intramedullary hypermetabolism can lead to missing the critical finding of early osteomyelitis. Awareness of the normal variants & pitfalls of ^{18}F-FDG distribution is important for both interpreting and treating doctors involved in patient management. Intramedullary hypermetabolism can be ignored as reactive uptake, or be confused with marrow-reconversion in special cases. Technical factors such as reconstruction algorithms, time-points of acquisition, subtle movement should also be taken into consideration to prevent erroneous reporting. Being biased by concurrent CT images or MRI images can also result in fallacious interpretation.

In summary, even if the MRI is negative while clinical suspicion is still high, physicians should utilize ^{18}F-FDG-PET /CT to assist with the diagnosis of osteomyelitis especially in patients with bacteremia.

References

1. Dioguardi P, Gaddam SR, Zhuang H, Torigian DA, Alavi A. FDG PET Assessment of Osteomyelitis: A Review. PET Clin. 2012 Apr;7(2): 161-79. doi: 10.1016/j.cpet.2012.01.011. PMID: 27157234.
2. Arter ZL, Barr R, Barr P, et al. BMJ Case Rep 2020;13:e236622. doi:10.1136/bcr-2020- 236622
3. Raja NS, Scarsbrook C. Burkholderia Pseudomallei Causing Bone and Joint Infections: A Clinical Update. Infect Dis Ther. 2016 Mar;5(1):17-29. doi: 10.1007/s40121-015-0098-2. Epub 2016 Jan 4. PMID: 26728713; PMCID: PMC4811834.
4. Inglis TJ, (February 1998). "Potential misidentification of Burkholderia pseudomallei by API 20NE". Pathology 30 (1): Lowe P, (December 2002). Journal of clinical microbiology 40 (12):
5. Elsheikh A, Elazazy M, Elkaramany M. Role of 18F-FDG PET-CT in Pre-Operative Planning of Surgical Debridement in Chronic Osteomyelitis. Indian J Orthop. 2022 Nov 19;56(12):2237-2244. doi: 10.1007/s43465-022-00771-9. PMID: 36507196; PMCID: PMC9705689.

Lab Medicine

Dealing with Rare Beta Chain HB Variants – Diagnostic Dilemmas

Scan QR Code for more

Dr Arpita Roy Dam
Head - Quality Assurance (A&C) and Head - Hematology Services, Agilus Diagnostic Ltd. Gurugram

Dr Ashutosh Awasthi
Pathologist - Haematology Department, Agilus Reference Lab, Gurugram

Dr Anurag Bansal
Technical Director N&E - Director Lab Operations, Agilus Reference Lab, Gurugram

Introduction

Hb Hope , a clinically silent variant ,[β136 (H14) Gly→Asp (GGT→GATOMIM: 141900.0112; dbSNP: 33949486)] has been reported in several African-American families, as well as in Japanese, Thai, Laotian, Cuban and Mauritanian families but is extremely rare in Indian population or is under reported. We bring forth two cases of probable Hb Hope peaks eluted in zone 10 of the electrophoretogram by capillary electrophoiresis (CE) and also show the comparative peaks on High Performance Liquid Chromatography(HPLC).

Clinical Presentations

Both the cases of Indian origin were asymptomatic with mild normocytic anaemia and no relevant blood transfusion or family history. The EDTA samples were run on HPLC at an external laboratory and referred to us, at Gurugram Agilus Reference Laboratory, for performing the assay on CE. The CBC findings along with CE and HPLC graphs are shown below in the Figures 1 &2.

Presumptive Diagnosis

Presumptive diagnosis of a rare beta chain variant – probability of Hb Hope. Confirmation by a molecular study and parental study was advised.

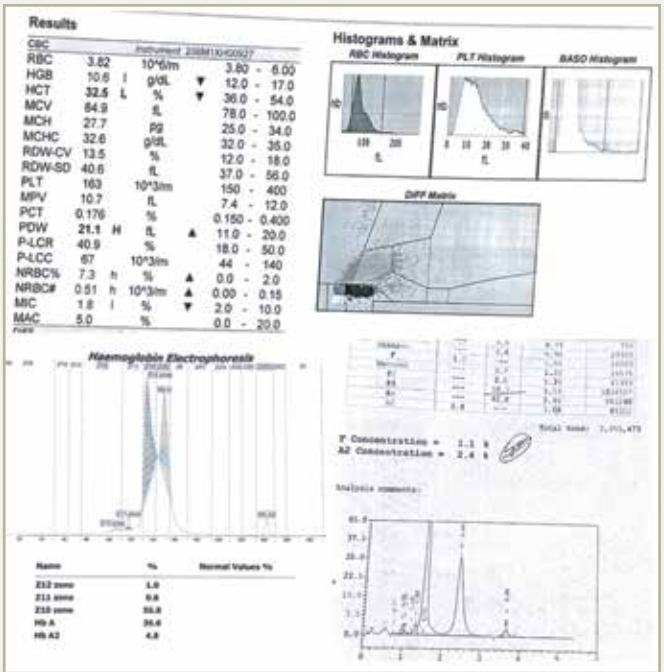

Figure 1: CBC, capillary electrophoresis & HPLC graphs of case 1

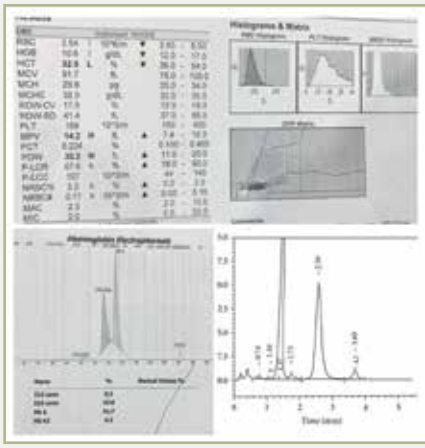

Figure 1: CBC, capillary electrophoresis & HPLC graphs of case 2

	Age/Gender	Ethnicity	Clinical Presentation	Hb (g/dl)	MCV (fL)	RDW-CV (%)	BT History
Case 1	29/F	Indian, R/O Pune	Asymptomatic Mild anaemia	10.6	84.9	13.5	No
Case 2	27/F	Indian, R/O Patna	Asymptomatic Mild anaemia	10.6	91.7	17.5	No

Discussion

Hb Hope, being a very rare beta chain variant in India, these two cases detected by the classical X (or inverted V) electrograph formation of Zone 10 and Hb A, makes one wonder the extent of undetected cases in the Indian sub-continent population.

The differential diagnosis between Hb Hope and some variants like Hb Pyrgos, Hb New York etc. is difficult on HPLC because these hemoglobinopathies are beta-globin chain variants which have similar elution pattern and elute in the P2 / P3 peaks. However, they can be classified by the CE system.

Another interesting fact which pathologist as well as clinicians should be aware of is that in c HPLC method, Hb Hope cases may be mistaken as erroneously high HbA1c, as it elutes in the same position as HbA1c. Hb Hope is characterized by a comparable charge altering mutation (β136 Gly Asp) and the intra chain salt bridge so formed between the carboxyl group of β136 Asp and the charged α-amino group of β1 valine. This salt bridge neutralizes the positive charges to the extent that HbA1c and Hb Hope co-elute from the HPLC column.

An important fact to be highlighted is that in both our Hb Hope cases there seems to be a falsely elevated Hb A2 values of 4.8% and 4.2% in CE whereas HPLC platforms show normal values of 2.4% and 2.5% respectively. An elevated HbA2 level in samples containing Hb Hope measured by CE may lead to an incorrect diagnosis of coinheritance of β-thalassemia with Hb Hope. The results of the RBC indices and molecular analysis would add value for β-thalassemia investigations. In reviewing the electrophoretogram in our cases, we noted that the Hb Hope and HbA overlap in the CE pattern. Because of this, the software shifts the baseline up to approximate the percentage of HbA and Hb Hope. Because the percentage of HbA2 is calculated as a percentage of the total haemoglobin, by not accounting for the overlap area, the percentage of HbA2 is falsely elevated.

Awareness of the limitations associated with the complementary screening methods (HPLC and CE) is essential to avoid false negative diagnosis of hemoglobinopathies. Genetic studies are indicated to confirm borderline cases and to detect silent carriers of beta thalassemia, alpha thalassemia, and rare and novel variants in routine practice.

References

1. R. Sachdev, A. R. Dam, and G. Tyagi, "Detection of Hb variants and hemoglobinopathies in Indian population using HPLC: report of 2600 cases," Indian Journal of Pathology and Microbiology, vol. 53, no. 1, pp. 57–62, 2010.
2. S. Chunpanich, et.al., "Molecular and hematological characterization of hemoglobin hope/hemoglobin E and hemoglobin hope/α-Thalassemia 2 in Thai patients," Laboratory Hematology, vol. 10, no. 4, pp. 215–220, 2004.
3. T. Sura, M. Busabaratana, et.al., "Haemoglobin Hope in a Northern Thai family: first identification of homozygous haemoglobin Hope associated with haemoglobin H disease," European Journal of Haematology, vol. 79, no. 3, pp. 251–254, 2007.
4. Bratati Singh, Debasis Debadatta Behera et.al. Hb Hope: A Rare Variant of Haemoglobin-Forged a Rise in HbA1c on Immunoturbidimetric Assay ;Indian J Clin Biochem. 2014 Oct; 29(4): 517–519
5. Sitthichai Panyasai et.al. Interference of hemoglobin Hope on beta-thalassemia diagnosis by the capillary electrophoresis Method: Am J Clin Pathol 2011 Jul;136(1):14-8.

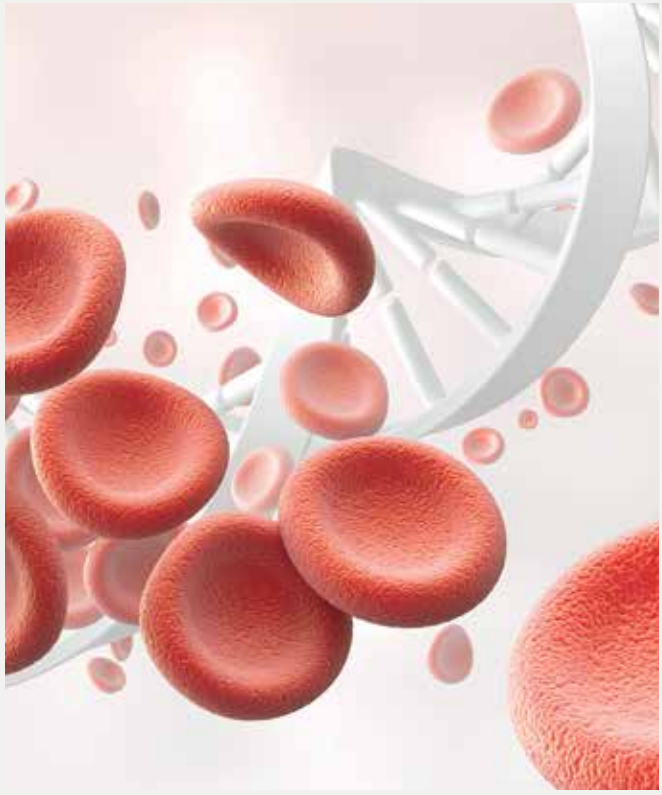

Novel Biomarkers for Screening and Diagnosis of Preeclampsia

Dr Avinash Phadke
President and Mentor,
Agilus Diagnostics Ltd.

Powerful Predictions: Novel Biomarkers for Screening and Diagnosis of Preeclampsia

The cause behind preeclampsia may be unknown- but its risks are clear. If left untreated, preeclampsia (PE) causes intrauterine growth restriction, preterm delivery and can lead to maternal mortality. Adoption of screening methods has predicted and prevented early-onset and preterm preeclampsia.

Right Timing leads to the Right Intervention

Early identification and treatment of preeclampsia gives better outcomes for both mother and child based on research from the ASPRE study. Due to the heterogeneous nature of PE, even in the presence of severe preterm disease, a woman can be asymptomatic. Assessment of maternal blood pressure and proteinuria used to identify PE has relatively low specificity and sensitivity. Recent studies reported that 38% of women who presented with an eclamptic fit did not have hypertension and proteinuria. Screening for PE is most effective when several biophysical and biochemical markers are used together for early prediction. These include maternal risk factors, mean maternal arterial pressure, ultrasound parameters, and biomarkers.

1st Trimester screening for PE

A combined screening program is recommended at 11 to 13 weeks of gestation. Screening tests include the following:

1. Maternal risk factors including family history of the condition, ethnicity, chronic hypertension, and smoking.
2. Calculated mean arterial pressure (MAP)
3. 3D power Doppler ultrasound, for placental vascularization and blood flow. Uterine artery pulsatility index (PI) by ultrasound examination
4. Biomarkers:
   - Human chorionic gonadotrophin (Free Beta hCG)
   - Maternal serum pregnancy-associated plasma protein - A (PAPP-A)
   - Placental growth factor (PlGF)
   - (PlGF tests can be done alone or in combination with the double marker test, which analyzes levels of Free Beta hCG and PAPP-A, as routine first-trimester screening for fetal anomalies)
   - Placental protein 13 (PP13)
   - Fetal hemoglobin levels
   - Cell-free fetal DNA (PE + aneuploidy screening)

2nd and 3rd Trimester Screening for PE

After 20 weeks of pregnancy, angiogenic markers can help identify women with at risk. One of the main features of pre-eclampsia is abnormal placental vasculature. The incomplete invasion of cytotrophoblastic cells and inadequate remolding of spiral arteries lead to decreased blood-carrying capacity and increased resistance. During the course of the disease, pro-angiogenic proteins like placental growth factor (PlGF) are reduced, and anti-angiogenic factors like soluble Flt1 and soluble endoglin, secreted by the placenta, are increased in the maternal circulation weeks before the onset of preeclampsia. These factors can be measured and have a significant role in the diagnosis and prognosis of PE.

Novel Tools: sFlt-1/PlGF ratio for PE Diagnosis and Management

In patients with pre-eclampsia, sFlt-1 levels are significantly increased while PlGF levels are significantly decreased compared to normal. To stratify the risk of developing PE and its stages of severity, the sFlt-1/PlGF ratio test requires specific data to be inputted into FMF-approved software. Accurate analysis and interpretation ensure that the sFlt-1/PlGF ratio can be used effectively as:

- A diagnostic test for PE as it differentiates between pre-eclampsia and other hypertensive disorders.
- A reliable prognostic indicator of adverse outcomes in a patient already diagnosed with pre-eclampsia. It predicts which patients may have worse outcomes and guides risk stratification and

treatment of patients due to the time-dependent slope of the sFlt-1/PlGF ratio. It reduces hospital costs, and hospital stays when it's not needed.

A ratio of 38 or lower can be used to predict the short-term absence of pre-eclampsia in women clinically suspected of having PE. Using the ratio after 20 weeks can diagnose and predict the severity of pre-eclampsia to guide a further course of therapy, like early delivery. Screening by biophysical and biochemical testing at 30-33 weeks could identify most pregnancies developing PE and requiring delivery within the subsequent four weeks. Measurement of circulating angiogenic proteins is rapidly becoming the "go-to" diagnostic and predictive test for preeclampsia.

Solitary Fibrous Tumor (SFT)

Dr Kunal Sharma
Associate Director and Head - Centre of Excellence and Histopathology, Global Reference Lab, Lead- DP and AI Initiatives,
Agilus Diagnostics Ltd.

Dr Priyanka Kembhavi
Histopathologist,
Agilus Diagnostics, Mumbai

Dr Brijesh Kumar
Consultant - Histopathologist,
Agilus Diagnostics, Mumbai

Dr Amit Kumar
Consultant - Histopathologist,
Mahavir Cancer Sansthan and Research Centre (MCSRC), Patna

Introduction

Solitary fibrous tumor (SFT) is a rare spindle cell mesenchymal tumor of poorly understood origin. It was first mentioned in pleura in 1870 (1), however the first description of this tumor was in 1931 by Klemperer, who called it "localized fibrous mesothelioma" (2). Although initially regarded as a pleural tumor, it is now recognized that SFT can occur in skin, nervous system, soft tissue, liver, lung, kidney, and thyroid (3). It accounts for less than two percent of all soft tissue tumors (4). More than 80% of SFTs are benign, asymptomatic and slow-growing tumors, however malignant SFTs are also known (5,6). Malignant SFT is the most aggressive form with a higher rate of local recurrence and distant metastases. (7)

The diagnosis is usually made by histopathological and immunohistochemical (IHC) examination of the excised sample. Surgery is considered as the primary treatment, but chemotherapy and radiation therapy is also indicated in some cases (4).

Case Report

A 60-year-old male patient presented with headache in the occipital region. On CT scan, a lytic lesion with soft tissue component measuring 5.2 x 4.5 cm was noted in the occipital bone in midline with extension into adjacent scalp and dura. There was mild indentation over the cerebral hemisphere. A suspicion of metastasis was raised clinically.

During primary histopathological reporting the core biopsy from the lesion was reported as pleomorphic vascular tumour with few mitoses and no necrosis. A possibility of angiosarcoma was suggested.

The case was sent to us for histopathological review and immunohistochemical evaluation. Microscopic evaluation revealed an oval to spindle cell tumor organised in irregular short fascicles with staghorn blood vessels. Tumor cells had rounded vesicular nuclei and conspicuous micronucleoli with a scant to moderate proportion of eosinophilic cytoplasm. Tumor cell nuclei exhibited a moderate degree of pleomorphism and frequent mitosis, including atypical forms. Necrosis was not seen in this biopsy. By IHC, tumor cells were positive for CK, Vimentin, p63, CD34, SMA and STAT6. They were negative for CD31, CD45, CK7, CK 20, EMA, TTF1, NKX3.1, Desmin, S100, HMB45 and CD117. ERG showed focal weak staining in the tumor cells. INI-1 was retained. Ki-67 labelling index was upto 70%.

Based on these morphological and immunohistochemical findings, a diagnosis of Malignant Solitary fibrous tumor

was rendered with and advice for NAB2-STAT6 gene fusion studies; which yielded a positive result. CK expression here was unusual and represents a diagnostic aberrancy which could result in a major misdiagnosis.

Discussion

SFT and hemangiopericytoma (HPC) have been originally regarded as separate entities, but according to the 2013 WHO classification of soft tissue tumors, they are now considered as one neoplasm, except for the central nervous system where meningeal HPC is still considered a separate entity (8). This tumor is most commonly seen in middle-aged adults, however rare cases in paediatric age groups have also been reported (9). Clinical manifestations are highly variable according to the location of the tumor (10). Cutaneous malignant SFT is an extremely rare tumor which resembles Dermatofibrosarcoma protuberans (DFSP) histologically and immunohistochemically with CD34 being positive in both (7).

The usual histomorphology of SFT is variable, ranging from a paucicellular to a moderate to highly cellular tumor, composed of round to spindle-shaped cells with scant cytoplasm. Prominent eosinophilic bands of collagen often arranged in a short storiform pattern, along with thin-walled branching vessels showing a staghorn (hemangiopericytoma-like) configuration.

Clinical behaviour can often be predicted by features such as hypercellularity, high mitotic figures (>4/10HPF), cytologic atypia, tumor necrosis and infiltrative margins (8). Absence of these criteria is not a definite predictor of benign behaviour and some SFTs with completely bland histomorphologic findings can have an aggressive course.

Immunohistochemistry is not widely accepted to be a predictor of malignancy (10). A combination of positive CD34 and STAT6 is highly characteristic of SFT. CD34 positivity has been reported in about 95% cases. However, some cases may be negative for the same, which are more likely to represent malignant and dedifferentiated SFT, which not only tend to loose CD34 positivity, but can also show in extremely rare case, an aberrant expression for cytokeratin. Thus, CK positivity and CD34 negativity in a solitary fibrous tumor, is highly indicative of its malignant and aggressive behaviour. NAB2-STAT6 fusion genes are specific for SFTs and the detection of the fusion gene can be helpful in diagnostically challenging cases. However, the molecular tests are costly, and are not available in every laboratory.

Recently, the use of immunohistochemistry for STAT6, as a pathognomic marker for detecting the fusion gene has widely gained popularity. It has been shown that a strong nuclear STAT6 immunoreactivity is highly sensitive and specific for SFTs (11,12) . By using this marker, we can accurately differentiate a case of SFT from other histologic mimics. Intense and diffuse nuclear staining of STAT-6 is highly characteristic of SFT and seen in more than 90% of cases (13,14). A few proportion of other spindle cell tumors in different locations of the body have also shown positivity for STAT-6, but most of these do not show as diffuse and intense a staining as seen in SFTs (15).

Malignant SFT is rare and malignancy has been reported in 12% to 37% of the cases. Several histomorphologic findings have been reported to be important predictors of malignancy and disease-free survival. These include high cellularity, mitotic activity (most of the studies have emphasized that >4 mitosis /10 HPF is a predictor of malignant and aggressive behaviour), with hemorrhage and necrosis (17). There are reports about the role of immunohistochemical biomarkers in prediction of behaviour in SFTs such as p53 and Ki67, however it has not been widely accepted (16, 17). Dedifferentiation has also been reported as a poor prognostic factor. It means that in a tumor, in addition to typical features of benign appearing SFT there is an abrupt transition to nondistinctive high-grade sarcoma. This can have round or spindle shaped cells or show an epithelioid morphology (18). There are reports of CD34 loss and p53 expression in these dedifferentiated SFTs (16). Besides, Ki67 staining shows a significant increase in dedifferentiated SFTs (18,19).

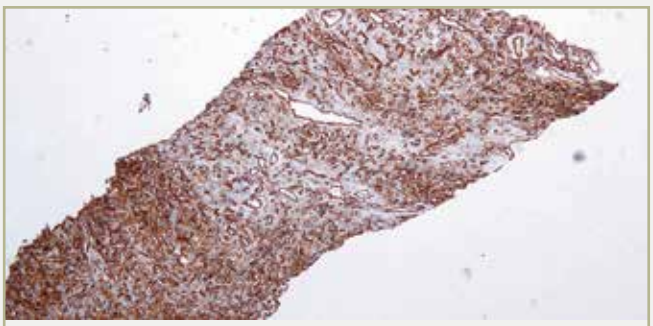

CD34

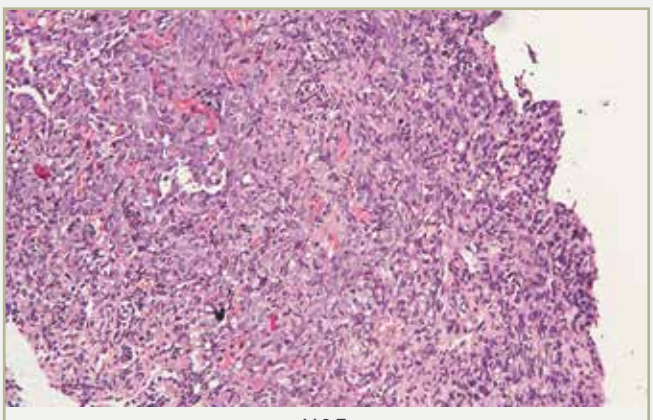

H&E

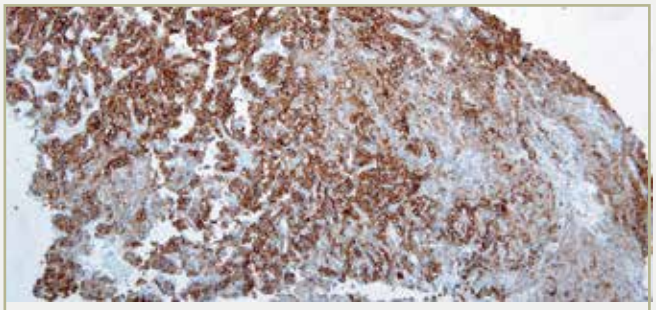

PAN CK

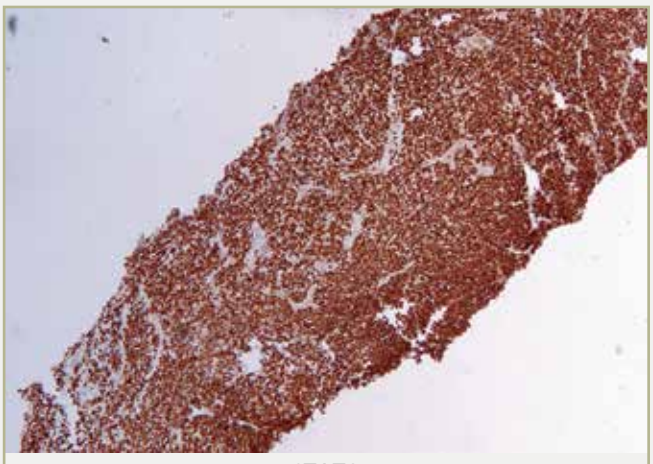

STAT6

Conclusion

SFT is a mesenchymal spindle cell tumor which is most commonly seen in the pleura. However, it can be seen in various extrapleural organs including cutaneous locations and should be differentiated from other spindle cell mesenchymal tumors. Immunohistochemical markers are very important for the histopathological diagnosis of this tumor; especially STAT-6 which is highly sensitive and specific. CK positivity is very rarely seen in SFTs and is likely to represent a more aggressive behaviour. It could result in misdiagnosis and thus, the knowledge of this aberrancy must always be kept in mind.

References

1. Wagner E. Das tuberkelähnliche Lymphadenom. (Der cytogene oder reticulirte Tuberkel). Leipzig: O. Wigand; 1871.
2. Klemperer P, Coleman BR. Primary neoplasms of the pleura. A report of five cases. Am J Ind Med 1992; 22(1):1-31.
3. Guo W, Xiao HL, Jiang YG, Wang RW, Zhao YP, Ma Z, et al. Retrospective analysis for thirty-nine patients with solitary fibrous tumor of pleura and review of the literature. World J Surg Oncol 2011;9: 134-140.
4. H. Neeff, R. Obermaier, K. Technau-Ihling, M. Werner, C. Kurtz, A. Imdahl, U.T. Hopt, Solitary fibrous tumour of the liver: case report and review of the literature, Langenbecks Arch. Surg. 389 (2004) 293–298.
5. J.A. Bishop, N. Rekhtman, J. Chun, P.E. Wakely Jr., S.Z. Ali, Malignant solitary fibrous tumor: cytopathologic findings and differential diagnosis, Cancer Cytopathol. 118 (2010) 83–89.
6. L. Peng, Y. Liu, Y. Ai, Z. Liu, Y. He, Q. Liu, Skull base metastases from a malignant solitary fibrous tumor of the liver, Diagn. Pathol. 6 (2011) 127.
7. Rabie A, Hasan A, Mohammed Y, Abdelmaksoud A, Rabaan AA. Recurrant Malignant Solitary Fibrous tumor of the scalp : a case report and literature review. J Pathol Transl Med. 2022 Mar ; 56(2): 103 - 108
8. Fletcher C DM, Bridge JA, Lee JC. Solitary fibrous tumor. WHO Classification of Tumors of Soft Tissue and Bone. Lyon, France: IARC Press; 2013; 81.
9. Geramizadeh B, Banani A, Moradi A, Hosseini SMV. Intrapulmonary solitary fibrous tumor with bronchial involvement: a rare case report in a child. J Pediat Surg 2010; 45(1): 249–251.
10. DeVito N, Henderson E, Han G,Reed D, Bui MM, Lavey R, et al. Clinical characteristics and outcomes for solitary fibrous tumor (SFT): A Single center experience. PLoS One 10(10): e0140362
11. Yoshida A, Tsuta k, Ohno M, Yoshida M, Narita y, Kawai A, et al. STAT6 Immunohistochemistry Is Helpful in the Diagnosis of Solitary Fibrous Tumors. Am J Surg Pathol 2014;38(4): 552–559.
12. Koelsche C, Schweizer L, Renner M, Warth A, Jones DTW, Sahm F, et al. Nuclear relocation of STAT6 reliably predicts NAB2–STAT6 fusion for the diagnosis of solitary fibrous tumour. Histopathology 2014; 65(5):613- 622.
13. Bauer JL, Miklos AZ, Thompson LDR. Parotid Gland Solitary Fibrous Tumor: A Case Report and Clinicopathologic Review of 22 Cases from the Literature. Head and Neck Pathol 2012; 6(1):21–31.
14. Mohajeri A,Tayebwa J, Collin A,Nilsson j,Magnusson l,Vult von Steyern F, et al. Comprehensive Genetic Analysis Identifies a Pathognomonic NAB2/ STAT6 Fusion Gene, Nonrandom Secondary Genomic Imbalances, and a Characteristic Gene Expression Profile in Solitary Fibrous Tumor. Genes Chromosomes Cancer 2013;52 (10):873–886
15. Barthelme S,Geddert H, Boltze C, Moskalev EA, Bieg M, Sirbu H, et al.Solitary Fibrous tumors/ hemangiopericytomas with different variants of the NAB2-STAT6 gene fusion are characterized by specific histomorphology and distinct clinicopathological features. Am J Pathol 2014;184(4): 1209-18.
16. Yokoi T, Tsuzuki T, Yatabe y, Suzuki M, Kurumaya H, Koshikawa T, et al. Solitary fibrous tumor: Significance of P53 and CD34 immunoreactivity in its malignant transformation. Histopathology 1998;32(5):423-32
17. Mosquera JM, Fletcher CD. Expanding the Spectrum of Malignant Progression in Solitary Fibrous Tumors. A Study of 8 Cases With a Discrete Anaplastic Component— Is This Dedifferentiated SFT? Am J Surg Pathol 2009;33(9): 1314-1321.
18. Demicco EG, Park MS, Araujo DM, Fox PS, Bassetts RL, Pollock RE, et al.Solitary fibrous tumor: a clinicopathological study of 110 cases and proposed risk assessment model. Mod Pathol 2012;25 (9): 1298-1306.
19. Subramaniam MM, Lim XY, Venkateswaran K, Shuen CS, Soong R, Petersson F. Dedifferentiated solitary fibrous tumour of the nasal cavity: the first case reported with molecular characterization of a TP53 mutation. Histopathology 2011;59(6):1269-79
20. Bita Geramizadeh, Mahsa Marzban, Andrew Churg. Role of Immunohistochemistry in the Diagnosis of Solitary Fibrous Tumor, a Review. Iranian Journal of Pathology, 2016 Summer;11(3): 195-203

Paragonimus Westermani Infection in Lung: Report of a Rare Case

Dr Gopendro Singh Naorem
Chief Histopathology,
Agilus Diagnostics Ltd.,
Fortis Flt Lt Rajan Dhall Hospital, Vasant Kunj,
New Delhi

Dr Nitin Dumeer
Histopathology,
Agilus Diagnostics Ltd.,
Fortis Flt Lt Rajan Dhall Hospital, Vasant Kunj,
New Delhi

Ms Abha K Sabhikhi
Advisor and Mentor, Technical CoE I Academics,
Co-Chair Council - Quality and Technical Excellence,
Agilus Diagnostics Ltd.

Introduction

Paragonimiasis is an important food-borne parasitic zoonosis caused by one or more of the trematode species of the genus Paragonimus. Fresh water snails, crabs, as well as crayfish act as first and second intermediate hosts, respectively. Humans acquire infection mostly by ingestion of undercooked crustaceans containing metacercariae, the larval stage of the parasite, and rarely by ingestion of infected, partially cooked meat of pig and wild boar. The latter are paratenic hosts.[1]

Case Presentation

A 34-year-old male patient, presented with the history of brownish red, hemoptysis. There was no history of fever, Jaundice or chest pain. The patient denied having anorexia or weighting loss. He had past history of recurrent hemoptysis for which empirical ATT was administered for 8 months. The patient was a non-vegetarian and a smoker. His general physical examination was within normal limits. No cackles or rhonchi were present. There was no family history of tuberculosis. Clinical differential diagnoses of tuberculosis, bronchiectasis, fungal infection, and malignancy were considered.

Routine investigations revealed hemoglobin to be 13.2 gm%, leukocyte count of 7600/cumm, eosinophilia of 11%, and a normal platelet count. The absolute eosinophil count was 840/cu mm, serum Ig E was 17321.0 KU/L . Contrast - enhanced computed tomography (CECT) revealed patchy consolidation with adjacent ground glass opacity and centrilobular nodules in the posterior basal segments of both lower lobes and anterior segment of right upper lobe (figure 1). The patient underwent CT guided aspiration cytology and biopsy from right upper lobe nodule to rule out malignancy.

All the specimens including issue biopsy and cell block preparation reveal ova characteristic of paragonimus species; likely Paragonimus Westernmani (figure 2). Patient also gave history of eating raw and pickled crabs on direct questioning.

Discussion

Paragonimiasis is an important food-borne parasitic zoonosis caused by one or more of the trematode species of the genus Paragonimus. This is endemic in some states of Northeastern India. Two Paragonimus species had been described from India – P. compactus from an Indian mongoose in 1859, and P. westermani from two Bengal tigers, in 1878.[2,]

P. Westernmani enters a human host after ingestion of metacercariae, its infective stage. They excyst in the small intestine, and the larvae then penetrate wall of intestinal and enter the peritoneum. Subsequently the diaphragm and pleura are penetrated thereafter made the way to invade the lung in three to eight weeks, where they mature to adult flukes. In general, Pulmonary paragonimiasis presenting with hemoptysis s commonly misdiagnosed as pulmonary tuberculosis, as had happened in our present case.

Definitive diagnosis of Paragonimiasis could be made by demonstrating characteristic golden brown, ellipsoidal operculated Paragonimus ova in the sputum, body fluids or feces. Occasionally, ova and an adult worm may be found in the biopsy specimens/autopsy/pleural fluid or sputum.[3,] In our current case we detected in

aspirated material and biopsy. Stool and sputum were continuously negative in three consecutive studies.

Conclusion

Paragonimus infection of the lung is a confounding diagnostic entity. The case is presented here to discuss the close differential of recurrent hemoptysis. It highlights the fact that all cases of hemoptysis are not pulmonary Koch`s and should not be treated as pulmonary tuberculosis. An underdiagnosed entity of 'endemic hemoptysis' is highlighted here.

References

1. Zhong HL, He LY, Xu ZB, Cao WJ. Recent progress in studies of paragonimus and paragonimiasis control in China. Chin Med J (Engl) 1981;94:483–94.
2. Cobbold TS. On some new forms of Entozoa. Trans Linn Soc London. 1859;22:363–6.
3. Vidamaly S, Choumlivong K, Keolouangkhot V, Vannavong N, Kanpittaya J, Strobel M. Paragonimiasis: A common cause of persistent pleural effusion in Lao PDR. Trans R Soc Trop Med Hyg. 2009;103:1019–23.

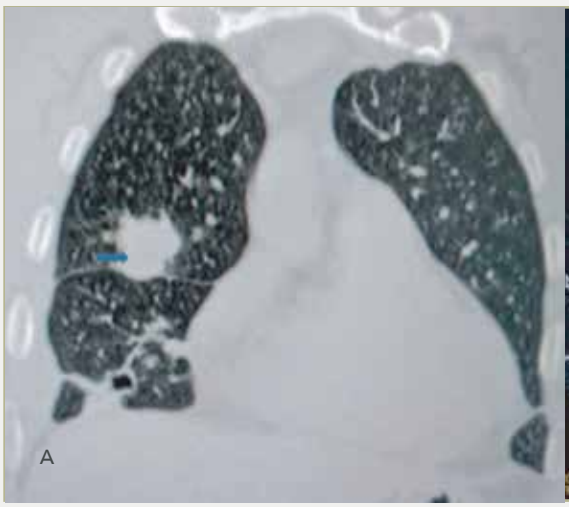

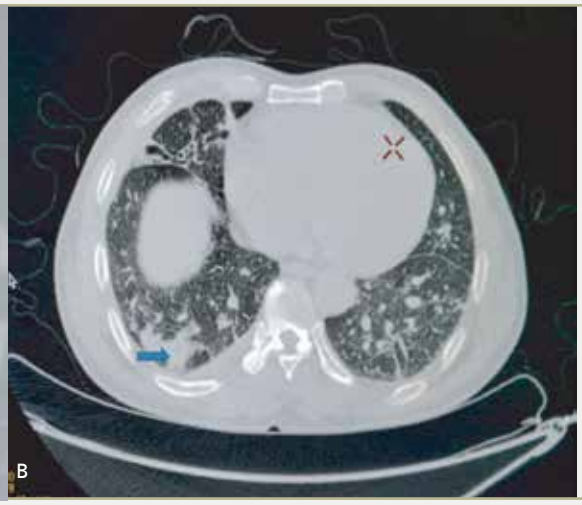

Figure 1:

HRCT showing consolidated lesion (arrow) in right upper lobe (A) and other ill-defined nodular lesion (arrow) on the right lower lobe (B)

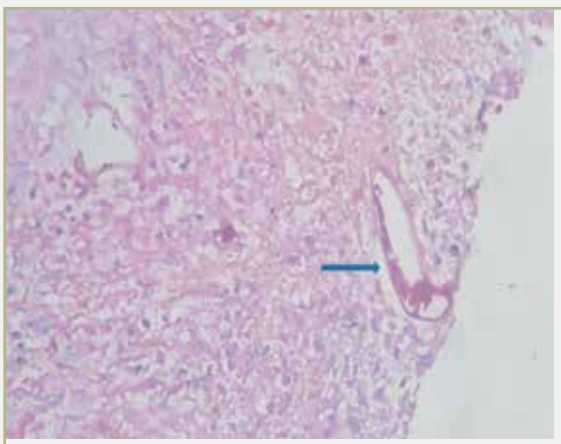

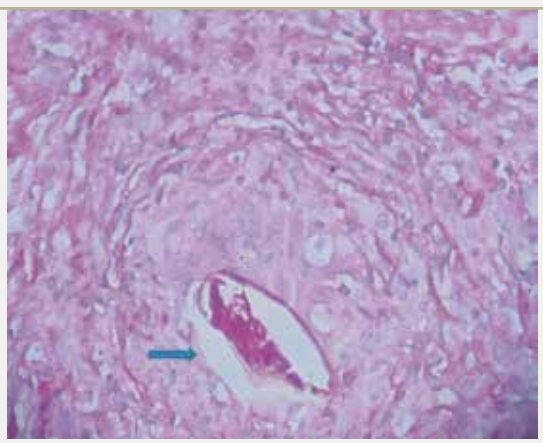

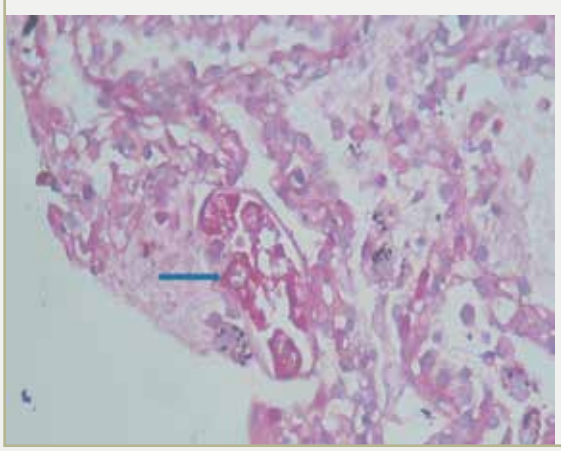

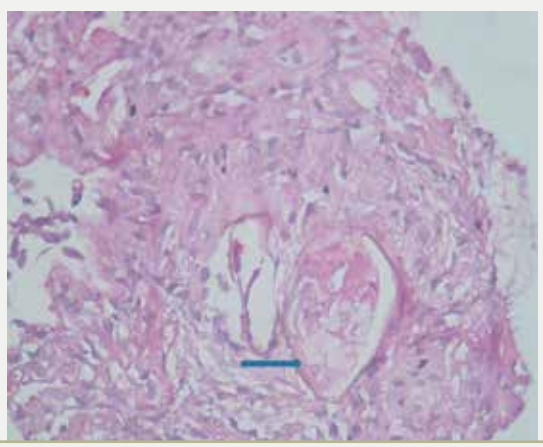

Figure 2: Photomicrograph of the Paragonium Westermani ova (arrows) which are seen entrapped in the parenchyma of lung. (H&E and PAS 400x)

An Unusual Case of Extensive Bone Marrow Involvement by NK/T Cell Lymphoma.

Dr Vishakha Tikeykar
Senior Consultant - Histopathology,
Agilus Diagnostics Ltd., Goregaon, Mumbai

Introduction

Clinically, NK/T cell lymphomas are predominantly extranodal. In about 80% of cases, the initially involved sites are nasal cavity, paranasal sinuses, nasopharynx, oropharynx and upper aerodigestive tract, collectively referred to clinically as the nasal subtype. In about 15-20% of cases, the primary presentation sites include the skin, gastrointestinal tract, testicles and salivary glands, collectively referred to clinically as the non-nasal subtype.

However in less than 5% of cases, the disease may be disseminated on presentation with hepatosplenomegaly, lymphadenopathy, marrow involvement and a leukemic phase. These disseminated cases are referred to clinically as the aggressive lymphoma / leukemic subtype and pathologically as aggressive NK cell leukemia by the WHO classification.

Case Description

Our patient was a 40 year old Asian female with no significant past history, presenting with anemia, malaise and fatigue, since two months. On CT abdomen, mild hepatosplenomegaly was reported. She was referred for bone marrow examination. The bone marrow aspirate was reported unremarkable and a suspected diagnosis of Myelodysplasia or an autoimmune hemolytic anemia was rendered on bone marrow biopsy at an outside hospital.

However, the bone marrow biopsy revealed diffuse infiltrate by atypical round cells on morphology and on IHC, the cells expressed CD45, CD3, CD56, CD4, TIA-1, Granzyme-B and CD30. EBERish was diffusely expressed by the neoplastic lymphoid cells. CD2 & CD7 T cell markers show downregulation. The cells were immunonegative for CD20, TdT, ALK-1 & CD5. Ki-t67 was 70-80%.

On further clinical investigation it was found that small; barely palpable axillary lymph nodes were noted, however those could not be sampled for histopathology reporting being non-accessible intraoperatively. The patient was initially given steroids and later one cycle of SMILE (Dexamethasone, methotrexate, ifosfamide, L-asparaginase and etoposide) regime of chemotherapy was administered, however unfortunately the patient succumbed.

Discussion

Usually, in a case of NK/T cell lymphoma, bone marrow involvement is rare and when it occurs, it is often minimal and is usually difficult to detect by routine morphologic examination. Our case showed near total replacement of the bone marrow by sheets of CD56 and EBER positive neoplastic lymphoid cells in a leukaemic fashion, which is highly unusual for a nasal NK/T cell lymphoma patients to develop. These morphologic and immunophenotypic features are similar to those seen in de novo aggressive NK cell leukaemia, which is defined in the WHO classification as systemic proliferation of NK cells with an aggressive and often fatal clinical course.In our case, however, there was no peripheral blood involvement.

Both disseminated Nasal NK/T cell lymphoma and aggressive NK cell leukaemia share common cytogenetic abnormalities in chromosomes 6, 7, 11 & 17. Both show lack of T cell receptor gene rearrangement and show similar ethnic background (Asian); morphology and immunophenotype. Disseminated nasal NK/T cell lymphoma present at an older age (average 50 years) and show no manifestations of B symptoms, less frequency of hepatosplenic and bone marrow involvement. higher frequency of cutaneous involvement; less frequent expression of CD16 & usually does not disseminate at presentation but rather later on during the course of the disease.

Whereas, in a case of aggressive NK/T cell leukaemia :-

1) Early age at presentation.
2) B symptoms.
3) Lymphadenopathy and Hepatospleenomegaly.
4) Extensive bone marrow involvement and spillage in peripheral blood.
5) Expression of CD16

Conclusion

It is very difficult to differentiate between the advanced disseminated nasal NK/T cell lymphoma and aggressive NK cell leukaemia due to many overlapping features between the two entities and lack of solid distinguishing criteria. Out case highlights such a diagnostic dilemma and we wish to share subtle nuances which help in distinguishing these two closely related entities.

References

1. Case Report :- Extranodal NK/T cell lymphoma, nasal type extensively involving the bone marrow. Sherif A. Rexk', Qin Huang2 Department of pathology and laboratory Medicine, university of California, Irvine, CA, USA; Department of pathology, City of Hope medical centre, Duarta, CA, USA, published Oct 31, 2011.
2. Diagnosis and management of NK/T cell lymphoma. Eric Tse & Yok-Lam Kwang J Hematol On col. 2017.

P204 Secondary Organizing Pneumonia Caused by Aspergillus Flavus in Immunocompromised Patients – PMC

Scan QR Code for more

Dr Ravneet Kaur
Head Lab Services and Microbiology,
Fortis Hospital, Noida, Agilus Diagnostics Ltd.

Introduction

Fungal pneumonia is a known complication in immunocompromised patients. However fungal infection leading to organizing pneumonia (OP) is a rare entity. Here we present two cases of co-occurrence of OP with Aspergillus lung infection

Case 1

A 33-year-old male with a history of recurrent oral-genital ulcerations and low-grade fever for the last 3 months presented with shortness of breath and high-grade fever for 10 days. On presentation he was hypotensive, tachycardic, and tachypnoeic, examination revealed bilateral crackles. His initial investigations were hemoglobin (Hb) 8.8, total leucocyte counts (TLC) 13 000, platelet 190 000, liver function test (LFT), and kidney function test (KFT) were normal. High-resolution commuted tomography (HRCT) revealed multifocal areas of interlobular septal thickening with ground glass opacity and patchy areas of consolidation seen in bilateral lung fields (Fig.1). He was initially managed with broad-spectrum antibiotics and oxygen support by a high flow nasal cannula (HFNC); as the condition deteriorated, he was mechanically ventilated. Fibreoptic bronchoscopy with bronchoalveolar lavage (BAL) was performed. Investigations for tuberculosis, nocardia, pneumocystis carinii, and bacterial infection was negative. Galactomannan index (GMI) in BAL was 3.15 and grew Aspergillus flavus. Transbronchial biopsy revealed features consistent with organizing pneumonia. He was on voriconazole and steroids. He was diagnosed with undifferentiated connective tissue disorder. As the patient's condition improved in due course of time, he was extubated and discharged in stable condition on voriconazole and steroids and is currently doing fine.

Case 2

A 56-year-old male known case of mantle cell lymphoma on consolidation therapy, presented with 15 days history of shortness of breath and high-grade fever. Chest examination revealed decreased breath sounds bilaterally in the lower lung zones with lower zone crackles. Initial investigations showed Hb 10.9, TLC 3.90, platelet 150000, KFT and LFT were normal. HRCT scan revealed multi lobular areas of consolidation showing air bronchogram with ground glass opacities in bilateral lung (Fig. 1). Bronchoalveolar lavage fluid (BALF) revealed the growth of Aspergillus flavus and was GMI 1.97. Investigations for tuberculosis, nocardia, pneumocystis carinii and bacterial infection was negative. Transbronchial biopsy revealed features consistent with organizing pneumonia. He was started

on combination therapy with voriconazole and micafungin along with steroids. Initially, he was managed with oxygen support but his oxygenation gradually worsened, he was mechanically ventilated, and received multiple pruning sessions. Patient had refractory organizing pneumonia, did not show any improvement even after 1 month, and left against medical advice.

Conclusion

Bacterial and viral infections are the common causes of secondary OP. Fungal infections implicated in secondary OP are rarely described, of which there are reports of Pneumocystis jiroveci (PJP) and Penicillium infection leading to secondary OP. Aspergillus flavus is a ubiquitous fungal agent and is considered as pathogenic in immunocompromised settings can lead to secondary organizing pneumonia. High index of suspicious for OP is always to be kept in mind while treating Aspergillus flavus pneumonia.

Pericentric Inversion of Chromosome 9 in a Non-consanguineous Couple with Spontaneous Abortions

Dr Rashmi Talwar
Senior GM, Deputy Lab Head, Head - Genetics,
Clinical Reference Lab, SRL Limited, Gurugram

Ms Kanika Gaur
Section Technical Coordinator,
Clinical Reference Lab, SRL Limited, Gurugram

Ms Priya
Section Technical Coordinator,
Clinical Reference Lab, SRL Limited, Gurugram

Mr Sabir Ansari
Scientific Officer,
Clinical Reference Lab, SRL Limited, Gurugram

Mr Sanjeet Kumar
Scientific Officer,
Clinical Reference Lab, SRL Limited, Gurugram

Case Description

The balanced pericentric inversion of chmmosome 9, inv(9) despite being considered a nomial variant has been frequently observed and reported in individual partners with spontaneous abortions.To tire best of our knowledge, we report the first case of this chromosomal abnomiality in both partners of a non-consanguineous marriage. This report highlights that invt 9) in both partners may be leading to unbalanced rearrangements in the fetus thereby leading to spontaneous abortions.

Keywords

Pericentric inversion, Chromosome, Sponmneous abortion.

Post SARS-CoV-2 Infection Related Colonic Ulcerations Masquerading as Gastrointestinal Mass

Source: Kumar P, Bhatia M. Role of Computed Tomography in Postoperative Follow-up of Arterial Switch Operation. J Cardiovasc Imaging. 2021 Jan;29(1):1-19. doi: 10.4250/jcvi.2020.0106. PMID: 33511796; PMCID: PMC7847786.

Dr Noopur Gupta
Senior Consultant - Pathology,
Fortis Hospital, Noida, Agilus Diagnostics Ltd.

Dr Abhishek Shekhar
Associate Consultant - Radiology,
Fortis Hospital, Noida

Dr Mukul Rastogi
Director - Liver Transplant and Hepatobiliary Sciences,
Fortis Hospital, Noida

Abstract

SARS-CoV-2 (COVID-19) infection has varied manifestations, ranging from predominant respiratory symptoms to only gastrointestinal manifestations to completely asymptomatic course. Coronavirus can be found in the stool even after other symptomatic recovery and nasal/ pharyngeal swab become negative. Gastrointestinal (GI) involvement in COVID-19 also has varied manifestations which can range from diarrheal illness to necrotizing colitis. We hereby reported a case of colonic ulcerations presented as caecal mass which developed during COVID-19 infection recovery.

Keywords

SARS-CoV-2 infection; COVID-19; Colonic ulcerations; Caecal mass; Colonoscopy; Colonic biopsy

Case Presentation

A case of 42 years old female, without any prior comorbidities, having fever of moderate severity, with shortness of breath, was diagnosed with SARS-CoV-2 (COVID-19) infection related pneumonia (COVID-19 RT-PCR Positive), for which she received steroids, ivermectin, azithromycin and other supportive treatment. There was no history of NSAIDs, or tocilizumab, Remdesivir treatment. She recovered gradually and discharged.

After 7 days of her COVID-19 therapy, she developed pain in right iliac fossa, which was radiating to umbilicus, non-colicky, severe in intensity; Visual Analogue Score (VAS) of 6/10, requiring analgesics, mimicking acute appendicular pain. It was associated with nausea and infrequent vomiting without loose stools, or abdominal distention. There was no history of bleeding per rectum. There were no residual symptoms of cough, shortness of breath, sore throat, or any other symptoms. She denied any chronic medicine use, prior Gastrointestinal (GI) symptoms, food allergies, lactose intolerance, alcohol abuse, smoking, and drug use. She was treated with metronidazole and other antibiotics for her abdominal symptoms before presenting to us, with no improvement in symptoms.

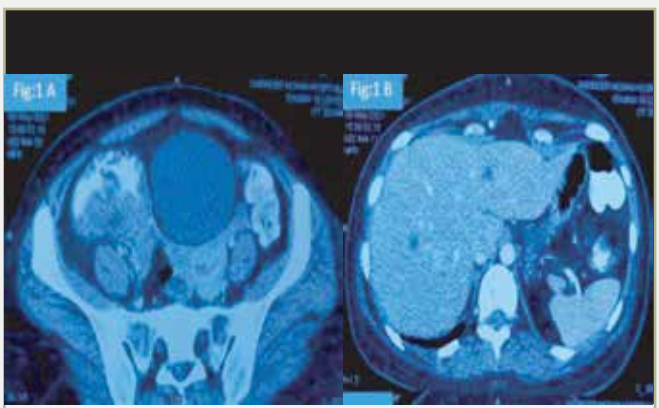

Figure 1A: Abdominal Computed tomography showing asymmetrical thickening of the cecum and IC junction. **Figure 1B:** Suggestive of <1cm hypodense lesions too small to characterie in the liver.

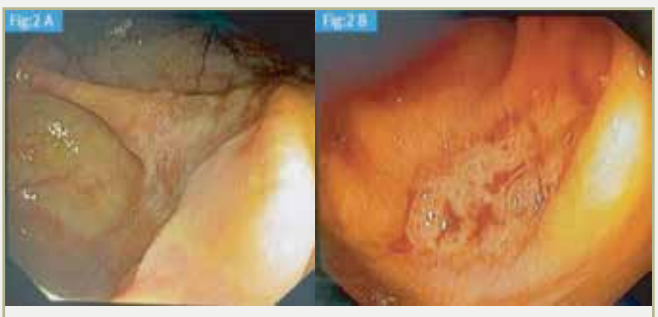

Figure 2: Colonoscopy Images of the cecum (Figure 2A) and ascending colon (Figure 2B) on flexible colonscopy examination showing ulcerations.

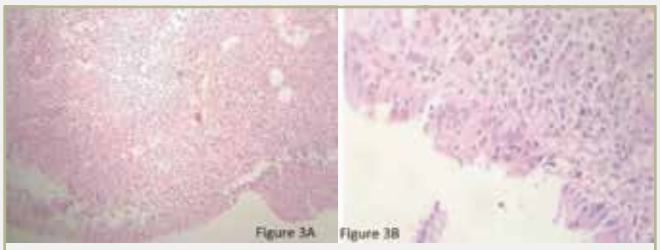

Figure 3: Colonic Biopsy images, H&E stain 10x (Figure 3A) and 40x (Figure 3B): Biopsy of the colonic ulcer showing inflammatory exudate, ulceration, Cryptitis and congested vessels. No microscopic coagulopathy, vrypt abscess, mucin depletion, hemosiderin, parasite, Vasculitis, malignancy, granuloma was seen.

Discussion

SSARS-CoV-2 (COVID-19) infection has varied manifestations, ranging from most common respiratory symptoms to less common gastrointestinal manifestations. It may have completely asymptomatic course as well. Initial case series reported that 3% to 10% of patients have initial GI symptoms, who eventually develop pulmonary manifestations [1]. GI involvement in COVID also has varied manifestations which can range from anorexia, dyspepsia, nausea, vomiting, diarrhoea illness, abdominal pain and necrotizing colitis. Gastrointestinal manifestations may be due to binding of the SARS-CoV-2 (COVID-19) virus to ACE 2 receptors (angiotensin converting enzyme-2 receptors) which are prevalent throughout the gut [2,3]. COVID-19 can results GIT inflammation directly via infection of the GI cells or indirectly mediated by cytokines which can results in systemic symptoms and multiple organ involvement [4]. Studies of colonoscopy from Italy, done in the COVID-19 patients showed segmental colitis associated with diverticulosis in 25% cases followed by, ischemic colitis in 20% and ulcerative haemorrhagic colitis in 5% of cases [5]. The colonic ulcers as manifestation or sequel of COVID infection has not reported in literature so far, probably this is the first case report of colonic ulcers as a sequel to COVID infection. There are some case reports of bloody diarrhoea as a clinical manifestation of COVID-19 with or without underlying inflammatory bowel disease [6,7].

There is also a case with colitis presenting as only presentation of COVID-19 infection [8]. Case reports of large bowel involvement in COVID-19 disease characterized by thickening of the ascending, transverse, left colon and case of colonic ileus with air fluid levels [9]. Due to the fear associated with the COVID-19 illness, and endoscopy being considered as a high-risk procedure [10]. As endoscopy and colonoscopy are aerosols generating procedures it may endanger medical staff, and therefore not routinely performed in COVID-19 patients unless patients with life-threatening gastrointestinal bleeding or oesophageal foreign-body obstruction [11]. So far no standardized methods established for stool COVID-19 analysis despite its prolonged shedding even after respiratory recovery. Coronavirus can be found in the stool even after other symptomatic recovery and nasal/pharyngeal swab become negative due to prolonged stool shedding [12]. Stool COVID-19 testing should done be in patients of gastrointestinal symptoms with negative nasopharyngeal swab test in a suspected COVID-19 disease [13], therefore methods should be sought for faecal isolation and stool testing for COVID-19.In the present case, the patient was referred to us as a case of ileocecal mass with possible metastasis to liver, in view of radiological findings, but clinical history was not in favor. There are case reports in the form of case series, where colonic ulcers were found to be masquerading as malignancy, particularly tuberculosis in India. It is very difficult to differentiate tuberculosis on endoscopic and radiological features from malignancy or inflammatory bowel disease, therefore biopsy remains the key in such cases [14,15]. Also case of ischemic colitis mimicking as tumour are reported [16]. One has to be at utmost awareness to rule out or rule in possible malignancy due to varied presentation, in the current pandemic COVID-19 related GI manifestation must be kept in mind, either treatment related adverse effects or virus related injury.

Therefore, patient was subjected to colonoscopy and biopsy with all standard precautions of COVID-19 protocols for the colonoscopy procedure to rule out the malignancy or other possible differential diagnosis. In present case we have considered multiple differential diagnoses for the cause of ulcerations which were masquerading as mass on radiological imaging. Firstly, NSAIDS related ulcerations, due to the proximal colonic nature, although history of NSAIDs or Over the Counter (OTC) drugs was not there. Secondly, tuberculosis related colonic ulcerations was considered, which is more common entity particular in developing countries like India, and suspected involvement of ileum and cecum on imaging, although on colonoscopy, ileum was normal up to 10 cm from ileo- caecal valve. Thirdly, possibility of amoebic ulceration was kept, which usually presents as punched out ulcerations, and also common in India, but this was also ruled out in the biopsy analysis. All the other possible differential diagnosis was ruled out on biopsy evaluation of the lesions. Since such presentation is never reported in contest to COVID-19 infection, it is worthwhile reporting this index case. Moreover, we have limitation of this case report is that the diagnoses is without any kinds of histologic confirmation of COVID-19, but we have ruled out all the alternative possible Etiologies.

Impact of Cytogenetic Evaluation in Haematological Malignancies: An Overview

Dr Anurita Pais
Head - Cytogenetics,
Agilus Diagnostics Ltd., Mumbai

Research aided by technological advancements linked Cancer and Genetics and indicated that Cancer is a heterogeneous disease with different genetic subtypes associated with differential prognosis and treatment. Genetic characterisation led to accurate diagnosis, better prognostication and an effective targeted treatment options.

Many cancer societies and groups such as NCCN, ELN, WHO, AMP and ASCO have set guidelines for classification based on cytogenetic as well as molecular risk markers on which treatment protocols are planned.

CML Karyotyping helps in identification of additional chromosomal abnormalities (ACAs) that leads to a better prognostication, help to define the disease phase and assess in risk of transformation.

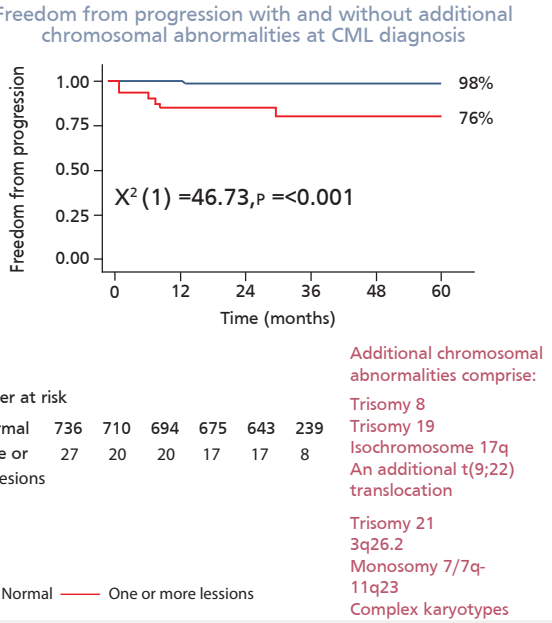

Source: Blood Adv (2021) 5 (4): 1102–1109

National Comprehensive Cancer Network (NCCN) and European Leukemia Net (ELN) guidelines recommend cytogenetics in case of atypical translocations, atypical transcripts, and additional chromosomal aberrations [1]. Cytogenetic monitoring is indicated when signs of progression surface and response to therapy is unsatisfactory [2,3].

In BCR/ABL negative myeloproliferative neoplasm we need to follow the algorithm. First identify the biomarker for targeted therapy and then look for any chromosomal abnormalities for better prognostication [4].

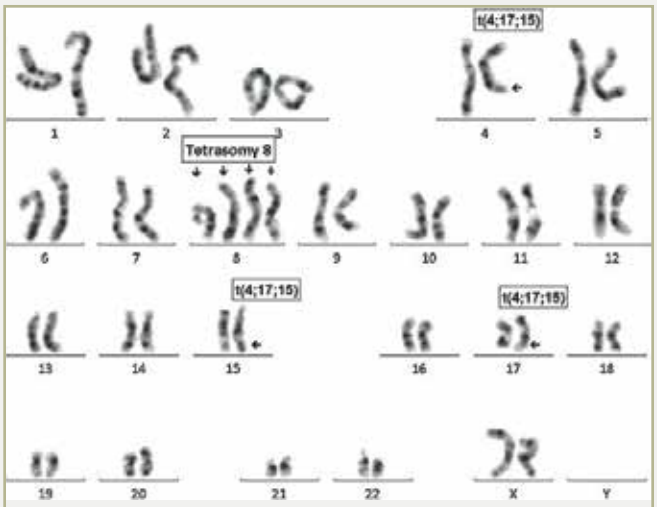

Source: A novel coexistence of tetrasomy 8 and FLT3-ITD along with variant 3 way translocation t(4;17;15) in acute promyelocytic leukemia.

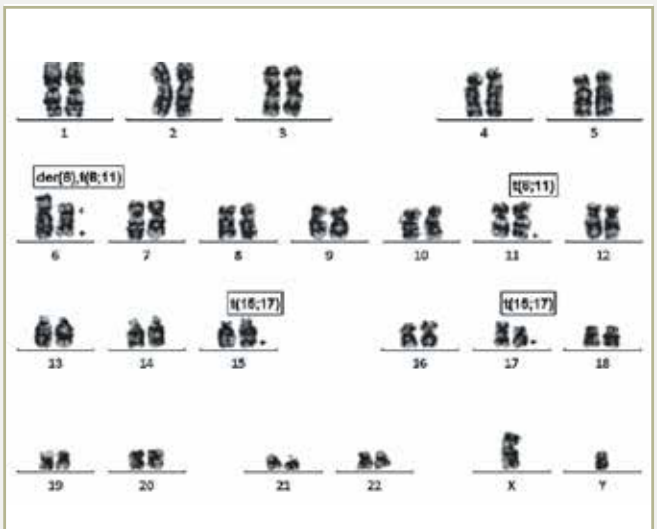

Source: Indian J Cancer 2022;59:419-21
Figure 3: Karyotype showing translocation t(15;17) (q22;q21) and derivative chromosome 6

ALL In Acute lymphoblastic leukemia survival rates have improved dramatically especially in pediatrics. There are various cytogenetic risk factors that have been identified that help to fine tune the therapy for improved outcomes. Children show a very good treatment outcomes as the favorable cytogenetic sub types such as hyperdiploidy and TEL/AML1 fusions are more common.

Unfavorable cytogenetic abnormalities such as hypodiploidy, MLL gene translocations and t(9;22) are considered as high risk groups that are followed on specific high risk protocols.

25% to 30% of B-cell ALL cases have a "high" hyperdiploid karyotype (generally defined as >50-67 chromosomes) and have good prognosis.

t(12;21):TEL/AML1 gene fusion is most common in children, accounting for 15 to 20% with favorable event free survival that are treated on standard risk [6]. The NCCN Guidelines for Acute Lymphoblastic Leukemia (ALL) focus on the classification of ALL subtypes based on immunophenotype and cytogenetic/molecular markers for risk assessment and stratification for risk-adapted therapy [7,8]. Unfavorable cytogenetic abnormalities such as hypodiploidy, MLL gene translocations and t(9;22) are considered as high risk groups that are followed on specific high risk protocols. 25% to 30% of B-cell ALL cases have a "high" hyperdiploid karyotype (generally defined as >50-67 chromosomes) and have good prognosis.

t(12;21):TEL/AML1 gene fusion is most common in children, accounting for 15 to 20% with favorable event free survival that are treated on standard risk [6]. The NCCN Guidelines for Acute Lymphoblastic Leukemia (ALL) focus on the classification of ALL subtypes based on immunophenotype and cytogenetic/molecular markers for risk assessment and stratification for risk-adapted therapy [7,8].

AML In Acute myeloid leukemia complex and monosomal karyotype are distinct cytogenetic entities with adverse prognostic impact requiring a more effective regimens for the prevention of relapse. Re-classification of cytogenetic risk is as (1) favourable risk: CBF-AML; (2) intermediate risk: normal karyotype, t(9;11); (3) adverse risk: three aberrations without specific adverse-risk abnormalities, without hyperdiploid karyotype (HDK); (4) very adverse risk: ⩾4 aberrations, HDK specific adverse-risk abnormalities, as defined by the ELN and Medical Research Council (MRC) [9-11].

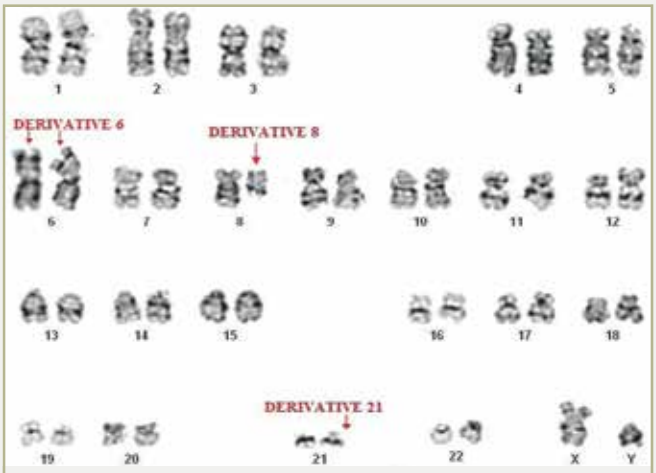

Source: International Journal of Medical Science and Advanced Clinical Research (IJMACR) 2018;1(4): 08-17.

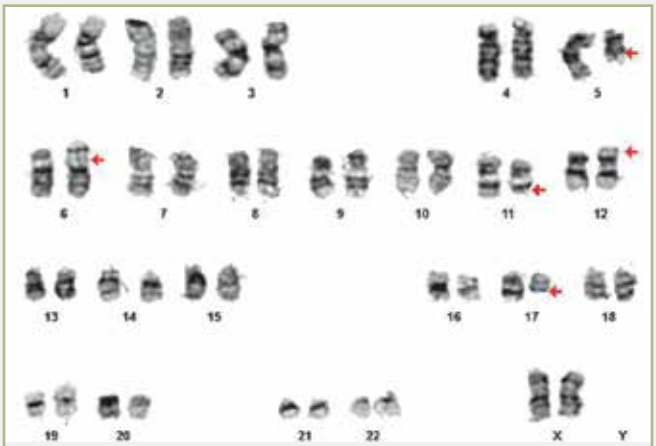

Source: Indian J Cancer. 2020 Jul-Sep;57(3):330-333

Figure 6: 46,XX,del(5)(q15q33),t(11;12)(q23;p13) [8]/46, sl,t(6;17) (p21;q21)[12]

Complex karyotype with involving MLL gene rearrangement with interstitial deletion 5q15q33 and translocation t(11;12)(q23;p13) and t(6;17)(p21;q21)

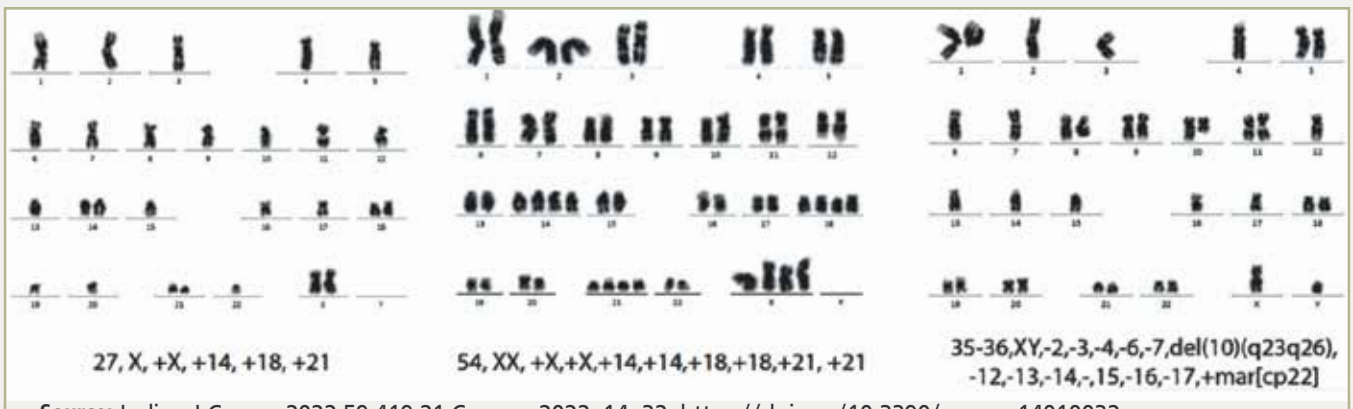

Source: Indian J Cancer 2022;59:419-21 Cancers 2022, 14, 32. https://doi.org/10.3390/cancers14010032

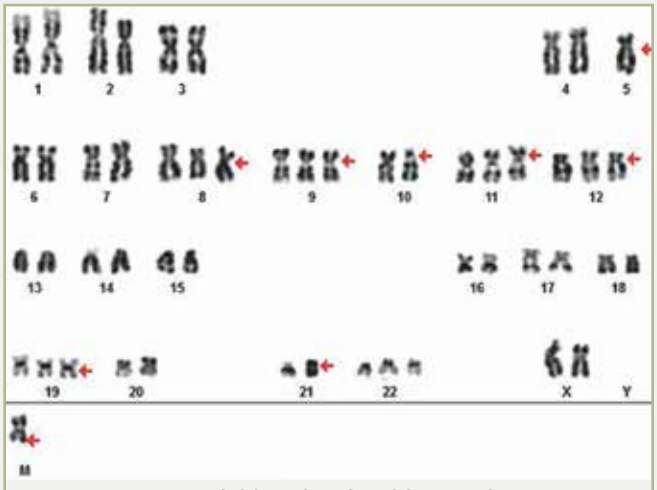

Source: Acute Myeloid Leukemia with Complex Hyperdiploid Karyotype with additional chromosomal abnormalities. Annals of Pathology and Laboratory Medicine. 2. 10.21276/APALM.2299.

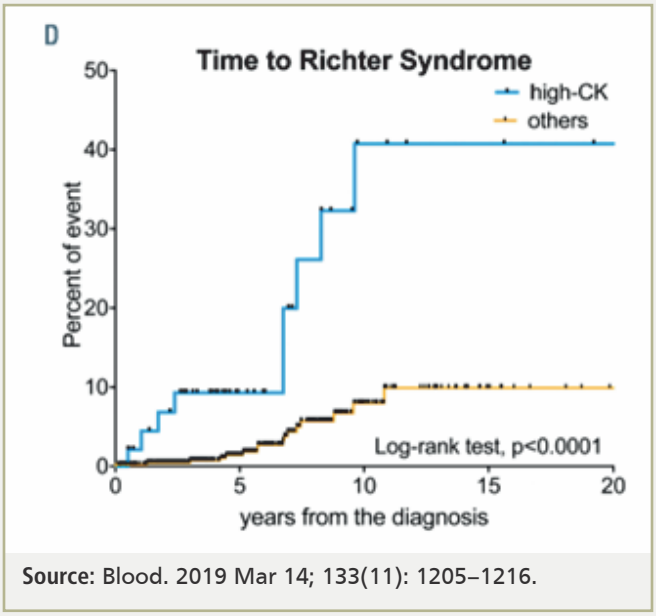

Source: Blood. 2019 Mar 14; 133(11): 1205–1216.

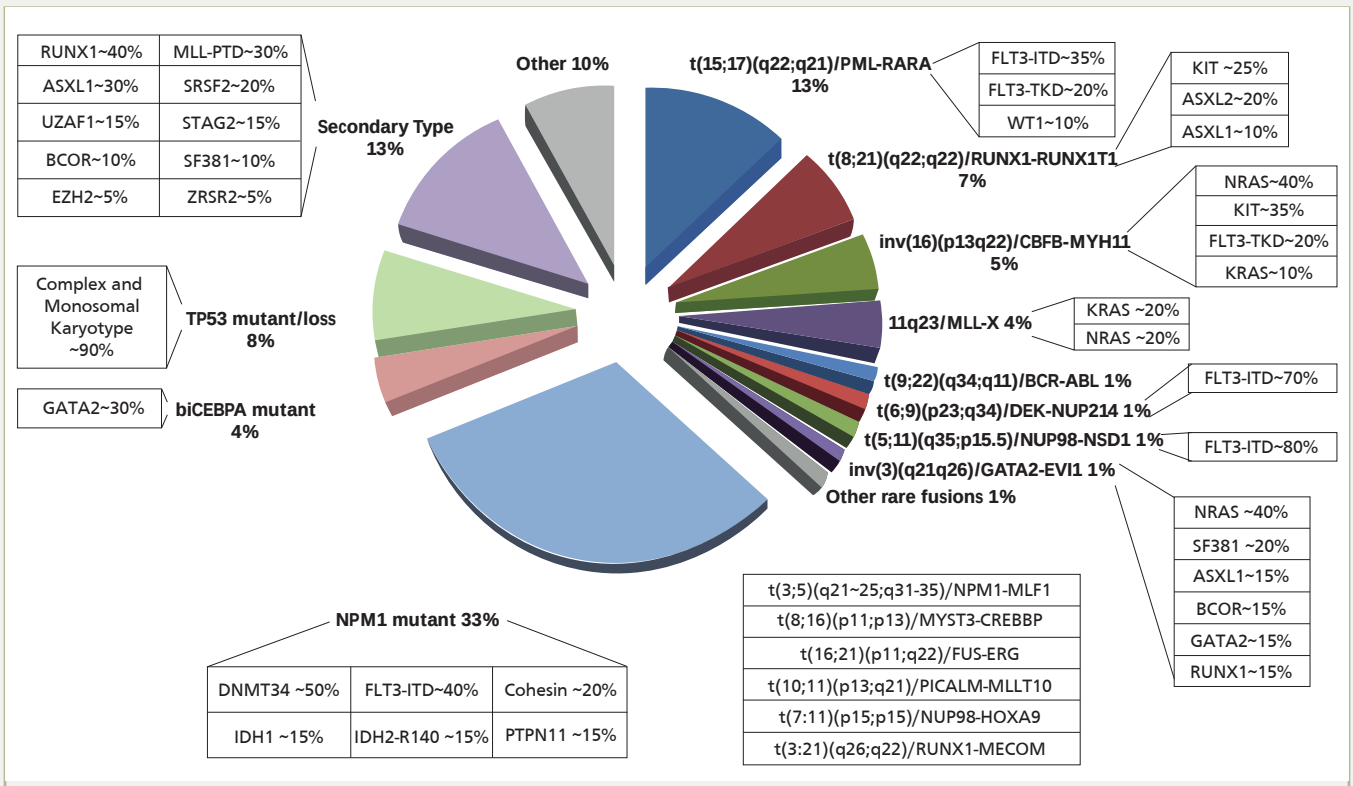

Source: Genomic classification with concurrent cytogenetic and Molecular subclasses Blood. 2017 Jan 26;129(4):424-447

CLL Chronic lymphocytic leukemia – Karyotyping before treatment initiation can reveal chromosomal aberrations not covered by the FISH. High cytogenetic complexity (High-CK) with ≥5 chromosomal aberrations emerge as prognostically adverse category and do not respond as well as other patients to targeted therapies [12].

MM The International Myeloma Working Group consensus updates the definition for high-risk (HR) multiple myeloma based on cytogenetic abnormalities such as t(4;14), del(17/17p), t(14;16), t(14;20), nonhyperdiploidy, and gain/amp(1q21), deletion 1p, and deletion 17p that confer poor prognosis. t(4;14), t(14;16), t(6;14), and t(14;20) are associated with high-risk disease characteristics, and IgH translocations ie t(11;14) and trisomies may be associated with better responses to PIs and IMiDs, respectively [13]. Modifying available treatments and introducing novel immunotherapies with specific helped to improve the outcomes of patients with high-risk MM [14]. Interphase Fluorescence in situ hybridization (I-FISH) is a most reliable method of cytogenetic profiling for relevant recurrent markers and cryptic abnormalities..

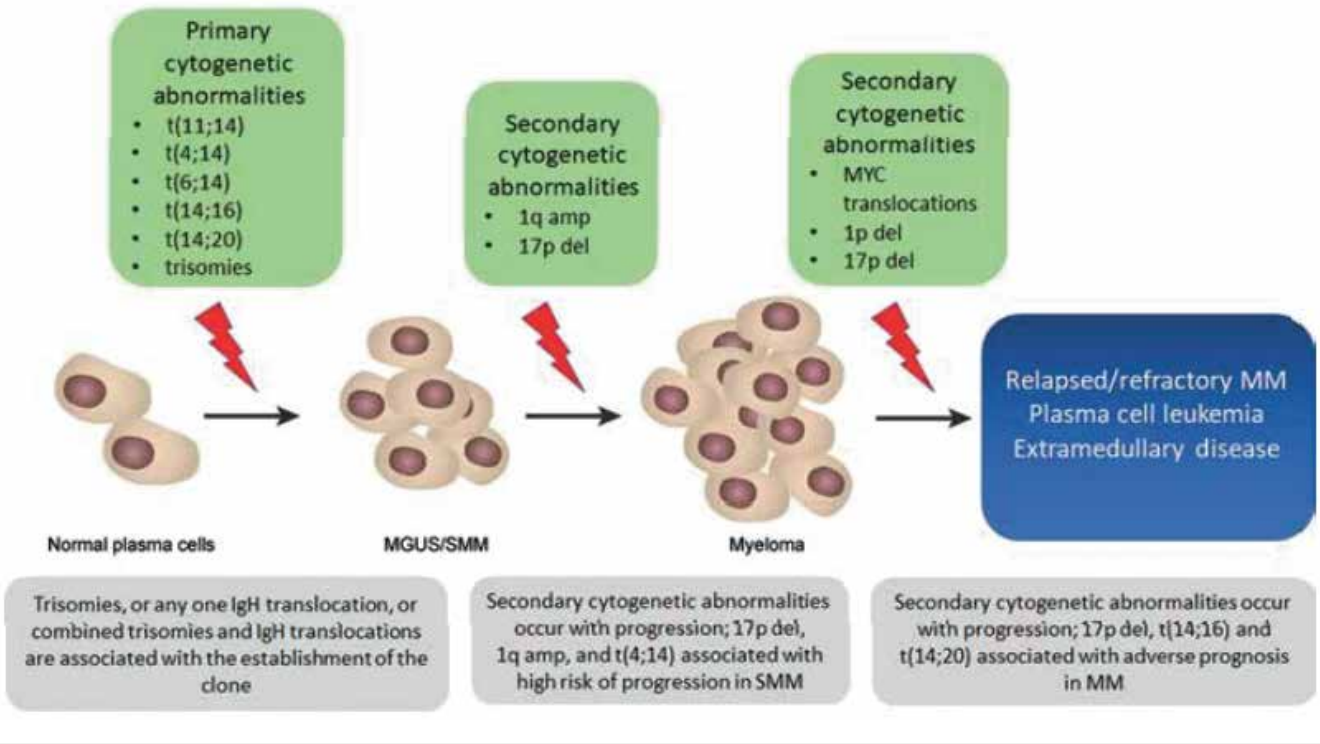

Source: Sequential genomic evolution in Multiple Myeloma. Acta Haematologic Polonica 2021;52(1):18–28

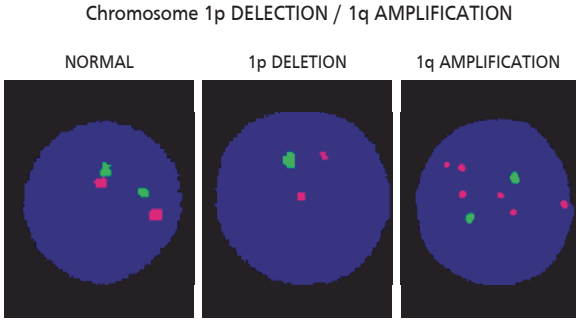

Figure 11

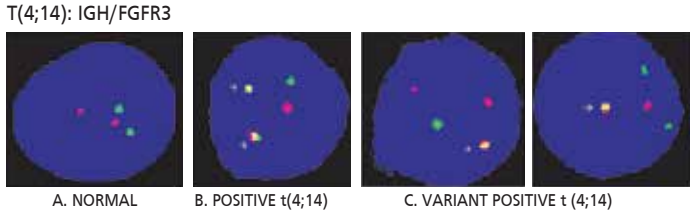

A. FISH signals with LSI IGH/FGFR3 probe showing 2 Green (IGH) and 20 (FGFR3) indicating normal status.

B. 1 Green (IGH), 1 Orange (FGFR3) and 2 yellow signals indicating fusion between IGH and FGFR3 genes.

C. Variant fusion patterns with loss of the 5' or 3' region of the labelled genes.

Figure 12

MDS In Myelodysplastic syndromes (MDS) Clonal cytogenetic evolution (CE) (i.e., acquisition of new chromosomal aberrations over time) is relevant for the progression of myelodysplastic syndromes.

Approximately 50–60% of cases of MDS present chromosomal abnormalities, like the deletions of chromosome 5q, monosomy 5,deletion 7q, monosomy 7, trisomy 8, and complex karyotypes [15]. Deletion 5q with ACAs and p53 will have a rapid transformation with autologous stem cell transplantation (ASCT) as only option. The International Prognostic Scoring System (IPSS-R) divides patients into low, intermediate and high categories based on cytopenias, chromosomal abnormalities, and percentage of bone marrow blasts and is used to estimate overall survival and predict progression to AML [16,17,18].

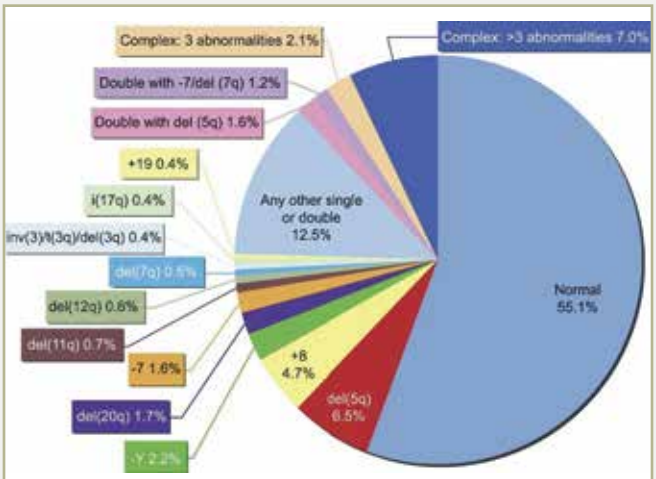

Source: The Journal of Molecular Diagnostics 2014;16(2):145-158.

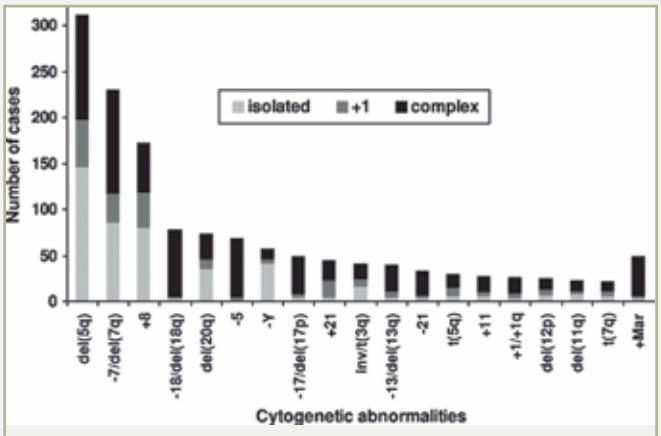

Source: Blood (2007) 110 (13): 4385–4395.

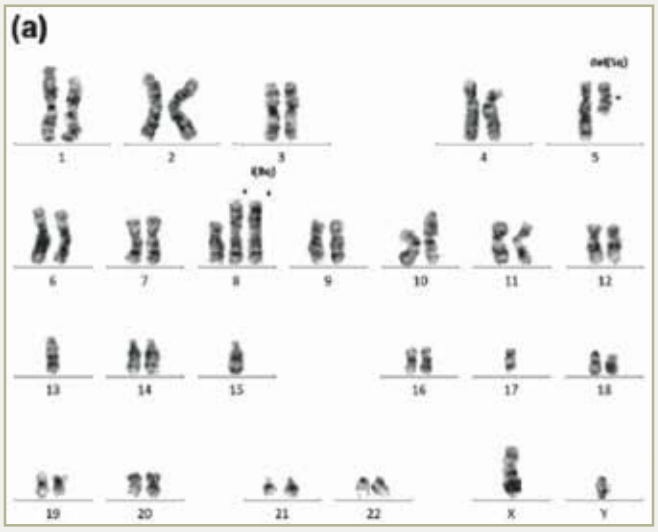

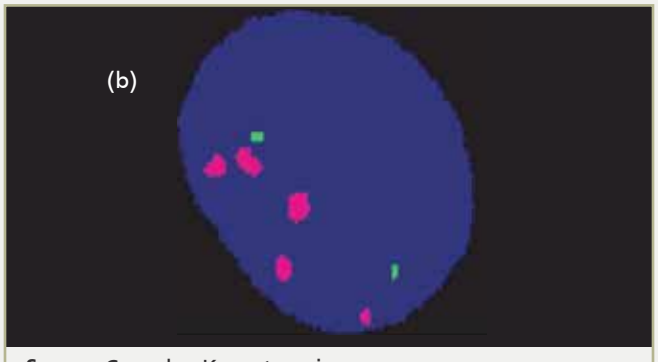

Source: Complex Karyotype in MDS:43~46,XY,del(5)(q13q33),-8,+i(8)(q10)x2,-13,-15,-17-[cp20]; Journal of Clinical and Diagnostic Research. 2021 Sep, Vol-15(9): GR01-GR03

References

1. Hochhaus, A.; Baccarani, M.; Silver, R.T.; Schiffer, C.; Apperley, J.F.; Cervantes, F. et al., European LeukemiaNet 2020 recommendations for treating chronic myeloid leukemia. Leukemia 2020;34:966–984.
2. Deininger MW, Shah NP, Altman JK, Berman E, Bhatia R, Bhatnagar B, et al., Chronic Myeloid Leukemia, Version 2.2021, NCCN Clinical Practice Guidelines in Oncology. J Natl Compr Canc Netw. 2020;18(10):1385-1415.
3. Wang W, Cortes JE, Tang G, Khoury JD, Wang S, Bueso-Ramos CE, DiGiuseppe JA, Chen Z, Kantarjian HM, Medeiros LJ, Hu S. Risk stratification of chromosomal abnormalities in chronic myelogenous leukemia in the era of tyrosine kinase inhibitor therapy. Blood. 2016;127(22):2742-50.
4. Li M, Wen L, Cen J, Feng Y, Chen S. JAK2V617F allele burden in patients with myeloproliferative neoplasms carrying Trisomy 9, and its relationship with clinical phenotypes. Int J Hematol. 2016;103(5):599-601.
5. Pais A, Fernandes C, Dalvi R, Bafna V, Pawar R, Chavan D, Ahmad F. A novel coexistence of tetrasomy 8 and FLT3-ITD along with variant 3 way translocation t(4;17;15) in acute promyelocytic leukemia: Case study and literature review. Cancer Genet. 2022;262-263:111-117.
6. Pais AP, Amare Kadam PS, Raje GC, Banavali S, Parikh P, Kurkure P, Arora B, et al., RUNX1 aberrations in ETV6/RUNX1-positive and ETV6/RUNX1-negative patients: its hemato-pathological and prognostic significance in a large cohort (619 cases) of ALL. Pediatr Hematol Oncol. 2008;25(6):582-97.
7. Lazaryan A, Dolan M, Zhang MJ, Wang HL, Kharfan-Dabaja MA, Marks DI, et al., Acute Leukemia Committee of the CIBMTR. Impact of cytogenetic abnormalities on outcomes of adult Philadelphia-negative acute lymphoblastic leukemia after allogeneic hematopoietic stem cell transplantation: a study by the Acute Leukemia Working Committee of the Center for International Blood and Marrow Transplant Research. Haematologica. 2020 May;105(5):1329-1338. Epub 2019 Sep 26. Erratum in: Haematologica. 2021;106(8):2295-2296.
8. Brown PA, Shah B, Advani A, Aoun P, Boyer MW, Burke PW, et al., Acute Lymphoblastic Leukemia, Version 2.2021, NCCN Clinical Practice Guidelines in Oncology. J Natl Compr Canc Netw. 2021;19(9):1079-1109.
9. Pollyea DA, Bixby D, Perl A, Bhatt VR, Altman JK, Appelbaum FR, et al., NCCN Guidelines Insights: Acute Myeloid Leukemia, Version 2.2021. J Natl Compr Canc Netw. 2021;19(1):16-27.
10. Slovak ML, Kopecky KJ, Cassileth PA, et al. Karyotypic analysis predicts outcome of preremission and postremission therapy in adult acute myeloid leukemia: a Southwest Oncology Group/Eastern Cooperative Oncology Group study. Blood. 2000;96:4075-83.
11. Stölzel, F., Mohr, B., Kramer, M. et al. Karyotype complexity and prognosis in acute myeloid leukemia. Blood Cancer Journal 2016;6, e386.
12. Baliakas, P., Jeromin, S., Iskas, M., Puiggros, A., Plevova, K., Nguyen-Khac, F., et al., Cytogenetic complexity in chronic lymphocytic leukemia: definitions, associations, and clinical impact. Blood 2019;133(11): 1205–1216.
13. Abdallah, N., Rajkumar, S.V., Greipp, P. et al. Cytogenetic abnormalities in multiple myeloma: association with disease characteristics and treatment response. Blood Cancer J. 2020;10:82.
14. Hanamura, I. Multiple myeloma with high-risk cytogenetics and its treatment approach. Int J Hematol 2022;115,762–777.
15. Mitelman F, Johansson B, Mertens F, editors: Mitelman Database of Chromosome Aberrations in Cancer [Internet]. 2008. Available from: http://cgap.nci.nih.gov/Chromosomes/Mitelman
16. Greenberg PL, Tuechler H, Schanz J et al. Revised international prognostic scoring system for myelodysplastic syndromes. Blood 2012;120:2454-65.
17. Schanz, J., Cevik, N., Fonatsch, C. et al. Detailed analysis of clonal evolution and cytogenetic evolution patterns in patients with myelodysplastic syndromes (MDS) and related myeloid disorders. Blood Cancer J. 2018 Mar 7;8(3):28.
18. Montalban-Bravo G, Garcia-Manero G. Myelodysplastic syndromes: 2018 update on diagnosis, risk-stratification and management. Am J Hematol. 2018;93(1):129-147.

World Pharmacist Day

Fortis Healthcare Medication Safety Summit, September 2023

Date: Friday, 29th Sep 2023 | Time: 04:00 pm to 05:30 pm

Opening Remarks *by Ms Gayatri Sapkale (Team Leader, Pharmacology, MSOG)*

ACTIVITY - 1

Panel Discussion - From Medications to Solutions: *Pharmacist the Key - Role players in Healthcare*

Dr Narayan Pendse
Vice President, MSOG

Dr Anita Arora
DMO & Group Head-Infection Prevention & Control, MSOG

Dr Gurvinder Kaur
FD, Fortis Memorial Research Institute, Gurugram

Dr Rajeev Nayyar
Director Medical Operations (MSOG)

Ms Nandini Gokhale
Business Partner SCM Ops & Governance - CBU

MODERATOR

Dr Shivani Juneja
FD, FMRI Associate Consultant, Clinical Pharmacology, Mohali

Closing Remarks *by Mr Dheeraj Jain (DGM, Business Head of Pharmacy)*

This summit was organized by the Fortis Healthcare Corporate Office and featured a range of meaningful activities to commemorate World Patient Safety Day (September 17, 2023) and World Pharmacist Day (September 25, 2023). It brought together healthcare professionals from various fields and included a panel discussion -"From Medication to Solution - Pharmacists as Key Players in Healthcare."

Dr Narayan Pendse (Vice President - MSOG), **Dr Anita Arora** (DMO & Group Head-Infection Prevention & Control-MSOG), **Dr Rajeev Nayyar** (DMO- MSOG), **Dr Gurvinder Kaur** (FD- FMRI) and **Ms Nandini Gokhale** (Business partner- SCM operation and governance-CBU), with **Dr Shivani Juneja** (Associate Consultant - Clinical Pharmacology-Mohali) as the moderator. This panel discussion shed light on various aspects of medication management, including patient safety, antimicrobial stewardship, supply chain management, Central Pharmacotherapeutics Committee (CPTC) functions, and the role of pharmacists and supporting staff in hospital formulary management and patient safety.

Ms Gayatri Prashant Sapkale (Team Lead – Pharmacology, MSOG) was instrumental in coordinating the whole event across the Fortis Network!

Activities 2: An online Quiz Competition on the theme "Caring for Patients by Ensuring Medication Safety" conducted during the summit.

Activities 3: A 1 Min video challenge - "Pharmacy Spotlight: Lights, Camera, Contribution!" was conducted.

More than 300 participants took part enthusiastically in the Summit – these included Pharmacists (covering Inpatient, Outpatient, Supply Chain Management, and Clinical Pharmacy), Quality and Patient Safety teams, Nurses, and Medical Admin teams.

"Medication safety start with each one of us!"

Congratulations to all the Winners and Participants!

Fortis Hospital, Mulund

Fortis Escorts Heart Institute, Delhi

Fortis Memorial Research Institute, Gurugram

Fortis Hospital, Mohali

Ms Gayatri Prashant

Fortis Hospital, Mohali

Activity	First Prize	Second Prize	Third Prize
Quiz Competition	Ms Ashlin Thomas– Quality (Mulund)	Dr Ansu Samuel– Clinical Pharmacist (CG road)	Dr Farmin Majeed– Clinical Pharmacist (Mulund)
1 min Video	Team **Mohali** *Topic: Look like sound alike medication safety aspect.* 1) **Ms Riya** - Clinical Pharmacist 3) **Mr Hemant Oberoi** - IP Pharmacist 3) **Ms Priya Chaudhary** - Intern Clinical Pharmacist 4) **Ms Riya Sharma** - Intern Clinical Pharmacist	Team **Kalyan** *Topic: Good Dispensing Practices.* 1) **Dr Jagruti Paste** - Clinical Pharmacist 2) **Mrs Ashwini Zunjarrao** - IPD Pharmacy In charge 3) **Mr Devdatta Korde** - IPD pharmacist	Team **Mulund** *Topic: Medication management with Good communication skills.* 1) **Mr Abdul Chaudhary** - IP Pharmacy 2) **Ms Ritika Nikam** - IP Pharmacy 3) **Mr Chinmay Dalvi** - IP Pharmacy 4) **Ms Priya Minde** - IP Pharmacy 5) **Mr Vinayak Hasnale** - IP Pharmacy 6) **Mr Nitin Kolge** - IP Pharmacy 7) **Mr Satyam Yadav** - IP Pharmacy

Role of Clinical Pharmacists in Preventing Antimicrobial Abuse - Can we Empower Them More?

Dr Murali Chakravarthy
Director - Clinical Affairs,
Director- Anaesthesia, Surgical Critical Care and Pain Relief,
Fortis Hospital, Bannerghatta Road, Bangalore

Introduction

Clinical pharmacists (CPs) as an allied medical specialty is rather novel in our country. They have been integral part of hospitals in the west. Their role is also predefined and they enjoy significant empowerment in preparing, dispensing, and controlling the use (and abuse) of medications; more so in special medications such as antimicrobial agents, anticancer therapy and targeted drug therapies. Let us discuss the role of CPs in preventing antimicrobial abuse.

Why clinical pharmacists?

CPs study pharmacology extensively and are in a vantage position in the healthcare facilities. They have an overview of all prescriptions; be it for inpatients or of those impending discharge. They also are privy to the hospital policy on antimicrobial use. They are alerted by electronic medical records either when restricted antimicrobials are prescribed or when hospital antimicrobial policy is flouted use of more than 3 antibiotics, continuance of surgical prophylaxis beyond 24 hours). They are also in a strategic position to monitor justification of use of restricted antimicrobials. Therefore, it is but natural that CPs have a job description that assists in monitoring appropriate antimicrobial use. In order to provide robust antimicrobial stewardship (AMS), it is pertinent to empower the CPs.

Empowerment of CPs:

In addition to the routine job description of CPs which involves monitoring of medication errors, checking duplicate medications, alerting drug interactions, they ought to be involved in more important administrative areas. They are

a. **Essential member of Hospital infection prevention and Control (HIPAC) committee.**

   The CPs provide useful inputs regarding appropriateness of antimicrobial combinations and also present to this committee the surgical prophylaxis/ use of restricted antimicrobials/ escalations and de-escalation. The CPs also enlighten at our unit the doctors who use irrational combinations/ inappropriate choices. If a type C error (the error reached the patient) has already taken place, a "Personal information Letter – PIL" is issued to the individual responsible for inappropriate prescription. Below are the samples of such PIL

a. **Measuring and spreading awareness about 'Drug Resistance Index' (DRI) and antibiograms:**

   The CPs are now enabled to measure DRI. DRI is a index developed from the following inputs Total number of antimicrobial days, total number of units of antimicrobial use. It is displayed a unit of 1. DRI of 0. 0 indicates pan sensitive nature of the antimicrobials while a value of 1.0 indicates pan resistance. We have taken 0.5 as the acceptable benchmark. The DRI value is clubbed with the antibiogram of the unit and the appropriate combinations for each department is arrived at. In a joint meeting of the chair of the HIPAC, the CPs inform the doctors of the appropriate antimicrobial based on the DRI and antibiogram of the particular specialty. This endeavour is a simple straight forward approach, liked very much by the doctors.

b. **Implementing AMS:**

   CPs play a pivotal role taking the hospital policy to the end users. At our unit, there were two instances where CPs played a great role in bringing AMS back on track.

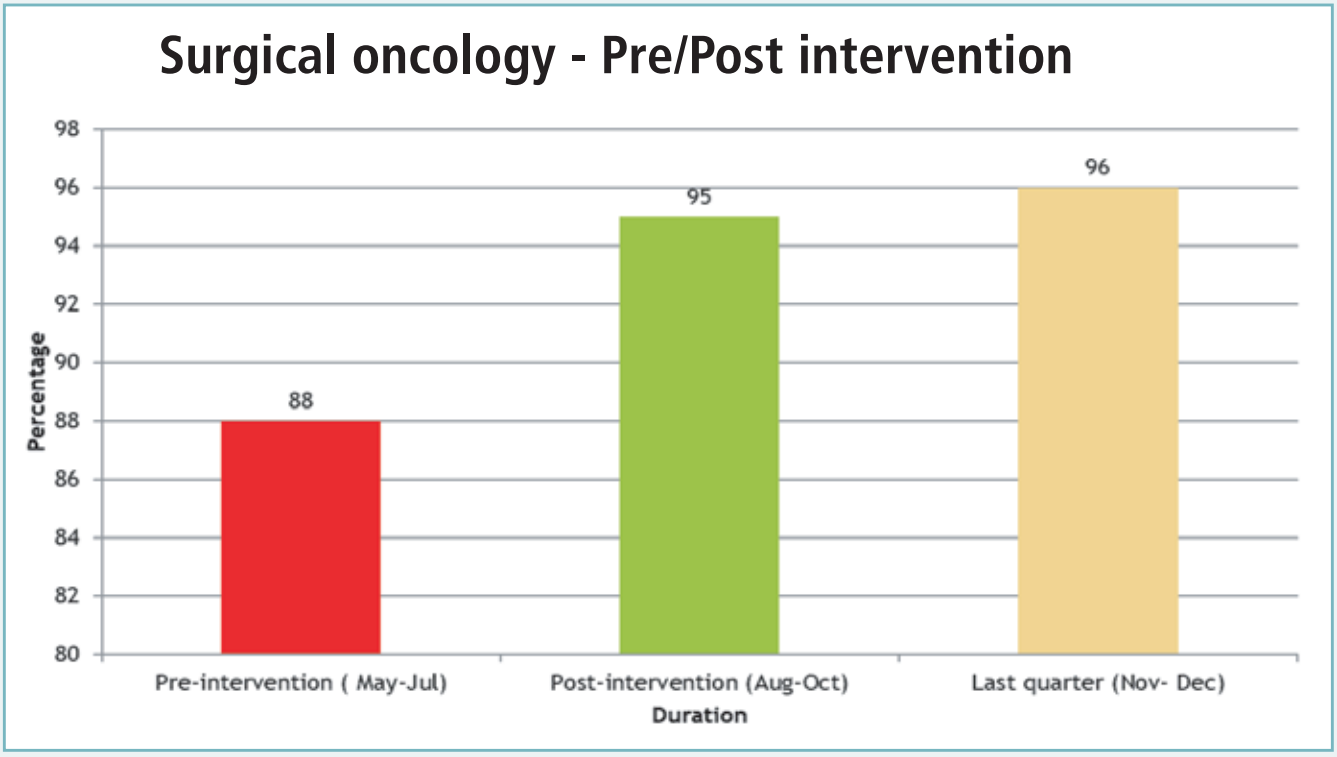

1. Surgical prophylaxis in surgical oncology: The compliance to surgical prophylaxis by the surgical oncology team improved with a few meetings with the team and appraising them of their current practices. Remarkably, with in a couple of weeks, the surgical prophylaxis of surgical oncology department came from 'not acceptable' to ' excellent'

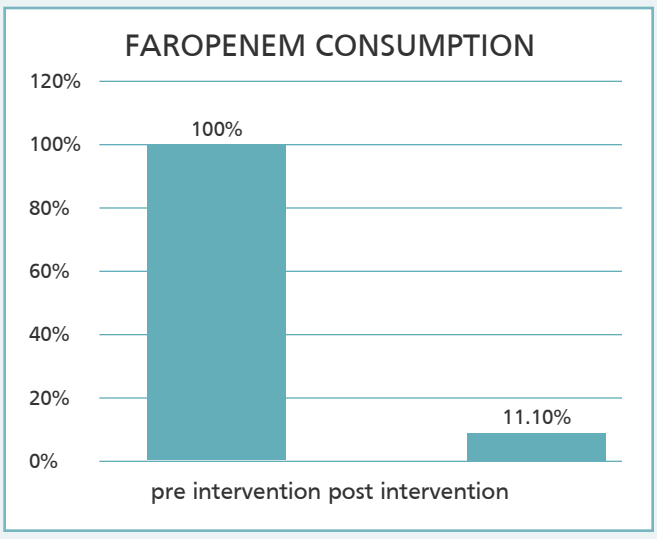

2. Inappropriate use of Faropenem: The urologist were prescribing faropenem for many of their discharges. The redundancy of this practice was identified by CPs and yet again, one on one meeting with the team uro rectified the problem in less than a week.

   The figure below is the testimony to the efforts of our CPs:

c. Preventing medication (antimicrobial) errors:

The CPs help percolate the knowledge regarding common mal practices. A colorful cartoon with the observed medication error and the potential harmful effect is circulated in the social media communication.

Below is the example of 'Dr Fixit"!

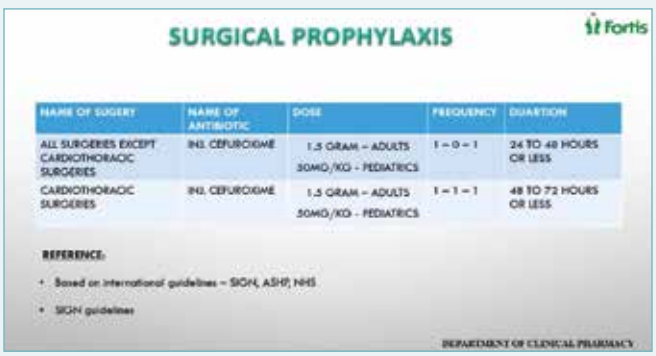

Conclusion

The CPs are a great resource in a healthcare setting. They have adequate knowledge and access to the problem areas. The bird view of the medications in the unit is perhaps one of their unique attributes. Enabling them to whistle blow and alert is a healthy practice; initially their finger pointing may cause heart burn, however, in the long run, healthy medication practices help all concerned: The physicians/ patients and the healthcare unit itself.

Role of Clinical Pharmacists in Medication Safety

Dr Shivani Juneja Bedi
Attending Consultant - Pharmacology,
Fortis Hospital, Mohali

Clinical pharmacists work directly with physicians, other health professionals and patients to ensure that the medications prescribed for patients contribute to the best possible health outcomes. Clinical pharmacists' practice in health care settings where they have frequent and regular interactions with physicians and other health professionals, contributing to better coordination of care.

The primary role of clinical pharmacists is medication management and ADR reporting.

Listed below are the various key areas of work of a Clinical pharmacist promoting medication safety:

- Evaluate the appropriateness and effectiveness of the patient's medications.
- Recognize untreated health problems that could be improved or resolved with appropriate medication therapy.
- Follow the patient's progress to determine the effects of the patient's medications on his or her health.
- Consult with the patient's physicians and other health care providers in selecting the medication therapy that best meets the patient's needs and contributes effectively to the overall therapy goals.
- Provide a consistent process of patient care that ensures the appropriateness, effectiveness, and safety of the patient's medication use.
- Consult with the patient's physicians and other health care providers to develop and implement a medication plan that can meet the overall goals of patient care established by the health care team.
- Apply specialized knowledge of the scientific and clinical use of medications, including medication action, dosing, adverse effects, and drug interactions, in performing their patient care activities in collaboration with other members of the health care team.
- Promoting rational use of medications and ways and means to combat antimicrobial resistance.

Thank you!

We would like to take a moment to thank Dr Vasundhra Atre and Dr Sulabh Tripathi for their invaluable contributions and efforts in putting up clinical connect together. Their dedication and hard work have been instrumental in bringing this Clinical Connect to fruition. We wish them all the best in their future endeavors.

TRIVIA

Crossword : Infectious Disease

Contributed by : Dr Aarti Gupta
Zonal Head, Lab Operations, Fortis Memorial Research Institute

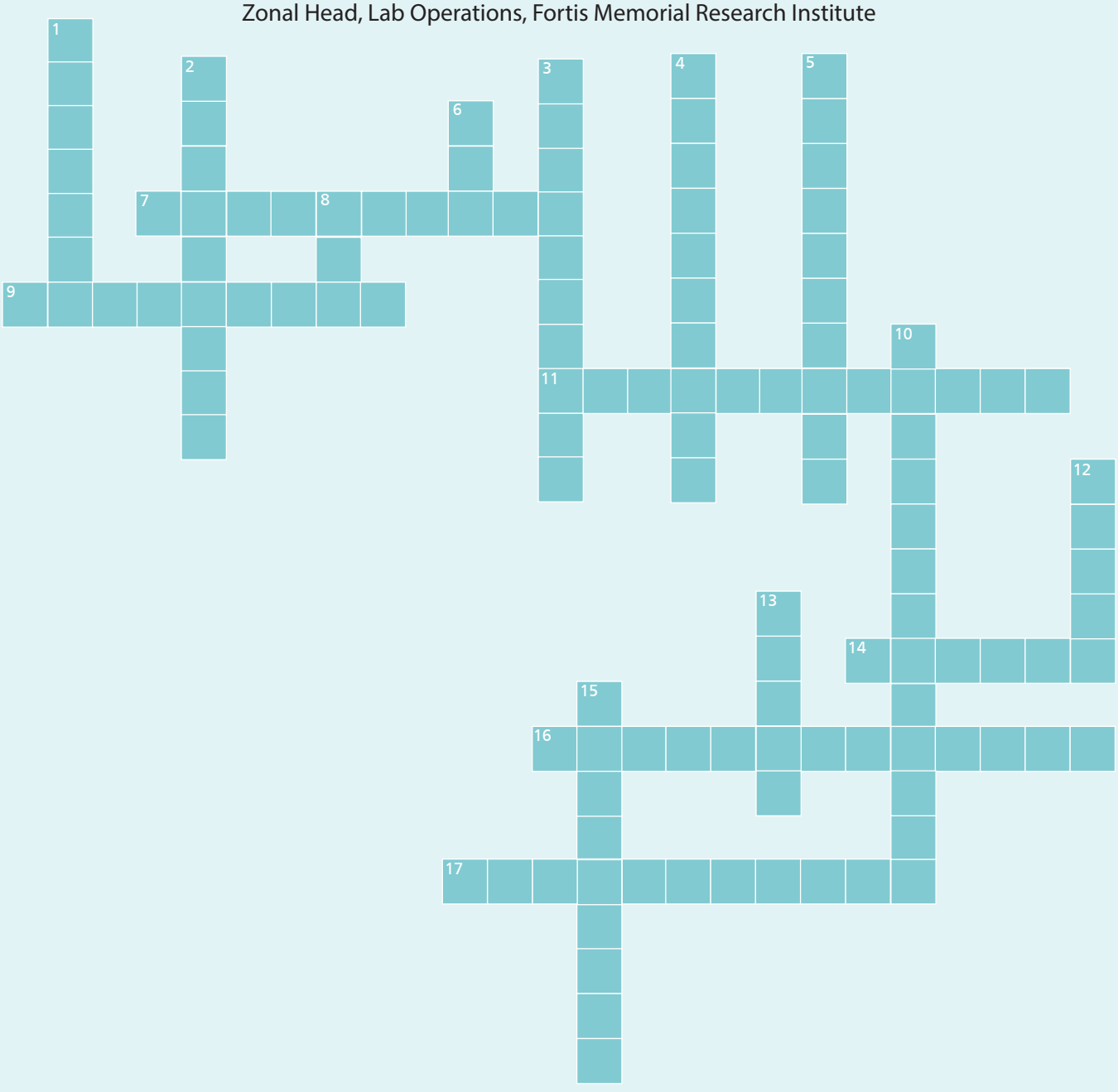

Across

7. Inflammation of cellular or connective tissue
9. Inflammation of the liver
11. The spread of disease from one person to another
14. The presence of pathogenic organisms in the blood
16. The capacity of microbes to cause disease
17. Proteins produced by human host cells in response to viral invasion

Down

1. The growth of microorganisms in lab media
2. Multiplication of organisms within the body
3. Inflammation of the membranes of the brain and spinal cord
4. The ability of a body to resist the effects of a microorganism
5. Infections that are acquired from a health care facility.
6. Urinary Tract Infection
8. Upper Respiratory Infection
10. Inflammation of the bone marrow and adjacent bone
12. Require a living host to survive and reproduce
13. Are molds or yeasts
15. A single celled microorganism

Answer To The Crossword

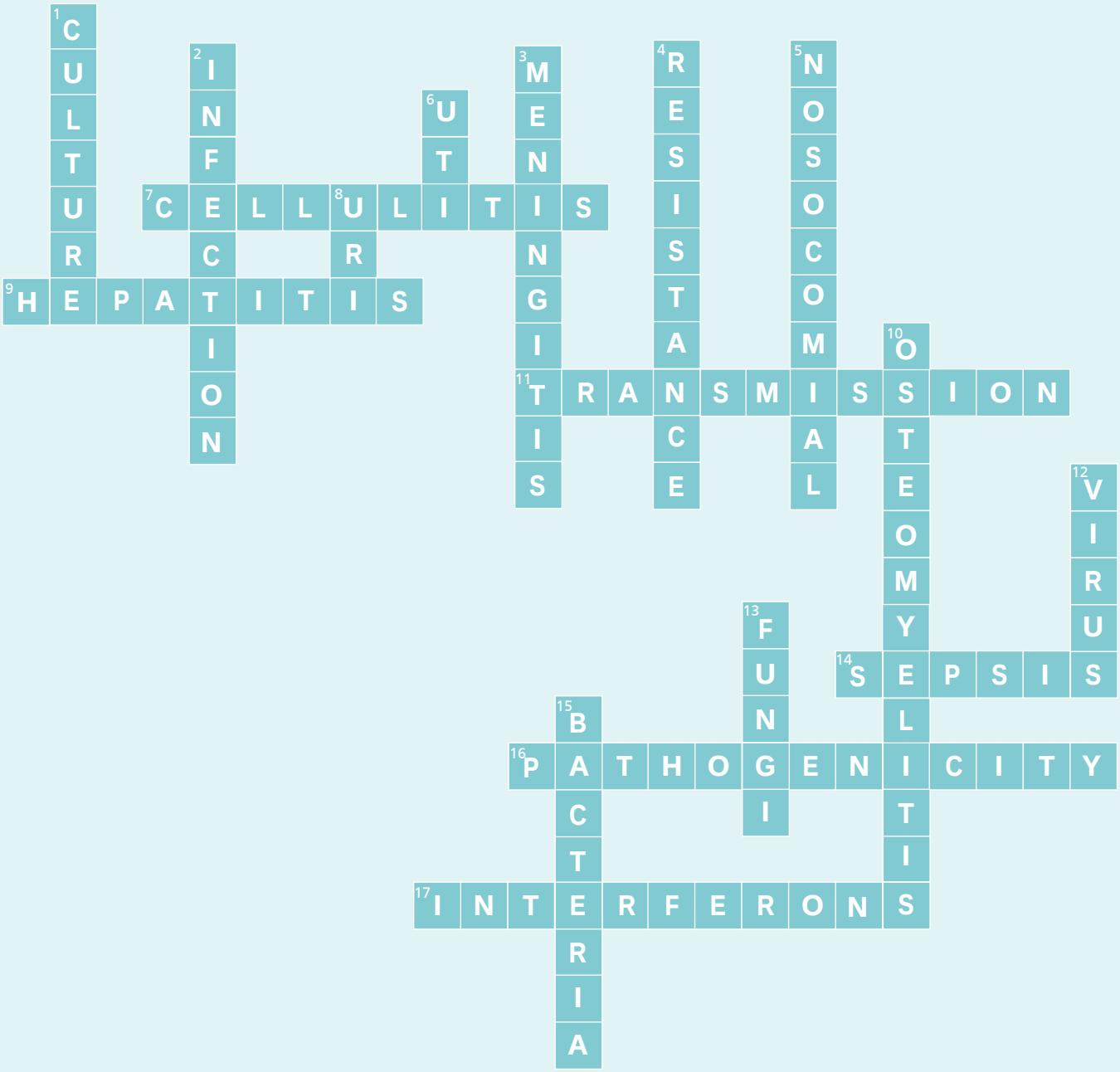

Across

7. Cellulitis
9. Hepatitis
11. Transmission
14. Sepsis
16. Patmogenicity
17. Interferons

Down

1. Culture
2. Infection
3. Meningitis
4. Resistance
5. Nosocomial
6. UTI
8. URI
10. Ostegmyelitis
12. Virus
13. Fungi
15. Bacteria

The Fortis Network

Amritsar


Anandapur, Kolkata


Bannerghatta Road, Bangalore

Chirag Enclave, New Delhi


Cunningham Road, Bangalore


Faridabad


FEHI, New Delhi


FHKI, Kolkata


FLF Greater Kailash, New Delhi


FMRI, Gurugram


Greater Noida


Jaipur

Kalyan


Ludhiana


Malar, Chennai


Mohali


Mulund, Mumbai


Nagarbhavi, Bangalore


Noida


Raigarh, Chhattisgarh

Rajajajinagar, Bangalore


Richmond Road, Bangalore

Shalimar Bagh, New Delhi


SL Raheja, Mumbai

Vadapalani, Chennai


Vasant Kunj, New Delhi


Vashi, Mumbai

Please send your comments, feedback and suggestions to
clinical.connect@fortishealthcare.com